

**Instability, Precipitation and Fouling  
in Heavy Oil Systems**

**by**

**Hong E**

B.A.Sc., The University of Petroleum (Beijing), 1991

M.A.Sc., The University of Petroleum (Beijing), 1994

A DISSERTATION SUBMITTED IN PARTIAL FULFILLMENT OF  
THE REQUIREMENT FOR THE DEGREE OF  
DOCTOR OF PHILOSOPHY

IN

THE FACULTY OF GRADUATE STUDIES  
CHEMICAL AND BIOLOGICAL ENGINEERING

THE UNIVERSITY OF BRITISH COLUMBIA

April 2005

© Hong E, 2005

## Abstract

Asphaltenes are the most polar, highest molecular mass species found in crude oils and bitumens. Depending on the nature of the surrounding species, the temperature and pressure, asphaltene may be dissolved, or may flocculate resulting in precipitation.

Asphaltene precipitation during oil production and processing is a very serious problem in many areas throughout the world. To avoid precipitation, much research has been directed to the solubility of asphaltenes in petroleum liquids as a function of temperature, pressure and composition. Bitumen from oil sands deposits contains about 13.5% asphaltenes, and during its processing is mixed with low molecular mass diluents, which can lead to precipitation and to fouling of processing equipment.

In this work, the effects of diluent composition on asphaltene precipitation from Cold Lake vacuum residue (VR) and Athabasca atmospheric tower bottoms (ATB) were determined using the hot filtration method at 60-85°C. The selected diluents include pure n-alkanes (heptane, decane and dodecane), a lube oil basestock—paraflex (PFX), a heavy vacuum gas oil (HVGO) and a resin enriched fraction (REF) recovered from Cold Lake vacuum residue by supercritical fluid extraction and fractionation. The latter three complex diluents were tested alone and in blends, in order to cover a range of saturates from 56 to 99.4wt%, aromatics from 0.6 to 25wt%, and resins from 0 to 19wt%. For pure n-alkanes, the amount of asphaltene precipitation at a given diluent/residue ratio decreases as the molecular mass of n-alkanes increases. With the increase of diluent-to-residue ratios  $R$ , the amount of precipitated asphaltene,  $W$ , increases sharply at first and then levels off. Similar behaviour can be found for the mixtures of both feedstocks with the aliphatic diluent PFX. With more aromatic diluents such as pure HVGO or blends of HVGO/PFX=1, the increases in  $W$  with  $R$  are modest or slight within the range of

experiment. The addition of the resin and aromatic-rich REF has a strong inhibition effect on asphaltene precipitation. For selected mixtures, the temperature effect on precipitation was investigated in the range of 60°C to 300°C. The results indicate that for the mixtures used in this work the solubility of asphaltenes increases monotonically with temperature.

Asphaltene solubility and precipitation using simple diluents has been analyzed traditionally using thermodynamic models; however, these models are based on the assumption that asphaltene precipitation is a reversible process. This has been a controversial issue, and because of lack of precise experimental data, it has remained unresolved. Another approach is a scaling model based on aggregation of clusters. The original form of scaling equation proposed by Rassamdana et al. gave good agreement of the precipitation data as a function of R for the pure n-alkane diluents (heptane, decane and dodecane). For the complex multi-component diluents of this work, an extended scaling equation with two additional variables (the density and saturate content of the diluents) was developed and provided good agreement with the data over a wide range of diluents to feed ratios. The scaling equation was also extended to correlate asphaltene precipitation from different feed oils by incorporating the colloidal instability index (CII) of the feed oil. This extended scaling equation correlates the experimental data from the two different feed oils well for both single and multi-component diluents. The scaling equation can also be put into a form more useful for thermal fouling studies by converting the ratio W to the precipitated asphaltene concentration (g precipitated asphaltene/L mixture) in the mixture.

The effects of different diluents on the stability of colloiddally dispersed heavy oil systems were tested by determining asphaltene precipitation onset points by titration. Cold Lake vacuum residue (VR), Athabasca atmospheric tower bottoms (ATB) and Cold Lake heavy oil (HO) were selected as sources of asphaltene. The diluents included toluene, Paraflex (PFX), heavy vacuum gas oil (HVGO), resin enriched fraction (REF), de-asphalted oil (DAO) and fuel

oil (FO). Mixtures of the asphaltene source liquids and the diluents were titrated in an automated flocculation titrimeter developed by Western Research Institute using two titrants (iso-octane, n-heptane) to get the flocculation onset points, which were defined by the condition of the beginning of the precipitation of asphaltenes from the sample solution. The inhibition effect of a few diluents (such as Toluene, REF and DAO) was evident, the inhibition effect of diluents increased with the increase of the mass fraction of the diluents and became appreciable when their mass fractions in the mixtures exceeded 30wt%. Two of the diluents (PFX, FO) were found to promote asphaltene precipitation by a slight degree. In other words, the onset point ratio decreases slightly with the increase of the mass fraction of these diluents. For all the mixtures tested in this work, the qualitative behavior of the onsets with titrant type were similar, and display an increase in the onset point with the higher solubility parameter titrant and a decrease for lower solubility parameter titrant.

To predict the stability of various oil blends, the Andersen/Pedersen model and the Wiehe model (Oil compatibility model) were applied to calculate the solubility parameter of all the feedstocks related to this work from the above flocculation results. The results show that the calculated solubility parameters of all the feedstocks lie in the range of 14.7-21.9 (MPa)<sup>0.5</sup>, which is in agreement with the values reported in the literature. Independent of applied diluents, solubility parameters at the flocculation point increase with the increase of the solubility parameter of the applied titrant. Data from the precipitation experiments were correlated with the solubility parameter of the oil blends.

For the purpose of linking precipitation and fouling, a series of fouling runs was carried out in an oil re-circulation loop equipped with an annular heat transfer probe. Vacuum residues from Cold Lake (VR), and Athabasca atmospheric tower bottoms (ATB) were blended with diluents of a range of saturates (56-99.4%), aromatics (0.6-25%), and resins contents (0-19%).

Selected heavy oil mixtures of 1.35-1.77% asphaltene content were re-circulated at constant velocity and a fixed bulk temperature of 85°C. The heat transfer probe was operated at constant heat flux, with initial surface temperatures in the range 230°C to 310°C. For both VR and ATB, fouling rates were much more severe when aliphatic diluents were used, and decreased as the aromaticity of the diluent was raised. The addition of small amounts (2-5%) of a resin and aromatics-rich fraction decreased substantially the extent of fouling at any time. The effects of surface temperature on fouling rates were determined. The extent and rate of fouling under fixed temperature and flow conditions were shown to correlate with the solubility parameters and colloidal instability index (CII) of the test fluids. Criteria from the Andersen/Pedersen model and the Wiehe model (Oil compatibility model) were applied to predict the stability of the test fluids. Thermal fouling deposits were characterized by elemental analysis, thermogravimetric analysis and scanning electron microscopy. A comparison was made of the composition of the thermal deposits and of asphaltene precipitates recovered by hot filtration from isothermal precipitation tests.

In summary, this research has shown that the extent of precipitation of asphaltenes from blends of complex fluids can be described by a modified scaling equation. Furthermore, both the precipitation extent and the fouling extent and rate can be related to solubility parameters of the fluid mixtures derived from flocculation titration measurements and the models of Andersen/Petersen and Wiehe. Temperature effects on asphaltene solubility, on solubility parameters and on fouling rate have been established. Relationships between instability, precipitation and fouling have been quantified.

## Table of Contents

Abstract	ii
Table of Contents	vi
List of Tables	x
List of Figures	xiii
Acknowledgement	xviii
1. INTRODUCTION	1
2. LITERATURE REVIEW	3
2.1 Petroleum Asphaltene Precipitation	3
2.1.1 Petroleum Asphaltene	3
2.1.2 Deposit Formation by Petroleum Asphaltene	8
2.1.3 Characterization Methods for Asphaltene-Containing Oils	10
2.1.4 Solubility Parameters of Heavy Oil Fractions	12
2.1.5 Solubility of Asphaltene	14
2.1.6 Experimental Methods for the Measurement of Asphaltene Precipitation	16
2.1.6.1 The Measurement for the Onset of Asphaltene Precipitation	16
2.1.6.2 Onset Criterion of Asphaltene Precipitation	19
2.1.6.3 The Measurement for the Amount of Asphaltene Precipitation	19
2.2 Mechanism for Deposit Formation by Asphaltene	20
2.3 Models for Asphaltene Precipitation	23
2.3.1 Thermodynamic Models for Asphaltene Precipitation	23
2.3.2 Thermodynamic-Micellization Models for Asphaltene Precipitation	24
2.3.3 The Scaling Equation for Asphaltene Precipitation	28

2.4 Prediction of Asphaltene Stability	29
2.5 Aims and Objectives of the Present Work	32
<b>3. EXPERIMENTAL MATERIALS, APPARATUS AND PROCEDURES</b>	<b>34</b>
3.1 Experimental Materials	34
3.1.1 Properties of Cold Lake Vacuum Residue	34
3.1.2 Properties of Athabasca Atmospheric Tower Bottoms	38
3.1.3 Properties of Diluents	40
3.1.3.1 Properties of Paraflex	40
3.1.3.2 Properties of Heavy Vacuum Gas Oil	40
3.1.3.3 Properties of Resin Enriched Fraction	40
3.2 Experimental Apparatus and Procedures	44
3.2.1 SFEF Apparatus and Procedures	44
3.2.2 Hot Filtration Apparatus and Procedures	46
3.2.3 Flocculation Titration Apparatus and Procedures	49
3.2.4 Thermal Fouling Test Apparatus and Procedures	52
<b>4. HOT FILTRATION EXPERIMENTAL RESULTS AND MODELING</b>	<b>57</b>
4.1 Effect of Diluents Composition on the Amount of Asphaltene Precipitation	57
4.2 Scaling Equation	68
4.2.1 Prediction of the amount and onset of Asphaltene Precipitation using Scaling Equation	68
4.2.2 Application to Deposition Studies	75
4.3 The Effect of Temperature on the Amount of Asphaltene Precipitation	81

5. FLOCCULATION TITRATION EXPERIMENTAL RESULTS AND STABILITY CRITERIA	84
5.1 Effect of Different Diluents on Asphaltene Precipitation Onset	84
5.2 Stability Criteria	98
5.2.1 The Andersen/Pedersen Model	98
5.2.2 The Wiehe Model	99
5.2.3 Colloidal Instability Index	104
5.3 Temperature Dependence Solubility Parameter	106
6. THERMAL FOULING EXPERIMENTAL RESULTS AND THE CORRELATION TO STABILITY CRITERIA	110
6.1 Composition Effect on Thermal Fouling	111
6.2 Surface Temperature Effect on Thermal Fouling	117
6.3 Deposit Characterization	124
6.3.1 Elemental Analysis of Deposits	124
6.3.2 Thermo-gravimetric Analysis	125
6.3.3 Scanning Electron Microscopy	129
6.4 Correlation of Thermal Fouling Data to Stability Criteria	139
6.4.1 Correlation of Thermal Fouling Data to the Andersen and the Wiehe Stability Criterion	139
6.4.2 Temperature Effect on the Stability Criterion	142
6.4.3 Correlation of Thermal Fouling Data to Colloidal Instability Index	146
6.4.4 Correlation of Thermal Fouling Data to Precipitation Data	148
6.4.5 Implications of Thermal Fouling Data	149

7. CONCLUSIONS AND RECOMMENDATIONS	150
7.1 Conclusions	150
7.2 Recommendations	152
Nomenclature	154
References	159
Appendix	173

## LIST OF TABLES

2.1	Analysis of Fractions of Cold Lake Vacuum Residue	6
2.2	Yields of Asphaltene Precipitated from Western Canadian Bitumen Using Various Solvents	14
2.3	Summarization of the Thermodynamic Models and the Thermodynamic-Micellization Models for Asphaltenes Precipitation	26
3.1	Properties for Cold Lake Vacuum Residue	36
3.2	SFEF Results and Analysis Data for Cold Lake Vacuum Residue	37
3.3	Properties for Athabasca Atmospheric Tower Bottoms	39
3.4	Properties of Paraflex	41
3.5	Properties of Heavy Vacuum Gas Oil	42
3.6	Properties of Resin Enriched Fraction	43
4.1	Hot Filtration Experiment Using ATB and Pure Diluent (heptane, decane, dodecane)	59
4.2	Hot Filtration Experiment Using VR and Pure Diluent (heptane, decane, dodecane)	60
4.3	Hot Filtration Experiment Using ATB and Multi-Component Diluents	62
4.4	Resin Effect on Hot Filtration Insolubles Adding REF to ATB Blends	63
4.5	Hot Filtration Experiment Using VR and Multi-Component Diluents	64
4.6	Resin Effect on Hot Filtration Insolubles Adding REF to VR Blends	65
4.7	Temperature Effect on Asphaltene Solubility and Precipitation	82
5.1	Properties of Cold Lake Heavy Oil	87
5.2	Properties of De-asphalted Oil	88
5.3	Properties of Fuel Oil	89
5.4	The Effect of Diluents on Asphaltene Precipitation Onset (iso-octane as titrant)	90
5.5	The Effect of Diluents on Asphaltene Precipitation Onset (iso-octane as titrant)	93

5.6	The Effect of Diluents on Asphaltene Precipitation Onset (n-heptane as titrant)	95
5.7	The Calculation of Solubility Parameter Using Titration Data (iso-octane as titrant, 25°C)	102
5.8	The Calculation of Solubility Parameter Using Titration Data (n-heptane as titrant, 25°C)	103
5.9	The Calculation of Solubility Parameter at Various Temperature Using Titration Data (n-heptane as titrant)	108
6.1	The Composition of the Mixtures for Thermal Fouling Runs	110
6.2	Thermal Fouling Parameter for Experiments of VR (17.7% asphaltene) with Various Diluents. ( $T_b = 85^\circ\text{C}$ , $T_{s0} = 260^\circ\text{C}$ , $U_b = 0.75\text{m/s}$ )	112
6.3	Thermal Fouling Parameter for Experiments of ATB (13.5% asphaltene) with Various Diluents. ( $T_b = 85^\circ\text{C}$ , $T_{s0} = 290^\circ\text{C}$ , $U_b = 0.75\text{m/s}$ )	113
6.4	Surface Temperature Effects on Fouling at $T_b = 85^\circ\text{C}$ , $U_b = 0.75\text{m/s}$	117
6.5	Curve Fitting Parameters from Arrhenius Type Plot	121
6.6	Simulation Distillation Data for PFX1 and PFX2 (ASTM D2887)	121
6.7	PNA Analysis for PFX1 and PFX2 (ASTM D2786, 3239)	122
6.8	Elemental Analysis of Fouling Deposits and Solids from Hot Filtration and Precipitation Tests	125
6.9	Thermal Analysis of Fouling Deposits and Solids from Hot Filtration and Precipitation Tests	128

6.10	SEM-EDX Analysis of Fouling Deposits and Solids from Hot filtration and Precipitation Tests	138
6.11	Solubility Parameters for the Mixtures Used in Thermal Fouling Experiments	143
A1.1	The Amount of Hot Filtration Insolubles (T=85°C) versus Time	173
A1.2	Hot Filtration Experiment Using Several Oil Cuts as Diluents	174
A1.3	Hot Filtration Experiment Using Several Oil Cuts as Diluents	175
A1.4	Resin Effect on Hot Filtration Insolubles Using REF as Diluent	176
A1.5	Resin Effect on Hot Filtration Insolubles Using REF as Diluent	177
A1.6	Hot Filtration Experiment Using Several Oil Cuts as Diluents	178
A1.7	Resin Effect on Hot Filtration Insolubles Using REF as Diluent	179
A1.8	Kinematic Viscosity for Thermal Fouling Test Fluids (85°C)	180
A2.1	Hot Filtration Insolubles for the Duplicate Runs with Various Diluents	181
A2.2	The Repeat Runs for Flocculation Titration Experiment (n-heptane as titrant, 25°C)	181
A2.3	Test of Reproducibility of Thermal Fouling Experiment	182
A3.1	The comparison of the initial fouling rate by two methods	186
A3.2	Average SARA analysis of test fluids	187
A3.3	Flocculation Titration Results for Cold Lake Vacuum Residue	188

## LIST OF FIGURES

2.1	Petroleum Separation Protocol	4
2.2	The Solvent-Resid Phase Diagram	7
2.3	Hypothetical Structure of Asphaltene Molecule	8
3.1	Schematic Diagram of SFEF Apparatus	45
3.2	Cumulative Weight of Extractable Residue as a Function of SFEF Pressure	45
3.3	Hot Filtration Apparatus	47
3.4	The Filter Holder	48
3.5	Schematic of the Automated Flocculation Titration Apparatus	51
3.6	Typical Result for Flocculation Titration Experiment	51
3.7	The UBC Fouling Test Apparatus	55
3.8	The Annular Test Section with PFRU Fouling Probe (not to scale)	56
4.1	Weight Percent of Residue Precipitated W (wt%), (a) Athabasca Atmospheric Tower Bottoms, (b) Cold Lake Vacuum Residue, as a Function of the Diluent to Residue ratio R (cm <sup>3</sup> /g) for Pure Alkane Diluent (T=60°C)	61
4.2	Weight Percent of Athabasca Atmospheric Tower Bottoms Precipitated W (wt%), as a Function of the Diluent to Residue Ratio R (cm <sup>3</sup> /g) for (a) PFX and HVGO Diluents, and (b) PFX-REF Diluents (T=85°C)	66
4.3	Weight Percent of Cold Lake Vacuum Residue Precipitated W (wt%), as a Function of the Diluent to Residue Ratio R (cm <sup>3</sup> /g) for (a) PFX and HVGO and PFX/HVGO Diluents, and (b) PFX/REF Diluents (T=85°C)	67
4.4	Inhibition Effect of REF on Asphaltene Precipitation	68
4.5	Various stages of formation of a 2-D diffusion-limited cluster-cluster aggregates	69

- 4.6 Scaling Equation with  $X=R/M^{1/4}$  and  $Y=WR^2$  for (a) Athabasca Atmospheric Tower Bottoms (Equation (4.5)), and  
(b) Cold Lake Vacuum Residue (Equation (4.6)) 77
- 4.7 Scaling Equation with  $X'=X*(Sa/\rho_{D,20})^{1.5}$  ( $X=R/M^{1/4}$ ) and  $Y=WR^2$  for  
(a) Athabasca Atmospheric Tower Bottoms (Equation (4.8)), and  
(b) Cold Lake Vacuum Residue (Equation (4.9)) 78
- 4.8 Scaling Equation with  $X=R/M^{1/4}$ ,  $X'=X*(Sa/\rho_{D,20})^{1.5}$  and  $Y'=Y*(CII)^2$   
( $Y=WR^2$ ) for both Athabasca Atmospheric Tower Bottoms and Cold lake Vacuum Residue with (a) n-alkanes Diluents (Equation (4.12)), and  
(b) Multi-Component Diluents (Equation (4.13)) 79
- 4.9 Scaling Equation with  $X'=X*(Sa/\rho_{D,20})^{1.5}$  ( $X=R/M^{1/4}$ ),  $Y'=Y*(CII)^2$   
( $Y=WR^2$ ), ( $2.0 \geq X' \geq X_c'$ ) for Cold Lake Vacuum Residue and Athabasca Atmospheric Tower Bottoms with Multi-Component Diluents (Equation (4.15)) 80
- 4.10 The Calculated Concentration of Precipitated Asphaltene  $C_{as,cal}$  (g/L)  
Using Equation (4.14) Versus the Measured Value  $C_{as}$  (g/L) for the Mixture of Cold lake Vacuum Residue and Athabasca Atmospheric Tower Bottoms with Multi-Component Diluents 80
- 4.11 Temperature Effect on (a) Asphaltene precipitation, (b) Asphaltene Solubility 83
- 5.1 The Effect of Diluents on Asphaltene Precipitation Onset (iso-octane as titrant, 25°C)  
(a) Athabasca Atmospheric Tower Bottom as Source of Asphaltene,  
(b) Cold Lake Vacuum Residue as Source of Asphaltene 92
- 5.2 The Effect of Diluents on Asphaltene Precipitation Onset at 25°C (Iso-octane as Titrant, Cold Lake Heavy Oil as Source of Asphaltene) 94
- 5.3 The Effect of Diluents on Asphaltene Precipitation Onset (n-heptane as titrant)

	(a) Athabasca Atmospheric Tower Bottom as Source of Asphaltene,	
	(b) Cold Lake Vacuum Residue as Source of Asphaltene	97
5.4	The Effect of Diluents on Asphaltene Precipitation Onset at 25°C (n-heptane as Titrant, Cold Lake Heavy Oil as Source of Asphaltene)	98
5.5	Linear Correlation between the Wiehe Model Criterion and the Andersen Model Criterion	102
5.6	Hot Filtration Insolubles Fraction W Versus (a) the Andersen Stability Criterion, (b) the Wiehe Stability Criterion. (n-heptane as titrant, 25°C)	104
5.7	Hot Filtration Insolubles Fraction W Versus Colloidal Instability Index (CII) of the Oil Blends	106
5.8	Weight Percent of Feed Precipitated Versus the Andersen Stability Criterion (a) 25°C (b) 35°C and (c) 50°C	109
6.1	Results of Typical Fouling Run with the Mixture of 10wt%VR and 90wt%PFX	114
6.2	Fouling Resistance over Time for a Repeat Run with the Mixture of 10%VR and 90%PFX	115
6.3	Comparison of Fouling Resistance of 10%VR-90%PFX and 10%ATB-90%PFX at the Same Clean Surface Temperature, (a) $T_{s0}=260^{\circ}\text{C}$ , (b) $T_{s0}=290^{\circ}\text{C}$	115
6.4	Fouling Resistance Versus Time for the Mixtures of VR and Various Diluents	116
6.5	Fouling Resistance Versus Time for the Mixtures of ATB and Various Diluents	116
6.6	Surface Temperature Effect on Thermal Fouling Runs Using the Mixture of 10%VR and 90% PFX1	119
6.7	Surface Temperature Effect on Thermal Fouling Runs Using the Mixture of 10%ATB and 90% PFX1	119

6.8	Surface Temperature Effect on Thermal Fouling Runs Using the Mixture of 10%VR and 90% PFX2	120
6.9	Dependence of Initial Fouling Rate on Surface Temperature	120
6.10	Total Ion Chromatogram (TIC) for PFX1 and PFX2	122
6.11	Selected Ion Chromatogram of m/z85 (Paraffins)	123
6.12	Selected Ion Chromatogram of m/z82 (Naphathenes)	123
6.13	Thermo-gravimetric Analysis (TGA) Curves (a) Fouling Deposits from 10%ATB-90%PFX1 at $T_{s0}=290^{\circ}\text{C}$ , (b) Fouling Deposits from 10%VR-90%PFX1 at $T_{s0}=290^{\circ}\text{C}$	127
6.14	SEM Micrographs of Fouling Deposits from the Runs of 10%ATB-90%PFX1 at $290^{\circ}\text{C}$ Initial Surface Temperature, (a) 45 times, (b) 500 times	131
6.15	SEM Micrographs of Fouling Deposits from the Runs of 10%VR-90%PFX1 at $290^{\circ}\text{C}$ Initial Surface Temperature, (a) 45 times, (b) 500 times	132
6.16	SEM Micrographs of Fouling Deposits from the Runs of 10%VR-90%PFX2 at $310^{\circ}\text{C}$ Initial Surface Temperature, (a) 45 times, (b) 500 times	133
6.17	SEM Micrographs of Hot Filtration Insolubles from 10%ATB-90%PFX1 Blends at $85^{\circ}\text{C}$ , (a) 45 times, (b) 500 times	134
6.18	SEM Micrographs of Hot Filtration Insolubles from 10%VR-90%PFX2 blends at $85^{\circ}\text{C}$ , (a) 45 times, (b) 500 times	135
6.19	EDX Plot for the Fouling Deposit from a Run of 10%ATB-90%PFX1 at $290^{\circ}\text{C}$ Initial Surface Temperature	136
6.20	EDX Plot for the Fouling Deposit from a Run of 10%VR-90%PFX1 at $290^{\circ}\text{C}$ Initial Surface Temperature	137
6.21	Final Fouling Resistance Versus (a) the Andersen Stability Criterion,	

	(b) the Wiehe Stability Criterion for ATB and Various Diluents (n-heptane as titrant, 25°C)	140
6.22	Initial Fouling Rate Versus (a) the Andersen Stability Criterion, (b) the Wiehe Stability Criterion for ATB and Various Diluents (n-heptane as titrant, 25°C)	140
6.23	Final Fouling Resistance Versus (a) the Andersen Stability Criterion, (b)the Wiehe Stability Criterion for VR and Various Diluents (n-heptane as titrant, 25°C)	141
6.24	Initial Fouling Rate Versus (a) the Andersen Stability Criterion, (b) the Wiehe Stability Criterion for VR and Various Diluents (n-heptane as titrant, 25°C)	141
6.25	Correlation of Initial Fouling Rate with the Andersen Stability Criteria for ATB and Diluents with Solubility Parameter at (a) 25°C, (b) 35°C, and (c) 50°C	144
6.26	Correlation of Initial Fouling Rate with the Andersen Stability Criteria for VR and Diluents with Solubility Parameter at (a) 25°C, (b) 35°C, and (c) 50°C	145
6.27	Correlation of Initial Fouling Rate with Colloidal Instability Index (CII) for ATB blends	147
6.28	Correlation of Initial Fouling Rate with Colloidal Instability Index (CII) for VR blends	147
6.29	The Correlation of Initial Fouling Rate Versus the Amount of Hot Filtration Insolubles for 10%VR or 10%ATB Blends	148

## ACKNOWLEDGEMENT

I wish to express my gratitude to Dr. A. P. Watkinson, my research supervisor, for his guidance, encouragement and support during this work.

I would like to thank Zhiming Xu, and Ruili Li in the State Key Laboratory of Heavy Oil Processing, University of Petroleum, Beijing, for performing the SFEF experiments and the SARA and elemental analysis on the samples.

Research funding from the Imperial Oil Charitable Foundation and the Natural Sciences and Engineering Research Council of Canada is gratefully acknowledged.

The support and helpful suggestions of fellow students Zhiming Fan, Eman Al-Atar and Xiaoyan Xu are greatly appreciated. I would like to thank all members of the Chemical & Biological Engineering faculty, staff, workshop, stores and graduate students for their assistance.

This thesis is dedicated to my family for their love and support.

## 1. Introduction

In the chemical process industry, organic fluid fouling can be found in the oil upgrading, polymer processing and petrochemical manufacturing industries. Deposit formation on the surface of equipment such as heat exchangers is a well known problem [1-5]. Fouling is especially severe during the upgrading of heavy crude oils where deposition occurs when heavy oil materials are heated, blended, or pyrolyzed in visbreaking or vacuum distillation processes. Increased processing of heavy crude oils, which have much higher asphaltene and heteroatom content than conventional crudes, has heightened researchers' interest in deposit formation by petroleum asphaltenes.

The species in crude oils are mutually soluble as long as a certain ratio of each kind of molecule (or particle) is maintained in the mixture. Variations in temperature, pressure or composition (such as an addition of a diluent) alter this ratio. Then the heavy and/or polar molecules such as asphaltene may separate from the mixture, leading to deposition problems. Petroleum asphaltenes are generally held as the main precursors of fouling by heavy crude oils. The polar asphaltene flocculation can result in deposition and fouling problems in both upstream and downstream operations [6,7]. Since the economic viability of petroleum companies requires processing large volumes of petroleum, any interruption of the flow or of the heat transfer through metal surfaces by the precipitation of asphaltenes is extremely costly. Therefore, it is imperative to be able to predict when and why asphaltenes precipitate in order to mitigate plugging and fouling.

Management of asphaltene deposition may be divided into two subject areas. The first concerns practical aspects in controlling asphaltene deposition problems through the use of solvent treatment, dispersant injection etc. [8]. The second is the prediction of asphaltene deposition by theoretical models. There are many deposition models, which enable the

prediction of asphaltene deposition under the influence of different parameters [9-11]. However it is not yet possible to predict asphaltene deposition for complex systems as occur in heavy oil processing and upgrading.

This thesis investigates the effect of the composition of various diluents and temperature on asphaltene solubility and precipitation using the hot filtration method. The effect of different diluents on asphaltene stability is also tested by measuring asphaltene precipitation onset when titrated with alkanes. The scaling equation [12], which is based on the concept of aggregation is used to predict the asphaltene precipitation onset and amount. The solubility parameter based the Wiehe model (Oil Compatibility Model) [13] and the Andersen/Pedersen model [14 ] are applied to predict the instability of oil blends within the experiment range. Selected fouling experiments are carried out to link the precipitation and fouling process.

## 2. Literature Review

### 2.1 Petroleum Asphaltene Precipitation

#### 2.1.1 Petroleum Asphaltenes

Crude oils are complex mixture of hydrocarbons which, for convenience, are divided into several classes of material. In order of increasing polarity, the classes are: saturates, aromatics, resins, and asphaltenes. Asphaltenes are usually defined as the fraction of oil that is soluble in toluene and insoluble in an n-alkane, usually n-pentane or n-heptane at room temperature. Resins can be defined as the fraction of crude oil not soluble in ethylacetate but soluble in n-heptane, toluene and benzene at room temperature.

Figure 2.1 shows one method for separating petroleum [15]. The first step is a vacuum distillation. This is done to correspond to refinery separation, to remove the fraction that would evaporate with solvent, and to concentrate on the more difficult to characterize fraction, the vacuum residue. Except for a slight amount of inorganic contaminants (salt, rust, clay, etc) petroleum crudes are toluene soluble. However, during conversion a black solid, toluene insoluble fraction—coke, can be formed. After evaporating off the toluene, asphaltenes are precipitated with n-heptane and removed by filtration. The resin fraction is removed from the heptane solution by adsorption on Attapulugus clay and desorption with a mixture of toluene and acetone. Meanwhile, the heptane is evaporated off the remaining oil and the saturates are precipitated by methyl ethyl ketone at dry ice temperature. The remaining oil after evaporation of the methyl ethyl ketone is the small ring aromatics (often called “aromatics”).

A key to understanding incompatibility during recovery and refining operations is to develop an understanding of the principal precursors—the asphaltenes. The chemical structure and physicochemical properties of asphaltenes are subjects of on-going research. Asphaltenes can be usually approximated as a series of polyaromatic hydrocarbons of increasing molar

mass and aromaticity with a variety of associated functional groups randomly distributed on a mass basis [16,17].

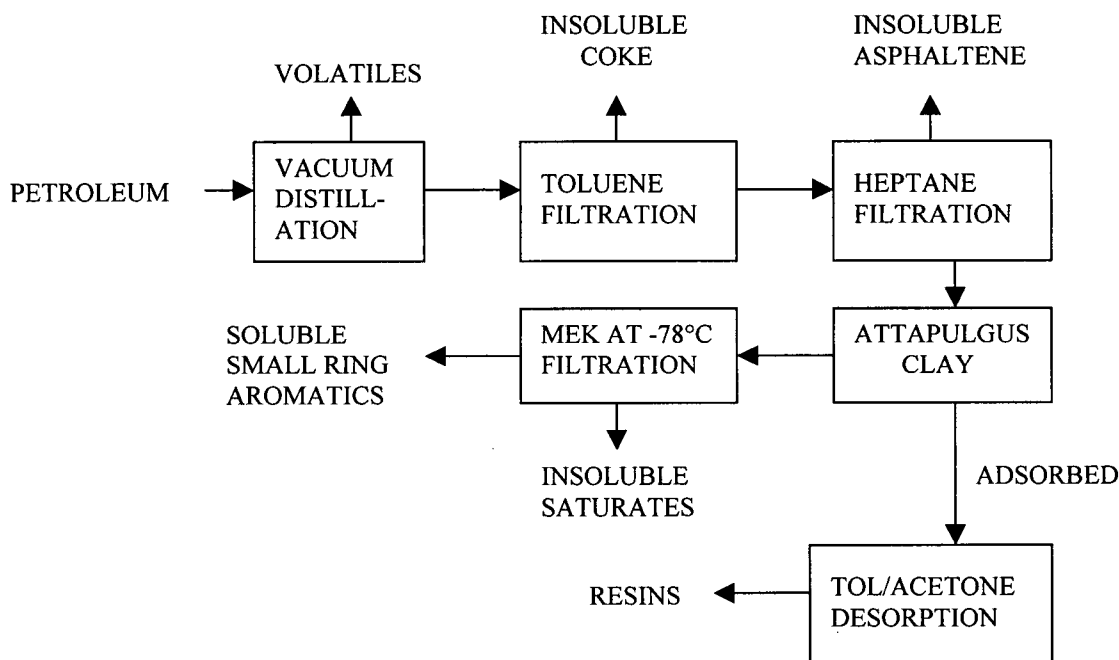


Figure 2.1 Petroleum Separation Protocol

The traditional approach is to investigate the properties of the entire asphaltene fraction and compare them with the properties of other fractions of petroleum macromolecules. Table 2.1 shows an example set of elemental analysis, molecular weight, and  $^{13}\text{C}$  NMR aromaticity values for the fractions of Cold Lake vacuum residue [18]. The asphaltene fraction is typically the highest molecular weight, most aromatic, highest heteroatom (atoms other than carbon and hydrogen) fraction of crude oil. The measurement of even the average molecular weight of asphaltene is a challenge because they are non-volatile, self-associate to form colloids in solvents, and strongly adsorb to most surfaces. Molecular weight can be determined using mass spectrometry (MS), vapor pressure osmometry (VPO), or gel permeation chromatography (GPC). Caution is required to avoid measuring the apparent molecular weight, which is the

molecular weight of the aggregates. The lack of volatility causes MS to measure values that are low; adsorption causes GPC to yield low values; and self association produces high values with measurement in solvents, such as VPO. Based on two-dimensional solubility parameter studies, o-dichlorobenzene at the highest temperature (130°C) is the best solvent for VPO technique [19]. Surface tension can also be used to measure the molecular weight of asphaltenes. It is a simple method and often operates at very low concentration below the asphaltene aggregation onset [20]. Recently, Sheu [21] used atmospheric pressure chemical ionization (APCI) mass spectrometry (MS) to determine the molecular weight distribution of Furrial crude oil and asphaltene. The samples were dissolved in THF (tetrahydrofuran) at 2.5 mg/L, much lower than the aggregation onset. Although the molecular weights of asphaltenes are variable, they usually fall into the range  $2000 \pm 500$ Da [22,23]. The molecular structure of resin has received less attention than that of asphaltene. It has been postulated that resin molecules contain long paraffinic chains with naphthenic rings and polar groups (such as hydroxyl groups, acid or ester functions) interspersed throughout. The molecular weights of resins are about 800Da, which is substantially lower than that of asphaltenes [19]. Unlike values for asphaltenes, the measured molecular weights of resins do not usually vary with the nature of the solvent or temperature. Therefore, chemical association between resin molecules is unlikely [19]. The problems surrounding molecular aggregation, covalent molecular weight, and their experimental investigation in asphaltene chemistry were reviewed by Strausz et al. [24].

Table 2.1 Analysis of Fractions of Cold Lake Vacuum Residue [18]

<i>Fraction</i>	<i>Yield</i> wt%	<i>C</i> wt%	<i>H</i> wt%	<i>H/C</i>	<i>S</i> wt%	<i>O<sup>a</sup></i> wt%	<i>VPO<sup>b</sup></i> <i>Mw</i>	<i>% arom</i> <i>C<sup>c</sup></i>	<i>CCR<sup>d</sup></i> wt%
Saturates	18	84.54	12.31	1.73	2.74	0.00	920	15	1.8
Aromatics	17	81.87	10.00	1.46	5.56	0.00	613	37	8.7
Resins	40	82.08	9.50	1.38	6.09	1.72	986	45	24.6
Asphaltenes	25	81.93	7.94	1.15	7.50	1.55	2980	50	49.6
Total	100	82.45	9.70	1.40	5.75	1.08	1040	40	24.2

<sup>a</sup>Oxygen determined by neutron activation.

<sup>b</sup>VPO number average measured in o-dichlorobenzene at 130°C.

<sup>c</sup>Aromatic carbon determined by <sup>13</sup>C NMR

<sup>d</sup>Conradson carbon residue determined by the Microcarbon test (ASTM D4530)

By investigating the properties of the fractions of the residues of a number of crudes before and after conversion, Wiehe [18] provided a plot of molecular weight versus hydrogen content to distinguish petroleum fractions from each other, as each fraction occupies a unique area on the plot, as shown in Figure 2.2. The hydrogen content is an inverse measure of aromaticity similar to H/C atomic ratio because the carbon content of all petroleum fractions, converted or not, is nearly constant at 80-85%. This plot indicates that asphaltenes are insoluble in n-heptane because of a combination of high molecular weight and high aromaticity. He believed that this solvent-residue phase diagram provides a better definition of asphaltenes and the other fractions than the usual separation definition as well as being a more quantitative version of the heavy oil map than the conceptual molecular weight versus polarity plot of Long [25].

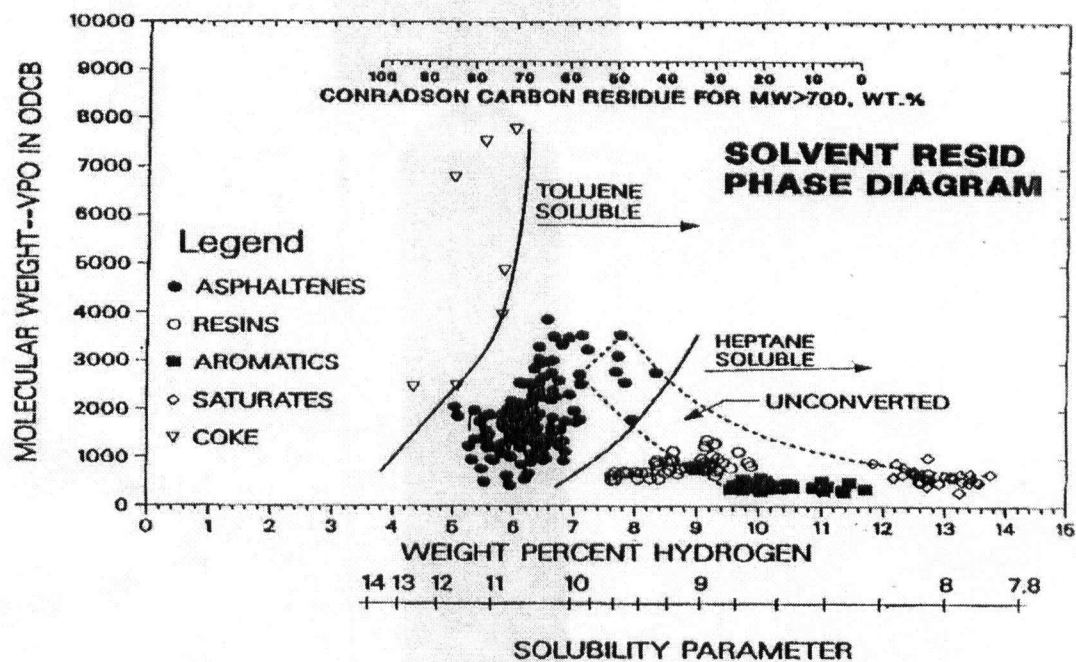
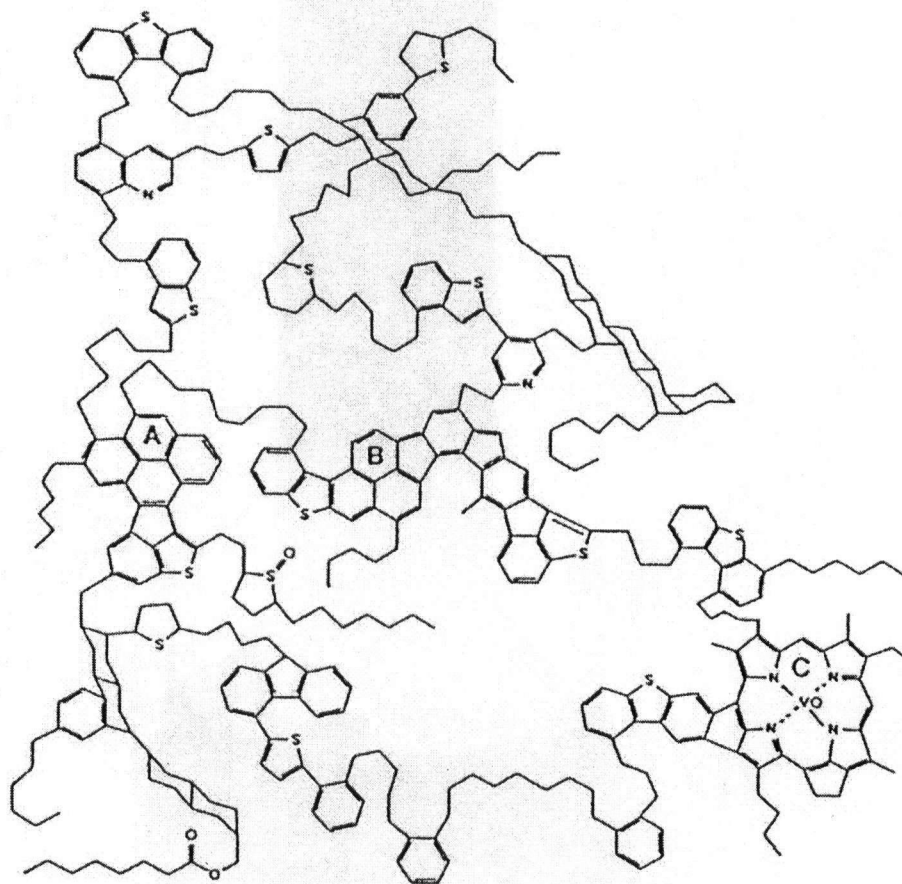


Figure 2.2 The Solvent-Resid Phase Diagram [18] (Solubility parameter in  $[\text{cal}/\text{cm}^3]^{0.5}$ ).

The complexity of asphaltene fractions has made it very difficult to determine a definite structure. Strausz et al. [16] introduced ruthenium-ion-catalysed oxidation (RICO) into petroleum chemistry. RICO is capable of selectively oxidizing aromatic carbon while leaving saturated carbon essentially unaffected. They proposed a hypothetical asphaltene molecule using Athabasca asphaltenes that incorporates in its structure condensed aromatic clusters with side chains and heteroatoms, as shown in Figure 2.3. The H/C atomic ratio is 1.18 and the molecular weight is 6191 daltons. The elemental composition (wt%) is C, 81, H, 8.0, S, 7.3, N, 1.4, O, 1.0, V, 0.8. The elemental formula of this asphaltene molecule can be deduced from the above data as  $\text{C}_{420}\text{H}_{496}\text{N}_6\text{S}_{14}\text{O}_4\text{V}$  [16].



A, B and C represent larger aromatic clusters

The rest of the structural units are based on experimental data

Figure 2.3 Hypothetical Structure of Asphaltene Molecule [16]

### 2.1.2 Deposit Formation by Petroleum Asphaltenes

One particular aspect of crude oil quality that often affects recovery and refining operations is the potential for untimely separation of a solid phase (such as asphaltene). Asphaltene precipitation from an oil can be induced by changes in temperature, pressure, and composition that reduce the stability of asphaltenes in crude oils. The formation of asphaltene deposits can

occur in wells, pipelines, and production equipment. This phenomenon seriously affects production operations and generates a large cost increase due to prevention and removal of deposits. However, although asphaltene deposition is a widespread problem, its causes remain incompletely understood. Asphaltene precipitation in crude oil production facilities is commonly accepted as a physical process, caused by changes of temperature, pressure and the composition of the crude oil that result in asphaltene precipitation. Below the bubble point of crude oils, the oil is single phase but as the crude oil is brought to the surface, a change in pressure leads to an increase in the relative volume fractions of the lighter fractions which induce asphaltene precipitation. However the process of deposit formation by asphaltene on heat transfer surfaces is still not clear. If it is controlled by physical precipitation, then knowing the critical precipitated asphaltene concentration and the factors (such as temperature, velocity etc.) which govern the deposition is crucial to prevent or mitigate asphaltene precipitation related fouling problems in oil refinery equipment.

It is widely believed that asphaltenes exist in petroleum as a colloidal suspension made up of micelles that consist of a dispersed phase (asphaltenes) and a dispersion medium (the rest of the crude) [19,26-28]. The self-aggregation of asphaltene is generally considered as the first step in the formation of precipitated asphaltene particles. The interaction between asphaltene molecules is claimed in the literature to be due to polarity, hydrogen bonding, acid-base,  $\pi$ - $\pi$  bonding etc.. Wiehe concluded that the primary interaction between asphaltene molecules is the Van der Waals attraction between large flat areas of polynuclear aromatics based on the solvent-resid phase diagram and investigating the solubility behavior of asphaltenes in a number of liquids [15]. Asphaltene precipitation depends on the colloidal stability of these complex systems [29]. It has been shown that without a resin fraction, asphaltene cannot dissolve in crude oil. The effect of resin fraction as the dispersing agent is diminished by the

addition of alkane liquids (in which the resins are soluble) leading to desorption of resin from the asphaltene molecules [30,26]. In addition, resin-asphaltene interactions appear to be preferred over asphaltene-asphaltene interactions [30]. Petroleum asphaltenes are held in a delicate balance that can be easily upset by the addition of saturates or the removal of resins or small ring aromatics. Aggregation may, in terms of micelle formation, be seen as a possible means of retaining the asphaltenes in solution without any precipitation [31]. Therefore, it has long been held that asphaltene in crude oil may exist as small aggregates of asphaltene molecules peptized by resin molecules, as recently pictured by Wiehe [13]. It is likely that resin molecules associate with asphaltene molecules through electron-donor-acceptor complexes or through hydrogen bonding [32]. Since resins and asphaltenes appear to coprecipitate when alkanes are added, some authors [12,23] refer to asphalt (which is defined as resins plus asphaltenes) deposition rather than asphaltene deposition during the crude oil production process.

On the other hand, since petroleum crude generally consists of a mixture of aromatic and other hydrocarbons (resins, waxes, and asphaltenes), some authors consider each of the constituent of this system as a continuous or discrete mixture interacting with the other constituents as pseudocomponents. The theory of continuous mixtures, the statistical mechanical theory of monomer/polymer solutions and the concept of Hildebrand's solubility parameter, are then used to analyze and predict the onset and amount of asphaltene precipitation in petroleum crudes [33].

### **2.1.3 Characterization Method for Asphaltene-Containing oils**

Molecular weight and specific gravity distribution data are required for characterizing asphaltene-containing oils, and this characterization information is essential for the computation of thermodynamic properties and phase equilibria. The accuracy of these

computations will be enhanced if molecular weight and specific gravity data of fractions containing similar groups/structures or common solubility properties are used. This is because the critical properties normally correlate better for a single fraction than for the whole oil.

The phase behavior of heavy oil fractions is normally described by their pressure-volume-temperature (PVT) properties. For lighter fractions ( $<C_7$ ), analysis by individual components is available. The heavier fractions ( $C_7-C_{30}$ ) can be separated into subfractions or pseudocomponents that contain related compounds, with a narrow boiling point range (usually  $30^\circ\text{C}$ ).

Experimental boiling curves are determined for the subfractions using any of batch distillation, simulated distillation, or true boiling point distillation. The true boiling point  $T_b$  is then determined from these boiling curves and the specific gravity (or density) and molecular weight are measured for the subfractions. The critical properties are then determined from correlations in the literature [34,35].

The non-volatile residue fraction ( $>524^\circ\text{C}$ ) can be considered as a single pseudocomponent or multiple pseudocomponents if the residue can be fully characterized. For heavy oils, the residue fraction can be up to 50 wt%. Thus the characterization for the residue becomes especially important for predicting asphaltene precipitation in heavy oils. The present residue oil characterization method is usually given a molecular-weight (or/and density) distribution (such as gamma distribution function) for heavy oils or asphaltenes and then using the measured average molecular weight and density value to predict the molecular weight and density for each subfraction or pseudocomponent. Peramanu et al. [36] provided some experimental molecular weight distribution data for Athabasca and Cold Lake bitumen and the specific gravity distributions were computed using the measured molecular weight distribution data and the correlation reported in the literature. Dabir et al. [37] also presented some new experimental data for the molecular weight (Mw) distributions of asphalt and asphaltene

aggregates formed when a solvent is injected into a crude oil (obtained from an oilfield in south-west Iran). The molecular weight distributions were determined by liquid size-exclusion chromatography, or gel permeation chromatography (GPC) methods.

Supercritical fluid extraction and fractionation (SFEF) is an emerging separation technology. Over the past ten years, the technique has been successfully developed by the State Key Laboratory of Heavy Oil Processing at the University of Petroleum, Beijing for separating petroleum residua into as many as 20 sub-fractions [38]. SFEF operation is similar to distillation, but distillation does not operate at high pressure. SFEF operates at a supercritical solvent temperature much lower than the cracking temperature of the feedstock [39]. The SFEF method is capable of producing sufficiently large quantities of each fraction for complete characterization and process scale studies.

#### 2.1.4 Solubility Parameters of Heavy Oil Fractions

The solubility parameter first proposed by Hildebrand [40] is valid only for regular solutions. For such solutions the solubility is controlled by their cohesive energy density or their energy of vaporization per unit volume. The solubility parameter is defined as:

$$\delta = \left( \frac{\Delta U^v}{V} \right)^{1/2} = \left( \frac{\Delta H^v - RT}{V} \right)^{1/2} \quad (2.1)$$

where  $\Delta U^v$  is the internal energy of vaporization (kJ/mol),  $\Delta H^v$  is the molar enthalpy of vaporization (kJ/mol) and  $V$  is the molar volume ( $\text{m}^3/\text{mol}$ ). The equation has been applied to show that solvents which are capable of dissolving asphaltenes are those with enough energy of solution to overcome the association forces of the asphaltene micelle. Thus the solubility parameter can be used to predict the action of particular solvents on asphaltenes. The solubility parameter of asphaltenes has been reported in the range of 20-22 [MPa]<sup>0.5</sup> [41,42]. Hirschberg [9] assumed that the solubility parameters of asphaltenes and resins are almost constant at

20.1[MPa]<sup>0.5</sup> (9.8 [cal/cm<sup>3</sup>]<sup>0.5</sup>), whereas Wiehe [18] provided a solvent-resid phase diagram, where the solubility parameters of asphaltenes and resins are within the range of 20.1~23.6[MPa]<sup>0.5</sup> (9.8~11.5[cal/cm<sup>3</sup>]<sup>0.5</sup>) and 18.0~20.1[MPa]<sup>0.5</sup> (8.8~9.8[cal/cm<sup>3</sup>]<sup>0.5</sup>) respectively. Rogel [43] classified asphaltenes according to their solubility parameters as being highly soluble if they are in the range of 17.0-22.5[MPa]<sup>0.5</sup>, fairly soluble within the range 22.5-25.5[MPa]<sup>0.5</sup>, and difficult to dissolve beyond 25.5[MPa]<sup>0.5</sup>. The solubility parameter of Cold Lake asphaltenes reported by Rogel [43] was 24.3[MPa]<sup>0.5</sup>, lying in the fairly soluble range. The application of solubility parameter data to correlate asphaltene precipitation, and hence asphaltene-solvent interaction, has been used on prior occasions [27,44]. Mitchell and Speight [27] precipitated asphaltenes from Athabasca bitumen using a range of nonpolar solvents and solvent blends. The results showed that the amount of asphaltene that precipitates upon the addition of a solvent varies linearly as the solubility parameter of the solvent. The yield of precipitate of each solvent depends on the difference between the solubility parameter of the asphaltenes and the solvent. Table 2.2 shows the solubility parameters and the asphaltene precipitate yield at 21°C for a variety of solvents. It is apparent that solvents with  $\delta$  values greater than 17.4[MPa]<sup>0.5</sup> (8.5 [cal/cm<sup>3</sup>]<sup>0.5</sup>) essentially dissolve all asphaltenes, whereas pentane with a  $\delta$  value of 14.3[MPa]<sup>0.5</sup> (7.0 [cal/cm<sup>3</sup>]<sup>0.5</sup>) precipitates all asphaltenes.

Table 2.2 Yields of Asphaltene Precipitated from Western Canadian Bitumen\* Using Various Solvents [19]

Hydrocarbon Solvent	Solubility Parameter		Asphaltene Precipitated (wt.% Bitumen)
	[cal/ml] <sup>0.5</sup>	[MPa] <sup>0.5</sup>	
Isopentane	6.8	13.9	17.6
N-Pentane	7.0	14.3	16.9
Isohexane	7.1	14.5	15.3
N-Hexane	7.3	14.9	13.5
Isoheptane	7.2	14.7	12.8
N-Heptane	7.5	15.3	11.4
Isodecane	7.6	15.6	9.8
N-Decane	7.7	15.8	9.0
Cyclopentane	8.2	16.8	1.0
Cyclohexane	8.2	16.8	0.7
Benzene	9.2	18.8	0
Toluene	8.9	18.2	0
Xylene	8.8	18.0	0
Isopropylbenzene	8.6	17.6	0
Isobutylbenzene	8.4	17.2	0

\*: Bitumen contains 16.9 wt% n-pentane asphaltenes

### 2.1.5 Solubility of Asphaltenes

As mentioned previously, much research has been directed to the solubility of asphaltenes in petroleum liquids as a function of temperature, pressure, and composition.

The effect of temperature on asphaltene solubility is somewhat controversial in the literature [45]. Lambourn and Durrieu [4] revealed an interesting behavior for asphaltenes at elevated temperatures. The study of three oils showed that for one oil suspended asphaltenes had a complex relationship with the bulk temperature, that asphaltenes dissolve in the temperature range 100-140°C, but the dissolved asphaltenes re-precipitate when the temperature was raised above 200°C. The other two oils showed either normal solubility behavior or no effect of temperature. Rheological studies of the flocculation of asphaltenes in heavy oil by Storm et al. [46] support the view of re-precipitation at higher temperatures. In contrast, Winans and Hunt [47] used small angle neutron scattering data on 5 wt% asphaltenes in 1-methyl naphthalene-d<sub>10</sub> measured directly at temperature and showed decreasing asphaltene aggregate size with increasing temperature to 340°C. Espinat and Ravey [48] showed that by small-angle X-ray scattering at temperature that the agglomerate size of asphaltenes in toluene decreased in heating from -27 to 77°C. This agreed with Andersen and Stenby [49] who observed increased asphaltene solubility on heating from 24 to 80°C and with Wiehe [50] who used hot stage microscopy to show insoluble asphaltenes redissolve in residue on heating from room temperature to 200°C. However, it is known [51] that petroleum crude that contains large amounts of dissolved gases (live oils) can precipitate asphaltenes on heating. As well, in commercial deasphalting with propane or butane, asphalt is precipitated on heating [52], however, this is due to the well known phenomenon [53] of the rapid change of density and other thermodynamic properties as a mixture approaches the critical point of one of its major components. Therefore, Wiehe [18] concluded that the solubility of asphaltenes always increases upon raising the temperature, unless one of the components is near or above its critical temperature.

Asomaning [54] used a hot filtration method to show that asphaltene solubility increased (i.e. insoluble asphaltenes decreased) with temperature over the range 60-120°C. Preliminary tests by Robin King [55] using a similar method indicated that asphaltene solubility increased as temperature increased, but the solubility curve may flatten out between 180°C and 200°C. This result, and those in [46] suggest that either a physical change or chemical reaction may occur within the oil at temperature approaching 200°C. This would be of key importance for heat exchanger fouling. Therefore, it was of interest to extend the temperature up to at least 300°C and determine if asphaltene solubility indeed increases with temperature as concluded by Wiehe [18].

## **2.1.6 Experimental Methods for the Measurement of Asphaltene Precipitation**

### **2.1.6.1 The Measurement for the Onset of Asphaltene Precipitation**

A number of methods are used to determine the point at which asphaltene flocculation and/or precipitation starts when a non-solvent such as pentane or heptane is added. The methods are typically based on microscopy, attenuation of electromagnetic radiation, gravimetric analysis, or measurement of a physical property such as particle size, viscosity or electrical conductivity, light transmission, acoustic resonance etc. Various detection techniques were proposed to find the onset while titrating a sample: U-VIS Spectrophotometry, NIR Spectrophotometry, Viscosimetry, Electrical conductivity, Thermal conductivity and Sound speed measurement etc.

Using a microscope magnification of 400×, Heithaus [56] visually determined the onset of flocculation upon n-heptane addition. Hirschberg et al. [9] also used a microscope but with a 200× magnification. Visual detection of this onset point in dark or heavy crude oils may be difficult and inaccurate. And the main inconvenience of such batch methods is that they are practically employable only at ambient conditions. An alternative method is to add precipitant

at constant flow rate. The Heithaus method was modified by Pauli [57] to an semi-automatic turbidimetric titration test. He also changed the precipitant from n-heptane to iso-octane to increase the versatility of the method. The principle of the method is to make a solution of bitumen in toluene. The titrant is added continuously at 0.5ml/min until precipitation occurs. The precipitation onset is determined with a UV/VIS spectrophotometer at 740nm as a decrease in light transmittance. Andersen et al. [14] also used light transmission method (UV/VIS spectrophotometer at 740nm) as detection principle including detection limits for low asphaltene concentration crude oils. The titration flow rate was kept as low as 60 $\mu$ l/min, which is much lower than titration rates reported by others. Hotier and Robin [58] and Fuhr et al. [59] used optical methods based on the scattering and absorbance of a beam, respectively. Yang et al. [60] modified Hotier and Robin method with a highly intensified light source, the wave length of the light is 800nm. The light path of the flow cell was reduced from the conventional 10mm to 1mm. A reference light path was used to increase the stability of light-transmittance measurements. This method was later employed by Hu et al. [61] for determining the onset point of asphaltene precipitation to various n-alkanes (n-C<sub>5</sub>~n-C<sub>12</sub>) at 20°C. Using a 633nm He-Ne 1mW laser with a photodiode, Thomas et al. [62] determined the onset of flocculation at reservoir conditions from a plot of photodiode voltage versus mole fraction of alkane solvent added. Asomaning [63] and Stark et al. [64] used NIR laser to determine the flocculation onset by titrating with n-heptane at a rate of 1ml/min and monitoring the transmittance. Most of the optical methods can usually be used at atmospheric pressure and are not suitable for opaque systems. In case of dark oils, solvent (such as toluene) dilution may be needed. As the asphaltene nucleation and separation have their own kinetics, using a continuous flow rate could perturb the system even after the threshold has been reached. In this way the sample stability would be overestimated. Hotier and Robin [58] explored this phenomenon in detail.

This drawback can be overcome by performing stepwise titrations: a finite volume of precipitant is added with a fixed frequency, and the sample is monitored between consecutive precipitant additions. If nucleation and growth are happening in the meantime between two consecutive precipitant additions, the observed variable should change. Due to the slow asphaltene aggregation kinetics, the time interval between successive precipitant addition should be at least 15-20 minutes [65].

To test the onset of live oil in PVT apparatus, the pressure losses to pass through a filter or in a capillary tube are employed. The asphaltene separation at the onset gives a large increase in the sample viscosity, which is detected as a sudden increase in pressure losses. Peramanu et al. [66] developed a flow loop apparatus to test asphaltene precipitation onset. With this technique, the precipitation onset is identified by an increase in the pressure drop across an in-line filter. The technique is capable of handling opaque samples at high temperature and pressure conditions. An asphaltene flocculation detection technique using viscosity measurements was presented by Escobedo and Mansoori [67]. Plots of kinematic and relative viscosity versus the amount of solvent added for both asphaltene flocculating solvents (for example, n-pentane, n-heptane and n-nonane) and dispersing solvents (such as toluene) were generated. For this rigorous method,  $\geq 30$  samples of different solvent/sample ratios were prepared. A small but abrupt deviation in the viscosity curve from the dispersing solvent baseline curve was evident at the point of asphaltene flocculation. Sivaraman et al. [68] used Acoustic Resonance Technology for obtaining high quality data on asphaltene onset in very dark live oil or dead oil at reservoir conditions. This mercury-free digital technology makes it possible to make fast, highly accurate measurement during depressurization runs to identify the onset of asphaltene precipitation. Measurements were performed at temperatures from 71°C to 116°C and at pressures from 9000 psia to 1200 psia. Carrier et al. [69] used the acoustic

technique of phase comparison to determine asphaltene flocculation onset in crude oils. The measurement were carried out at atmospheric pressure and 50°C, n-hexane and n-octane were selected as flocculants. Jones et al. [70] also proposed a method--acoustic scattering to determine the size and concentration of asphaltene particles in crude streams. Unlike conventional methods, this technique was capable of making in situ measurements of oil stability without adulteration with solvents or reagents.

#### **2.1.6.2 Onset Criterion of Asphaltene Precipitation**

An often-applied criterion related to asphaltene precipitation onset is to monitor a minimum or a maximum in the tested variable (absorbance, light transmission, etc). It is assumed that before the onset there is a monotonic behavior due to the dilution effect on the observed variable, while after the onset asphaltene nucleation causes a change of the trend in the opposite direction. This is why it is assumed that the onset condition is related to a minimum or a maximum. While to find the onset from a stepwise titration, the “slope” criterion should be adopted instead [65].

#### **2.1.6.3 The Measurement for the Amount of Asphaltene Precipitation**

Measurement of the amount of asphaltene precipitated is a very difficult problem. The experimental methods can be typically divided into direct and indirect methods. The former methods usually use a filter to separate and weigh the precipitates [62,71-73, 61]. The latter methods usually measure the asphaltene contents in the original oil and the final oil (after precipitation), with the difference taken as the amount of asphaltene precipitated at the given conditions (temperature, pressure and composition) [74,60]. The measurement accuracy of the direct methods will decrease due to the deposition on equipment surface, residual oil in the precipitate, and precipitate entrained in the oil. The material-balance approach (indirect method) of estimating precipitate from the difference in asphaltene content between original

and diluted oil can also be misleading. The difference is low if precipitate is entrained in the diluent oil or if additional components are precipitated from the diluted oil because its composition is changed. The composition of the precipitate also changes with the nature of the precipitant [75].

## **2.2 Mechanism for Deposit Formation by Asphaltenes**

It has been found that asphaltene precipitation during crude oil production is a physical process, however, it is not clear whether deposit formation by asphaltenes on heat transfer surfaces is a physical process, a chemical reaction, or a combination of both chemical reaction and physical processes. Deposit formation mechanisms in heat exchangers proposed by Dickakian and Seay [2], Lambourn and Durrieu [4] are based on the incompatibility between asphaltenes and components of the crude oil as the basis of foulant generation in the bulk solution. By contrast, Eaton and Lux [1] proposed that asphaltene fouling of heat exchangers is principally via chemical reactions.

The mechanism proposed by Dickakian and Seay [2] can be summarized in the following steps:

1. Precipitation of asphaltenes due to incompatibility between asphaltenes and rest of the crude oil.
2. Adherence of precipitated asphaltenes to heat transfer surfaces.
3. Coking of asphaltenes on heat transfer surface.

The crucial step of fouling precursor generation in this mechanism is the precipitation of asphaltene in the bulk of the crude oil. In this mechanism, both the physical process of precipitation and the chemical process of coking are involved. Adherence can be described as physico-chemical. The role of chemical reactions in the coking step is only secondary to the most important step of asphaltene precipitation, and only occur at elevated temperatures. The

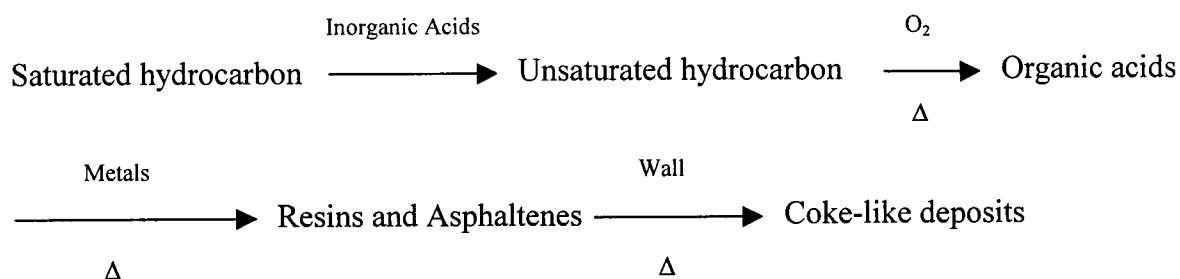
exact method by which asphaltenes precipitate and the role of the other polar species, resins, are not given in this mechanism.

Lambourn and Durrieu [4] found that asphaltene precipitation in the bulk is the major cause of fouling in crude oil preheat exchangers. They proposed a mechanism involving the following steps:

1. Asphaltene precipitation in the bulk.
2. The interactions of the asphaltenes, water and particulates to form a stable emulsion.
3. The deposition of the emulsion on the heated surfaces and its subsequent aging to form coke like materials.

Clearly this mechanism applies only when water and particulates are present.

Eaton and Lux [1] proposed that fouling by asphaltene is principally via chemical reactions. They suggested that saturated hydrocarbon convert to coke as follows:



Eaton and Lux's[1] mechanism assumes that mainly chemical processes (especially polymerization and condensation reactions in the presence of oxygen) result in fouling by asphaltenes. Asphaltenes content in conventional virgin crude oil may be relatively low. Under severe heating conditions, resins and aromatics are converted to asphaltenes [76]. Hence upon exposure to heat, the concentration of asphaltenes in virgin crude can increase. Two processes are assumed to be responsible for this increase, the first is the hydrocracking of

maltenes (saturates, aromatics and resins) to asphaltenes [76,77] and the second is the dealkylation of resins and aromatics followed by condensation reactions that result in the formation of asphaltenes of varying molecular weight, and the production of lower molecular weight compounds. These views seem to support the chemical reaction model of Eaton and Lux [1]. However, data from Blažek and Šebor [76] show that these processes take place at very high temperature (400-500°C). While chemical reactions can lead to the conversion of components of crude oil to coke via asphaltenes, the bulk and surface temperature conditions of Eaton and Lux's study were not high enough to justify the presence of such reactions.

Asomaning [54] also proposed a mechanism for asphaltene deposition based on his experimental data, which consists of the following steps:

1. Depending on the composition of the test fluid, asphaltenes will either aggregate or solubilize in solution. This process is well correlated by the Colloidal Instability Index.
2. In the colloid system, the asphaltenes form aggregated solids, which are filterable and of similar composition to the asphaltenes. Increasing the bulk temperature reduces the concentration of insolubles, therefore the fouling rate decreases.
3. At the heated surface, the high apparent activation energy and negative velocity effect suggest that the adhesion of asphaltene solids is an important step.
4. Attached asphaltene solids age to form coke-like deposits which differ from the original asphaltenes.

Al-Atar [78] investigated the effect of de-asphalted oil (DAO) on asphaltene precipitation and found that adding a DAO which contained no asphaltenes caused increased fouling. Also, as DAO% increased, deposits were higher in H/C atomic ratio, suggesting asphalt (resin plus asphaltene) deposition rather than simply asphaltene deposition. Further, all tests showed the DAO to de-stabilize asphaltenes. Hence, resin/asphaltene interactions need further explanation.

## **2.3 Models for Asphaltene Precipitation**

The models describing asphaltene precipitation in the literature basically fall into two classes: the models that involve the use of asphaltene properties (such as the thermodynamic models, the thermodynamic micellization models, etc); and the models based on the scaling approach.

### **2.3.1 Thermodynamic Models for Asphaltene Precipitation**

The thermodynamic models for predicting asphaltene precipitation under oil production or conditions of pure solvent addition [27] usually involve the phase behavior of asphaltene fractions and some form of equation of state. They generally seek to predict the amount of asphaltenes deposited under specified conditions of temperature, pressure and crude oil composition. There has been no attempt to link such models, or precipitation data, to thermal fouling.

Most thermodynamic models in the literature are based on the classical Flory-Huggins polymer-solution theory coupled with Hildebrand regular-solution theory to describe the phase behavior of asphaltene-containing fluid, such as the Hirschberg et al. model, the Kawanaka et al. model and the Kokal et al. model, etc. [9,10,62,79-81]. Two main factors that determine the precipitation of asphaltenes from crude oil are not addressed in these classical models: one is the chemical association between asphaltene molecules and the other is the peptizing effect of resin molecules. Moreover, most classical models do not explicitly take into account the effect of liquid density. So these models can not provide good quantitative representation for some experimental data.

The thermodynamic models are based on the assumption that asphaltene precipitation is a reversible process. This has been a controversial issue, and because of lack of precise experimental data, it has remained unresolved. The assumption that asphaltene precipitation is

not a reversible process is based mainly on titration experiments in which, after precipitation by addition of a precipitant, one redissolves the asphaltenes by the addition of a solvent [56,13]. The re-dissolution appears to be possible only up to a limited amount of added precipitant [56,13]. Up to now, there has been no firm indication for complete irreversibility of this phenomenon, since the addition of a solvent is not the reverse process of the addition of a precipitant. Further, asphaltene re-dissolution may take considerable time to reach equilibrium time. Rassamdana et al. [12] gave some experimental data and confirmed that this phenomenon is at best partially reversible. Peramanu et al. [66] investigated the precipitation and redissolution of asphaltenes upon the addition and removal of solvent for Athabasca and Cold Lake bitumens using a flow-loop apparatus. In both cases, the precipitation could be completely reversed.

While most thermodynamic models have successfully predicted the precipitation point, they have been less successful in predicting the amount of precipitated material. It has been recently shown that more accurate results can be obtained when the ranges of molar volume and solubility parameter are accounted for with a solid-liquid equilibrium method [79,82]. The last method has been particularly successful with wax precipitation where the physical properties of the wax are reasonably well-known [83].

### **2.3.2 Thermodynamic-Micellization Models for Asphaltene Precipitation**

An alternate method for describing solubility is provided by colloid theory. Asphaltenes were considered to be solid-like particles that are suspended colloidally in the crude oil, stabilized by resin molecules. Irreversible deposition of asphaltenes has been described using colloid-science theories by Leontaritis and Mansoori [84]. This model can be used to assess the possibility of precipitation, however, it does not explicitly deal with the dependence of the micellization process on the characteristics of the micelle. A micelle can be defined as a

submicroscopic aggregation of molecules, formed usually by self-association. On the other hand, a thermodynamic micellization model proposed by Victorov and Firoozabadi [11] assumed that micelles of asphaltene and resin molecules are always soluble in crude oil; asphaltene precipitation is due to the concentration of asphaltene monomers becoming higher than the solubility of asphaltenes in the crude oil without forming micelles. These micelle-based models are helpful for understanding the effect of resin on asphaltene precipitation and the mechanism of asphaltene precipitation from crude oil. While most of these models can not easily explain the observed effect of oil density and oil composition on asphaltene-precipitation phenomena, a recent study by Pan and Firoozabadi [85] indicated marked improvement.

The application of thermodynamic models and thermodynamic-micellization models are summarized in Table 2.3. For the simplest model due to Hirschberg et al., it is clear that  $\Phi_{\max}$  (the maximum volume fraction of asphaltenes soluble in the crude) is dependent on molar volumes of asphaltene and oil, temperature and the square of the difference between solubility parameters of the asphaltene and the oil. For the model of Yarranton et al., a correlation of the equilibrium ratio  $K_i = x_i^s/x_i^l$  for the solid-liquid equilibrium calculation was derived, by which the onset and amount of asphaltene precipitation was determined. In this model, the density, molar volume and solubility parameter of each fraction was related to molar mass based on their experimental data.

Table 2.3 Summarization of the Thermodynamic Models and the Thermodynamic-Micellization Models for Asphaltenes Precipitation

Models		Summarizing Equations	Basic Features	Model Shortcoming	Application
Thermodynamic Models	Hirschberg et al.'s Model [9]	$\Phi_{\max} = \exp\left(\frac{V_a}{V_L} \left[1 - \frac{V_a}{V_L} - \frac{V_L}{RT} (\delta_a - \delta_L)^2\right]\right)$	Modified BWR EOS, Soave EOS and a modified Flory-Huggins theory [86] were applied in this model.	The oil phase and the solid phase were both treated as a single component, this is apparently not reasonable.	The prediction for the onset was better than the amount of asphaltene precipitated. This model is relatively simple.
	Kawanaka et al.'s Model [10]	$V_{fA}^L = \int_0^{\infty} \left\{ \frac{(M_{Ai} / \overline{M}_A) V_a^c}{V^L + V^s \exp(-N_{SAi} \theta)} \right\} F(M_{Ai}) dM_{Ai}$ $W_{Ad} = W_{At} - \rho_A V_{fA}^L V^L$ $W_{At} = \rho_A (V_{fA}^L V^L)_{\text{onset}}$	This is a modified Hirschberg's model [9] by assuming that both petroleum crudes and asphaltenes are solutions of heterogeneous polymers. Scott and Magat's [87] statistical mechanical theory of polymer mixtures incorporating a molecular weight distribution (gamma distribution) was applied.	This model is relatively complex and the application of this model is limited by the absence of extensive and accurate experimental data for the molecular weight distribution of asphaltenes.	The prediction of the onset and amount of asphaltene precipitation were found to improve considerably over Hirschberg et al.'s model [9].

Chapter 2: Literature Review

	<p>Yang et al.'s Model [60]</p>	$F = \ln \Phi_a + 1 - \frac{V_a}{V_m} + \frac{V_a}{RT} \sum_i \sum_j \Phi_i \Phi_j [D_{ia} - 0.5D_{ij}] = 0$ $D_{ij} = (\delta_i - \delta_j)^2 + 2I_{ij} \delta_i \delta_j$ $\delta = 0.500765 (T_B)^{0.982382} \left( \frac{SG}{MW} \right)^{0.482472}$	<p>This is a modified Hirschberg's solubility model [9]. The oil phase was treated as a multicomponent mixture and a new solubility parameter correlation for <math>C_7^+</math> fraction in the oil was proposed.</p>	<p>The solid phase was still be treated as a single component, and this is obviously not valid in reality and may affect the predictive accuracy of the model.</p>	<p>The calculation results based on the new model was in good agreement with experimental data (measured in their work [60] and those reported in literature [9,71]).</p>
	<p>Yarranton et al's Model [88]</p>	$K_i = \exp \left\{ 1 - \frac{v_i'}{v_m} + \ln \left( \frac{v_i'}{v_m} \right) + \frac{v_i'}{RT} (\delta_m - \delta_i')^2 \right\}$ $\rho_i = 0.017M_i + 1080$ $v_i = \frac{1000M_i}{0.017M_i + 1080}$ $\delta_i' = \left( \frac{\Delta H^{vap} - RT}{v_i} \right)^{1/2} = \left( \frac{AM_i + B - RT}{M_i / \rho_i} \right)^{1/2}$	<p>Solid-liquid equilibrium calculations based on the Scatchard-Hildebrand solubility theory and the Flory-Huggins theory were used to predict asphaltene precipitation. Molar mass distribution of asphaltenes were measured and correlations were used to calculate the molar volume and solubility parameters.</p>	<p>For the purpose of simplification, there are many assumptions in this model. Thus the predictive accuracy of this model is not clear without the many assumptions used.</p>	<p>This model has successfully predicted the amount of asphaltene precipitated, but it has been less successful in predicting asphaltene precipitation onset.</p>
<p>Thermodynamic -Micellization Models</p>	<p>Victorov et al's Model [11]</p>	$d \left[ \mu_{ai}^*(T, P, x^*) + kT \ln X_{ai}^{ons} \right] = 0$ $X_{ai}^{ons}(T, P, ratio) = X_{ai}^{ons}(T, P, ratio=0) \frac{\varphi_{ai}^\beta(T, P, ratio=0)}{\varphi_{ai}^\beta(T, P, ratio)}$	<p>A simple form of the standard Gibbs free energy of micellization was used. The Peng-Robinson equation of state (PR-EOS) was applied to describe the fugacity of monomeric asphaltene in the bulk of the petroleum.</p>	<p>This model need many parameters (such as the molecular structure and volume of asphaltene, etc) and most of them need to be fitted from experimental data. Some of them are very difficult to measure accurately.</p>	<p>This model gave good agreement for the amount of asphaltene precipitation (Burke et al. [71]). The model prediction accuracy could be improved by relaxing some of the assumptions.</p>

### 2.3.3 The Scaling Equation for Asphaltene Precipitation

As an alternative, Rassamdana et al. [12] proposed a new model that employed a scaling equation, somewhat similar to those encountered in aggregation and gelation phenomena. This model is discussed later in detail in Section 4.2.

The three variables in the scaling equation are  $W$ , the weight percent of the precipitated asphaltene,  $R$ , the ratio of the volume of the injected solvent and the weight of the crude oil, and  $M$ , the molecular weight of the solvent. They combine the three variables into two by taking  $X=R/M^Z$  and  $Y=W/R^{Z'}$ . Indeed, they choose  $Z=1/4$  and  $Z'=-2$  and then their experimental data for alkanes ( $n\text{-C}_5\text{~}n\text{-C}_8$ ,  $n\text{-C}_{10}$ ) collapse onto a single curve. They claim that  $Z'$  of  $-2$  is universal, whereas the value of  $Z$  will depend on the system used. For  $X>X_c$ , where  $X_c$  is the value of  $X$  at the onset of precipitation, the scaling function was represented very accurately by a third-order polynomial given by:

$$Y = A_1 + A_2X + A_3X^2 + A_4X^3 \quad (2.25)$$

The scaling equation takes on a very simple form, and its predictions are in very good agreement with their experimental data.

Hu et al. [89] investigated the universality of exponents and  $Z'$  in the scaling equation. The results show that  $Z'$  can be taken as a universal constant ( $Z'=-2$ ) as claimed by Rassamdana et al. [12], while  $Z$  depends on oil composition but is independent of the specific precipitant used. They proposed that the optimum value of exponent  $Z$  is in the range of  $0.10 \leq Z \leq 0.5$ . Hu et al. [61] also investigated the effect of temperature ( $20\text{-}65^\circ\text{C}$ ), molecular weight of  $n$ -alkane precipitants and dilution ratio on asphaltene precipitation. New scaling equations were proposed to correlate and predict the asphaltene precipitation data measured at different temperatures using various  $n$ -alkane precipitants.

## 2.4 Prediction of Asphaltene Stability in Blending of Oils

A widely used approach to modeling asphaltene stability is based on regular solution theory, as adapted by the Flory-Huggins approach to account for large size difference between solute and solvent molecules [9]. The onset condition can be quantified by the solubility parameter of mixtures at the onset of asphaltene flocculation.

Andersen and Pedersen [14] proposed a solubility parameter based model to predict the stability of oil blends. According to the Andersen/Pedersen approach, asphaltenes will precipitate when the solvent phase or oil reaches conditions where the average solubility parameter of the phase equals a critical solubility parameter obtained through titration. The solubility parameter of an oil was estimated based on parameters derived from the cubic equation of state (SRK EOS) description of the vapor-liquid equilibrium. The evaluation is derived from a gas chromatographic composition, a molecular weight and the density of the oil. A few oil samples (including stable and unstable oils) were tested using tetrahydrofuran (THF) as the oil solvent. The results show that this method can be used as a simple and reliable empirical tool in assessing possible problems with instability by flocculation titration tests. They claimed that the lowest limit of asphaltene content of the oils for the test was in the range of 0.5% C<sub>7</sub> asphaltene, below which no precipitation can be observed using turbidimetry with the applied detection system.

Wiehe [13] also proposed a solubility parameter based model—the Oil Compatibility Model (OCM) to determine the correct order and proportions of blending petroleum oils to prevent the precipitation of asphaltenes and hence rapid fouling and coking. The basic hypothesis of the Oil Compatibility Model (OCM) is that the asphaltene/resin dispersion has the same flocculation solubility parameter, whether the oil is blended with nonpolar liquids or the other oils. A second hypothesis is that the solubility parameter of a mixture is the

volumetric average solubility parameter of its constituents. As a result, the solubility parameter of a crude oil and its flocculation solubility parameter on a toluene-n-heptane scale can be determined based on mixing the crude oil with toluene and n-heptane and determining if each mixture dissolves or precipitates asphaltenes. Thereafter, the correct proportions and correct order of blending oils to ensure compatibility can be specified. The correct order and proportions of two potentially incompatible crude oils, Souedie and Forties crudes, were predicted using OCM and the results show good agreement with the application in the refinery. If these two crude oils were blended in a tank in the correct proportions for compatibility but in the wrong order at a refinery, then black sludge in the desalter, high fouling of preheat exchangers, and rapid coking of vacuum pipestill furnace tubes occurred. Therefore, blending order is important. One should blend potentially incompatible oils in the order of decreasing solubility blending number. The Oil Compatibility Model was also investigated by Al-Atar [78] with the addition of de-asphalted oil (DAO) into the heavy oil (HO). The fuel oil (FO) was then added as a diluent to this binary mixture for a further fouling experiment. The OCM parameters for these three oil samples were determined by titration and it was confirmed that the addition of the DAO to the HO made the system less stable. For the DAO-HO containing mixtures, the trend of fouling behaviour for asphaltene concentrations greater than 0.8% was consistent with the OCM, approaching zero fouling rate where the calculations showed the mixture to be compatible. The OCM predictions were verified in terms of fouling measurements for these ternary oil mixtures.

The models of Andersen/Pedersen and Wiehe use different nomenclature, but are closely related, as will be shown in Section 5.2.

Wang et al. [90] investigated the effects of compositional changes on asphaltene stability for different crude oils, asphaltene fraction and resins with hydrocarbons that act either as

asphaltene solvents or flocculating agents. The refractive index of onset mixtures was used to quantify solution properties with respect to asphaltene stability, and the results were compared to predictions of an asphaltene solubility model. The effect on asphaltene stability of adding aromatic solvents to an oil was also tested. Buckley et al. [91,92] proposed that the refractive index (RI) of a solution can be measured in place of solubility parameter as an indicator of asphaltene stability.

Rogel et al. [93] evaluated asphaltene stability using the flocculation onset titration technique. It was found that stable crude oils are characterized by possessing asphaltenes with lower density and lower aromaticity, compared with asphaltenes from unstable crude oils. Their resins show a higher stabilizing activity than the ones from unstable crude oils, and their maltenes also exhibit higher asphaltene stabilization effectiveness. Flocculation onsets of stable crude oils are higher than the flocculation onsets of unstable oils, at the same asphaltene content in the sample to be titrated. On the basis of this finding, they proposed an empirical equation for predicting the possible risk of asphaltene precipitation.

## 2.5 Aims and Objectives of the Present Work

Fouling of heat exchangers in the refinery is a major cost element. Petroleum asphaltene are generally held as the main precursors of fouling by heavy crude oils. The polar asphaltene flocculation and precipitation can result in deposition and fouling problems in both upstream and downstream operations. Fouling is especially severe during the upgrading of heavy crude oils where deposition occurs when heavy oil materials are heated, blended, or pyrolyzed in visbreaking or vacuum distillation processes. It is realized that fouling cannot be completely eliminated, but should be reduced to an economic optimum. Thus the overall aim of the present work is to investigate asphaltene precipitation and fouling from blends of heavy oil residues and diluents of varying aromaticities. The main objectives of the current work are as follows:

1. Investigate the effects of diluent composition on asphaltene precipitation from Cold Lake vacuum residue and Athabasca atmospheric tower bottoms using the hot filtration method at 60-85°C. Diluents include pure n-alkanes (heptane, decane and dodecane) and multi-component blends with a wide range of saturates, aromatics and resin contents.
2. Study the temperature effect on asphaltene precipitation and solubility in selected mixtures with temperature over the range of 60°C to 300°C, due to the conflicting views in the literature.
3. Evaluate the effect of different diluents on asphaltene precipitation onset using the automated flocculation titrimeter (AFT) developed by Western Research Institute, Inc.
4. Investigate the possibility of the prediction for the amount and onset of asphaltene precipitation using the original form of scaling equation for pure n-alkane diluents and the feasibility of scaling equations for multi-component diluents in this work. Explore the adaptability of the scaling equations for asphaltene precipitation from different feed oils.

5. Predict the stability of oil blends by the solubility parameter based Wiehe model (Oil Compatibility Model) and the Andersen/Pedersen model by means of flocculation titration techniques (AFT). Investigate the correlation of oil blends stability with the Colloidal Instability Index (CII).
6. Investigate the temperature effect on the solubility parameters of the feedstocks in this work.
7. Investigate the correlation of thermal fouling data with various stability criteria in the literature. Study the link of thermal fouling results with asphaltene precipitation data.
8. Study the composition and surface temperature effect on thermal fouling using a flow loop equipped with an annular, electrically-heated probe. Characterize the fouling deposits from the probe surface and investigate their relations to the insoluble species in the test fluids.

### 3. Experimental Materials, Apparatus and Procedures

This chapter describes the materials used in this work. The physical properties are shown in the following tables. It also describes the equipment used in carrying out the hot filtration, flocculation titration and the thermal fouling experiments.

#### 3.1 Experimental Materials

Cold Lake vacuum residue (VR) supplied by Imperial Oil Company and Athabasca atmospheric tower bottoms (ATB) provided by Syncrude Canada Ltd. were selected as sources of asphaltenes. The diluents include pure n-alkanes (n-heptane, n-decane and n-dodecane), a lube oil base-stock—Paraflex (PFX) supplied by Petro Canada Ltd., a heavy vacuum gas oil (HVGO) provided by Imperial Oil Company and a resin-enriched fraction (REF) recovered from the Cold Lake vacuum residue by supercritical fluid extraction and fractionation (SFEF) [94]. The latter three diluents were tested alone and in blends, in order to cover a range of saturates from 56 to 99.4wt%, aromatics from 0.6 to 25wt%, and resins from 0 to 19wt%.

##### 3.1.1 Properties of Cold Lake Vacuum Residue

Cold Lake vacuum residue, supplied by Imperial Oil Ltd., was produced from Cold Lake bitumen. Cold Lake bitumen is recovered by an in-situ steam displacement process (steam stimulation) [95]. This involves the injection of a steam water (80:20) mixture into the reservoir at 300-315°C for weeks to months. The steam-water mixture serves as the drive-fluid which mobilizes the heavy oil, that can then be recovered at the surface. The latent heat of steam mobilizes the highly viscous bitumen, creating a bitumen-water emulsion which can be produced by conventional means. Production of bitumen is achieved through blowdown of the reservoir pressure, then by pumping the well. The cycle is terminated when either production rates or temperatures become too low, or the water/bitumen ratio becomes too high. The entire cycle can be repeated several times. After the bitumen is pumped to the central plant, water and

gas are removed in separators, and the residual water is removed by heat and electrostatic dehydration. Raw bitumen from these cleaning and separation steps is first desalted and then distilled in atmospheric or vacuum fractionating units. Then different fractions will be sent out to the refineries off site.

Cold Lake vacuum residue is a black viscous liquid with high density and high boiling point range. It mainly consists of high molecular weight hydrocarbons. The asphaltene content is about 17.7%, which is much higher than that of conventional crude oils. The properties of Cold Lake vacuum residue in this work are shown in Table 3.1.

The elemental analysis, specific gravity, molecular weight and SFEF test of Cold Lake vacuum residue were carried out at the State Key Laboratory of Heavy Oil Processing, Beijing, China. The ash and fixed carbon content was determined with the Thermogravimetric Analyzer at the Department of Chemical & Biological Engineering, at the University of British Columbia.

True boiling point (TBP) distillation curves are very useful for classification of petroleum and correlation of petroleum properties, and have been accepted worldwide. However when applied to heavy oils or petroleum residues, difficulties are often encountered due to the limit of distillation temperature (maximum 350°C), in order to prevent feed decomposition or cracking.

In this work, Cold Lake vacuum residue was separated into 15 sub-fractions including the end-cut using the supercritical fluid extraction and fractionation (SFEF) method, and each sub-fraction was further characterized by SARA analysis, elemental analysis, molecular weight, etc. These data are very useful for the understanding of the detailed composition of Cold Lake vacuum residue. A new characterization factor,  $K_H$ , and correlation for boiling point ( $T_B$ ) calculations for fractions of residue were proposed by the State Key Laboratory of Heavy Oil Processing and had shown some success for Chinese vacuum residues [96]. The SFEF method

allowed the extraction of an aromatics and resin rich fraction (REF) in sufficient quantity for our research. Table 3.2 shows the conditions of the SFEF extraction and the properties of each subfraction.

Table 3.1 Properties for Cold Lake Vacuum Residue \*

Properties		Cold Lake vacuum residue
SARA Analysis	Saturates, wt%	11.0
	Aromatics, wt%	38.7
	Resins, wt%	32.6
	Asphaltenes, wt%	17.7
Elemental Analysis	C wt%	83.64
	H wt%	10.0
	S wt%	4.88
	N wt%	0.53
	H/C (atomic)	1.42
	Ash (wt%)	1.40
Molecular Weight		756
Specific gravity		1.0402
CII		0.4009

\* Cold Lake Vacuum Residue: Supplied by Imperial Oil Ltd.

SARA analysis: ASTM D2007 method.

Molecular weight: VPO method.

Table 3.2 SFEF Results and Analysis Data for Cold Lake Vacuum Residue\*

No.	1	3	5	7	8	9	10	11	12	13	14	end
Separation pressure (MPa)	4.0	5.49	5.72	6.03	6.24	6.49	6.86	7.33	8.00	8.95	10.3	12.0
Yield, wt%	6.4	4.9	5.2	5.4	5.2	5.5	5.0	4.8	4.6	4.6	2.5	26.1
Cumulative yield, wt%	6.4	17.6	27.9	38.7	43.9	49.4	54.4	59.2	63.8	68.4	70.9	100
Saturates, wt%	45.50	36.18	25.24	18.52	14.19	6.14	3.84	1.08	0	0	0	-
Aromatics, wt %	47.79	54.76	60.59	64.76	66.06	76.36	72.64	69.71	63.35	55.50	47.98	-
Resins, wt%	6.71	9.07	14.17	16.72	19.75	17.50	23.52	29.21	36.35	44.50	52.02	-
Asphaltenes, wt%	0	0	0	0	0	0	0	0	0	0	0	-
C, wt%	85.01	85.02	85.13	84.35	84.41	83.83	83.77	83.39	83.12	82.85	82.68	82.36
H, wt%	11.79	11.43	11.63	10.71	10.67	10.65	10.62	10.60	10.40	9.96	9.74	8.54
N, wt%	0.13	0.15	0.16	0.15	0.16	0.33	0.33	0.32	0.36	0.49	0.57	1.02
H/C (atomic)	1.653	1.601	1.628	1.513	1.506	1.513	1.510	1.514	1.492	1.432	1.403	1.236
Molecular weight	444	525	573	622	646	670	669	763	711	1098	1510	12778
Specific gravity	0.9591	0.9653	0.9737	0.9876	0.9969	1.0094	1.0219	1.0347	1.0446	1.0567	1.0652	1.1009
Boiling point, K (Calculated)	738.0	784.2	810.4	836.8	849.7	863.0	864.8	908.4	887.7	1038.2	1164.3	2500.5
K <sub>H</sub> (Calculated)	8.11	7.65	7.63	6.92	6.80	6.71	6.53	6.09	5.97	5.70	5.33	3.49

\*: Cold Lake Vacuum Residue: Supplied by Imperial Oil Ltd.

### 3.1.2 Properties of Athabasca Atmospheric Tower Bottoms

Athabasca atmospheric tower bottoms provided by Syncrude Canada Ltd., is a black viscous liquid with lower molecular weight and lower amount of asphaltenes (13.5%) compared to Cold Lake vacuum residue. The properties are shown in Table 3.3.

Athabasca bitumen is extracted from Athabasca oil sands by the mining and hot water extraction method. There are two objectives in the mining and hot water process: (1) To separate the bitumen from the coarse and fine (clay) solids, which are predominantly water-wet, (2) To aerate the bitumen globules but not the solids, so that the bitumen will rise quickly in a flotation vessel to form a froth layer.

Three major steps are involved in this process:

(1) Oil sand is agitated in hot water (at about 80°C) with a small amount of sodium, to maintain the pH in the range of 8.0~8.5. The role of sodium hydroxide in the process is not to adjust the slurry pH, but mainly to produce carboxylate surfactants from precursors occurring in the bitumen. The ionization of these surfactants at slightly alkaline pH gives the bitumen a highly negatively-charged and hydrated surface, which is beneficial to bitumen liberation [97,98].

(2) The sand grains that have settled to the bottom of the settling tank are removed and the oil froth that floats to the top is recovered by skimming the surface. Fine particulate matter, dominated by clay minerals remains in what is called the middle stream.

(3) The suspended bitumen is recovered by conventional froth flotation [99]. Then the bitumen is treated with naphtha diluent, and passed through settlers or a centrifuge before going to the upgrading plants. The ATB is the bottom fraction from the atmospheric distillation column.

Table 3.3 Properties for Athabasca Atmospheric Tower Bottoms \*

Properties		Athabasca atmospheric tower bottoms
SARA Analysis	Saturates, wt%	21.2
	Aromatics, wt%	45.5
	Resins, wt%	19.8
	Asphaltenes, wt%	13.5
Elemental Analysis	C, wt%	82.82
	H, wt%	10.32
	S, wt%	4.47
	N, wt%	0.45
	H/C (atomic)	1.49
	Ash, wt%	1.77
Molecular Weight		581
Specific gravity		1.0163
CII		0.5311

\* ATB: Provided by Syncrude Canada Ltd.

SARA analysis: ASTM D2007 method.

Molecular weight: VPO method.

### 3.1.3 Properties of Diluents

In this work, the diluents include a lube oil base-stock—Paraflex (PFX), a heavy vacuum gas oil (HVGO) and a resin-enriched fraction (REF). The three diluents were tested alone and in blends, which were selected to cover a range of properties with saturates from 56 to 99.4wt%, aromatics from 0.6 to 25wt%, and resins from 0 to 19wt%. These diluents provided a means of studying the effects of diluent composition on asphaltene precipitation, asphaltene flocculation onset point and the deposit formation in heavy oil systems.

#### 3.1.3.1 Properties of Paraflex

Paraflex HT 10 is the commercial name of a lube oil base stock, which is supplied by Petro Canada Ltd. It is colorless. The properties of paraflex are shown in Table 3.4. It contains mainly saturates, with very little aromatic content. As will be described later in Section 6.2, a second sample of Paraflex used in some of the work had somewhat different properties.

#### 3.1.3.2 Properties of Heavy Vacuum Gas Oil

Heavy vacuum gas oil used in this work was provided by Imperial Oil Ltd. It is yellowish brown in colour. Table 3.5 shows the properties of heavy vacuum gas oil. It has a high H/C atomic ratio of 1.76 and low values of sulphur and nitrogen. It has high content of saturates and low amount of aromatics and resins, and contains asphaltenes.

#### 3.1.3.3 Properties of Resin Enriched Fraction (REF)

The resin enriched fraction (REF) was recovered from the Cold Lake vacuum residue by supercritical fluid extraction and fractionation in the State Key Laboratory of Heavy Oil Processing, University of Petroleum, Beijing, China. This fraction is a combination of fractions 10-14 of Table 3.2, which contains almost no saturates, 63 wt% aromatics, 36 wt% resins and no asphaltenes. The properties of this fraction are shown in Table 3.6.

Table 3.4 Properties for Paraflex \*

Properties		PFX
SARA analysis	Saturates, wt%	99.4
	Aromatics, wt%	0.6
	Resins, wt%	0.0
	Asphaltenes, wt%	0.0
Elemental analysis	C, wt%	85.66
	H, wt%	13.73
	S, wt%	0.0
	N, wt%	0.0
	H/C (atomic)	1.92
Kinematic viscosity	25°C (m <sup>2</sup> /s, × 10 <sup>6</sup> )	17.91
	40°C (m <sup>2</sup> /s, × 10 <sup>6</sup> )	10.37
	85°C (m <sup>2</sup> /s, × 10 <sup>6</sup> )	3.63
Molecular Weight		314
Specific gravity		0.8554
Boiling curve:		
1 wt%		293°C
10wt%		324°C
30wt%		344°C
50wt%		358°C
70wt%		374°C
90wt%		400°C
99wt%		465°C

\* Paraflex HT 10: Provided by Petro Canada Ltd.

Table 3.5 Properties for Heavy Vacuum Gas Oil \*

Properties		Heavy Vacuum Gas Oil
SARA analysis	Saturates, wt%	68.3
	Aromatics, wt%	15.9
	Resins, wt%	15.8
	Asphaltenes, wt%	0.0
Elemental analysis	C, wt%	86.55
	H, wt%	12.65
	S, wt%	0.98
	N, wt%	0.03
	H/C (atomic)	1.76
Kinematic viscosity	25°C (m <sup>2</sup> /s, × 10 <sup>6</sup> )	10.84
	40°C (m <sup>2</sup> /s, × 10 <sup>6</sup> )	6.62
	85°C (m <sup>2</sup> /s, × 10 <sup>6</sup> )	2.51
Molecular Weight		285
Specific gravity		0.8685
Boiling curve:		
1wt%		240°C
10wt%		277°C
30wt%		314°C
50wt%		336°C
70wt%		354°C
90wt%		372°C
99wt%		408°C

\* Heavy Vacuum Gas Oil: Supplied by Imperial Oil Ltd.

Table 3.6 Properties for Resin Enriched Fraction (REF) \*

Properties		Resin Enriched Fraction
SARA analysis	Saturates, wt%	0.9
	Aromatics, wt%	62.8
	Resins, wt%	36.3
	Asphaltenes, wt%	0.0
Elemental analysis	C, wt%	81.99
	H, wt%	9.70
	S, wt%	5.47
	N, wt%	0.56
	H/C (atomic)	1.42
Molecular Weight		905
Specific gravity		1.0436

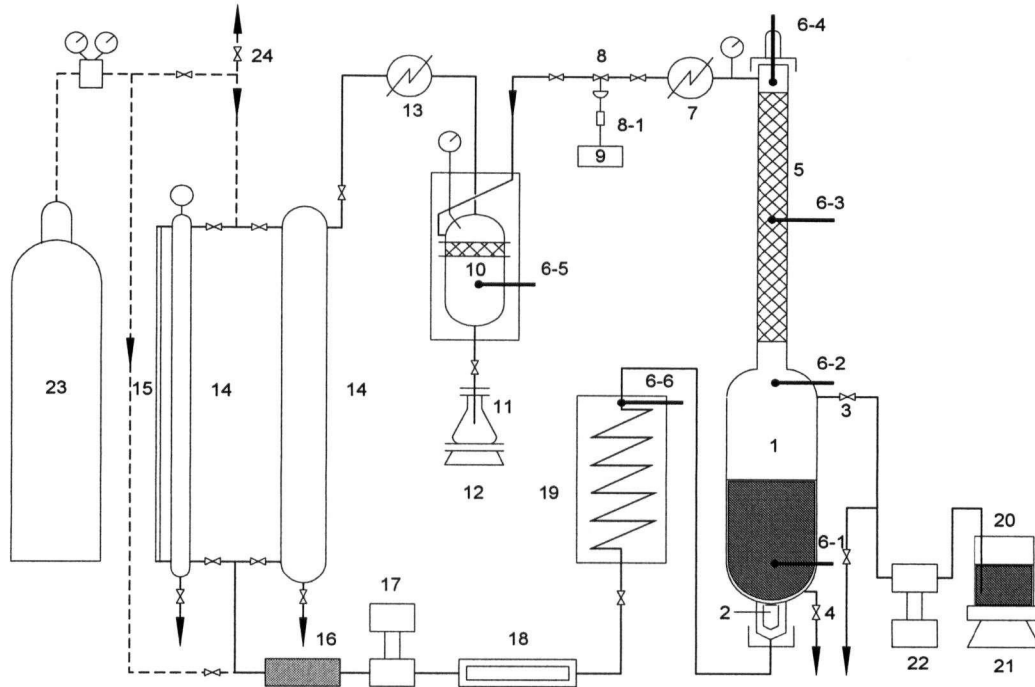
\* Resin Enriched Fraction: SFEF Experiment in the State Key Laboratory of Heavy Oil Processing, University of Petroleum, Beijing, China.

## 3.2 Experimental Apparatus and Procedures

### 3.2.1 Supercritical Fluid Extraction and Fractionation Apparatus and Procedures

The schematic of SFEF is shown in Figure 3.1 [94]. About 1.5 liters of residue was fractionated with n-pentane as supercritical solvent (the critical temperature of n-pentane is 469.6 K and the critical pressure, 3.37 MPa). The recirculation rate of n-pentane was set at 60ml/min. The extraction and fractionation sections of the supercritical fluid extraction unit were maintained at 200°C and 210°C respectively. The pressure of the SFEF unit was initially set at 4.0MPa and was increased to 12MPa over 8hr. The cumulative weight of extractable residue as a function of SFEF pressure is shown in Figure 3.2. Total recovery was 74wt% for Cold Lake vacuum residue. The remaining end-cut was treated as a single fraction. The unit was operated by personnel of the State Key Laboratory of Heavy Oil Processing, University of Petroleum, Beijing, China; in the presence of the author (Hong E).

The residue feed 20 was pumped into the extractor 1 while the heated solvent from the solvent train was distributed evenly through the distributor 2 to the extractor. In operation of the extractor 1 and fractionation column 5, their temperature were so adjusted that a temperature gradient was created with the lowest temperature at the bottom and the highest at the top. As the supercritical fluid went up, its solution power would decrease and some heavier component would separate out serving as a reflux of the column 5. Then a transfer of mass and heat would take place between the extract and raffinate phases. Coming out of the column, the pressure was reduced at valve 8 and the solvent evaporated. A fraction of the residue could be collected in collection flask 11. The solvent through condenser 13 was sent back to the solvent train 14→16→17→18→19→2. By stepping up the pressure of the system linearly or stepwise, fractions of the residue as desired could be collected and their characteristic properties determined by further analysis.



1-Extractor; 2- SCF Distributor; 3-Feed inlet valve; 4-Residue outlet valve; 5-Packed bed; 6-Thermocouple; 7-Cooler; 8-Pressure adjusting valve; 9-Computer Controlling SYS; 10-Solvent evaporator; 11-Collection flask; 13-Condenser; 14- Solvent Cylinder; 15-Solvent Level indicator; 16-Filter; 17- Solvent pump; 18- Flowrate gauge; 19- Preheater; 20-Feed Cylinder, 21- Electronic balance; 22-Feed Pump; 23-N<sub>2</sub> Cylinder; 24- Vent

Figure 3.1 Schematic Diagram of SFEF Apparatus

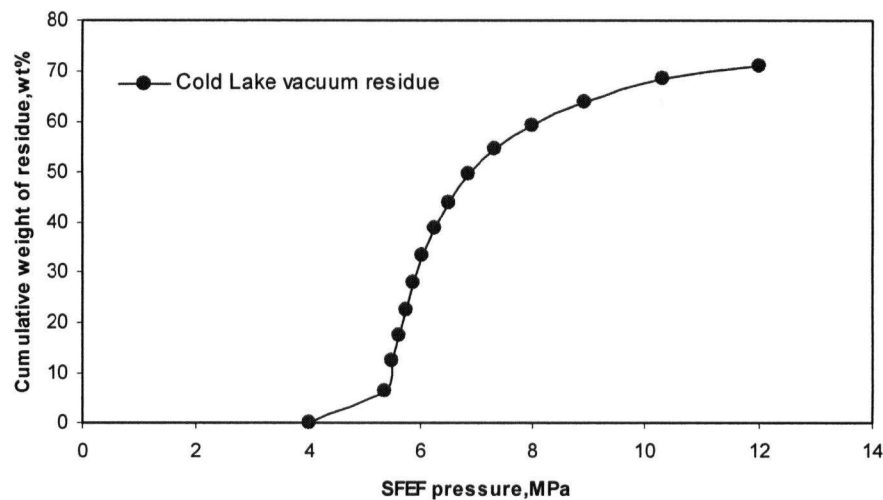


Figure 3.2 Cumulative Weight of Extractable Residue as a Function of SFEF Pressure

### 3.2.2 Hot Filtration Apparatus and Procedure

Hot filtration insolubles were determined by filtration at bulk temperatures of 60 or 85°C using a 47mm dia. Millipore glass filter funnel equipped with pre-weighed 1 $\mu$ m or 3 $\mu$ m pore size glass fiber PALL Gelman filters. Ten grams of sample was heated and mixed in a vial or a beaker on a hot plate to the selected bulk temperature, then equilibrated, while being subjected to intermittent agitation. Tests showed essentially no difference in suspended asphaltene concentrations between times of 30 minutes and 3 hours (as shown in Appendix A1.1), which is consistent with the results of Asomaning [54], hence a time of 30 minutes was used in subsequent experiments. The sample was filtered under vacuum, and then the precipitate was washed with n-heptane until the filtrate was clear. The filter and the precipitate were placed in an aluminum dish and dried over night in an oven at 100°C until successive weighings produced no change in weight. Experiments using alkane diluents were carried out at 60°C; those with multi-component diluents were done at 85°C.

The temperature effect (60-300°C) on asphaltene insolubles concentration was investigated using a stainless steel pressure filtration device. The schematic of this apparatus is shown in Figure 3.3. The apparatus consisted of a 1-liter cylindrical closed tank with a Millipore filter holder mounted underneath, both in a common furnace. The detailed structure of the filter holder is shown in Figure 3.4. Glass fiber filters 90mm in diameter, with a pore size 1 $\mu$ m or 3 $\mu$ m from PALL Gelman were employed. One hundred grams of sample were mixed in a beaker at 50°C and then poured into the tank. A nitrogen purge was started and then the furnace was turned on. After the sample reached the desired temperature, it was held there for half an hour. The filtration was then carried out under nitrogen pressure, and the glass fiber filter was treated in the same manner as stated above.

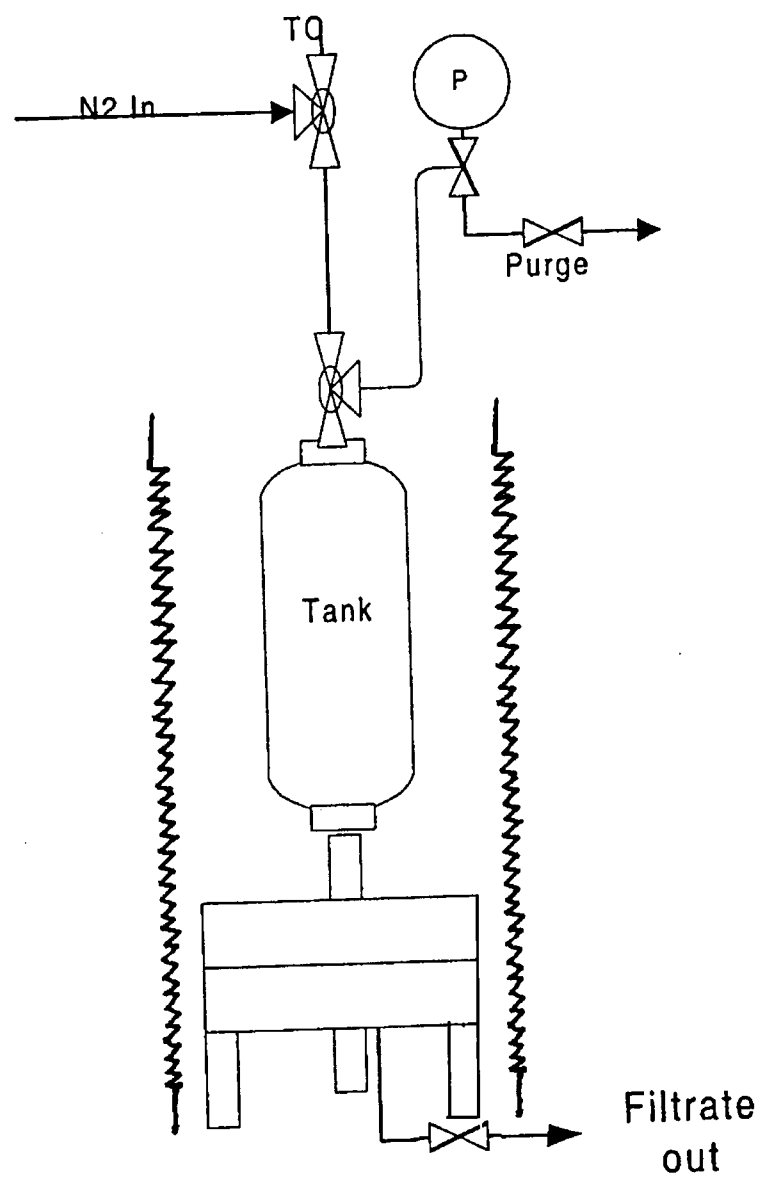
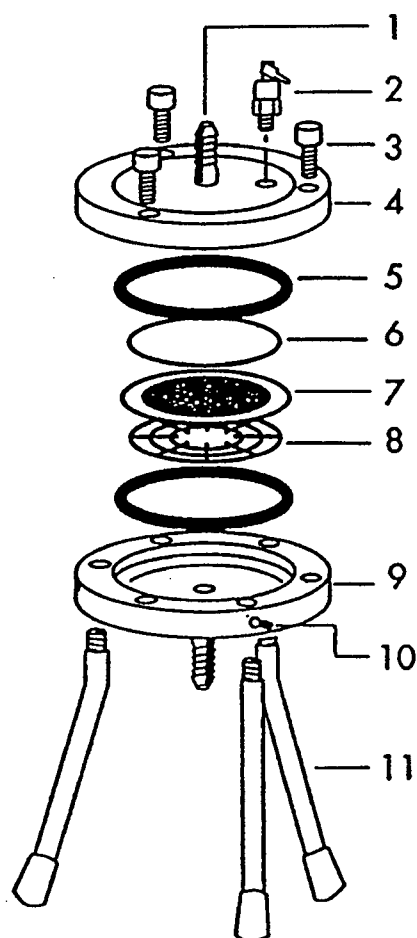


Figure 3.3 Hot Filtration Apparatus



1. Connector
2. Vent Valve
3. Allen-head cap screws
4. Inlet plate
5. O-ring
6. 90 mm diameter filter

7. Filter support screen
8. Underdrain support
9. Outlet plate
10. Allen set screws
11. Legs

Figure 3.4 The Filter Holder

### 3.2.3 Flocculation Titration Apparatus and Procedures

The onset point of asphaltene flocculation is determined by titration with iso-octane or n-heptane, using the automated flocculation titrimer (AFT) developed by Western Research Institute, Inc.; a schematic of this apparatus is shown in Figure 3.5 [57].

The AFT consists of intersecting sample circulation and titration loops. A reaction vial is housed in a water-jacketed reaction vessel and sealed with a custom-designed cover from which the sample flows through small-bore Teflon tubing through the sample circulation loop. One of these tubes connects a short-pathlength (0.1mm) quartz flow cell housed in a fiberoptic UV-visible spectrophotometer to the reaction vial. A second tube connects the reaction vial to a high-flow-rate (10ml/min) metering pump. A third tube connects the quartz flow cell to the high-flow-rate metering pump to complete the circulation loop. The titration loop is made by two additional tubes which connect the reaction vial to a low flow rate (0.5ml/min) metering pump, which is connected via a second tube to a water-jacketed reaction vessel filled with titrant (usually n-heptane or iso-octane). While the sample solution circulates through the sample circulation loop, the titrant is pumped into the sample reaction vial at a constant rate by the low-flow-rate metering pump. During this process, the output signal from the spectrophotometer is computer recorded. The change in percentage of transmittance (%T) of detected radiation at 740 nm passing through the quartz cell is plotted versus the time,  $t$ , during which titrant is added to the sample reaction vial.

The spectrophotometer output signal detects the onset of turbidity of the sample solution. This is the flocculation onset point, corresponding to the beginning of the precipitation of asphaltenes from the sample solution. In this work, samples of approximately 0.5-1.0g heavy oil are transferred into a specially designed reaction vial, into which 3.0ml toluene is added to dissolve the heavy oil. Thus each reaction vial contains a solution of a different concentration

of heavy oil in toluene. Reaction vials are resealed with Teflon-lined caps and stored away from sunlight for at least 24 hours for sample dissolution. With a given solution of heavy oil and toluene, different amounts of the diluents are added and then the onset points are determined by titration with precipitant at 0.5ml/min. In the present study, tests are performed by titrating a sample at three or more concentrations with both iso-octane and n-heptane precipitants. Most of the tests were conducted at 25°C, selected runs were performed at 35°C and 50°C for the purpose of testing the temperature effect. The light transmission of the sample first increases due to the dilution effect of the titrant, and then decreases with the occurrence of precipitating asphaltenes, as shown in Figure 3.6. The onset is taken as the volume of titrant which has been added at the point of maximum light transmission.

When the test is completed, the circulation pump intake tube is removed from the sample and placed into a small beaker containing toluene. The residual sample solution along with a few milliliters of toluene is pumped back into the reaction vial. The second tube is removed and placed into the same small beaker containing toluene and several milliliters of toluene is re-circulated through the system. After a short period of time the rinse toluene is removed from the beaker and the fresh toluene is re-circulated through the circulation loop flow cell. The spectrometer is re-zeroed. The sample vial is removed from the water jacket beaker and Teflon cap.

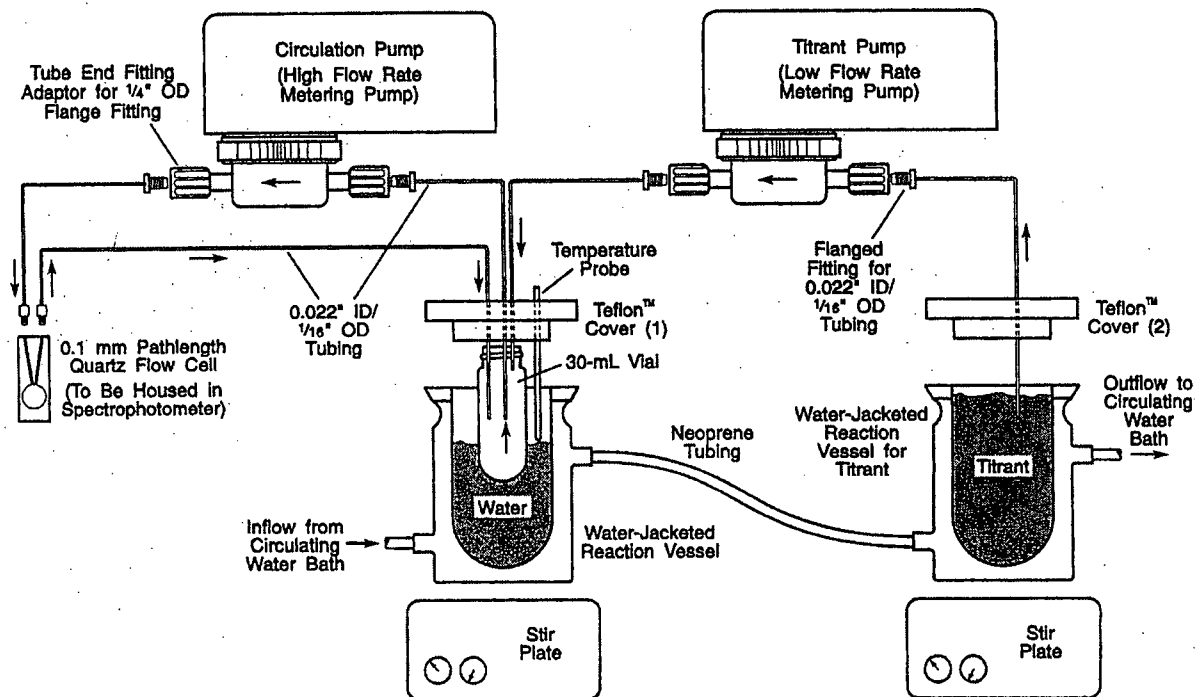


Figure 3.5 Schematic of the Automated Flocculation Titration Apparatus

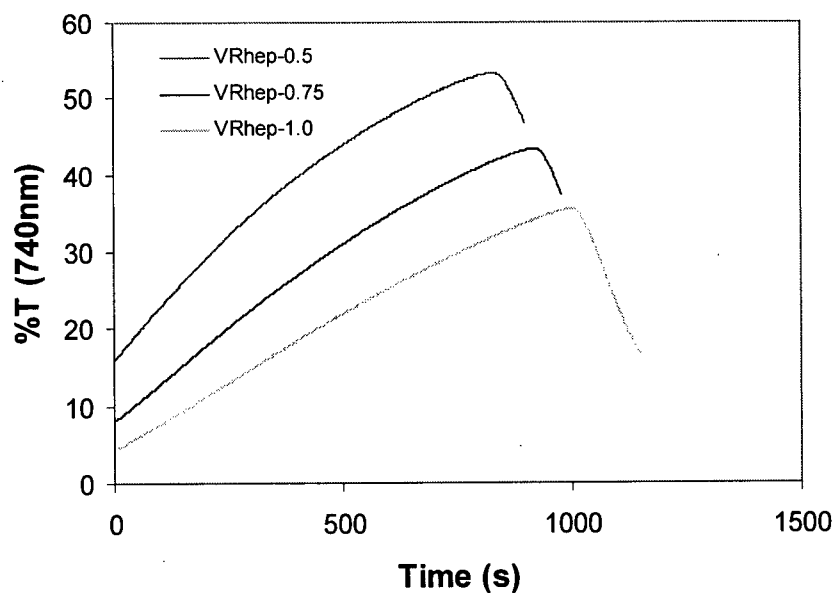


Figure 3.6 Typical Result for Flocculation Titration Experiment for VR with n-heptane as Precipitant at Ratios of 0.5gVR/3.0ml Toluene, 0.75gVR/3.0ml Toluene, 1.0gVR/3.0ml Toluene.

### 3.2.4 Thermal Fouling Apparatus and Procedures

Fouling experiments were conducted in a flow loop shown in Figure 3.7, and described in [100]. The loop is equipped with an annular, electrically-heated probe (Figure 3.8), designed by Heat Transfer Research Incorporated and supplied by Ashland Drew Chemicals.

Due to the high viscosity of VR or ATB, it is heated on a hot plate to 40-50°C, then the necessary amount of diluent oil (also heated to 40-50°C) is added gradually, before mixing on a hot plate. In the case of blending diluent oils (such as HVGO+PFX, etc.), the more aromatic diluent oil always mixed first with VR or ATB. In this work, 860 grams of VR or ATB are used and 7740 grams of diluent oils required to make the 10 wt% solution. After the supply tank has been filled, the test fluid (8.6kg) is purged with nitrogen for one hour under 410kPa absolute pressure to eliminate any dissolved oxygen. After purging, the pump and immersion heater were turned on and the control panel activated. Once the desired pressure was reached, the vent valve was closed. When the bulk temperature reached the desired temperature of 85°C, the flow control valve was set to yield the desired bulk velocity based on a calibration of the orifice plate. Before the probe heater was started, a sample of the test fluid was taken for analysis. The power to the heat transfer probe was adjusted to achieve the desired initial surface temperature ( $T_{s0}$ ). The datalogger and the PC were activated to record system variables at a scanning interval of 10 minutes. A small flow of cooling water was used to maintain a constant bulk temperature throughout the run.

At the end of ~40 hours or when power to the probe was cut off due to high surface temperatures, a sample of the test fluid was taken once again for analysis. The cooling water flow rate was increased to cool the system, the pressure of the system released and the test fluid drained. The probe was taken out of the test section and rinsed with varsol, a paint thinner sold by Esso Chemicals, to dissolve the oil, followed by n-heptane to evaporate varsol. The probe is

photographed and then the deposit is mechanically removed and stored for further analysis. The apparatus was cleaned by circulating 9 liters of varsol for one hour. The probe was cleaned with varsol and n-heptane prior to each run.

The fouling probe operates at constant heat flux over time. Four thermocouples embedded within the wall measure the temperature at a single axial position shown in Figure 3.8. The thermocouples are embedded into the probe wall at a distance from the heater surface. This distance  $x_w$  is normally unknown and has to be determined through calibration, as shown by Asomaning [54]. The PFRU thermocouples measure the wall temperature  $T_w$  which is then corrected to give the metal surface temperature, and then averaged to give  $T_s$  [54]. Under constant heat flux the fluid/deposit interface is assumed to be constant at  $T_{s0}$ . The overall heat transfer coefficient can be calculated as follows:

Under clean conditions,

$$\frac{1}{U_0} = \frac{T_{s0} - T_b}{Q/A} \quad (3.1)$$

Under fouled conditions,

$$\frac{1}{U} = \frac{T_s - T_b}{Q/A} \quad (3.2)$$

where the power input  $Q=VI$ . The thermal fouling resistance, which is a function of time, is given by:

$$R_f = \frac{1}{U} - \frac{1}{U_0} \quad (3.3)$$

The thermal fouling resistance is related to the deposit thickness and the mass of deposit per unit surface as follows [101]:

$$R_f = \frac{x}{k_f} = \frac{m}{\rho_f k_f} \quad (3.4)$$

Where  $x$  is the deposit thickness,  $m$  is the mass of deposit per unit surface area ( $\text{kg/m}^2$ ),  $\rho_f$  is the density of the foulant and  $k_f$  is the thermal conductivity of the foulant.

The initial fouling rates were obtained by a fit of the linear section of the fouling resistance-time plots over the first few hours of a run:

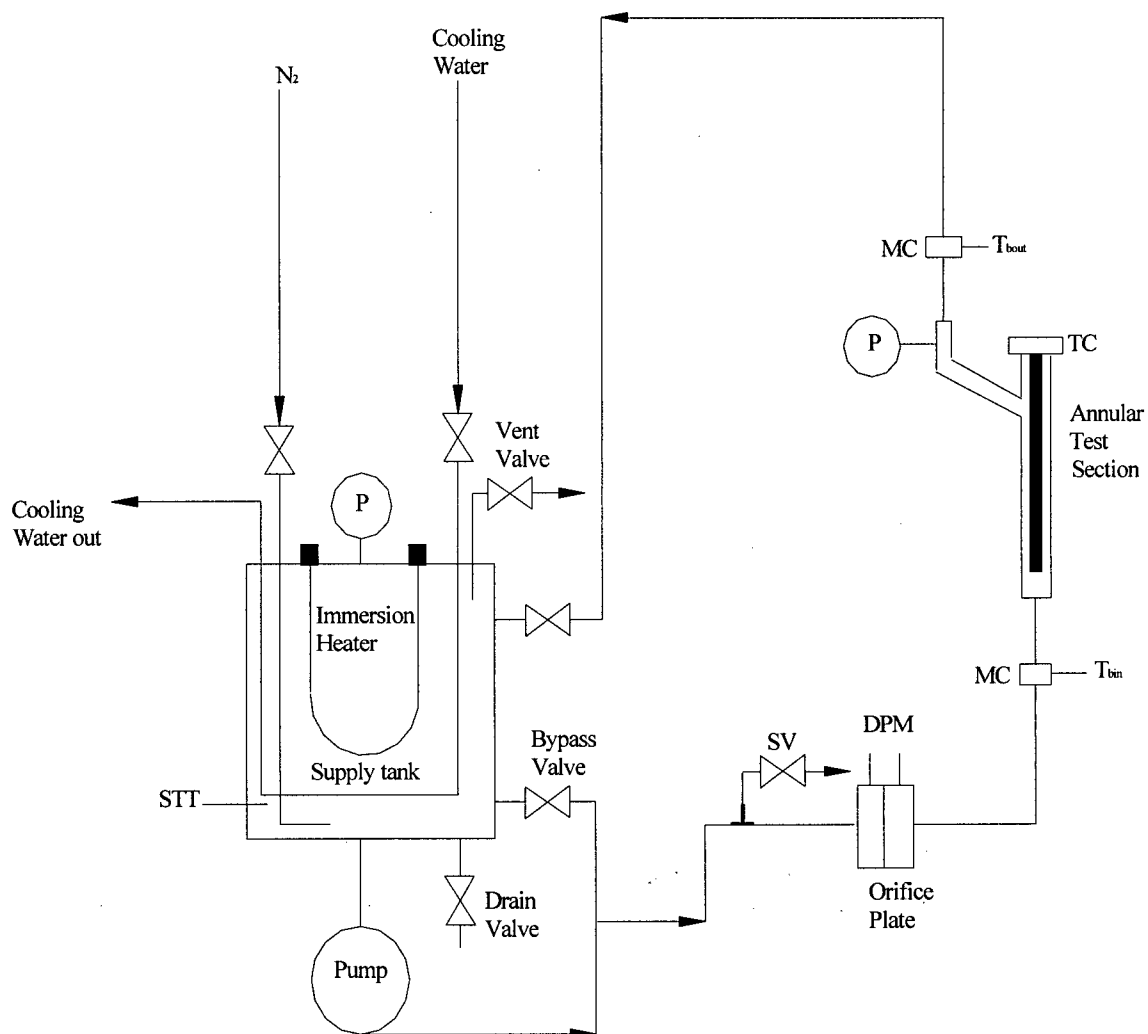
$$\frac{dR_f}{dt} = \frac{d}{dt} \left( \frac{1}{U(t)} \right) \quad (3.5)$$

In case where asymptotic fouling behavior is observed, the Kern-Seaton [101] asymptotic fouling resistance model can be used to fit the data and the initial fouling rate obtained as follows:

$$R_f = R_f^* (1 - \exp(-bt)) \quad (3.6)$$

where  $R_f^*$  is the asymptotic resistance. The initial fouling rate is given by

$$R_{f0}^* = \left. \frac{dR_f}{dt} \right|_{t=0} = b \times R_f^* \quad (3.7)$$



DPM- Differential Pressure Manometer

TC- PFRU Thermocouples SV- Sampling Valve

STT- Supply Tank Thermocouple 00000

MC- Mixing Chamber

$T_b$ - Bulk Temperature Thermocouples

P- Pressure Gauge

Figure 3.7 The UBC Fouling Test Apparatus

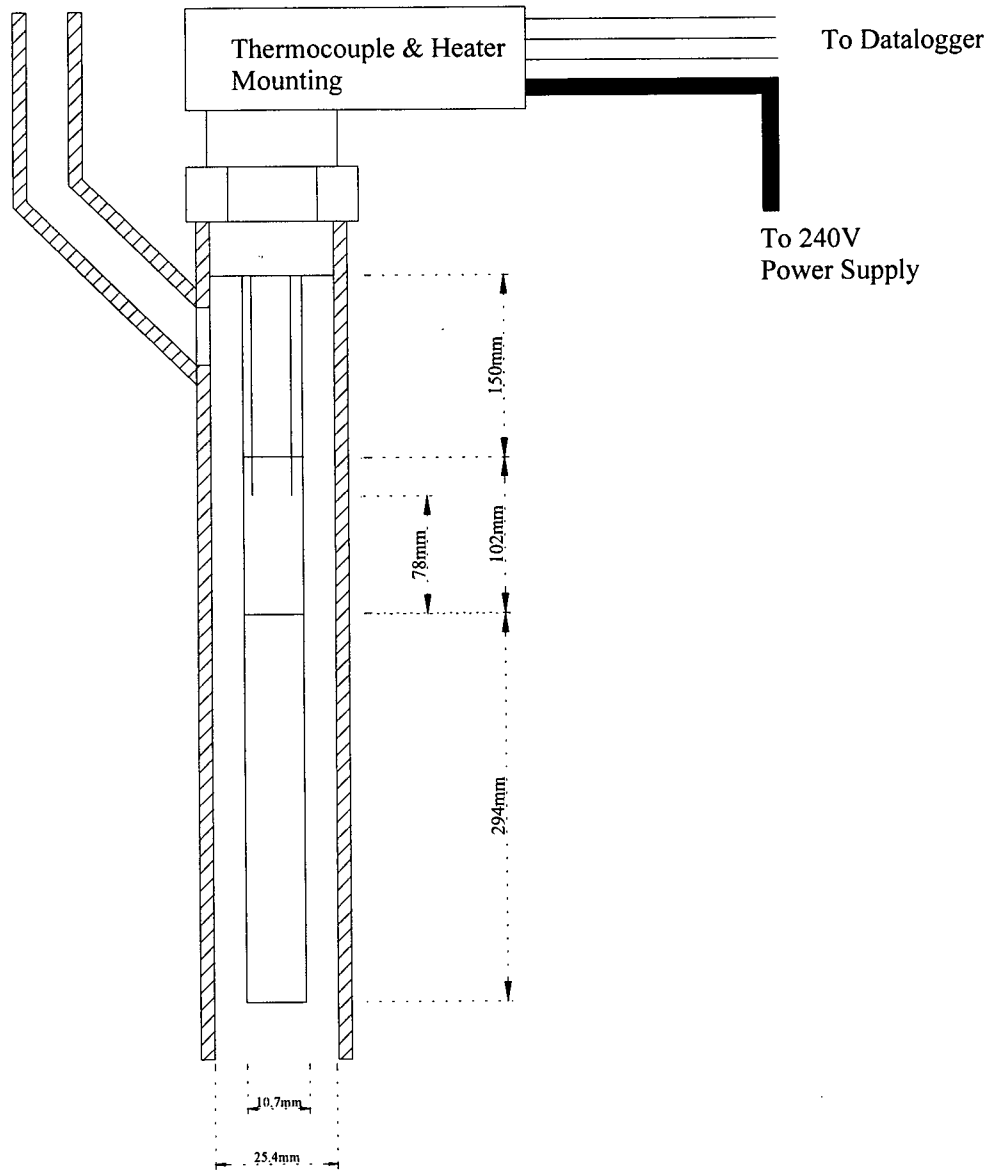


Figure 3.8 The Annular Test Section of the PFRU Fouling Probe (not to scale).

## 4. Hot Filtration Experimental Results and Modeling

### 4.1 Effect of Diluents Composition on the amount of Asphaltene Precipitation

Asphaltene precipitation can be a serious problem during oil production and processing. Considerable research has been directed to the issue of solubility of asphaltenes in petroleum liquids in order to avoid conditions for precipitation. The species in crude oils are mutually soluble as long as certain ratio of each kind are maintained in the mixture. Variations in temperature, pressure or composition (such as due to the addition of a diluent, or blending of different oils) alter this ratio. The heavy and/or polar molecules such as asphaltene may consequently separate from the mixture, leading to deposition problems. In this work, the effects of diluent composition on asphaltene precipitation from Cold Lake vacuum residue (VR) and Athabasca atmospheric tower bottoms (ATB) were determined using the hot filtration method at 60-85°C. The diluents include pure n-alkanes, a lube oil base stock-paraflex (PFX), a heavy vacuum gas oil (HVGO) and a resin-enriched fraction (REF) recovered from Cold Lake vacuum residue by supercritical fluid extraction and fractionation (SFEF). The latter three complex diluents were tested alone and in blends, in order to cover a range of saturates from 56 to 99.4 wt%, aromatics from 0.6 to 25 wt%, and resins from 0 to 19 wt%.

Figure 4.1 and Table 4.1, 4.2 show experimental results for the weight percent of Athabasca atmospheric tower bottoms (ATB) and Cold Lake vacuum residue (VR) precipitated, by three pure-component diluents (heptane, decane, dodecane) at various diluent-to-residue ratios,  $R$  (1.33-13.16) at 60°C. For both feedstocks the percentage of residue which precipitated,  $W$  decreases with the increase of carbon number or molecular mass of the diluents. As the diluent-to-residue ratio  $R$  is raised, the amount of precipitated asphaltene,  $W$ , increases sharply at first

and then levels off. Values of  $W$  were in the range of 0.88-9.26wt% for ATB and 3.62-17.32 wt% for VR. These data are consistent with results in the literature [9,12].

Figures 4.2, 4.3 and Table 4.3-4.6 show experimental results at 85°C for the weight percent of precipitated Athabasca atmospheric tower bottoms and Cold Lake vacuum residue, for the multi-component diluents - Paraflex HT 10 (PFX), heavy vacuum gas oil (HVGO), resin - enriched fraction (REF) and their blends. When ATB or VR respectively are mixed with PFX, a diluent which is over 99 wt% saturates, the amount of precipitated asphaltene first increases sharply with the increase of diluent-to-residue ratio  $R$ , and then levels off, similar to the behaviour with pure alkane diluents shown in Figure 4.1. But for diluents which are lower in saturates, such as the mixtures with HVGO (68 wt% saturates) or the blend of HVGO/PFX=1 (84 wt% saturates), the increases in percent precipitation of ATB (Figure 4.2a) or VR (Figure 4.3a) are modest or slight within the range of experiment. The addition of REF, which is rich in aromatics and resins, has a strong inhibition effect on the amount of asphaltene precipitated with both ATB (Figure 4.2b) and VR (Figure 4.3b). This inhibition effect is especially strong within the initial 0-10 wt% addition of REF, as shown in Figure 4.4.

Results in the above tables are the average values for duplicate experiments. Reproducibility is discussed in Appendix A2.

Table 4.1 Hot Filtration Experiment for ATB Using Pure Diluent (Heptane,Decane,Dodecane)\*

Test fluid	T (°C)	R (cm <sup>3</sup> /g)	W (wt%)
10%ATB+90%Heptane	60	13.16	9.26
20%ATB+80%Heptane	60	5.85	7.87
30%ATB+70%Heptane	60	3.41	4.78
40%ATB+60%Heptane	60	2.19	2.36
50%ATB+50%Heptane	60	1.46	1.04
10%ATB+90%Decane	60	12.33	8.46
20%ATB+80%Decane	60	5.48	7.38
30%ATB+70%Decane	60	3.2	4.26
40%ATB+60%Decane	60	2.05	2.12
50%ATB+50%Decane	60	1.37	0.98
10%ATB+90%Dodecane	60	11.98	7.96
20%ATB+80%Dodecane	60	5.33	6.89
30%ATB+70%Dodecane	60	3.11	3.98
40%ATB+60%Dodecane	60	2.0	1.96
50%ATB+50%Dodecane	60	1.33	0.88

\* ATB: Athabasca Atmospheric Tower Bottoms (Syncrude Canada Ltd.).

R: the ratio of the volume of the injected diluent to the weight of the feed oil, R (cm<sup>3</sup> diluent/g feed oil).

W: the weight percent of the feed which precipitated ((g asphaltene precipitate/g feed oil)×100%).

Table 4.2 Hot Filtration Experiment for VR Using Pure Diluent (Heptane, Decane, Dodecane)\*

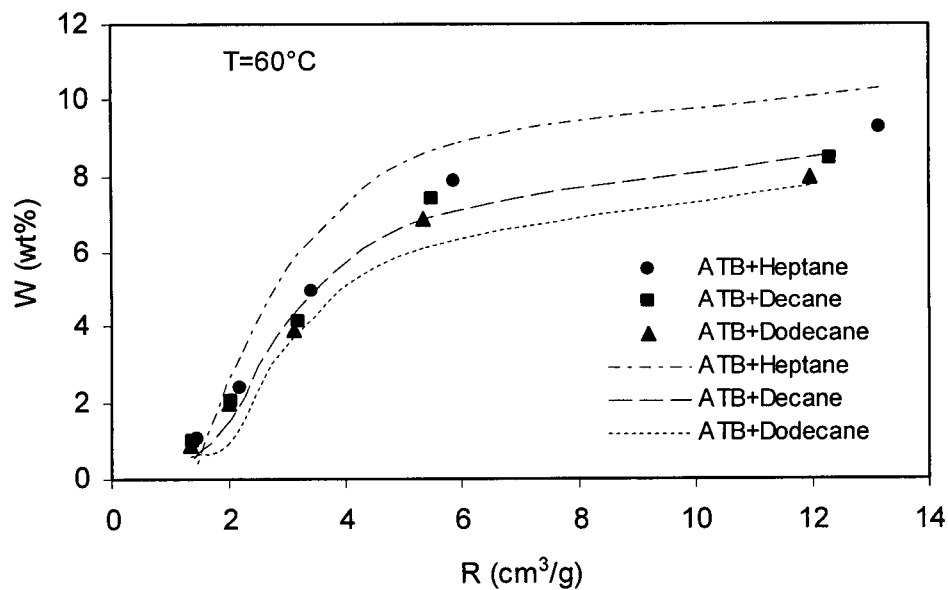
Test fluid	T (°C)	R (cm <sup>3</sup> /g)	W (wt%)
10%VR+90%Heptane	60	13.16	17.32
20%VR+80%Heptane	60	5.85	16.3
30%VR+70%Heptane	60	3.41	14.4
40%VR+60%Heptane	60	2.19	9.85
50%VR+50%Heptane	60	1.46	4.16
10%VR+90%Decane	60	12.33	16.18
20%VR+80%Decane	60	5.48	15.02
30%VR+70%Decane	60	3.2	12.68
40%VR+60%Decane	60	2.05	8.49
50%VR+50%Decane	60	1.37	3.93
10%VR+90%Dodecane	60	11.98	15.05
20%VR+80%Dodecane	60	5.33	14.21
30%VR+70%Dodecane	60	3.11	11.96
40%VR+60%Dodecane	60	2.0	7.32
50%VR+50%Dodecane	60	1.33	3.62

\* VR: Cold Lake Vacuum Residue (Imperial Oil Ltd.).

R: the ratio of the volume of the injected diluent to the weight of the feed oil, R (cm<sup>3</sup> diluent/g feed oil).

W: the weight percent of the feed which precipitated ((g asphaltene precipitate/g feed oil)×100%).

(a)



(b)

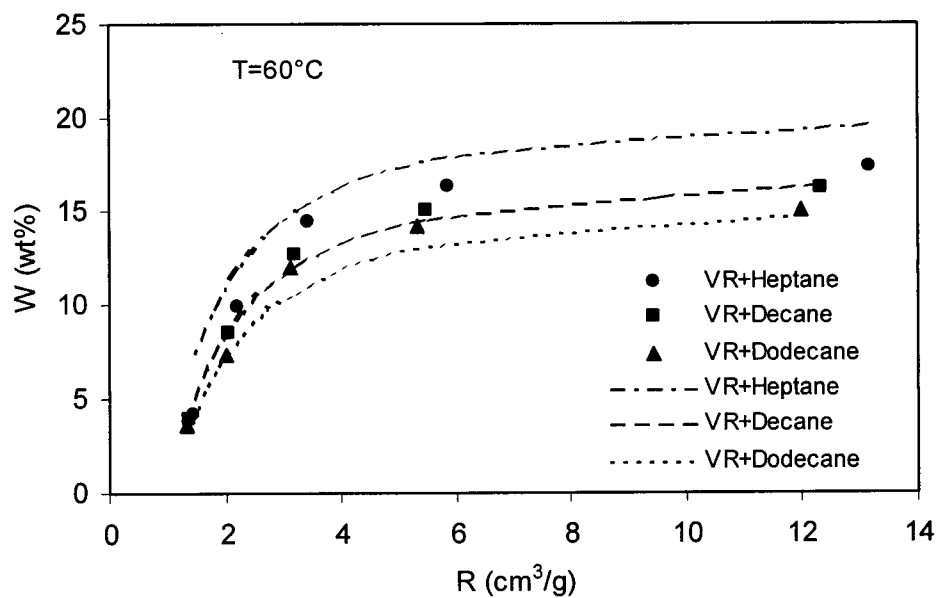


Figure 4.1 Weight Percent of Residue Precipitated  $W$  (wt%) (a) Athabasca Atmospheric Tower Bottoms (b) Cold Lake Vacuum Residue, as a Function of the Diluent to Residue Ratio  $R$  ( $\text{cm}^3/\text{g}$ ) for Pure Alkane Diluents.

Table 4.3 Hot Filtration Experiment Using ATB and Multi-Component Diluents \*

Test fluid	T (°C)	Re/As	CII	R (cm <sup>3</sup> /g)	W (wt%)
5%ATB+95%PFX	85	1.47	25.08	22.21	5.24
10%ATB+90%PFX	85	1.47	13.14	10.52	3.84
15%ATB+85%PFX	85	1.47	8.70	6.62	2.48
20%ATB+80%PFX	85	1.47	6.39	4.68	1.53
25%ATB+75%PFX	85	1.47	4.96	3.51	1.15
5%ATB+95%HVGO	85	23.73	2.0	21.88	0.88
10%ATB+90%HVGO	85	12.01	1.85	10.36	0.85
15%ATB+85%HVGO	85	8.11	1.72	6.52	0.79
20%ATB+80%HVGO	85	6.15	1.60	4.61	0.75
25%ATB+75%HVGO	85	4.98	1.49	3.45	0.72

\* ATB: Athabasca Atmospheric Tower Bottom (Syncrude Canada Ltd.).

HVGO: Heavy Vacuum Gas Oil (Imperial Oil Ltd.).

PFX: Paraflex HT 10 (Petro Canada Ltd.).

Table 4.4 Resin Effect on Hot Filtration Insolubles Adding REF to ATB blends \*

Test fluid	T (°C)	Re/As	CII	R (cm <sup>3</sup> /g)	W (wt%)
0%REF+5%ATB+95%PFX	85	1.47	25.08	22.21	5.24
5%REF +5%ATB+90%PFX	85	4.16	10.42	22.0	3.60
10%REF +5%ATB+85%PFX	85	6.84	6.31	21.79	2.84
15%REF +5%ATB+80%PFX	85	9.53	4.37	21.58	2.32
0%REF +10%ATB+90%PFX	85	1.47	13.14	10.52	3.84
5%REF +10%ATB+85%PFX	85	2.81	7.34	10.42	2.34
10%REF +10%ATB+80%PFX	85	4.16	4.91	10.31	1.78
15%REF +10%ATB+75%PFX	85	5.50	3.58	10.21	1.66
0%REF +15%ATB+85%PFX	85	1.47	8.70	6.62	2.48
5%REF +15%ATB+80%PFX	85	2.36	5.57	6.55	1.72
10%REF +15%ATB+75%PFX	85	3.26	3.96	6.48	1.48
15%REF +15%ATB+70%PFX	85	4.16	2.99	6.41	1.32

\* ATB: Athabasca Atmospheric Tower Bottoms (Syncrude Canada Ltd.).

REF: Resin Enriched Fraction (SFEF Experiment in China).

PFX: Paraflex HT 10 (Petro Canada Ltd.).

Table 4.5 Hot Filtration Experiment Using VR and Multi-Component Diluents \*

Test fluid	T (°C)	Re/As	CII	R (cm <sup>3</sup> /g)	W (wt%)
5%VR+95%PFX	85	1.84	23.18	22.21	7.56
10%VR+90%PFX	85	1.84	12.04	10.52	6.86
15%VR+85%PFX	85	1.84	7.92	6.62	5.72
20%VR+80%PFX	85	1.84	5.78	4.68	3.1
25%VR+75%PFX	85	1.84	4.47	3.51	1.82
30%VR+70%PFX	85	1.84	3.59	2.73	0.83
5%VR+95%HVGO	85	18.82	1.92	21.88	1.23
10%VR+90%HVGO	85	9.89	1.81	10.36	1.16
15%VR+85%HVGO	85	6.91	1.66	6.52	0.88
20%VR+80%HVGO	85	5.42	1.52	4.61	0.75
25%VR+75%HVGO	85	4.52	1.40	3.45	0.66
30%VR+70%HVGO	85	3.93	1.30	2.69	0.56
5%VR+47.5%HVGO+47.5%PFX	85	10.33	4.29	22.05	3.14
10%VR+45%HVGO+45%PFX	85	5.86	3.62	10.44	2.43
15%VR+42.5%HVGO+42.5%PFX	85	4.37	3.10	6.57	1.66
20%VR+40%HVGO+40%PFX	85	3.63	2.68	4.64	1.27
25%VR+37.5%HVGO+37.5%PFX	85	3.18	2.34	3.48	0.84

\* VR: Cold Lake Vacuum Residue (Imperial Oil Ltd.).

HVGO: Heavy Vacuum Gas Oil (Imperial Oil Ltd.).

PFX: Paraflex HT 10 (Petro Canada Ltd.).

Table 4.6 Resin Effect on Hot Filtration Insolubles Adding REF into VR blends \*

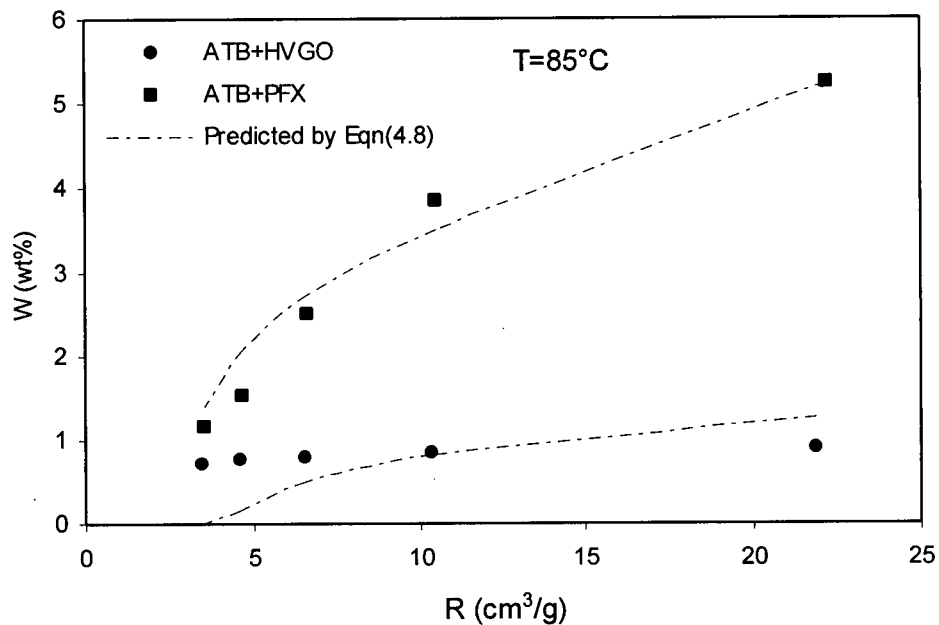
Test fluid	T (°C)	Re/As	CII	R (cm <sup>3</sup> /g)	W (wt%)
0%REF +10%VR+90%PFX	85	1.84	12.04	10.52	6.86
5%REF+10%VR+85%PFX	85	2.87	6.94	10.42	3.61
10%REF+10%VR+80%PFX	85	3.89	4.71	10.31	2.18
15%REF+10%VR+75%PFX	85	4.92	3.46	10.21	1.95
0%REF+15%VR+85%PFX	85	1.84	7.92	6.62	5.72
5%REF+15%VR+80%PFX	85	2.53	5.20	6.55	2.79
10%REF+15%VR+75%PFX	85	3.21	3.75	6.48	1.68
15%REF+15%VR+70%PFX	85	3.89	2.85	6.41	1.59
0%REF+20%VR+80%PFX	85	1.84	5.78	4.68	3.1
5%REF+20%VR+75%PFX	85	2.35	4.09	4.62	1.89
10%REF+20%VR+70%PFX	85	2.87	3.26	4.57	1.29
15%REF+20%VR+65%PFX	85	3.38	2.39	4.52	1.16

\* VR: Cold Lake Vacuum Residue (Imperial Oil Company).

REF: Resin Enriched Fraction (SFEEF Experiment in China).

PFX: Paraflex HT 10 (Petro Canada Ltd.)

(a)



(b)

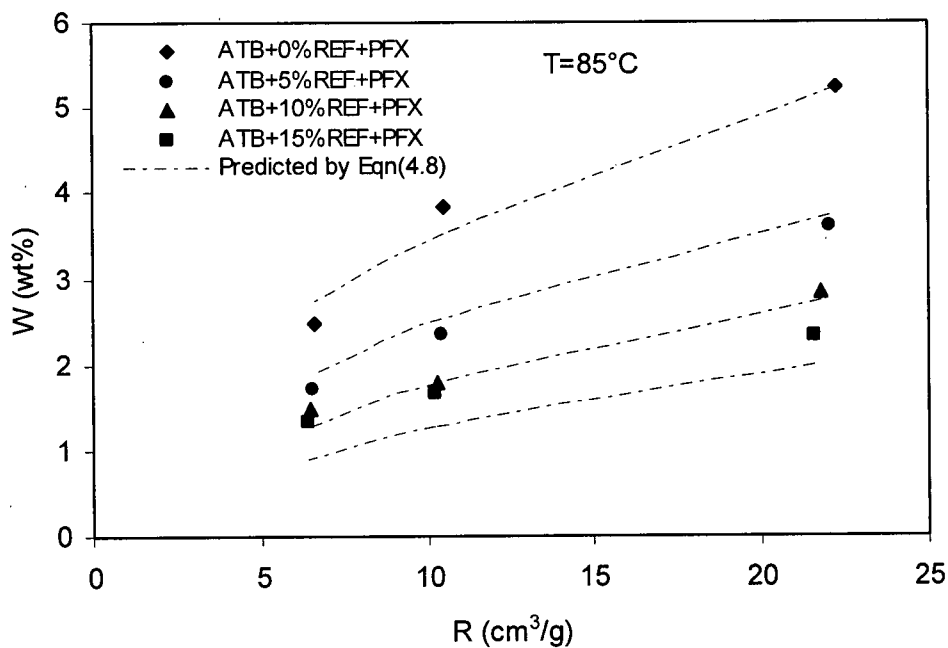
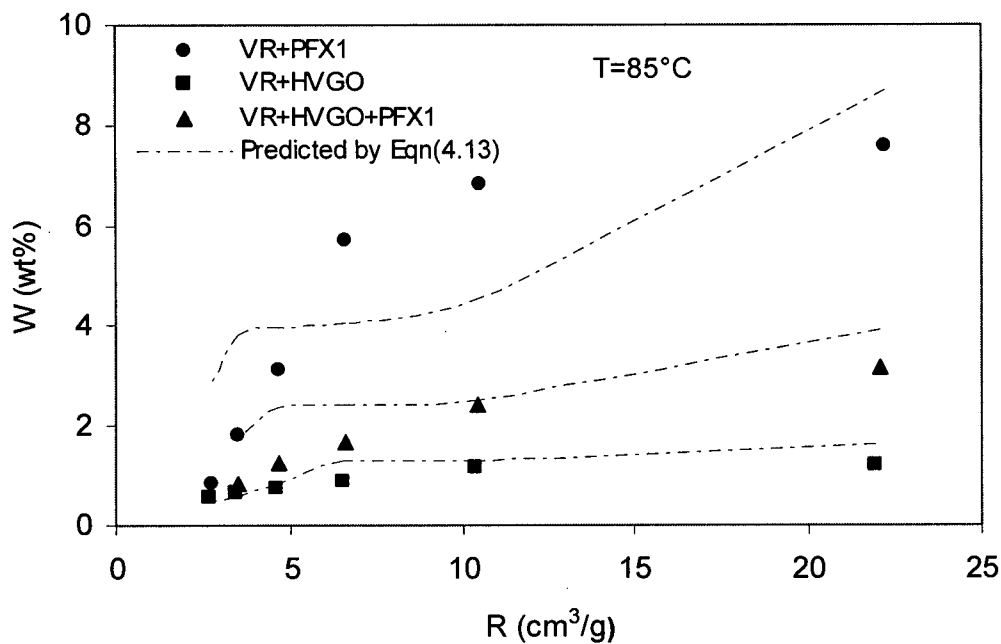


Figure 4.2 Weight Percent of Athabasca Atmospheric Tower Bottoms Precipitated  $W$  (wt%), as a Function of the Diluent to Residue Ratio  $R$  ( $\text{cm}^3/\text{g}$ ) for (a) PFX-HVGO Diluents, and (b) PFX-REF Diluents.

(a)



(b)

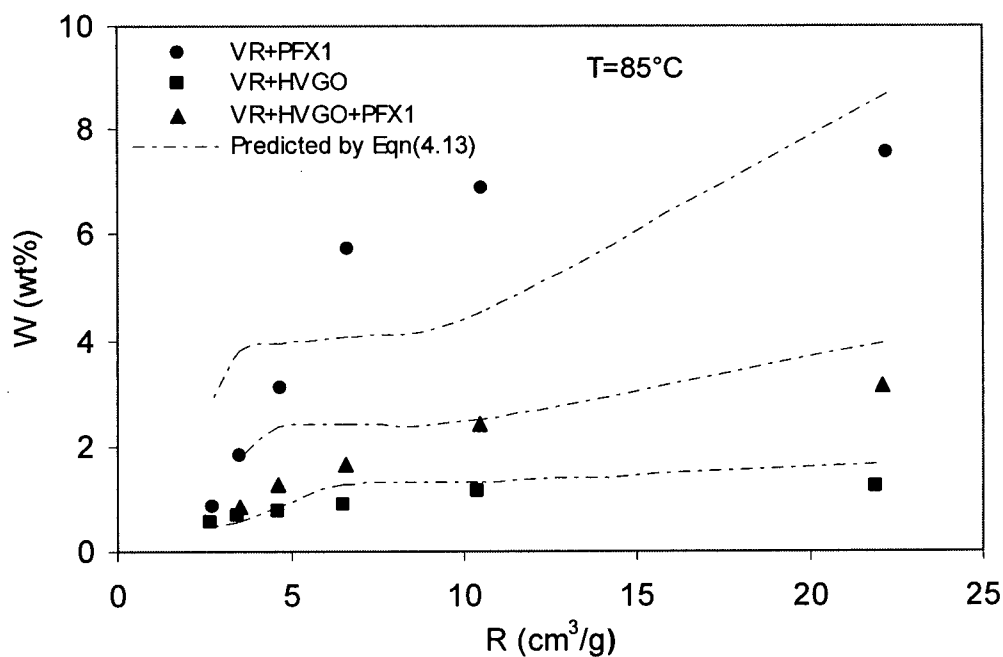


Figure 4.3 Weight Percent of Cold Lake Vacuum Residue Precipitated  $W$  (wt%), as a Function of the Diluent to Residue Ratio  $R$  ( $\text{cm}^3/\text{g}$ ) for (a) PFX and HVGO and PFX/HVGO Diluents, and (b) PFX/REF Diluents.

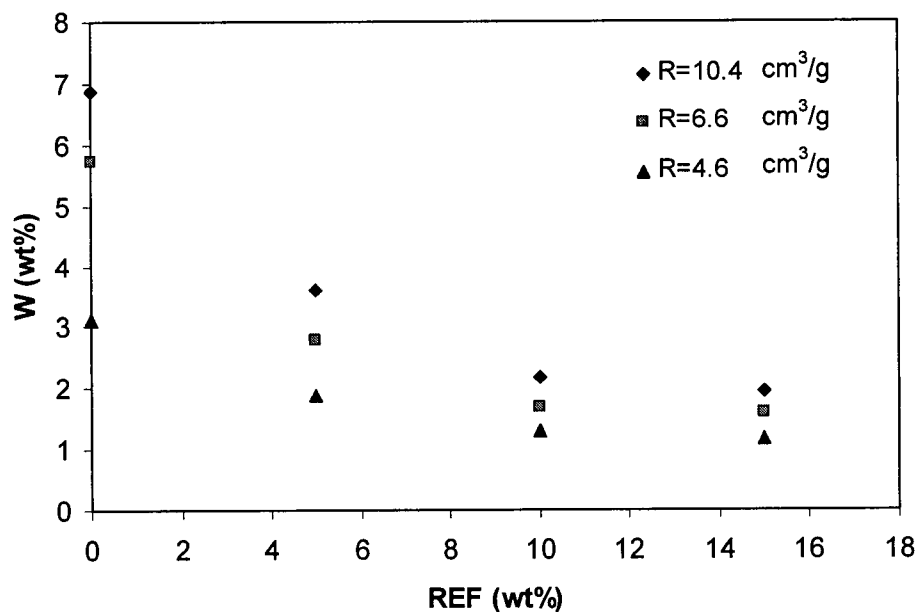


Figure 4.4 Inhibition Effect of REF on Asphaltene Precipitation

## 4.2 Scaling Equation

### 4.2.1 Prediction of the Amount and Onset of Asphaltene Precipitation Using Scaling Equations [12]

The scaling equations proposed by Rassamdana et al. [12] are applied in this work for the prediction of asphaltene precipitation amount. Rassamdana et al. [12] suggested that asphaltene precipitation was similar to aggregation and gelation phenomena [102], which possess universal properties, independent of many microscopic properties of their structure. In particular, the structural and physical properties of aggregates obey universal scaling equations [103, 104]. According to Rassamdana et al. [12], the experimental results of asphaltene precipitation were amenable to description by a scaling equation, since all the curves start at about the same point, and at large values of  $R$  they become more or less parallel, as shown in Figures 4.1-4.3. As a result, the data would collapse onto a single curve. Two important aggregation processes--

diffusion-limited particle (DLP) [105] and diffusion-limited cluster-cluster (DLCC) [106] aggregation were reviewed by Meakin [103]. A brief summary of these processes that are directly related to asphaltene precipitation was proposed by Rassamdana et al. [107]. Figure 4.5 shows various stages of formation of a 2-D DLCC aggregate.

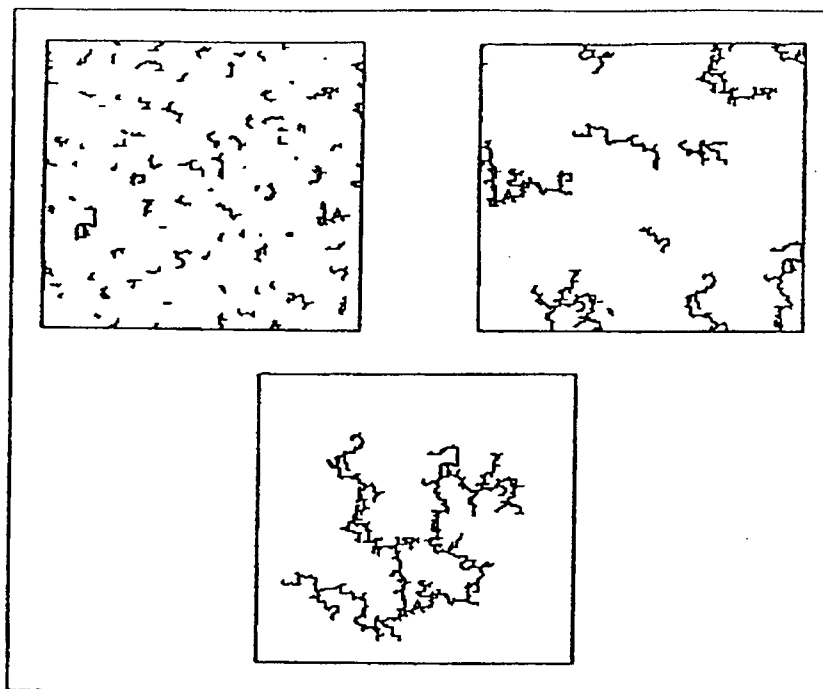


Figure 4.5 Various stages of formation of a 2-D diffusion-limited cluster-cluster aggregate [107].

An important property of the DLCC aggregates is their cluster-size distribution. Suppose that  $s$  is the cluster size and  $n_s(t)$  is the number of clusters of size  $s$  at time  $t$  (cluster size distribution). Then,  $n_s = s^{-\tau} f(s/\langle s \rangle)$ , where  $\tau$  is a universal exponent, and  $\langle s \rangle$  is the mean cluster (aggregate) size. Here  $f(x)$  is a universal scaling function. For the DLCC aggregates  $\tau=2$ . Obviously, the mean cluster size increases with the time  $t$ , and therefore  $\langle s \rangle \sim t^w$ . Where  $w$  is a dynamical exponent that may depend on  $\zeta$ , the exponent that relates the diffusivity of the

clusters to their molecular weight. Therefore, for DLCC process,  $s^2 n_s(t) = f(s/t^w)$ . This implies that the universal scaling function  $f(x)$  can be expressed only in terms of  $s^2 n_s(t)$ .

Rassamdana et al. [107] proposed that the formation of asphalt and asphaltene aggregates obeys the DLCC aggregation model based on the results of small-angle scattering data in the literature. Therefore, the original form of the scaling equation [12] as applied to asphaltene precipitation involves three variables (corresponding to the three variables  $n_s(t)$ ,  $s$  and  $t$  in the DLCC process) —  $W$ , the weight percent of the feed which precipitated, ((g asphaltene/g feed oil)×100%);  $R$ , the ratio of the volume of the injected diluent to the weight of the feed oil, ( $\text{cm}^3$  diluent/g feed oil) , and  $M$ , the molecular mass of the diluent. The three variables were combined into two variables ( $X, Y$ ) as follows:

$$X = R / M^Z \quad (4.1)$$

$$Y = W / R^{Z'} \quad (4.2)$$

where  $Z$  and  $Z'$  are constants. It has been shown [12,89,108] that  $Z'$  is a universal constant ( $Z'=-2$ ) and does not depend on the solvent or the oil type, while  $Z$  depends on the composition of the oil and its value is generally within the range of  $0.10 \leq Z \leq 0.50$ . Whence for asphaltene precipitation,  $R^2 W = f(R/M^Z)$ . As stated by Rassamdana et al. [107], the scaling functions  $s^2 n_s(t) = f(s/t^w)$  and  $R^2 W = f(R/M^Z)$  are not the same. The roles of  $s$  and  $n_s(t)$  in the dynamic cluster-size distribution are played by  $R$  and  $W(t)$ , respectively. It is not unreasonable to infer that the size of the asphaltene aggregates may be proportional to the ratio  $R$ , and indeed, as Figures 4.1-4.3 indicate, with increasing  $R$  the amount of precipitation, and thus the size of the aggregates, do increase. As a rough estimate,  $W(t)$  is also proportional to  $n_s(t)$ , the number of clusters or aggregates of size  $s$  at time  $t$  for all  $s \geq s_{min}$ . Here  $s_{min}$  is the minimum cluster size for precipitation, since only when a cluster is large enough, can it precipitate; otherwise it will

remain suspended in the solution. The analogy between these two scaling functions also implies that the role of the mean cluster size  $\langle s \rangle \sim t^w$  in the dynamic cluster-size distribution, is played by  $M^Z$  in the scaling equation for the precipitation data. That is, the mean size of the asphaltene aggregates is proportional to the molecular weight  $M$  of the solvent, raised to some power  $Z$ . As mentioned previously, the exponent  $w$  depends on  $\zeta$ , the exponent that relates the diffusivity of an aggregate to its molecular weight. They also conclude that the exponent  $Z$ , the analog of  $w$ , may also be nonuniversal and presumably depend on the type of solvent and/or asphaltene-containing oil, whereas the exponent  $Z' = -2$  is universal and does not depend on the solvent or the oil type. This universality is the result of mass conservation in the system, which also results in DLCC model scaling function with  $\tau=2$ .

The scaling equation can be represented in terms of  $X$  and  $Y$  by a third-order polynomial function [12], which is valid for  $X \geq X_c$  where  $X_c$  is the value of  $X$  at the onset of asphaltene precipitation:

$$Y = A_1 + A_2X + A_3X^2 + A_4X^3 \quad (4.3)$$

It can be seen from Equations (4.1)-(4.3) that the properties of asphaltene (which are difficult to measure) are not involved in the scaling equation.

In this work,  $Z'$  was taken as  $-2$ , and the exponent  $Z$  was adjusted to get the best fits and predictions of the experimental data. Hu et al. [89] studied the effect of  $Z$  value on the accuracy of the scaling equation and conclude that an increase of  $Z$  from 0.25 to 0.50 has little effect. In this work,  $Z$  values ranging from 0.1-0.8 in steps of 0.01 were investigated. The value of  $Z=1/4$  (0.25) was obtained by the optimum fits and predictions for the experimental data (using Equation (4.4)), following Rassamdana et al. [12]. As shown in Figure 4.6 and Equations (4.5)

and (4.6), the original form of scaling equation gives a satisfactory fit to the data for the pure alkane diluents (heptane, decane and dodecane) with both ATB and VR feedstocks.

$$\sigma = \frac{1}{n} \sum_{i=1}^n \left| \left( Y_i^{Exp} - Y_i^{Cal} \right) / Y_i^{Exp} \right| \quad (4.4)$$

where  $Y^{Exp}$  and  $Y^{Cal}$  stand for the rescaled experimental data and the corresponding calculated  $Y$  respectively.

Some other types of function, such as linear, quadratic polynomial, exponential and logarithmic functions were also tested in this work. The third order polynomial proposed by Rassamdana et al. [12] was found to give the best fit of the experimental data in this work.

For ATB at ( $X \geq X_c$ ),

$$Y = 9.8573 - 87.081X + 139.78X^2 - 3.9074X^3 \quad (4.5)$$

where  $X_c=0.4838$ ;  $r^2=0.9987$ . The absolute and relative derivations are 22.53 for the calculated  $Y$  (corresponding to 0.69wt% or 1.77 g/L) and 29.46% respectively.

For VR at ( $X \geq X_c$ ),

$$Y = 4.801 - 80.082X + 225.52X^2 - 2.3887X^3 \quad (4.6)$$

where  $X_c=0.2799$ ;  $r^2=0.9992$ . The average absolute and relative deviations for the calculated  $Y$  (corresponding to 1.03wt% or 2.57g/L) are 41.47 and 12.37% respectively.

The critical value of  $R$  for the onset of precipitation,  $R_c = X_c M^{1/4}$ , is higher for the ATB which had a lower asphaltene content than for the VR. A similar result was found in a flocculation titration (Section 5.1), which indicated that the Heithaus  $P$  value [56] was higher for ATB than for VR. Using Equations (4.2), (4.5) and (4.6), the weight percent of the feed which precipitated,  $W$ , can be calculated and then plotted versus  $R$ , the ratio of the volume of the injected diluent to the weight of the feed oil. The results are shown as the curves in Figure

4.1, where the data predictions in terms of W and R are reasonably good for n-decane and n-dodecane, but for heptane the predicted amount of asphaltene precipitation is significantly higher than the experiment results for both ATB and VR.

With the multi-component diluents (PFX, HVGO, REF and their blends), two additional variables (the saturates content, Sa, and the density in g/cm<sup>3</sup> at 20°C,  $\rho_{D,20}$ ) were combined with the variable X in the scaling equation through the following relation:

$$X' = X * \left( \frac{Sa}{\rho_{D,20}} \right)^{1.5} \quad (4.7)$$

These properties were chosen because of the earlier noted effect of diluent density and the fact that saturates are the precipitants or non-solvents for the asphaltenes. The value of the exponent was determined by the best fit of the experimental data. This modified scaling equation provides good agreement with the data over a wide range of diluents to feed ratios, as shown in Figure 4.6 and in Equations (4.8) and Equation (4.9).

For ATB

$$Y = -4.7858 - 17.663X' + 32.718X'^2 + 4.2079X'^3 \quad (4.8)$$

where  $X'_c = 0.6904$ ;  $r^2 = 0.9956$ . The average absolute and relative deviations for the calculated Y (corresponding to 0.26wt% or 0.33g/L) are 31.22 and 19.43% respectively.

For VR,

$$Y = -72.534 + 162.07X' - 55.808X'^2 + 17.283X'^3 \quad (4.9)$$

where  $X'_c = 0.5278$ ;  $r^2 = 0.9940$ . The average absolute and relative deviations for the calculated Y (corresponding to 0.73wt% or 1.11g/L) are 49.74 and 54.45% respectively.

These modified equations also fitted the data for pure alkanes as diluents, but less well than Equations (4.5) and (4.6). Using Equations (4.2) and (4.8), the predicted values of W for ATB with different complex diluents was determined and then plotted versus R in Figure 4.2. It is

shown that the predicted values were in reasonably good agreement with the raw data for ATB with all the three complex diluents (PFX, HVGO and REF) used individually or in blends. However the data for ATB+HVGO (Figure 4.2 a) showed that ATB might contain sufficient inorganics (clays) that we always get about 0.5wt% insolubles, hence Figure 4.2a with HVGO is nearly flat.

Since the properties of the feed oils (the source of asphaltenes) are not involved in the original scaling equation, it is not feasible to use it directly for correlating asphaltene precipitation from different feedstocks. A number of variables (such as asphaltene concentration ( $C_{As}$ ), the ratio of resin and asphaltene ( $Re/As$ ), colloidal instability index, C.I.I., etc.) were tested to extend the scaling equation to describe asphaltene precipitation from the two different feed oils, and the colloidal instability index, C.I.I. [109] of the feed oil (VR or ATB) was found to provide the best correlation. It was added into the variable Y in the scaling equation by means of the following relation, found by fitting the data:

$$Y' = Y * (CII)^2 \quad (4.10)$$

$$CII = \frac{\text{saturates} + \text{asphaltenes}}{\text{aromatics} + \text{resins}} \quad (4.11)$$

As shown in Figure 4.8 and Equations (4.12) and (4.13), the new scaling equations correlate the experimental data from the two different feed oils (VR and ATB) well for both pure alkane and complex diluents.

For alkane diluents at 60°C:

$$Y' = 0.5594 - 15.809X + 36.167X^2 - 0.4791X^3 \quad (4.12)$$

where  $X_c=0.4006$ ;  $r^2=0.9962$ .

For multi-component diluents at 85°C:

$$Y' = -12.006 + 22.634X' - 6.6665X'^2 + 2.851X'^3 \quad (4.13)$$

where  $X'_c = 0.6118$ ;  $r^2 = 0.9694$ .

The diluents in Figure 4.6 cover a range of saturates from 56 to 99.4 wt%, aromatics from 0.6 to 25 wt%, and resins from 0 to 19 wt%; density from 0.8554 to 0.8946 g/cm<sup>3</sup>; and molecular mass from 285 to 408. Using Equations (4.2) and (4.13), the predicted W for the mixtures of VR with various complex diluents was calculated, as shown by the curves in Figure 4.3. For those cases of VR with HVGO, HVGO/PFX=1 and the blends of PFX with REF as diluents, the predicted values were reasonably close, but did not agree as well as those for ATB. For the mixtures of VR with PFX, agreement of some of the fitted data was poor (especially at the middle two values of R). The large deviations which resulted when re-casting the equation into the form of the raw data, indicates that fitting of the general scaling equation (Equation (4.13)) to these data points could be improved.

#### 4.2.2 Application to Deposition Studies

As indicated above in Figures 4.6-4.8, the scaling equation from the asphaltene precipitation literature [12,89,108] is usually plotted as Y vs X. For deposition and thermal fouling studies, the concentration of suspended asphaltenes rather than the fraction of oil precipitated is of greater importance. For example, it has been shown [13], that the rate of asphaltene thermal fouling from unstable oil blends at a given bulk temperature, velocity and heat flow is affected strongly by the concentration of suspended asphaltene solids. The percentage, W, can be converted to the suspended asphaltene concentration in the mixture, using the following equation:

$$C_{as} = 10Wm_F / (m_F / \rho_F + m_D / \rho_D) \quad \text{g/L} \quad (4.14)$$

where  $W$  is given in Equations (4.2) and (4.3),  $m_F$ ,  $m_D$ , are the masses of the feed oil and diluent respectively, and  $\rho_F$ ,  $\rho_D$  are their corresponding densities ( $20^\circ\text{C}$ ,  $\text{g/cm}^3$ ). Hence using Equations (4.2), (4.3) and (4.14) one can calculate all the suspended asphaltene concentration values for the single or multi-component diluents. In the asphaltene precipitation research literature, a full range of extent of precipitation is of interest. For industrial operations, processing of oils with high concentrations of suspended asphaltenes is generally problematic, whereas low concentrations might be tolerated. Precipitation results for the subsets of experimental data with  $X' \leq 2.0$  (Figure 4.9), for the mixtures of VR and ATB with multi-component diluents were re-fitted to Equation (4.15).

$$Y' = -13.467 + 47.845X' - 47.409X'^2 + 18.001X'^3 \quad (2.0 \geq X' \geq X'_c) \quad (4.15)$$

$$X'_c = 0.4436, \quad r^2 = 0.9369$$

Here suspended asphaltene concentrations were below about 5 g/L. Figure 4.10 shows the concentration results. The average absolute and relative derivations are 0.3g/L and 20.8% respectively. These results are satisfactory for industrial or engineering application.

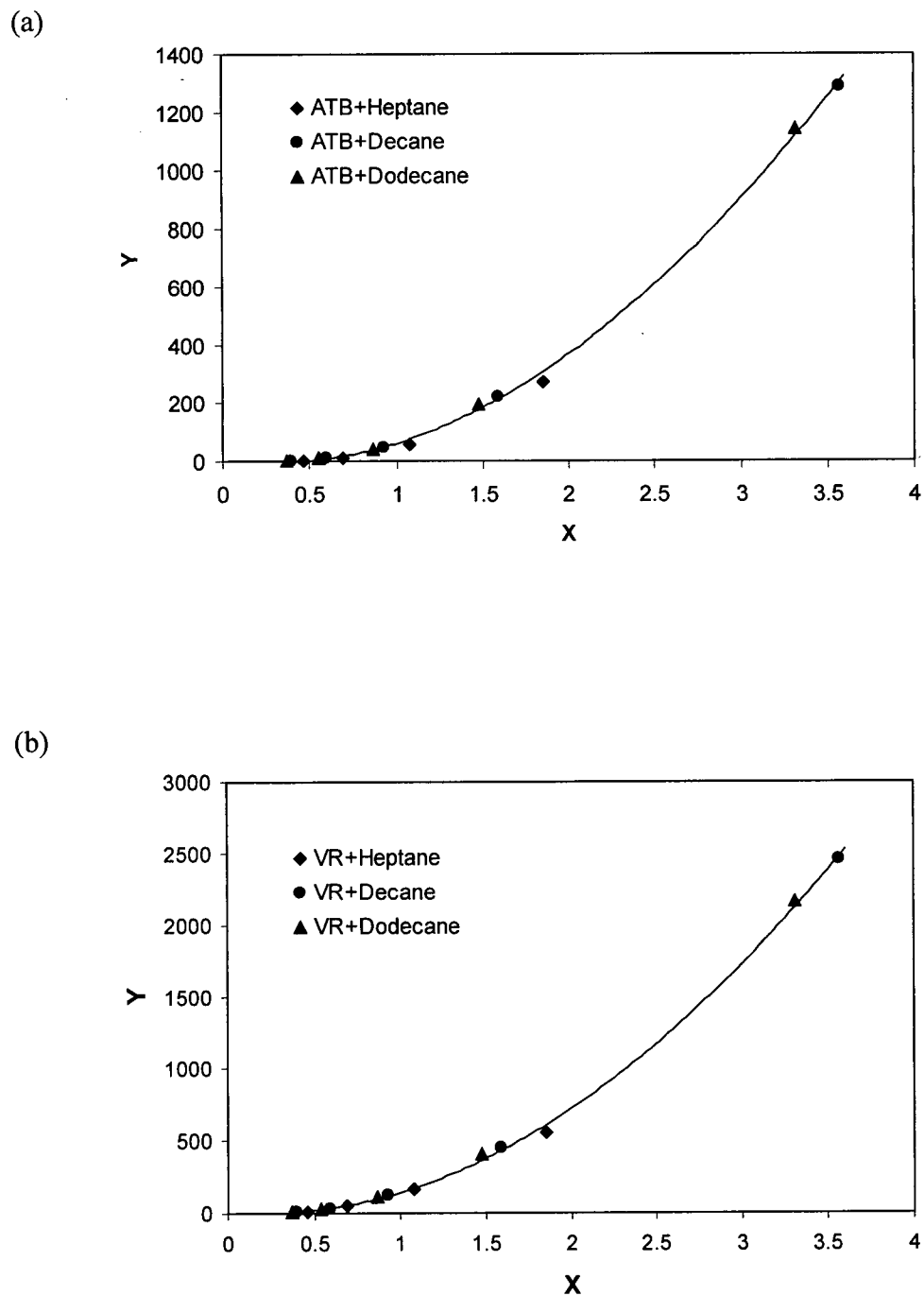
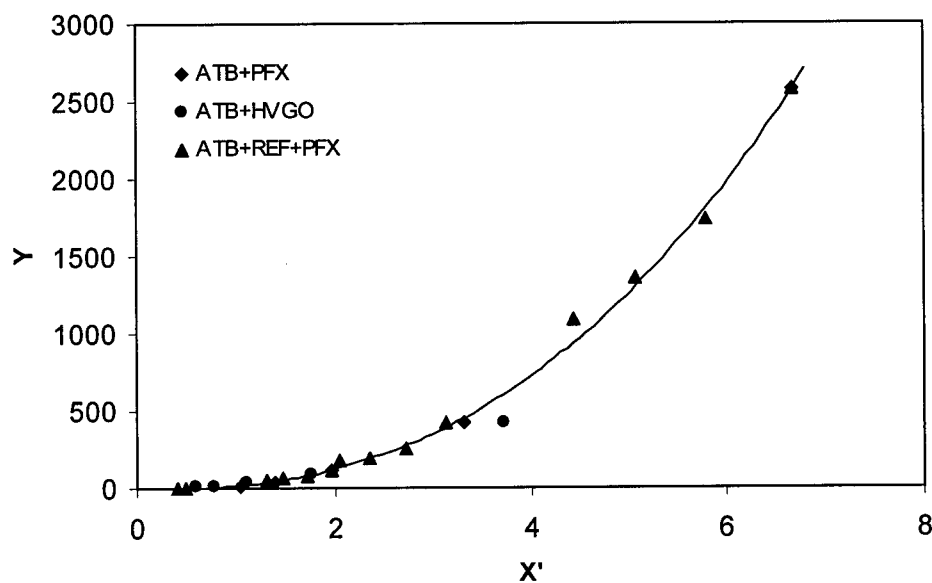


Figure 4.6 Scaling Equation with  $X=R/M^{1/4}$  and  $Y=WR^2$  for (a) Athabasca Atmospheric Tower Bottoms (Equation (4.5)), and (b) Cold Lake Vacuum Residue (Equation (4.6)).

(a)



(b)

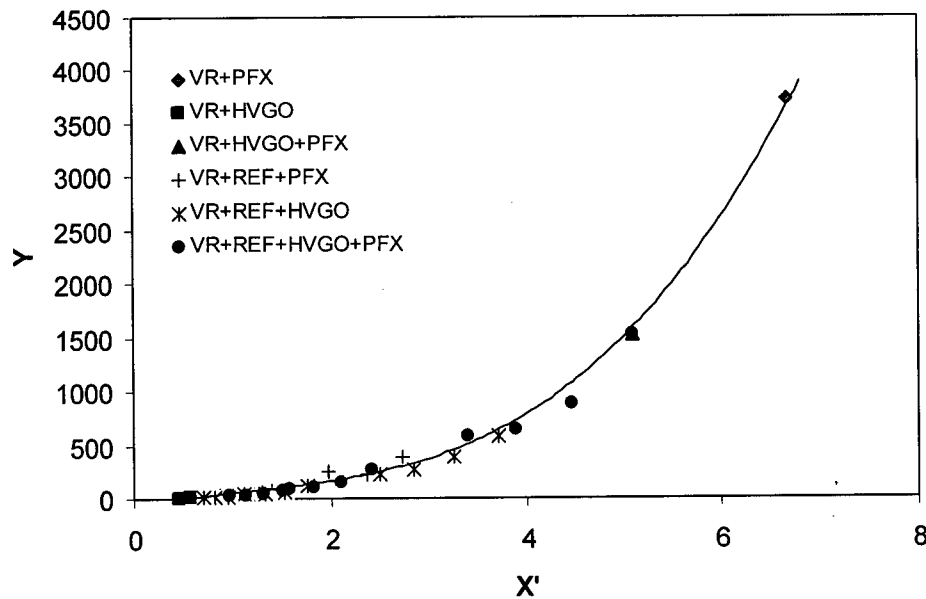
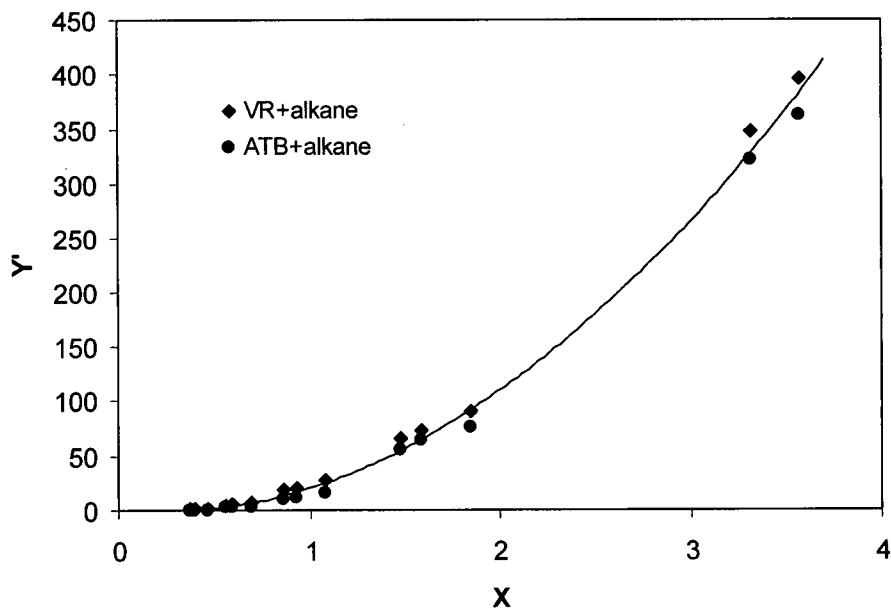


Figure 4.7 Scaling Equation with  $X'=X*(S_a/\rho_{D,20})^{1.5}$  ( $X=R/M^{1/4}$ ) and  $Y=WR^2$  for (a) Athabasca Atmospheric Tower Bottoms (Equation (4.8)), and (b) Cold Lake Vacuum Residue (Equation (4.9)).

(a)



(b)

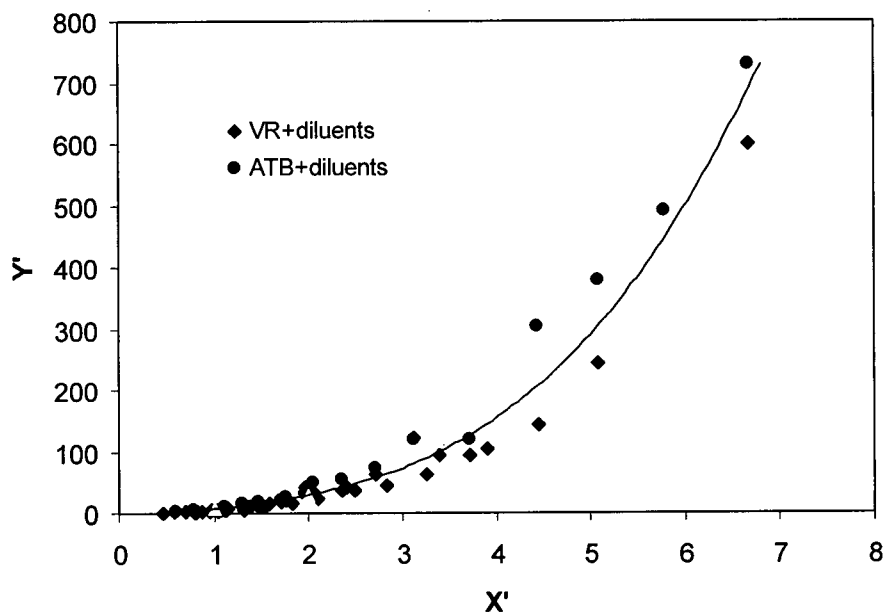


Figure 4.8 Scaling Equation with  $X=R/M^{1/4}$ ,  $X'=X*(Sa/\rho_{D,20})^{1.5}$  and  $Y'=Y*(CII)^2$  ( $Y=WR^2$ ) for both Athabasca Atmospheric Tower Bottoms and Cold Lake Vacuum Residue with (a) n-Alkanes Diluents (Equation (4.12)), and (b) Multi-Component Diluents (Equation (4.13)).

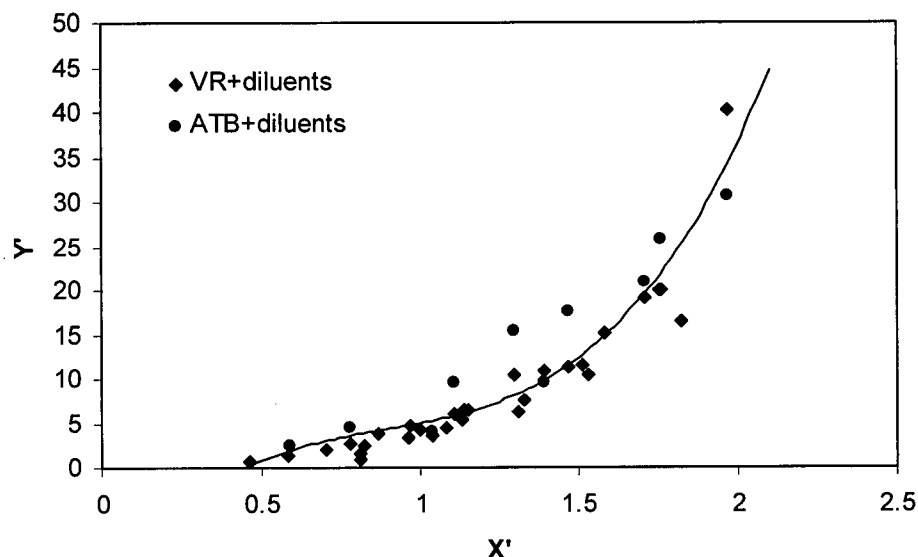


Figure 4.9 Scaling Equation with  $X' = X * (S_a / \rho_{D,20})^{1.5}$  ( $X = R / M^{1/4}$ ),  $Y' = Y * (CII)^2$  ( $Y = WR^2$ ), ( $2.0 \geq X' \geq X_c'$ ) for Cold Lake Vacuum Residue and Athabasca Atmospheric Tower Bottoms with Multi-Component Diluents (Equation (4.15)).

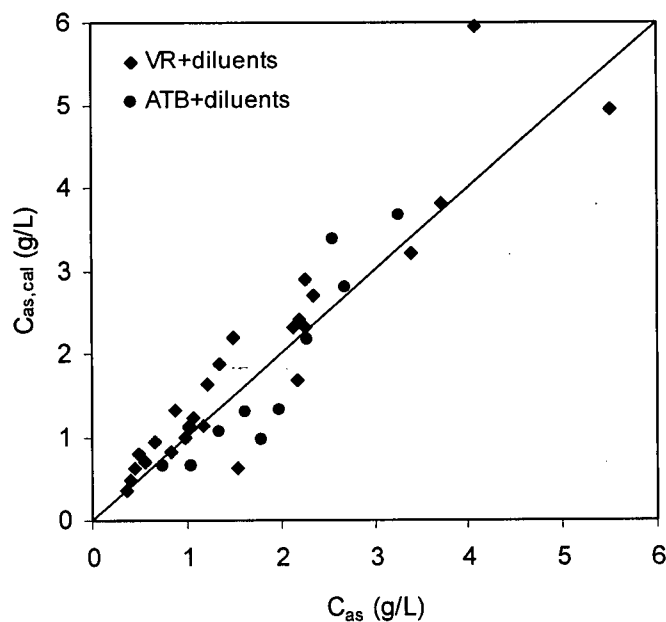


Figure 4.10 The Calculated Concentration of Precipitated Asphaltene  $C_{as,cal}$  (g/L) Using Equation (4.14) Versus the Measured Value  $C_{as}$  (g/L) for the Mixture of Cold Lake Vacuum Residue and Athabasca Atmospheric Tower Bottoms with Multi-Component Diluents.

### 4.3 The Effect of Temperature on Asphaltene Solubility and Precipitation

There are conflicting views in the literature on the effect of temperature on asphaltene solubility [4,46-50]. Some results show that a higher temperature will generate more asphaltene precipitation [110], while some other results indicate an opposite temperature effect [111,112]. Andersen [45] has discussed this controversy in the temperature effect. Most of the work on the effect of temperature on asphaltene solubility and precipitation has been done below 200°C, while the main inconsistent observations have been reported around 200°C [4,46,50]. Therefore, the effect of temperature on asphaltene solubility and precipitation in the present mixtures was investigated for selected mixtures over the range of 60-300°C (333-573 K), as shown in Table 4.7 and Figure 4.11. The results indicate that the dissolved asphaltene concentration (or suspended asphaltene concentration) from these mixtures increased (or decreased) monotonically with temperature over the range of the experiment, in agreement with the conclusion of Wiehe [18]. The temperature effect is not large for Cold Lake vacuum residue, where significant variation with temperature occurs only below 160°C (433K).

Table 4.7 Temperature Effect on Asphaltene Solubility and Precipitation \*

Test fluid	T (K)	Weight percent of asphaltene precipitated W (wt%)	Suspended asphaltene concentration $C_{as,p}$ (g/L)	Dissolved asphaltene concentration $C_{as,d}$ (g/L)
10wt%ATB +45wt%HVGO +45wt%PFX	333	1.65	1.44	10.02
	358	1.51	1.32	10.14
	393	1.35	1.18	10.28
	433	1.16	1.02	10.45
	473	0.98	0.86	10.61
	513	0.86	0.75	10.71
	553	0.80	0.70	10.76
10wt%VR +45wt%HVGO +45wt%PFX	333	3.39	2.97	12.58
	358	2.97	2.60	12.94
	393	2.46	2.16	13.39
	433	2.12	1.86	13.69
	473	1.83	1.60	13.94
	513	1.67	1.46	14.08
	553	1.52	1.33	14.22
	573	1.46	1.28	14.27

\* ATB: Athabasca Atmospheric Tower Bottoms (Syncrude Canada Ltd.).

VR: Cold Lake Vacuum Residue (Imperial Oil Ltd.).

HVGO: Heavy Vacuum Gas Oil (Imperial Oil Ltd.).

PFX: Paraflex HT 10 (Petro Canada Ltd.).

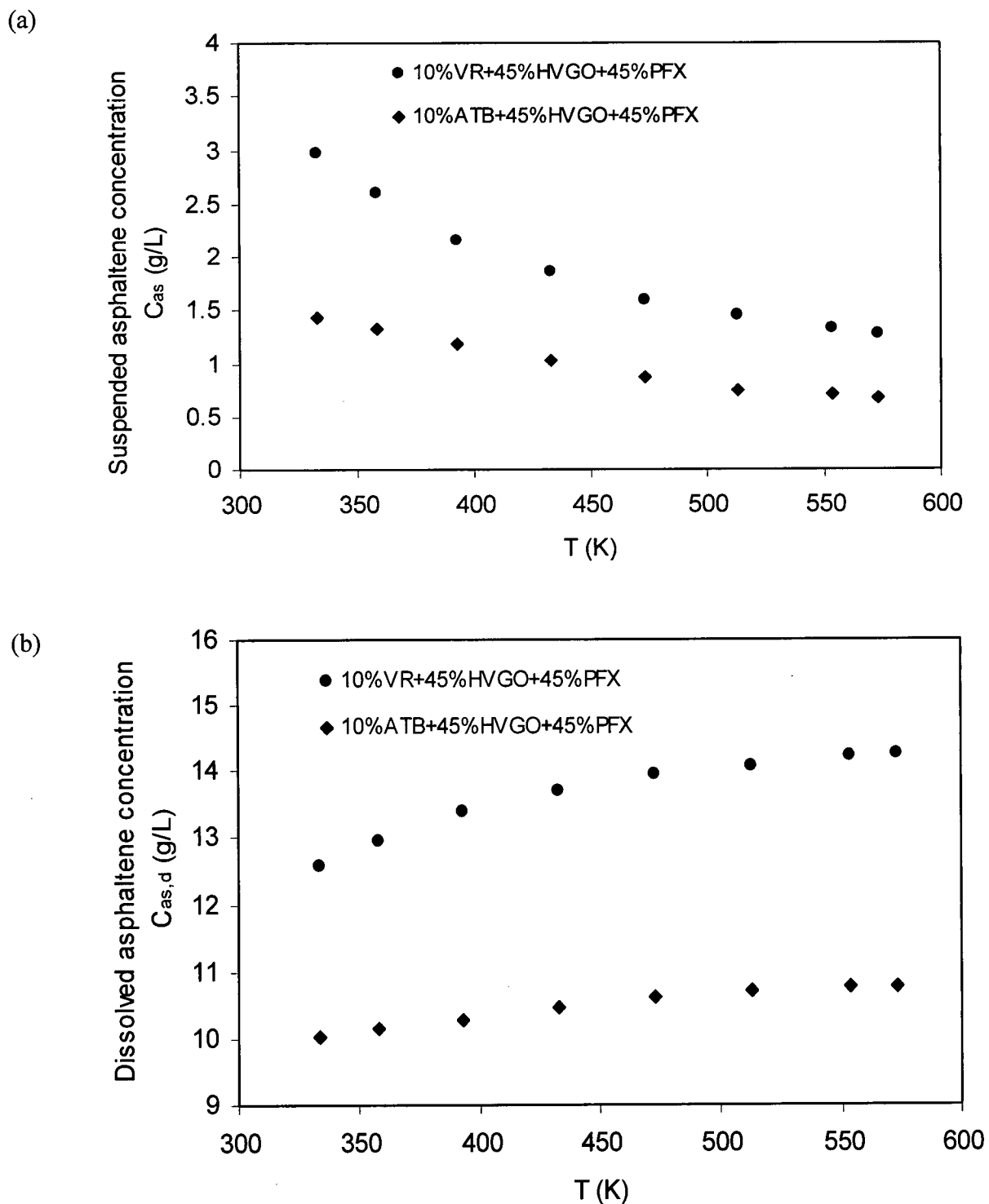


Figure 4.11 Temperature effect on (a) Asphaltene Precipitation, (b) Asphaltene Solubility.

## 5. Flocculation Titration Experimental Results and Modeling

### 5.1 Effect of Different Diluents on Asphaltene Precipitation Onset

As stated previously, the precipitation of asphaltene in petroleum fluids can cause serious operating problems. For this reason, prevention or minimization of asphaltene precipitation is a major goal for many oil corporations. Under laboratory conditions, the asphaltene precipitation tendency is usually measured using titration techniques. The incipient precipitation or flocculation onset is usually caused by adding n-heptane or n-pentane to the sample. Flocculation onset measurements have usually been employed to determine the stability of crude oils at ambient conditions [113] and also evaluate the effectiveness of commercial inhibitors of asphaltene precipitation [114-116]. Sheu and Storm [117] and Rogacheva et al. [118] discussed the effect of aromatic solvents on asphaltenes. Gonzalez and Middea [119], Chang and Fogler [120,121] and De Boer [122] studied the effect of adding surfactants on the inhibition of asphaltene precipitation. The effect of any additive on the stabilization of asphaltenes in the crude oil and the inhibition of precipitation relies mainly on direct attractive interaction between the molecules of the additive and the asphaltene. The adsorption of the resin or amphiphile on the asphaltene core and the acid-base interaction is the main reason for asphaltene stabilization [120]. Chang and Fogler [121] used infrared spectroscopy to characterize and quantify the acid-base interactions between asphaltene and amphiphiles. Pan and Firoozabadi [123] presented a thermodynamic micellization model to describe the asphaltene precipitation inhibition mechanism for both aromatic solvents and oil-soluble amphiphiles. Taher A.Al-Sahhaf et al. [8] investigated the inhibition effect on asphaltene precipitation by addition of toluene, resins, deasphalted oil and surfactants. They found that toluene and deasphalted oil are not effective asphaltene precipitation inhibitors. While the addition of resin has a pronounced effect on asphaltene stabilization. Resin molecules have

polar groups, hence there was a marked improvement of their inhibition effect in comparison to non polar solvents like toluene.

In this work, the effects of different diluents on asphaltene precipitation onset were investigated by conducting a series of flocculation titration experiments in which blends of the asphaltenes-containing residues with diluents and toluene were titrated with normal alkanes. The automated flocculation titrimeter (AFT) developed by Pauli [57] was used with two titrants (iso-octane, n-heptane) to get the flocculation points, i.e. the volume of titrant added to cause flocculation. In addition to the experimental materials in this work (Chapter 3), the feed stocks used previously for thermal fouling studies [54,78]--Cold Lake Heavy Oil (HO) and De-asphalted Oil (DAO) supplied by Imperial Oil Canada Ltd., Fuel oil (FO) provided by Burnaby refinery of Chevron Canada Ltd. were also tested. The properties of these additional materials are shown in Tables 5.1, 5.2 and 5.3.

The titration results are shown in Tables 5.4-5.6, and Figures 5.1-5.4. As the mass fraction of the diluents is increased in the mixture to be titrated, the asphaltene concentration decreases. The inhibiting effect of the highly aromatic diluents Toluene, REF and DAO on precipitation are obvious from the increases in onset point. This inhibition effect increases with the increase of the mass fraction of diluents, and becomes most appreciable where their mass fraction in the mixtures exceed 30wt%. The inhibition effect is not solely due to aromatics content, since REF, which is high in resins content (36 wt% resins, 63 wt% aromatics) gives more inhibition than does toluene. The reason that REF is more effective than toluene is that the latter contains no polar groups, and the effectiveness of any inhibitor is determined by the acid-base interaction which causes adsorption of the inhibitor on the surface of the asphaltene molecules. DAO has a slightly higher inhibition power than toluene since this oil contains natural resins. There is also a considerable amount of saturates in DAO, which lower its inhibition effect. The HVGO has

enough resins plus aromatics, while containing considerable (68 wt%) amounts of saturates, to inhibit flocculation slightly. Two of the diluents (PFX and FO), which are both high in saturates and low in resins promote asphaltene precipitation by a slight degree. In other words, the onset point ratio decreases slightly with the increase of the mass fraction of these diluents. Both the inhibition effect and the promotion effect discussed above occur in all three of the asphaltic feedstocks (ATB, VR and HO).

In each onset calculation, three different concentrations were used, an in addition one concentration was duplicated. The repeatability of the titrations is discussed in Appendix A2.

Table 5.1 Properties of Cold Lake Heavy Oil [78]

Test Description	Value
<b>SARA Analysis (HPLC)</b>	
Saturates (wt.%)	21.94
1 Ring Aromatics (wt.%)	12.4
2 Ring Aromatics (wt.%)	14.4
3 Ring Aromatics (wt.%)	8.9
4 Ring Aromatics (wt.%)	18.4
Aromatics (total wt.%)	54.1
Resins (wt.%)	8.4
Asphaltenes (wt.%)	15.6
<b>SARA Analysis (ASTM D2007M)</b>	
Saturates (wt.%)	24.37
Aromatics (wt.%)	45.58
Resins (wt.%)	12.39
Asphaltenes (wt.%)	17.66
<b>Average SARA Analysis</b>	
Saturates (wt.%)	23.1
Aromatics (wt.%)	49.8
Resins (wt.%)	10.4
Asphaltenes (wt.%)	16.6
<b>Elemental Analysis</b>	
Carbon (wt.%)	84.14
Hydrogen (wt.%)	10.52
Nitrogen (wt.%)	0.41
Sulfur (wt.%)	4.51
H/C atomic ratio	1.57
Specific Gravity (@ 15°C)	1.038
API Gravity	10.1
Kinematic Viscosity (@ 80°C, m <sup>2</sup> /s)	4.25E-3
350°C ~ 525°C	23.75%
525°C <sup>+</sup>	76.25%

Table 5.2 Properties of De-asphalted Oil [78]

Test Description	Value
<b>SARA Analysis (HPLC)</b>	
Saturates (wt.%)	20.48
1 Ring Aromatics (wt.%)	12.9
2 Ring Aromatics (wt.%)	17.5
3 Ring Aromatics (wt.%)	15.8
4 Ring Aromatics (wt.%)	22.4
Aromatics (total wt.%)	68.6
Resins (wt.%)	10.1
Asphaltenes (wt.%)	0.8
<b>SARA Analysis (ASTM D2007M)</b>	
Saturates (wt.%)	20.93
Aromatics (wt.%)	68.3
Resins (wt.%)	10.05
Asphaltenes (wt.%)	0.72
<b>Average SARA Analysis</b>	
Saturates (wt.%)	20.7
Aromatics (wt.%)	68.5
Resins (wt.%)	10.0
Asphaltenes (wt.%)	0.8
<b>Elemental Analysis</b>	
Carbon (wt.%)	86.71
Hydrogen (wt.%)	11.15
Nitrogen (wt.%)	0.28
Sulfur (wt.%)	3.54
H/C atomic ratio	1.58

Table 5.3 Properties of Fuel Oil [78]

Test Description	Value
<b>SARA Analysis (HPLC)</b>	
Saturates (wt.%)	70.88
1 Ring Aromatics (wt.%)	12.4
2 Ring Aromatics (wt.%)	7.2
3 Ring Aromatics (wt.%)	3.7
4 Ring Aromatics (wt.%)	2.2
Aromatics (total wt.%)	25.5
Resins (wt.%)	3.7
Asphaltenes (wt.%)	Trace
<b>SARA Analysis (ASTM D2007M)</b>	
Saturates (wt.%)	68.34
Aromatics (wt.%)	29.92
Resins (wt.%)	1.74
Asphaltenes (wt.%)	Trace
<b>Average SARA Analysis</b>	
Saturates (wt.%)	69.6
Aromatics (wt.%)	27.7
Resins (wt.%)	2.7
Asphaltenes (wt.%)	Trace
<b>Elemental Analysis</b>	
Carbon (wt.%)	86.41
Hydrogen (wt.%)	12.76
Nitrogen (wt.%)	0.21
Sulfur (wt.%)	0.56
H/C atomic ratio	1.77
Density (@25°C,kg/m <sup>3</sup> )	851
Kinematic Viscosity (@ 80°C,m <sup>2</sup> /s)	2.15E-6

Table 5.4 The Effect of Diluents on Asphaltene Precipitation Onset at 25°C, (Iso-octane as Titrant)\*

Composition of mixtures	Asphaltene precipitation onset, ml iso-octane/g Sample oil
0.5gATB+2.0gToluene	2.04
0.5gATB+2.0gToluene+1.0gToluene	2.75
0.5gATB+2.0gToluene+2.0gToluene	3.57
0.5gATB+2.0gToluene+3.0gToluene	4.30
0.5gATB+2.0gToluene+5.0gToluene	5.83
0.5gATB+2.0gToluene+0.5gREF	2.79
0.5gATB+2.0gToluene+1.0gREF	3.56
0.5gATB+2.0gToluene+2.0gREF	5.19
0.5gATB+2.0gToluene+3.0gREF	6.72
0.5gATB+2.0gToluene+0.5HVGO	2.26
0.5gATB+2.0gToluene+1.0gHVGO	2.35
0.5gATB+2.0gToluene+2.0gHVGO	2.71
0.5gATB+2.0gToluene+3.0gHVGO	2.97
0.5gATB+2.0gToluene+5.0gHVGO	3.54
0.5gATB+2.0gToluene+0.5PFX	2.02
0.5gATB+2.0gToluene+1.0gPFX	2.01
0.5gATB+2.0gToluene+2.0gPFX	1.94
0.5gATB+2.0gToluene+3.0gPFX	1.72
0.5gATB+2.0gToluene+5.0gPFX	1.50
0.5gVR+2.0gToluene	1.87

0.5gVR+2.0gToluene+1.0gToluene	2.63
0.5gVR+2.0gToluene+2.0gToluene	3.37
0.5gVR+2.0gToluene+3.0gToluene	4.08
0.5gVR+2.0gToluene+5.0gToluene	5.35
0.5gVR+2.0gToluene+0.5gREF	2.66
0.5gVR+2.0gToluene+1.0gREF	3.30
0.5gVR+2.0gToluene+2.0gREF	4.67
0.5gVR+2.0gToluene+3.0gREF	5.67
0.5gVR+2.0gToluene+0.5HVGO	2.03
0.5gVR+2.0gToluene+1.0gHVGO	2.24
0.5gVR+2.0gToluene+2.0gHVGO	2.40
0.5gVR+2.0gToluene+3.0gHVGO	2.53
0.5gVR+2.0gToluene+5.0gHVGO	2.79
0.5gVR+2.0gToluene+0.5PFX	1.92
0.5gVR+2.0gToluene+1.0gPFX	1.87
0.5gVR+2.0gToluene+2.0gPFX	1.62
0.5gVR+2.0gToluene+3.0gPFX	1.33
0.5gVR+2.0gToluene+5.0gPFX	1.02

\*: Sample oil: 0.5g ATB (or VR) + 2.0g Toluene

ATB: Athabasca Atmospheric tower bottom (Syncrude Canada Ltd.)

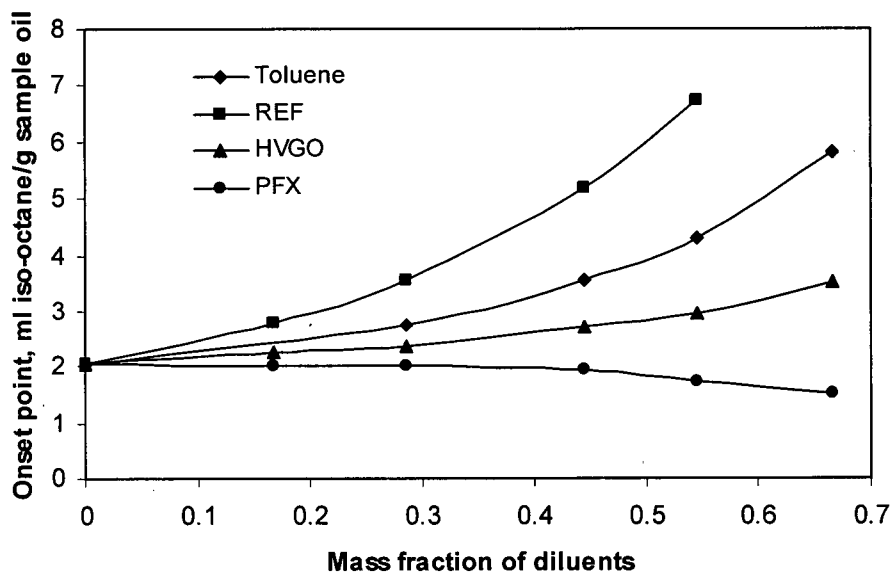
VR: Cold Lake vacuum residue (Imperial Oil Ltd.)

PFX: Paraflex HT 10 (Petro Canada Ltd.)

HVGO: Heavy vacuum gas oil (Imperial Oil Ltd.)

REF: Resin enriched fraction (SFEEF Experiment in China)

(a)



(b)

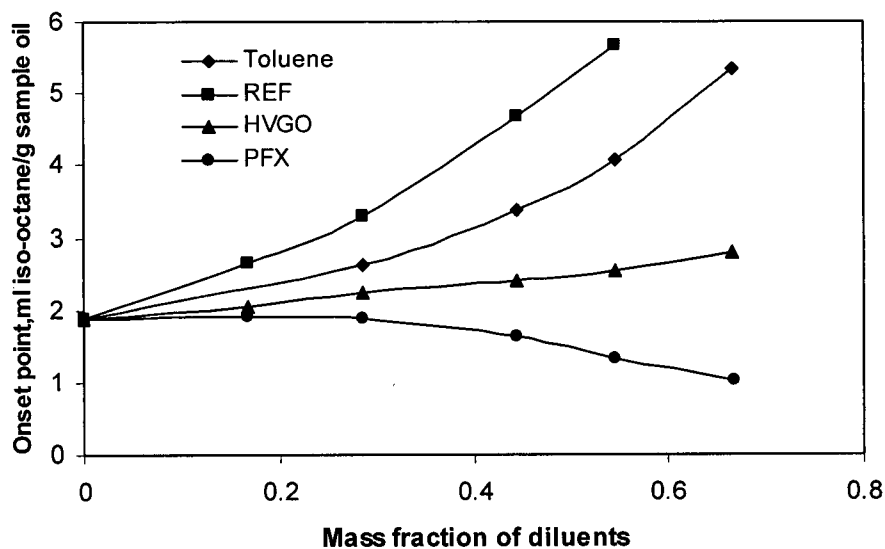


Figure 5.1 The Effect of Diluents on Asphaltene Precipitation Onset at 25°C, (Iso-octane as Titrant) (a) Athabasca Atmospheric Tower Bottom as Source of Asphaltene, (b) Cold Lake Vacuum Residue as Source of Asphaltene.

Table 5.5 The Effect of Diluents on Asphaltene Precipitation Onset at 25°C (Iso-octane as Titrant)\*

Composition of mixtures	Asphaltene precipitation onset, ml iso-octane/g Sample oil
0.5gHO+3.0mlToluene	1.17
0.5gHO+3.0mlToluene+0.5gToluene	1.28
0.5gHO+3.0mlToluene+1.0gToluene	1.53
0.5gHO+3.0mlToluene+2.0gToluene	1.86
0.5gHO+3.0mlToluene+0.5gDAO	1.35
0.5gHO+3.0mlToluene+1.0gDAO	1.53
0.5gHO+3.0mlToluene+2.0gDAO	1.86
0.5gHO+3.0mlToluene+0.5gFO	1.17
0.5gHO+3.0mlToluene+1.0gFO	1.15
0.5gHO+3.0mlToluene+2.0gFO	1.02

\*: Sample oil: 0.5gHO (ATB or VR) + 3.0ml Toluene

HO: Cold Lake heavy oil (Imperial OilLtd.)

FO: Fuel Oil (Imperial Oil Ltd.)

DAO: De-asphalted Oil (Imperial Oil Ltd.)

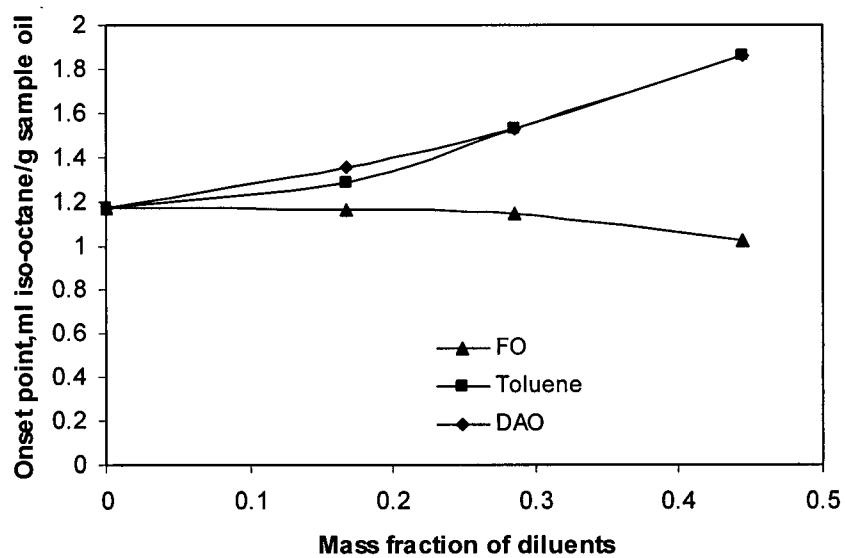


Figure 5.2 The Effect of Diluents on Asphaltene Precipitation Onset at 25°C, (Iso-octane as Titrant, Cold Lake Heavy Oil as Source of Asphaltene).

Table 5.6 The Effect of Diluents on Asphaltene Precipitation Onset at 25°C (n-Heptane as Titrant)\*

Composition of mixtures	Asphaltene precipitation onset, ml heptane/g Sample oil
0.5gATB+3mlToluene	2.45
0.5gATB+3.0mlToluene+1.0gToluene	3.30
0.5gATB+3.0mlToluene+2.0gToluene	4.05
0.5gATB+3.0mlToluene+3.0gToluene	4.63
0.5gATB+3.0mlToluene+0.5gREF	3.52
0.5gATB+3.0mlToluene+1.0gREF	4.30
0.5gATB+3.0mlToluene+2.0gREF	5.96
0.5gATB+3.0mlToluene+1.0gHVGO	2.68
0.5gATB+3.0mlToluene+2.0gHVGO	2.99
0.5gATB+3.0mlToluene+3.0gHVGO	3.26
0.5gATB+3.0mlToluene+1.0gPFX	2.44
0.5gATB+3.0mlToluene+2.0gPFX	2.25
0.5gATB+3.0mlToluene+3.0gPFX	2.08
0.5gVR+3.0ml Toluene	2.24
0.5gVR+3.0mlToluene+1.0gToluene	2.92
0.5gVR+3.0mlToluene+2.0gToluene	3.60
0.5gVR+3.0mlToluene+3.0gToluene	4.24
0.5gVR+3.0mlToluene+0.5gREF	3.15
0.5gVR+3.0mlToluene+1.0gREF	3.91
0.5gVR+3.0mlToluene+2.0gREF	5.31
0.5gVR+3.0mlToluene+1.0gHVGO	2.61

0.5gVR+3.0mlToluene+2.0gHVGO	2.75
0.5gVR+3.0mlToluene+3.0gHVGO	2.87
0.5gVR+3.0mlToluene+1.0gPFX	2.21
0.5gVR+3.0mlToluene+2.0gPFX	2.00
0.5gVR+3.0mlToluene+3.0gPFX	1.74
0.5gHO+3.0mlToluene	1.23
0.5gHO+3.0mlToluene+1.0gToluene	1.63
0.5gHO+3.0mlToluene+2.0gToluene	1.93
0.5gHO+3.0mlToluene+3.0gToluene	2.31
0.5gHO+3.0mlToluene+0.5gDAO	1.47
0.5gHO+3.0mlToluene+1.0gDAO	1.65
0.5gHO+3.0mlToluene+2.0gDAO	1.98
0.5gHO+3.0mlToluene+0.5gFO	1.22
0.5gHO+3.0mlToluene+1.0gFO	1.16
0.5gHO+3.0mlToluene+2.0gFO	1.07

\*: Sample oil: 0.5g ATB (or VR) + 3.0mlToluene

ATB: Athabasca Atmospheric tower bottom (Syncrude Canada Ltd.)

VR: Cold Lake vacuum residue (Imperial Oil Ltd.)

PFX: Paraflex (Petro Canada Ltd.)

HVGO: Heavy vacuum gas oil (Imperial Oil Ltd.)

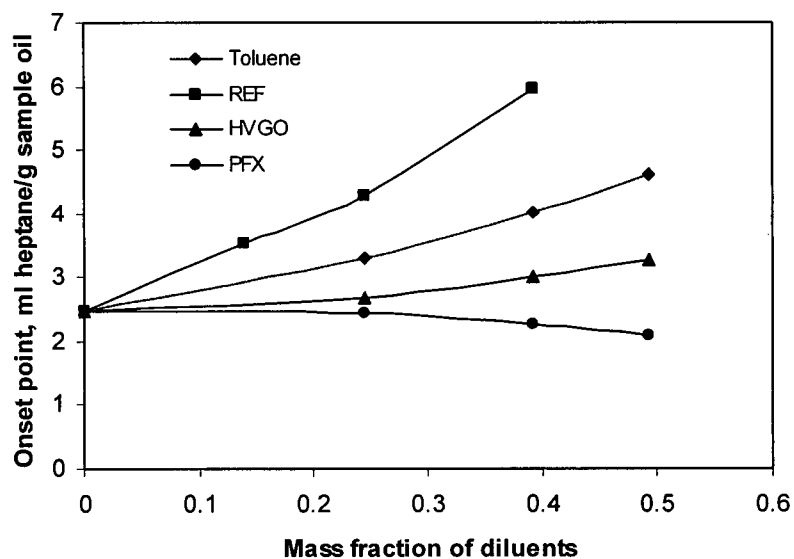
REF: Resin enriched fraction (SFEEF Experiment in China)

HO: Cold Lake heavy oil (Imperial Oil Ltd.)

FO: Fuel Oil (Imperial Oil Ltd.)

DAO: De-asphalted Oil (Imperial Oil Ltd.)

(a)



(b)

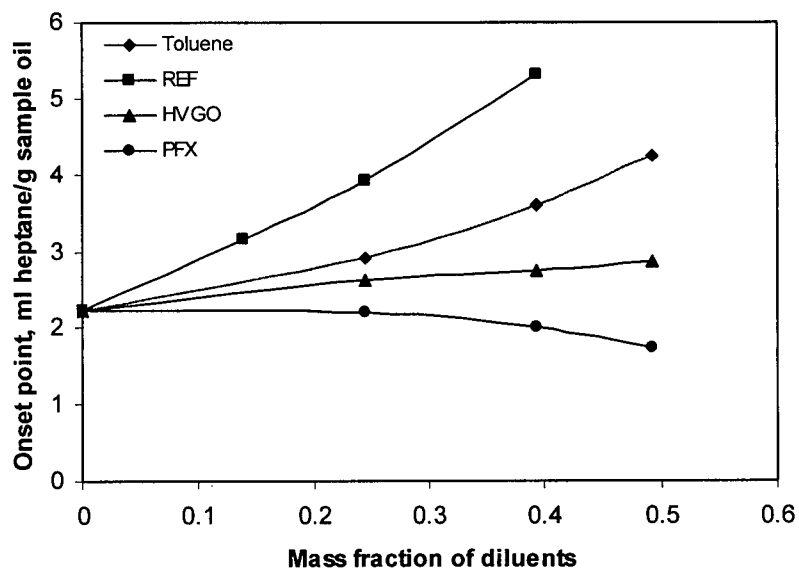


Figure 5.3 The Effect of Diluents on Asphaltene Precipitation Onset (n-Heptane as Titrant) (a) Athabasca Atmospheric Tower Bottoms as Source of Asphaltene, (b) Cold Lake Vacuum Residue as Source of Asphaltene.

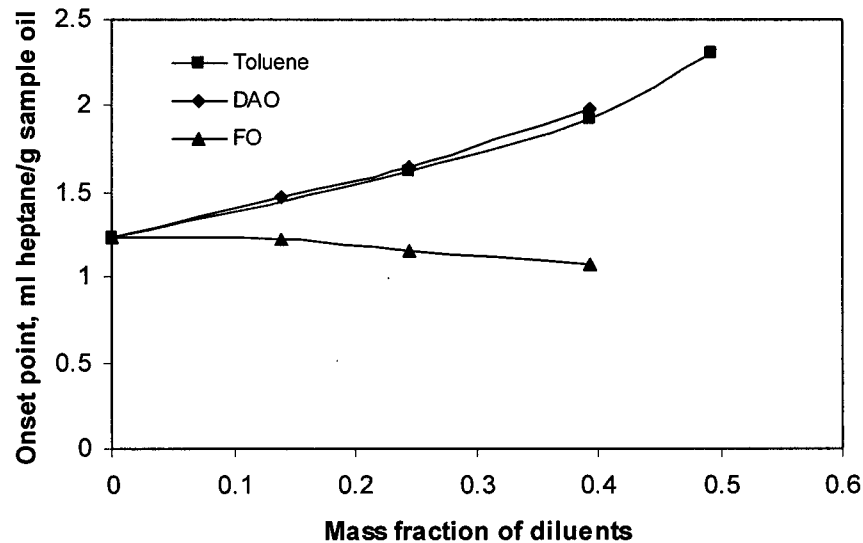


Figure 5.4 The Effect of Diluents on Asphaltene Precipitation Onset at 25°C, (n-Heptane as Titrant, Cold Lake Heavy Oil as Source of Asphaltene).

## 5.2 Stability Criteria

To predict the stability of various oil mixtures, the Andersen/Pedersen model [14] and Wiehe's Oil Compatibility Model [13] are applied to calculate the solubility parameter of the feedstocks and the blends. These two approaches to asphaltene precipitation use different nomenclature, but are closely related.

### 5.2.1 Andersen/Pedersen's Model

According to the Andersen/Pedersen approach [14], asphaltenes will precipitate when the solvent phase or oil reaches conditions where the average solubility parameter of the phase equals a critical solubility parameter obtained through the titration. The critical solubility parameter for the mixture,  $\delta_{cr}$ , is given as

$$\delta_{cr} = \phi_o\delta_o + \phi_p\delta_p + \phi_s\delta_s \quad (5.1)$$

where  $\delta_o$ ,  $\delta_p$ , and  $\delta_s$  are the solubility parameters of oil, precipitant and solvent respectively and  $\phi_o$ ,  $\phi_p$ ,  $\phi_s$  are volume fractions of the corresponding components such that  $\sum \phi_i = 1$ . Assuming that Equation (5.1) fully describes the onset of asphaltene precipitation, a plot of  $V_p/V_o$  vs  $V_s/V_o$  is a linear function with each point being a flocculation condition. The slope,  $s = (\delta_s - \delta_{cr}) / (\delta_{cr} - \delta_p)$ , and the intercept,  $I_y = (\delta_o - \delta_{cr}) / (\delta_{cr} - \delta_p)$ . The criterion for the oil blend to be stable is that  $\delta_o > \delta_{cr}$ . A few oil samples (including stable and unstable oils) were tested [14] using THF as the oil solvent. The results showed that this method can be used as a simple and reliable empirical tool in assessing possible problems with instability by flocculation titration tests.

### 5.2.2 Wiehe's Model

The Oil Compatibility Model (OCM) of Wiehe [13], expresses Equation (5.1) as

$$\delta_f = \phi_o \delta_o + \phi_H \delta_H + \phi_T \delta_T \quad (5.2)$$

where  $\delta_f$  is the flocculation solubility parameter, and  $\delta_H$ ,  $\delta_T$ ,  $\delta_o$  are the solubility parameters of n-heptane (precipitant), toluene (solvent) and the oil respectively. The slope and intercept for the flocculation titration plot are defined as :

$$S_{BN} = 100(\delta_o - \delta_H) / (\delta_T - \delta_H) \quad (5.3)$$

$$I_N = 100(\delta_f - \delta_H) / (\delta_T - \delta_H) \quad (5.4)$$

where  $S_{BN}$ , and  $I_N$  are defined as the solubility blending number and insolubility number.

For mixtures,

$$S_{BNmix} = \frac{V_1 S_{BN1} + V_2 S_{BN2} + V_3 S_{BN3} + \dots}{V_1 + V_2 + V_3 + \dots} \quad (5.5)$$

Therefore, if the oil is completely soluble in n-heptane and thus, contains no asphaltenes, the insolubility number is 0 but if the asphaltene-resin dispersion is barely soluble in toluene, the insolubility number is 100. Likewise, an oil that is as poor a solvent as n-heptane has a solubility blending number of 0 and an oil that is as good of solvent as toluene has a solubility blending number of 100. A first hypothesis of this model is that the asphaltene will precipitate from the oil at the same mixture solubility parameter, no matter whether the oil is blended with non-complexing liquids or other oils. A second assumption, given by equation (5.5) is that the solubility parameter of a mixture is the volumetric average solubility parameter. Since for compatibility, the solubility parameter of the mixture of oils must be higher than the flocculation solubility parameter of any oil in the mixture, the maximum insolubility parameter of all the oils in the mixture is the only one required. Thus, for a mixture of oils, the compatibility criterion is  $S_{BNmix} > I_{Nmax}$ . The correct order and proportions of two potentially incompatible crude oils-Souedie and Forties crudes were predicted in their work using OCM (Oil Compatibility Model) and the results show good agreement with the application in the refinery. The Oil Compatibility Model was also investigated by Al-Atar [78] with the addition of de-asphalted oil (DAO) into the heavy oil (HO). The fuel oil (FO) was then added as a diluent to this binary mixture for further fouling experiment. The OCM predictions were verified in terms of fouling measurements for these ternary oil mixtures.

From consideration of the above equations and using for toluene and heptane respectively  $\delta_T=18.3 \text{ (MPa)}^{0.5}$  and  $\delta_H=15.2 \text{ (MPa)}^{0.5}$  [124], the solubility parameters of all the components of the blends can be calculated, the results are shown in Table 5.7 and 5.8. The calculated solubility parameters lie in the range of 14.7-21.9  $\text{(MPa)}^{0.5}$ , which is in agreement with the values reported in the literature [14,28,29]. Independent of applied diluents, solubility parameters at the flocculation point increase with the increase of the solubility parameter of the

applied titrants, as reported by [29]. A linear plot of the titration data from which the above parameters derived, is shown in Appendix A3.

Based on the acquired solubility parameter of the feedstocks from the above titrations the parameters of the Andersen model and the Wiehe model can be calculated for the blends used in the precipitation experiments of Chapter 4. A linear relation is found between the criterion of Wiehe and that of Andersen, as shown in Figure 5.5 and Equation (5.6).

$$S_{BNmix} - I_{Nmax} = 32.331(\delta_{mix} - \delta_f) \quad (5.6)$$

The correlation of the precipitation data of Section 4.1 where filtration was used versus Andersen's and Wiehe's stability criterion determined from the titration are shown in Figure 5.6 and Tables A1.2-1.7. It is clear that although there is considerable scatter at  $W > 2\%$ , there is a good correlation of the trend of the precipitation data with either method of presentation of the mixture solubility parameter. However, even for conditions where the system is expected to be stable (ie  $S_{BNmix} - I_{Nmax} > 0$ , or  $\delta_{mix} > \delta_f$ ), such that  $W$  should be zero, a finite value of  $W$  is found. This may be due to non-asphaltene insolubles such as clays present in the heavy oils, or due to other factors in the experiments or models. One such experimental factor - the difference in temperature between the precipitation experiments and the titration is explored in Section 5.3. Nevertheless, the flocculation titration approach does lead to good correlation of the asphaltene precipitation data for both Athabasca and Cold Lake blends.

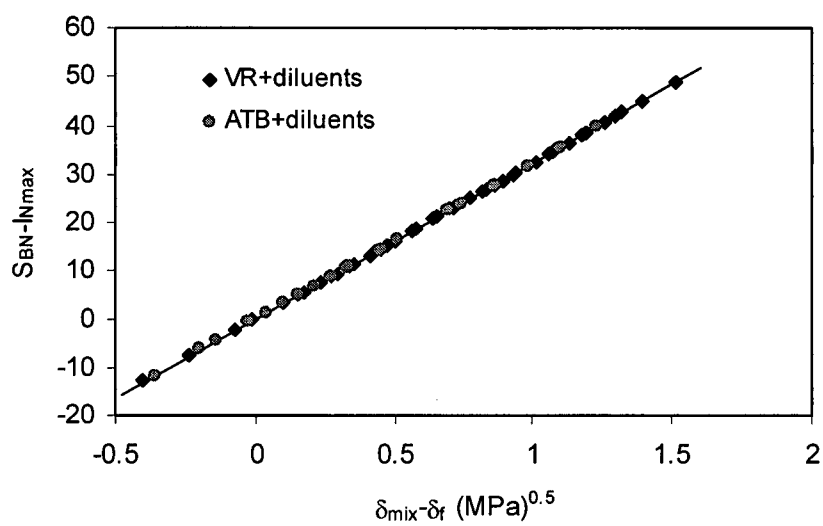


Figure 5.5 Linear Correlation between Criterion of the Wiehe Model and of the Andersen Model.

Table 5.7 The Calculation of Solubility Parameter Using Titration Data (Iso-octane as Titrant, 25°C)

Sample	Solubility parameter, $\delta$ [MPa] <sup>0.5</sup>	The flocculation solubility parameter, $\delta_f$ [MPa] <sup>0.5</sup>	$S_{BN}$	$I_N$
ATB	19.83	15.56	149.4	11.6
VR	19.31	15.60	132.6	12.9
REF	21.88	-	215.5	0
PFX	14.74	-	-14.8	0
HVGO	16.60	-	45.2	0
HO	18.63	16.13	110.6	30.0
FO	15.61	-	13.2	0
DAO	18.25	-	98.4	0

Table 5.8 The Calculation of Solubility Parameter Using Titration Data (n-Heptane as Titrant, 25°C)

Sample	Solubility parameter, $\delta$ [MPa] <sup>0.5</sup>	The flocculation solubility parameter, $\delta_f$ [MPa] <sup>0.5</sup>	S <sub>BN</sub>	I <sub>N</sub>
ATB	19.57	16.20	141.0	32.3
VR	19.53	16.23	139.7	33.2
REF	21.12	-	191.0	0
PFX	15.67	-	15.2	0
HVGO	16.82	-	52.3	0
HO	19.12	16.70	126.5	48.3
FO	16.31	-	35.8	0
DAO	18.20	-	96.8	0

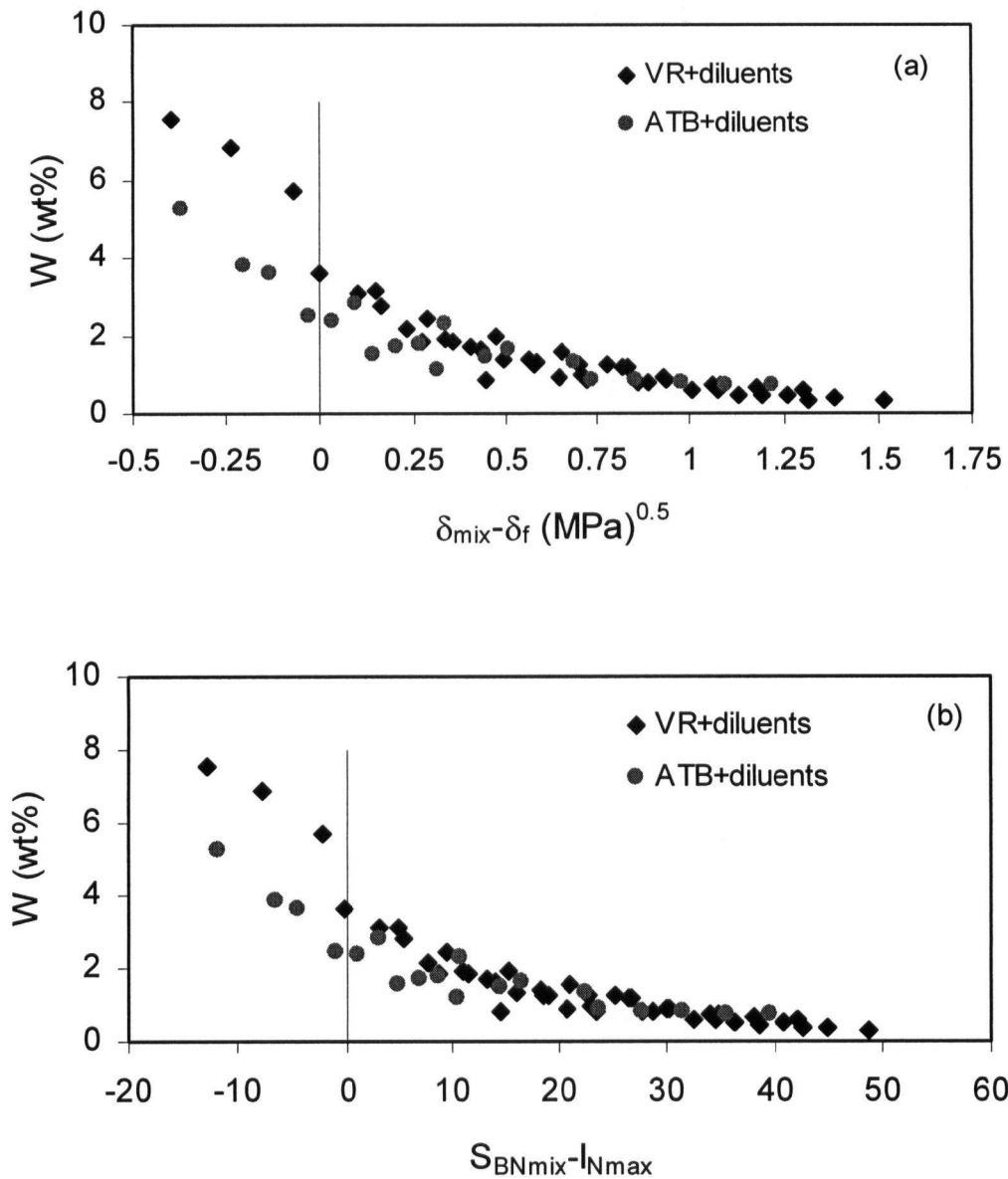


Figure 5.6 Hot Filtration Insolubles Versus (a) the Andersen Model Stability Criterion, (b) the Wiehe Stability Criterion. (n-Heptane as Titrant, 25°C).

### 5.2.3 Colloidal Instability Index

The Colloidal Instability Index (CII) considers the crude oil as a colloidal suspension made up of the pseudocomponents saturates, aromatics, resins, and asphaltenes. The CII based instability or incompatibility of the petroleum depends on its composition of the oil fractions,

saturates, aromatics, resins and asphaltenes. The index is an expression of the colloidal nature of petroleum fractions and is defined as a mass ratio of the sum of asphaltenes and saturates which precipitate asphaltenes, to the sum of the aromatics which dissolve and the resins that peptize asphaltenes as follows:

$$CII = \frac{(Saturates + Asphaltenes)}{(Aromatics + Resins)} \quad (5.7)$$

The CII uses the weight percentages obtained from SARA analysis. The CII has been used to predict the stability of asphalts by Gastel [109], and the stability of asphaltenes in crude oil – solvent blends by Asomaning and Watkinson [125]. The CII measures relative stability, the higher the value, the more unstable the asphaltenes in the oil are. Asomaning [63] reported that based on their large database of crude oils, the values of 0.9 or more indicate an oil with unstable asphaltene, while values below 0.7 indicate an oil with stable asphaltenes; between 0.7 and 0.9 the stability of the asphaltenes falls in the uncertain region. In their work, the performance of the CII index was compared to that of Asphaltene-Resin ratio, Oliensis Spot Test number and the Asphaltene Precipitation Detection Test (APDT) number from the solvent titration method [126]. The results showed that CII predicted the stability of asphaltenes in crude oils better than all the other indices. As mentioned previously, the CII index can be obtained from SARA analysis data, which can easily be measured. The utility of the index for oils of very low asphaltene concentrations could be limited however.

In this work, the correlation of hot filtration insolubles versus CII of the oil blends is shown in Figure 5.7 and Table A1.2-1.7. The results show that CII correlate reasonably well with the amount of hot filtration insolubles for each of ATB and VR, particularly for values of  $CII < 2.5$ . The amount of hot filtration insolubles decreased with decreasing CII and reached very low values at  $CII < 1$  (from the extrapolation of experimental results). At  $CII > 3$ , there was

considerable scatter, and as might be expected, large W values at a given CII for the VR mixtures. This may be due to the higher asphaltene concentration for VR mixtures than that for the ATB mixtures, as shown in Table A1.2-A1.7.

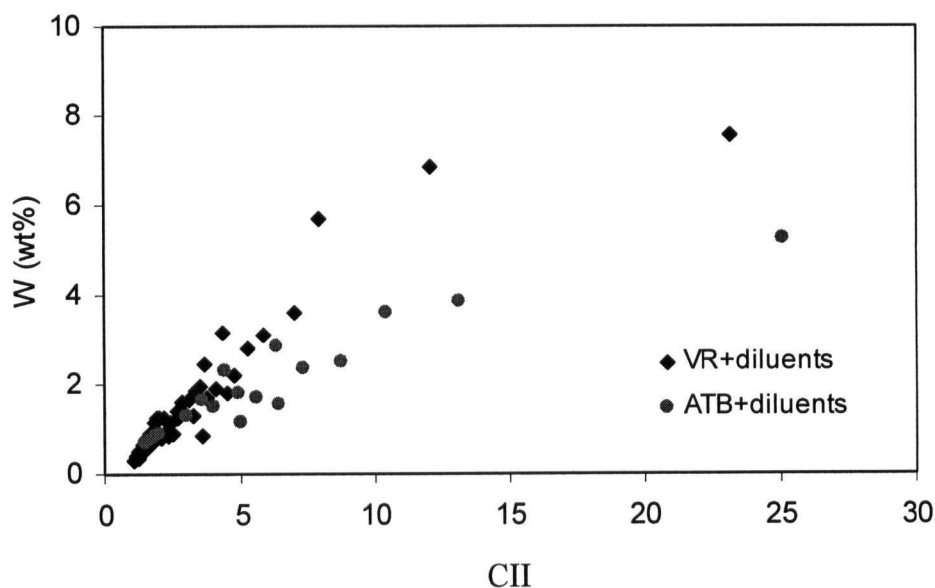


Figure 5.7 Hot Filtration Insolubles Versus Colloidal Instability Index (CII) of the Oil Blends.

### 5.3 Temperature Dependence of the Solubility Parameter

Since the hot filtration and later fouling tests were conducted at bulk temperatures (85°C) higher than those of the titrations (25°C), the effect of temperature on solubility parameters was investigated. It was thought that the finite values of W at the stability point in Figure 5.6 might be related to this temperature effect. Flocculation titration experiments with n-heptane as titrant were conducted at a higher temperature of 35°C and 50°C. The latter value was the highest achievable with the AFT apparatus since the 0.1mm quartz flow cell from Starna Cell Ltd. failed at temperature of 85°C. The results are shown in Table 5.9. With the 25°C increase in temperature from 25 to 50°C, the solubility parameters for all the feedstocks decreased by around 0.67-1.26 (MPa)<sup>0.5</sup>, while the flocculation solubility parameters ( $\delta_f$ ) for ATB and VR decreased by 0.57-0.61(MPa)<sup>0.5</sup> (0.023-0.024[MPa]<sup>0.5</sup>/°C). These changes are in agreement with

reported values by Sajedi [127] for one oil using single point titration, where the critical solubility parameter has a decrease of  $1.1(\text{MPa})^{0.5}$  from  $1-49^\circ\text{C}(0.022[\text{MPa}]^{0.5}/^\circ\text{C})$  was found according to a few experiments performed. The solubility parameters for all the hot filtration oil blends at  $35^\circ\text{C}$  and  $50^\circ\text{C}$  were calculated using the same method as mentioned previously. At the higher temperature of  $35^\circ\text{C}$  and  $50^\circ\text{C}$ , the stability criteria line was shifted to the right, as shown in Figures 5.8, giving an improved prediction for zero insolubles, as compared to Figure 5.6. According to the extrapolation of the above experimental data, if the titrations were done at  $85^\circ\text{C}$ , the flocculation solubility parameters ( $\delta_f$ ) for ATB and VR will decrease to  $14.74(\text{MPa})^{0.5}$  and  $14.87(\text{MPa})^{0.5}$  respectively. As might be expected, the stability criteria line will be shifted further to the right and give better prediction for zero insolubles. The model predictions are conservative in that if the titration is done at  $25^\circ\text{C}$ , the amount of precipitation at higher temperature will be over-predicted. Hence if it is predicted that no precipitation occurs at  $25^\circ\text{C}$  by either solubility model, it will definitely be safe at higher temperatures.

Table 5.9 The Calculation of Solubility Parameter at Various Temperatures Using Titration Data (n-Heptane as Titrant)

Sample	$\delta$ [Mpa] <sup>0.5</sup> (25°C)	$\delta_f$ [MPa] <sup>0.5</sup> (25°C)	$\delta$ [Mpa] <sup>0.5</sup> (35°C)	$\delta_f$ [MPa] <sup>0.5</sup> (35°C)	$\delta$ [Mpa] <sup>0.5</sup> (50°C)	$\delta_f$ [MPa] <sup>0.5</sup> (50°C)
Athabasca atmospheric tower bottom	19.57	16.20	18.90	16.0	18.46	15.59
Cold lake vacuum residue	19.53	16.23	18.83	16.04	18.38	15.66
Enriched resin fraction (REF)	21.12	-	20.51	-	19.86	-
Paraflex 1	15.67	-	15.43	-	15.0	-
Paraflex 2	16.09	-	15.78	-	15.34	-
Heavy vacuum gas oil	16.82	-	16.47	-	15.96	-

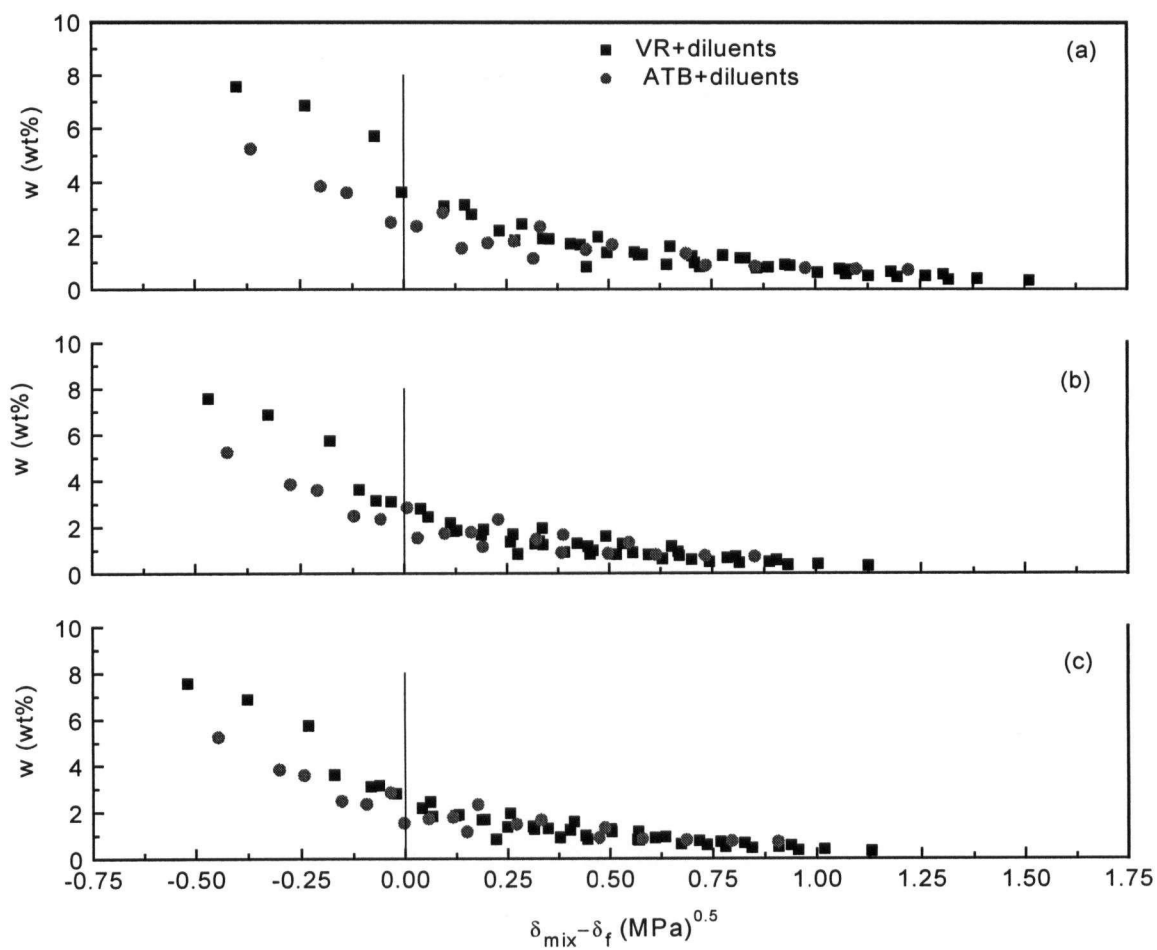


Figure 5.8 Weight Percent of Feed Precipitated versus the Andersen Stability Criterion (a) 25°C, (b) 35°C and (c) 50°C.

## 6. Thermal Fouling Experimental Results and the Correlation to Stability Criteria

Based on the results from hot filtration and flocculation titration experiments, selected fouling runs were conducted to explore fouling behaviour. The fouling loop which was described in Section 3.2.4, is equipped with a Heat Transfer Research Incorporated (HTRI) heat transfer probe. The composition of the test fluids are given in Table 6.1, which were chosen to cover both stable and non-stable blends. For both VR and ATB, percentage precipitated varied from <1 wt% to over >7 wt%. For unstable asphaltene blends the fouling rate has been found previously [128] to depend on initial surface temperature, bulk temperature, and velocity as well as composition of the mixtures. In this work, the velocity and bulk temperatures were held constant at 0.75m/s and 85°C respectively.

Table 6.1 The Composition of the Mixtures for Thermal Fouling Runs

Test fluid	W (wt%)*	$\delta_{mix}$ [MPa] <sup>0.5</sup>	$\delta_f$ [MPa] <sup>0.5</sup>	$S_{BNmix}$	$I_{Nmax}$
10%VR+90%HVGO	0.96	17.05	16.23	59.7	33.2
10%VR+45%HVGO+45%PFX	2.46	16.52	16.23	42.6	33.2
10%VR+5%REF+85%PFX	3.96	16.22	16.23	33.1	33.2
10%VR+90%PFX	7.28	15.99	16.23	25.6	33.2
10%ATB+90%HVGO	0.80	17.06	16.20	60.0	32.3
10%ATB+5%REF+85%PFX	2.08	16.24	16.20	33.5	32.3
10%ATB+2%REF+88%PFX	2.62	16.09	16.20	28.9	32.3
10%ATB+0.5%REF+89.5%PFX	3.16	16.03	16.20	26.7	32.3
10%ATB+0.1%REF+89.9%PFX	3.58	16.01	16.20	26.1	32.3
10%ATB+90%PFX	4.02	16.0	16.20	26.0	32.3

\* W: Hot filtration insolubles (85°C), the weight percent of the feed which precipitated ((g asphaltene/g feed oil)×100%)

### 6.1 Composition Effect on Thermal Fouling

Figure 6.1 shows the results of a typical fouling run carried out with the mixture of 10% VR and 90% PFX. The bulk temperature is 85°C, and the clean surface temperature is 290°C, bulk velocity is 0.75m/s. After about 45 hours of operation, the probe temperature has increased to 346°C, and the overall heat transfer coefficient has decreased from 1.50 kW/m<sup>2</sup>K to 1.16 kW/m<sup>2</sup>K, resulting in a fouling resistance of about 0.19 m<sup>2</sup>K/kW.

The result of duplicated runs with the mixture of 10%VR and 90%PFX is shown in Figure 6.2. The bulk temperature is 85°C, the clean surface temperature is 290°C, and the bulk velocity is 0.75m/s. Both runs show very similar results (initial fouling rates are 0.0068 and 0.0066 m<sup>2</sup>K/kWh respectively), which indicated that the results of the thermal fouling experiment are reliable and reproducible. The absolute and relative deviations are 0.0002 m<sup>2</sup>K/kWh and 2.9%.

The comparison of thermal fouling resistance for the mixture of 10%VR-90%PFX and 10%ATB-90%PFX at the same clean surface temperature (260°C and 290°C) is shown in Figure 6.3. Thermal fouling resistance (290°C) at the end of the experiment is lower by 36.8% for the ATB which has a lower asphaltene content than that for the VR (13.5 wt% versus 17.7 wt%), as shown in Figure 6.3. This result is consistent with our previous hot filtration experimental results in which the amount of insolubles are lower by 44% for the ATB than that for the VR, as shown in Table A1.2 and A1.6. In Figure 6.3a, the run of 10%ATB-90%PFX (260°C) shows very low thermal fouling resistance ( $R_f < 0.01$  m<sup>2</sup>K/kW). So the fouling runs for ATB and various diluents are carried out at the higher clean surface temperature (290°C) than for VR (260°C).

Figure 6.4 and Table 6.2 show the results of thermal fouling runs with the mixtures of VR and various diluents. Fouling resistance is much higher for the mixture of VR with aliphatic

diluent PFX, a diluent which is over 99wt% saturates, compared with the more aromatic diluent HVGO (15.9 wt% aromatics, 68.3 wt% saturates). The inhibition effect of resin on fouling was investigated in detail by the addition of 0.1-5 wt% REF. With the addition of 5 wt% REF (36.3 wt% resins) into the mixture of VR and PFX, the fouling resistance and initial fouling rate decrease significantly by about 50%. A similar trend can be found for the mixtures of ATB and various diluents. However the inhibition effect is much stronger for ATB than that for VR. Thermal fouling for ATB decreases by a factor of about three to six with only 0.5 wt% REF addition. The results are shown in Figure 6.5 and Table 6.3. This may be due to the lower value of  $R_e/A_s$  ratio for ATB (0.44) than that for VR (0.84). As mentioned previously, asphaltene cannot dissolve in crude oil without a resin fraction. Resin-asphaltene interactions appear to be preferred over asphaltene-asphaltene interactions [30]. The ratio of  $R_e/A_s$  for the ATB test fluids increase much higher with the addition of REF than that for the VR test fluids, as shown in Tables A1.3 and A1.7.

Table 6.2 Thermal Fouling Parameter for Experiments of VR (17.7% Asphaltene) with Various Diluents. ( $T_b = 85^\circ\text{C}$ ,  $T_{s0} = 260^\circ\text{C}$ ,  $U_b = 0.75\text{m/s}$ )

Test fluid	Initial fouling rate ( $\text{m}^2\text{K/kWh}$ )	Final $R_f$ ( $\text{m}^2\text{K/kW}$ ) at ~40 hours	$\delta_{\text{mix}}$ [ $\text{MPa}$ ] <sup>0.5</sup>	Hot filtration insolubles, W (wt%)	
				Start	End
10%VR+90%PFX	0.0051	0.09	15.99	7.28	5.16
10%VR+5%REF+85%PFX	0.0022	0.04	16.22	3.96	3.12
10%VR+45%HVGO+45%PFX	0.0007	0.02	16.52	2.46	1.98
10%VR+90%HVGO	0.0007	0.01	17.05	0.96	0.80

Table 6.3 Thermal Fouling Parameter for Experiments of ATB (13.5% Asphaltene) with Various Diluents. ( $T_b = 85^\circ\text{C}$ ,  $T_{s0} = 290^\circ\text{C}$ ,  $U_b = 0.75\text{m/s}$ )\*

Test fluid	Initial fouling rate ( $\text{m}^2\text{K/kWh}$ )	Final $R_f$ ( $\text{m}^2\text{K/kW}$ ) at ~40 hours	$\delta_{\text{mix}}$ [MPa] <sup>0.5</sup>	Hot filtration insolubles W(wt%)	
				Start	End
10%ATB+90%PFX	0.0025	0.12	16.0	4.02	2.06
10%ATB+0.1%REF+89.9%PFX	0.0020	0.08	16.01	3.58	2.12
10%ATB+0.5%REF+89.5%PFX	0.0008	0.02	16.03	3.16	2.38
10%ATB+2%REF+88%PFX	0.0003	0.012	16.09	2.62	2.26
10%ATB+5%REF+85%PFX	0.0001	0.004	16.24	2.08	1.86
10%ATB+90%HVGO	0.0002	0.006	17.06	0.80	0.72

\*: ATB: Athabasca Atmospheric Tower Bottoms (Syncrude Canada Ltd.)

REF: Resin Enriched Fraction (SFEF Experiment in China).

HVGO: Heavy Vacuum Gas Oil (Imperial Oil Ltd.).

PFX: Paraflex HT 10 (Petro Canada Ltd.).

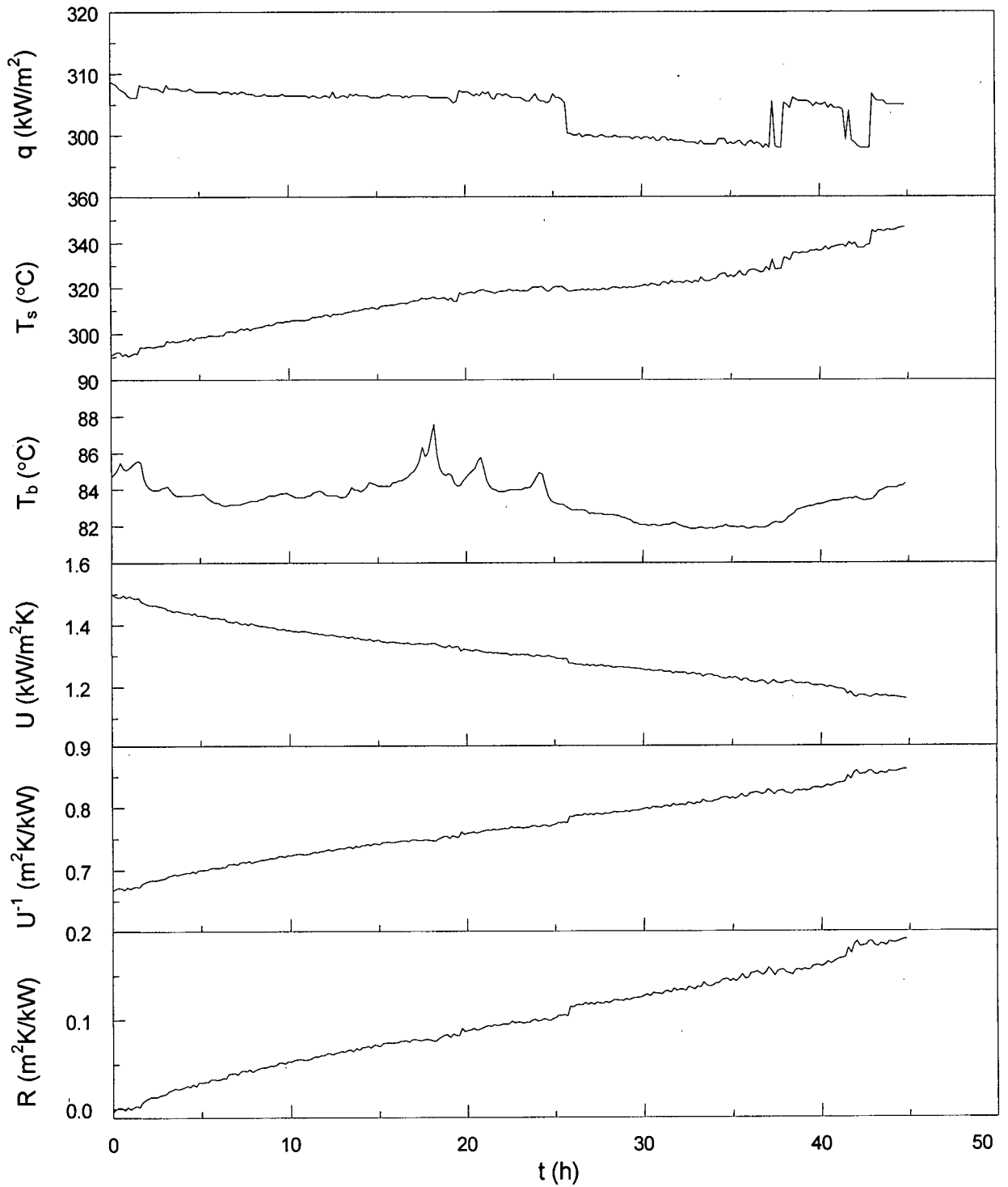


Figure 6.1 Results of typical fouling run with the mixture of 10%VR and 90%PFX.

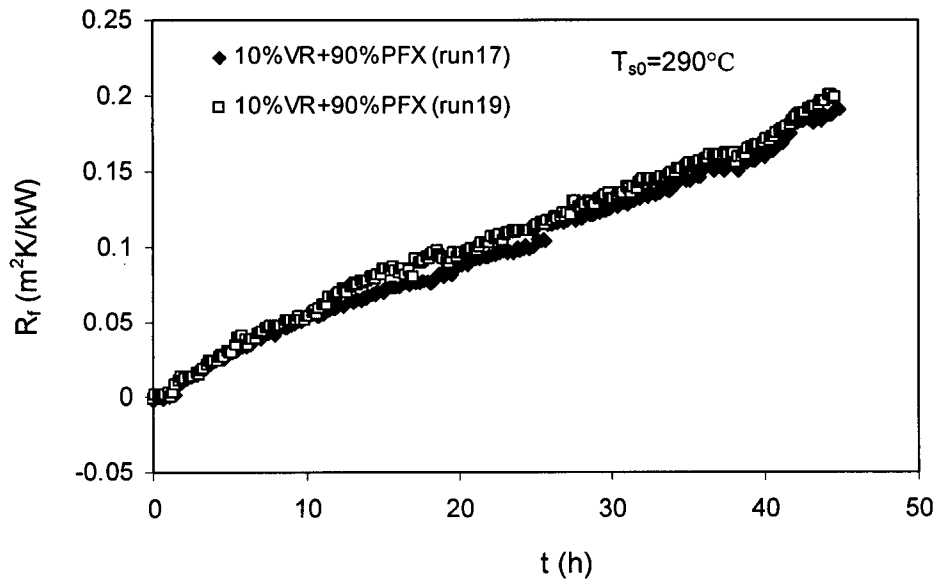


Figure 6.2 Fouling Resistance over Time for a Repeat Run with the Mixture of 10%VR and 90%PFX.

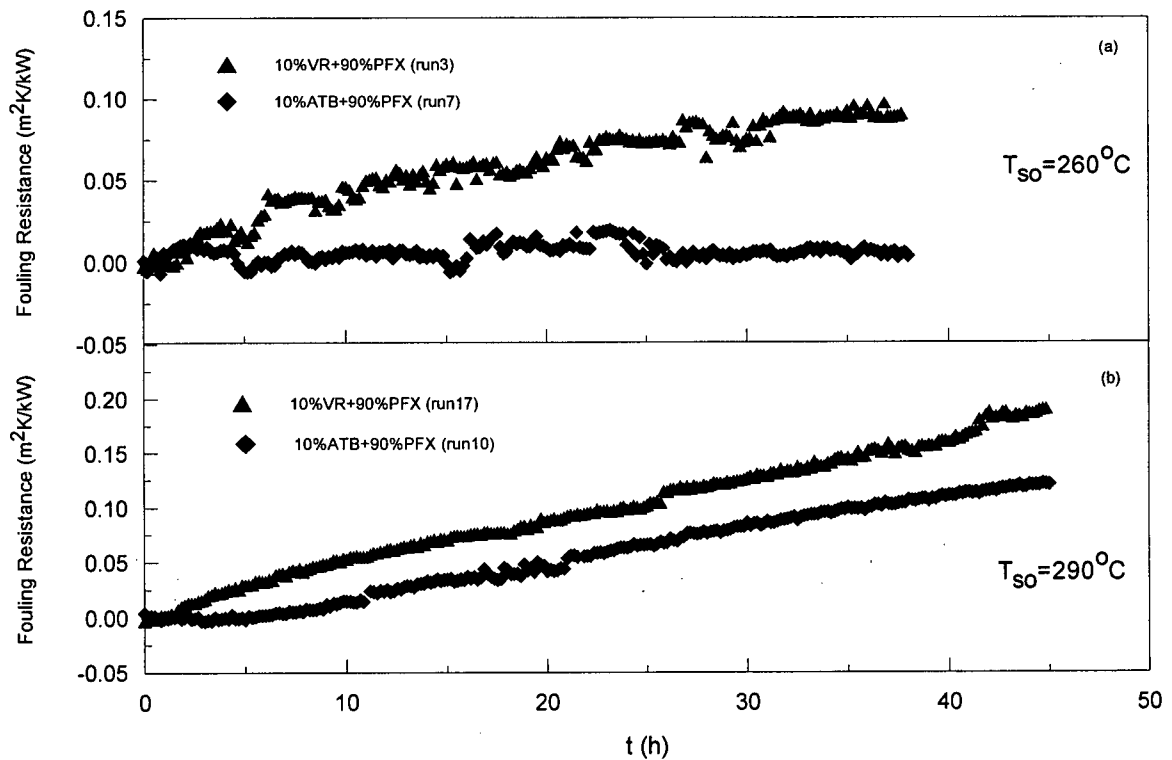


Figure 6.3 Comparison of Fouling Resistance of 10%VR-90%PFX and 10%ATB-90%PFX at the Same Clean Surface Temperature, (a)  $T_{so}=260^{\circ}\text{C}$ , (b)  $T_{so}=290^{\circ}\text{C}$ .

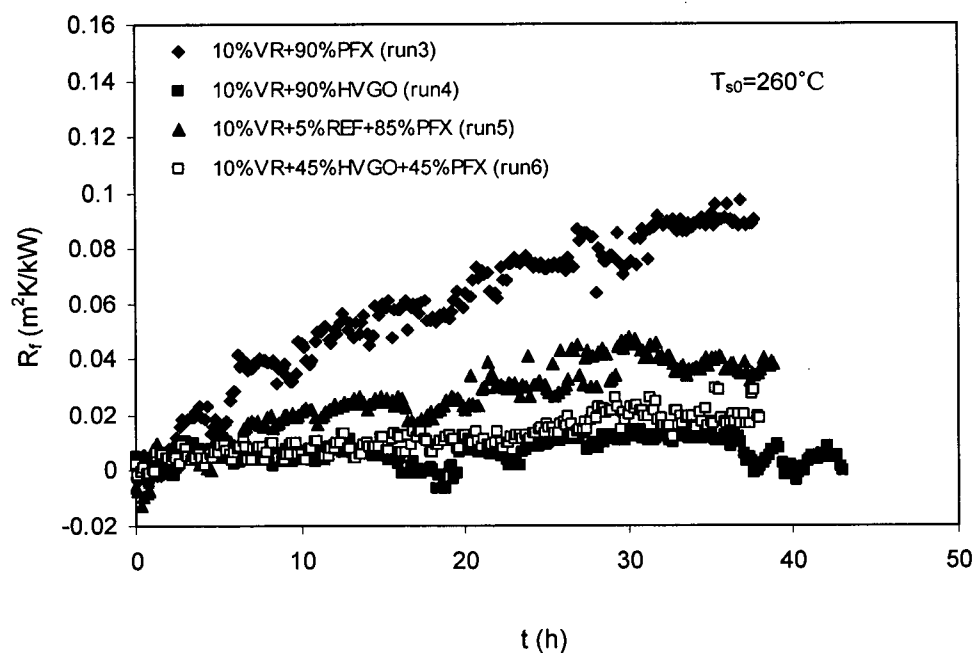


Figure 6.4 Fouling Resistance Versus Time for the Mixtures of VR and Various Diluents

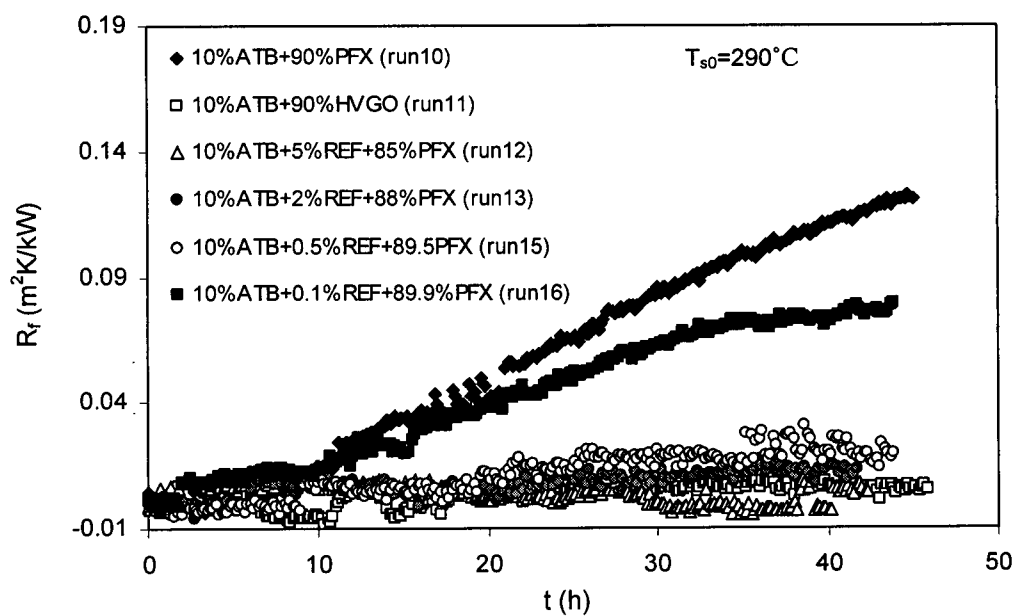


Figure 6.5 Fouling Resistance Versus Time for the Mixtures of ATB and Various Diluents

## 6.2 Surface Temperature Effect on Thermal Fouling

The thermal fouling resistance versus time plots for runs with varying surface temperature at constant bulk temperature and flow rate are shown in Figures 6.6-6.8. The fouling parameters for these runs shown in the plots are given in Table 6.4. During this investigation, the supply of Paraflex was replenished. The sample was designated PFX2, and the original sample as PFX1.

Table 6.4 Surface Temperature Effects at  $T_b = 85^\circ\text{C}$ ,  $U_b = 0.75\text{m/s}$

Test fluid	$T_{s0}$ ( $^\circ\text{C}$ )	Initial fouling rate ( $\text{m}^2\text{K/kWh}$ )	Final $R_f$ ( $\text{m}^2\text{K/kW}$ ) at ~40 hours	$\delta_{\text{mix}}$ [MPa] <sup>0.5</sup>
10%VR+90%PFX1 (run2)	230	0.0012	0.025	15.99
10%VR+90%PFX1 (run3)	260	0.0051	0.09	15.99
10%VR+90%PFX1 (run17)	290	0.0068	0.19	15.99
10%ATB+90%PFX1 (run7)	260	0.0011	0.006	16.0
10%ATB+90%PFX1 (run10)	290	0.0025	0.12	16.0
10%VR+90%PFX2 (run24)	310	0.0029	0.12	16.38
10%VR+90%PFX2 (run25)	290	0.0019	0.063	16.38
10%VR+90%PFX2 (run26)	260	0.0013	0.045	16.38

Fouling resistances increased with increasing surface temperature for all the runs in this work. The surface temperature was in the range of 230-310 $^\circ\text{C}$ . The fouling resistance-time profiles were near linear, especially for the runs at higher surface temperature. The dependence of the initial fouling rates on surface temperature was expressed by an Arrhenius type equation of the form  $(dR_f/dt)_0 = A \exp(-E/RT_{s0})$ , where  $E$  is a fouling activation energy and  $R$  the gas

constant. The parameters of the fitting equation are shown in Table 6.5 and the corresponding Arrhenius type plot is shown in Figure 6.9. For 10%VR-90%PFX1, four data points were available. While for the other test fluids, only two or three data points were provided. For the fitting of the test fluid 10%VR-90%PFX2, the lowest temperature run (260°C) was not included. Almost the same activation energies were obtained for all cases, so the reported value ~68 kJ/mol is representative of the data. The activation energies are for the overall fouling process and can best be regarded as apparent activation energies. The magnitude of the apparent activation energies reported here were higher than expected for fouling being only a physical process. From studies of temperature and velocity effects with similar oils, Asomaning [54] concluded that adhesion controlled the fouling. The magnitude of the activation energies reported here supports this conclusion.

It was also noticed that the initial fouling rates were considerably lower for the mixture of 10%VR and 90%PFX2 compared with the mixture of 10%VR and 90%PFX1 at the same surface temperature. This result was unexpected, since the PFX1 and PFX2 were both samples of Paraflex HT 10, which is the commercial name of a lube oil base stock and supplied by Petro Canada Ltd.. Sample PFX1 was received one and a half years earlier than PFX2. Therefore, we conducted further analysis for the properties of PFX1 and PFX2, such as simulated distillation, GC-MS analysis, PNA analysis etc. The results are shown in Table 6.6, 6.7 and Figure 6.10-6.12. Simulated distillation analysis (Table 6.6) shows that PFX1 is a little heavier than PFX2, with boiling points at 50% recovered some 9°C higher and at 90% recovered some 17°C higher. GC-MS results (Figures 6.10-6.12) qualitatively indicate that PFX1 contains more paraffins than PFX2 (6.11) and is heavier than PFX2 (6.10). The PNA analysis (ASTM D2786,3239; Table 6.7) shows that paraffins content for PFX1 (34.7%) is much higher than that of PFX2

(23.0%). That is probably the main reason that the mixtures of VR and PFX1 yielded more fouling than that of VR and PFX2 at the same conditions.

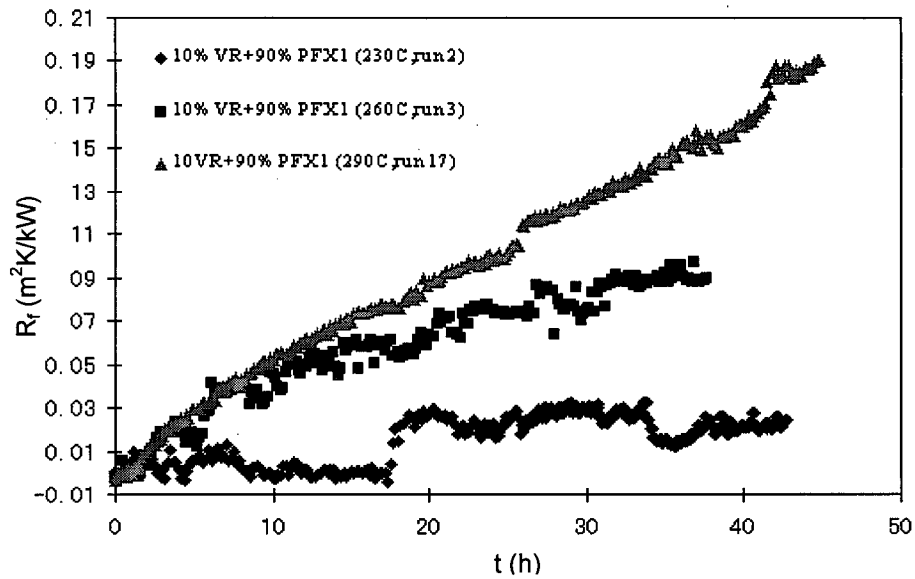


Figure 6.6 Surface Temperature Effect on Thermal Fouling Runs Using the Mixture of 10%VR and 90% PFX1.

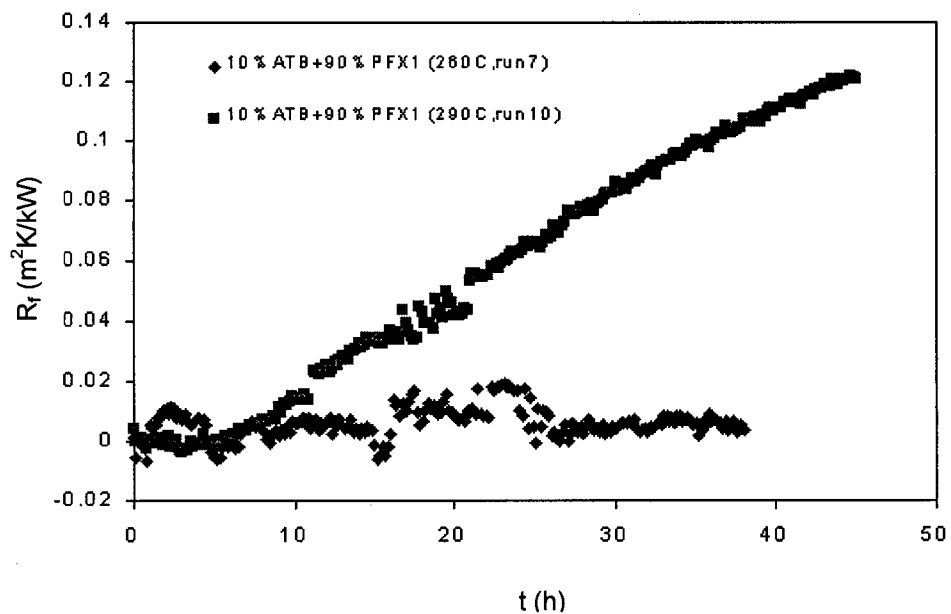


Figure 6.7 Surface Temperature Effect on Thermal Fouling Runs Using the Mixture of 10%ATB and 90% PFX1.

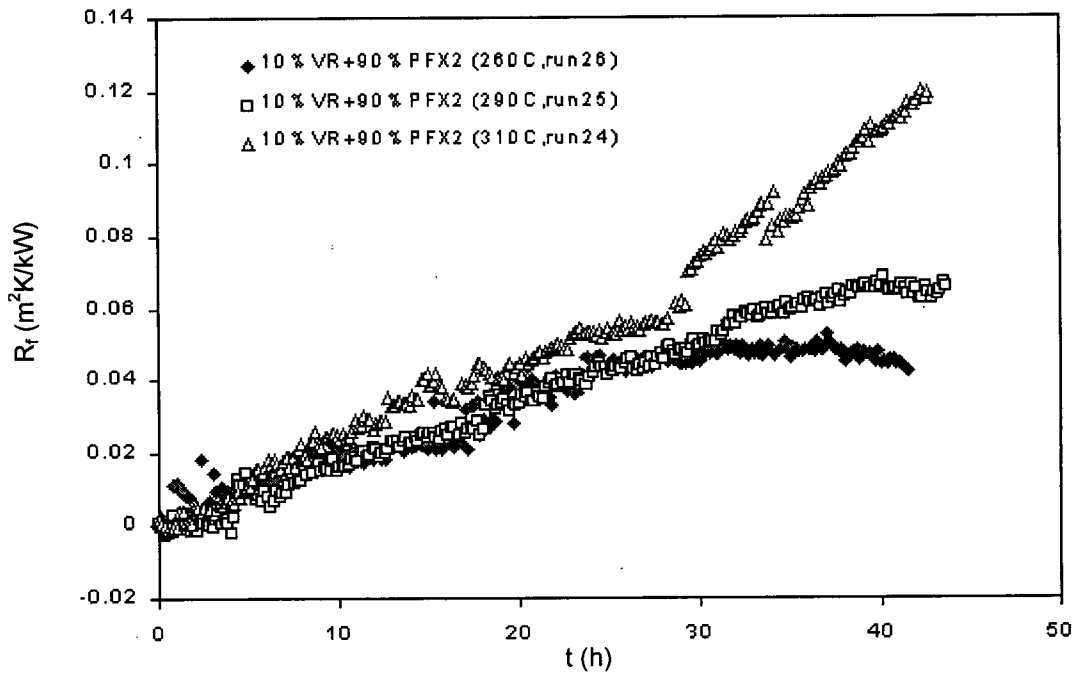


Figure 6.8 Surface Temperature Effect on Thermal Fouling Runs Using the Mixture of 10%VR and 90% PFX2

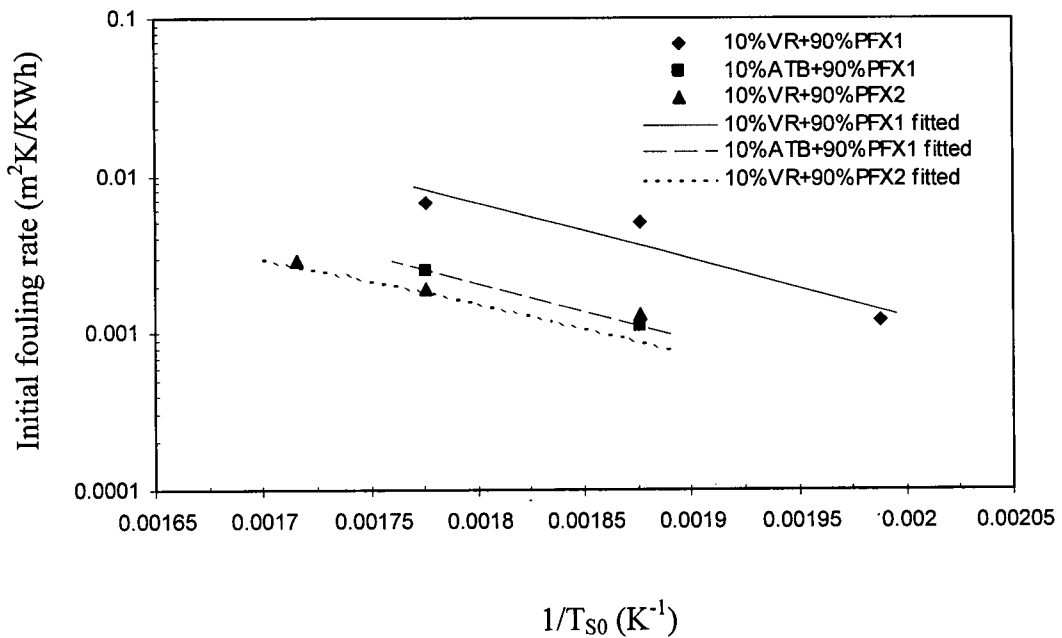


Figure 6.9 Dependence of Initial Fouling Rate on Surface Temperature

Table 6.5 Curve Fitting Parameters from Arrhenius Type Plot

Test fluids	A	$E_{act}$ (kJ/mol)	Initial surface temperature range, $T_{s0}$ (°C)
10%VR+90%PFX1	20018	68.8	230-290
10%ATB+90%PFX1	5402.5	68.3	260-290
10%VR+90%PFX2	4135.3	68.5	260-310

Table 6.6 Simulated Distillation Data for PFX1 and PFX2 (ASTM D2887)

	PFX1 (°C)	PFX2 (°C)
IBP	293	279
1wt%	299	287
10wt%	324	314
20wt%	335	325
30wt%	344	334
40wt%	351	342
50wt%	358	349
60wt%	366	355
70wt%	374	362
80wt%	384	370
90wt%	400	383
99wt%	465	429
FBP	493	443

Table 6.7 PNA Analysis for PFX1 and PFX2 (ASTM D2786, 3239)

PNA results		PFX1	PFX2
Paraffins (wt%)		34.7	23.0
Naphthenes ( total, wt%)		65.3	77.0
Naphthenes (wt%)	1-ring naphthene	21.6	21.1
	2-ring naphthene	20.6	22.1
	3-ring naphthene	12.7	17.6
	4-ring naphthene	8.1	12.5
	5-ring naphthene	2.3	3.7

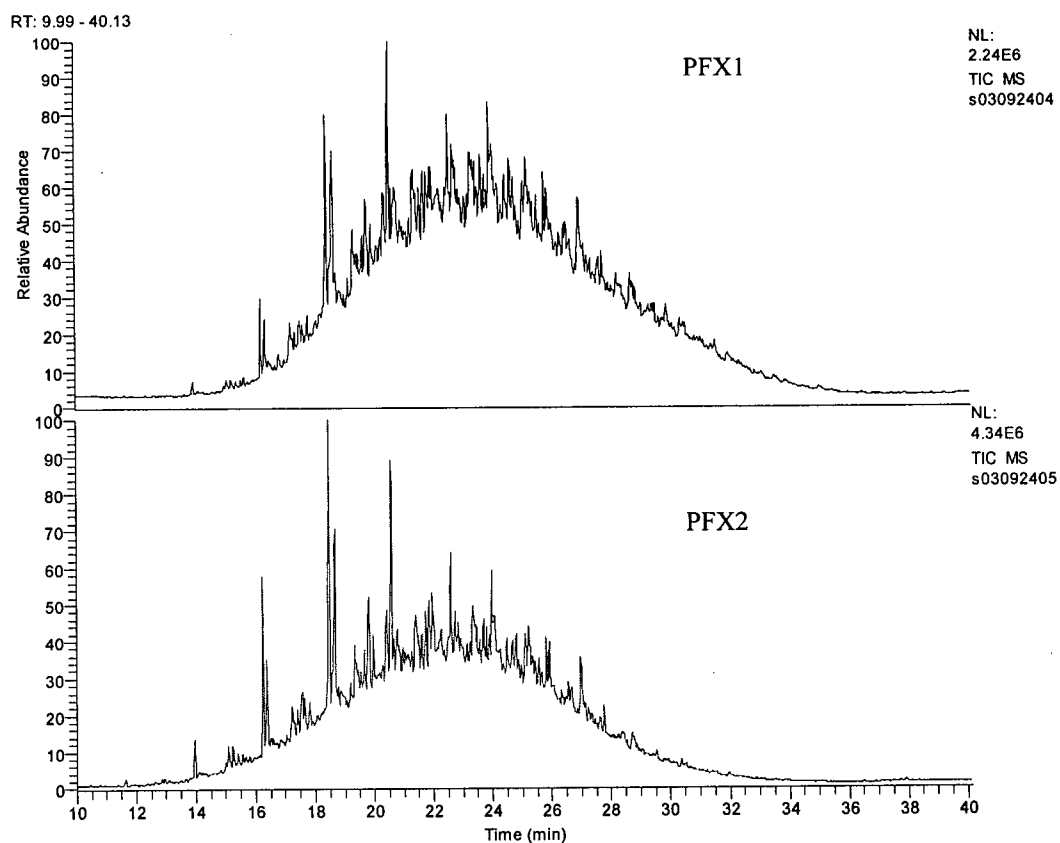


Figure 6.10 Total Ion Chromatogram (TIC) for PFX1 and PFX2

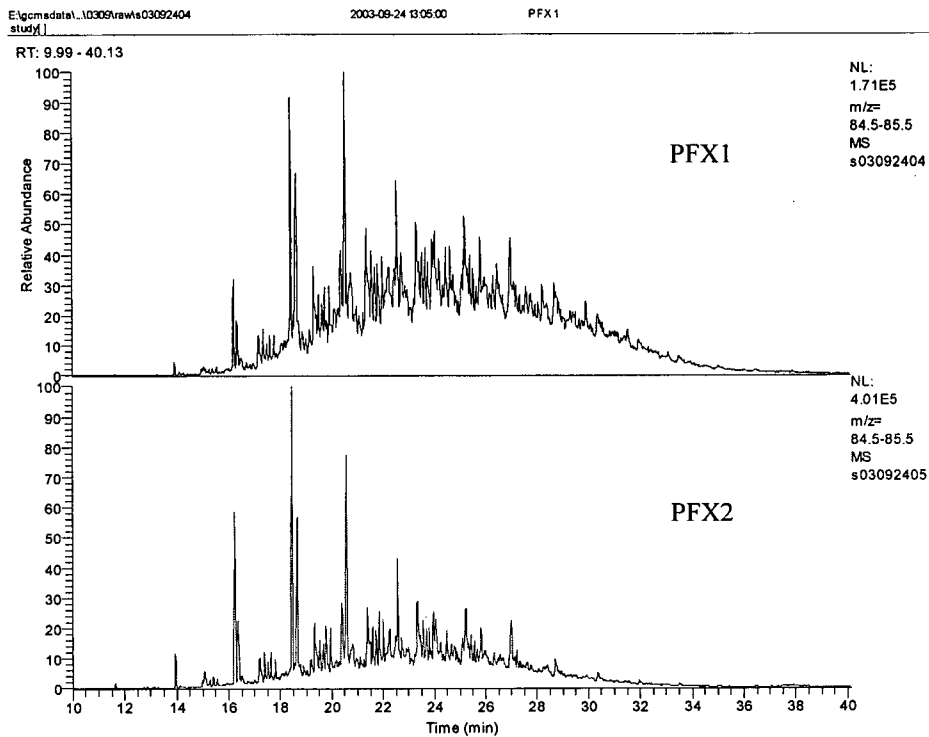


Figure 6.11 Selected Ion Chromatogram of m/z85 (Paraffins)

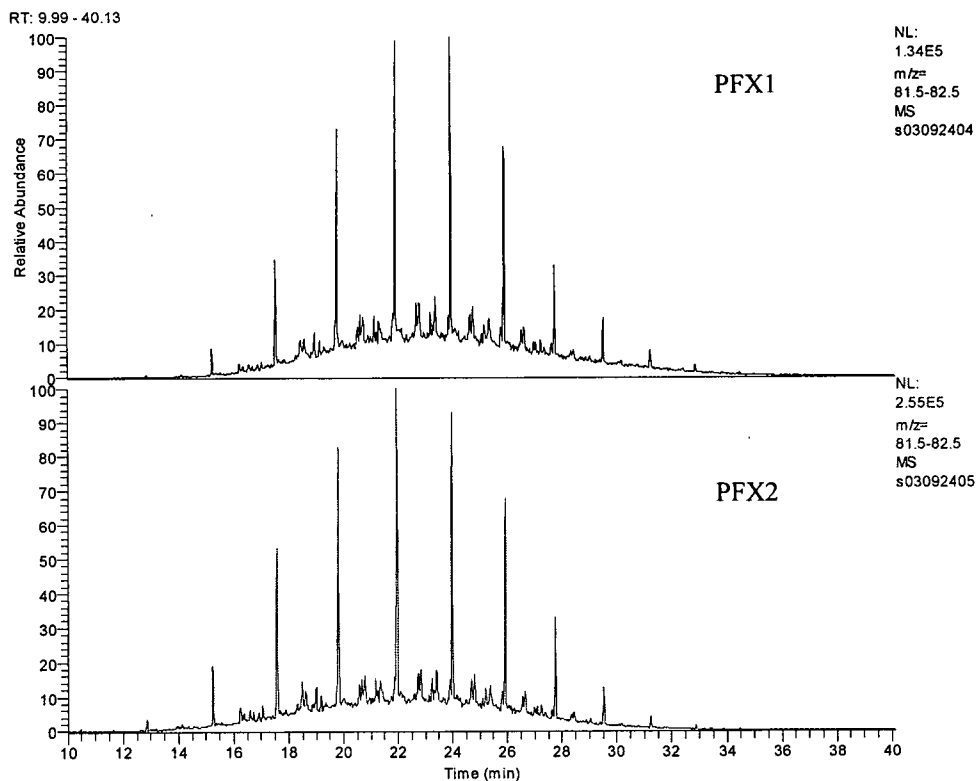


Figure 6.12 Selected ion chromatogram of m/z82 (Naphthenes)

### 6.3 Deposit Characterization

Thermal fouling deposits for selected runs were characterized by elemental analysis, thermogravimetric analysis (TGA), and scanning electron microscopy with energy dispersion X-ray (SEM-EDX). Deposit analyses were compared with results for selected insolubles recovered by hot filtration of the blends used in fouling, and for the selected n-heptane insolubles.

#### 6.3.1 Elemental Analysis of Deposits

Table 6.8 shows the elemental analysis results for the thermal fouling deposits, the insolubles recovered by hot filtration of the blends used in fouling and the n-heptane insolubles. The hot filtration insolubles and the n-heptane insolubles from VR and ATB show identical H/C ratios of 1.1-1.2, which is close to the reported value of 1.1 for Cold Lake asphaltenes [129]. The results show that the H/C ratios were very high for the fouling deposits originating from ATB (1.51-1.70), and much lower for the deposits and the precipitates (0.94-1.20) originating from VR. The higher H/C ratios for the ATB deposits suggest that some PFX is incorporated in the ATB deposits in spite of the rinsing step incorporated in the procedure. Physically, deposits from ATB appeared thick and loose, and were easily removed; while those from VR were thin and hard, and were firmly attached. In most cases the latter deposits could only be removed by scraping with a sharp blade. The high H/C ratios for ATB deposits are closer to the H/C ratios of 1.4 to 1.5 quoted by Asomaning [54] for the fouling deposits originating from Cold Lake heavy oil, where the possibility of contamination of the fouling deposits by the test solution was mentioned. The sulphur and nitrogen contents of the deposits from ATB are also considerably below those of the hot filtration insolubles and the n-heptane insolubles. This also suggests that the PFX1 which has non-detectable levels of S and N (Table 3.4) contributes to the deposit. For the VR deposits, S and N values are roughly similar to those of the hot filtration insolubles and n-heptane insolubles.

Table 6.8 Elemental Analysis of Fouling Deposits and Solids from Hot Filtration and Precipitation Tests

Solids type	C (%)	H (%)	S (%)	N (%)	H/C
Fouling Deposit (290°C, run10) 10%ATB+90%PFX1	72.78	9.18	2.30	0.49	1.51
Fouling Deposit (290°C, run16) 10%ATB+0.1%REF+89.9%PFX1	75.00	10.64	1.91	0.36	1.70
Hot filtration Insolubles, 10%ATB+90%PFX1	72.06	7.08	6.43	1.41	1.18
ATB-Heptane Insolubles	77.69	7.75	5.61	1.17	1.20
Fouling Deposit (260°C, run3) 10%VR+90%PFX1	80.49	7.03	5.73	0.95	1.05
Fouling Deposit (290°C, run17) 10%VR+90%PFX1	82.48	8.16	4.35	0.94	1.19
Fouling Deposit (310°C, run24) 10%VR+90%PFX2	82.63	6.45	5.46	1.03	0.94
Hot Filtration Insolubles, 10%VR+90%PFX2	80.63	7.40	6.08	1.12	1.10
VR-Heptane Insolubles	81.21	7.95	5.63	0.97	1.17

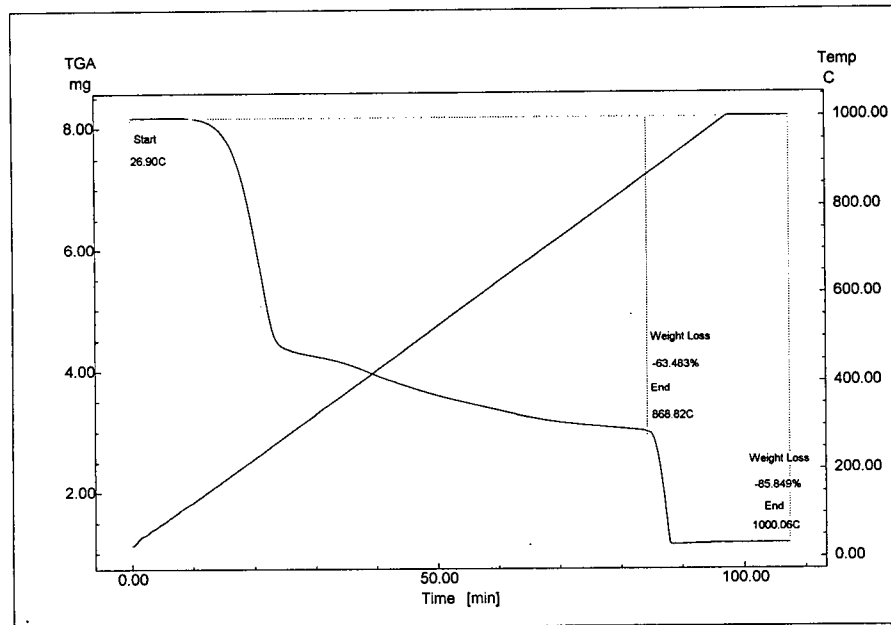
### 6.3.2 Thermo-gravimetric Analysis

Thermo-gravimetric analyses (TGA) were also done for the thermal fouling deposits, the insolubles recovered by hot filtration of the blends used in fouling and the n-heptane insolubles. The TGA test was conducted in a nitrogen atmosphere with a flow rate of 50ml/min and a

heating rate of 10°C /min. The weight loss at 850°C is termed the volatiles; the remainder is the fixed carbon plus ash. After the temperature reached 850°C, the oxygen supply was turned on to burn off the fixed carbon. The temperature was then raised to 1000°C and held for 10 minutes yielding the ash. This procedure gives a “proximate analyses” such as is commonly used in the coal industry. Figure 6.13 shows the TGA curves for the deposits from a run of 10%ATB-90%PFX1 and 10%VR-90%PFX1 at 290°C initial surface temperature. A period of gradual weight loss was observed for both cases, during which 55-65% of the weight of the sample was lost. After the oxygen supply was turned on, a further weight loss was observed when the fixed carbon was burnt leaving a residue of ash.

The TGA results are summarized in Table 6.9. For ATB samples, volatiles for the fouling deposits were 64-79%, compared to 50-57% for the hot filtration insolubles and n-heptane insolubles. The high volatiles content for the ATB fouling deposits is in agreement with the results of the elemental analysis (high H/C ratio for ATB deposits) and further indicate that some PFX is incorporated in the deposits. The high ash content for ATB (7.7-14.2%) deposits suggests that inorganic particulates in the bulk fluid are incorporated into the deposit or that the heteroatoms, combine with some components of the solids to form inorganics salts on the probe surface. The deposit ash content with ATB are consistent with the results of Asomaning [54], who found ash contents of 13.45 to 26.97 wt%. For the VR samples, volatiles in the deposits were much lower than for ATB, ranging from 38-57%, and were close to those of the hot filtration insolubles and n-heptane insolubles. Ash contents were uniformly low at 1.3-4.3%. These low ash contents probably reflect the source of the fouling oil-VR is produced by steam stimulation, and is low in clays and ash content, whereas ATB originates in a mining operation, which is known to produce fine clays in the bitumen, and accompanying higher ash content, as shown in Section 3.1.

(a)



(b)

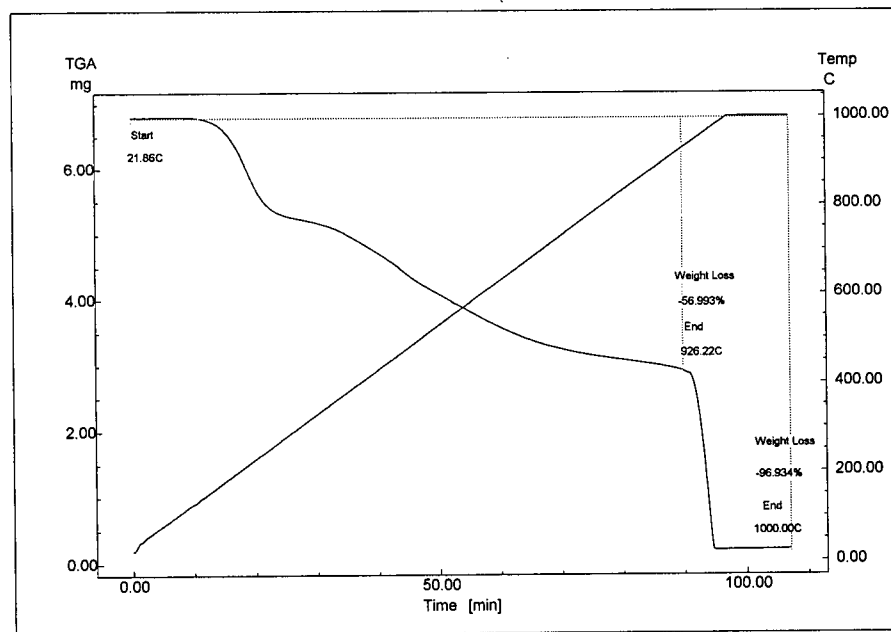


Figure 6.13 Thermo-Gravimetric Analysis (TGA) Curves for (a) Fouling Deposits from 10%ATB-90%PFX1 at  $T_{s0}=290^{\circ}\text{C}$ , (b) Fouling Deposits from 10%VR-90%PFX1 at  $T_{s0}=290^{\circ}\text{C}$ .

Table 6.9 Thermal Analysis of Fouling Deposits and Solids from Hot Filtration and Precipitation Tests

Solid Type	Moisture and Volatiles, wt%	Fixed Carbon and Ash, wt%	Fixed Carbon, wt%	Ash wt%
Fouling Deposit (290°C, run10) 10%ATB+90%PFX1	63.5	36.5	22.3	14.2
Fouling Deposit (290°C, run16) 10%ATB+0.1%REF+89.9%PFX1	79.3	20.7	13.0	7.7
Hot filtration insolubles, 10%ATB+90%PFX1	50.5	49.5	39.4	10.1
ATB-heptane insolubles	57.7	42.3	32.9	4.7
Fouling Deposit (260°C, run3) 10%VR+90%PFX1	45.4	54.6	-	-
Fouling Deposit (290°C, run17) 10%VR+90%PFX1	57.0	43.0	39.9	3.1
Fouling Deposit (310°C, run24) 10%VR+90%PFX2	37.6	62.4	61.1	1.3
Hot filtration insolubles, 10%VR+90%PFX2	46.7	53.3	49.0	4.3
VR-heptane insolubles	57.7	42.3	40.1	2.2

### 6.3.3 Scanning Electron Microscopy

The thermal fouling deposits, the insolubles recovered by hot filtration of the blends used in fouling and the n-heptane insolubles were further analyzed by scanning electron microscopy with energy dispersion X-ray (SEM-EDX). The EDX analyzer generates peaks of elements present at specific locations of observation on the surface of the sample. These may differ significantly from bulk chemical analyses. As well, hydrogen is not detected. EDX analysis can quantify the elements it detects. A quantitative analysis can be performed by a standard or standardless analysis. A standardless analysis is generally used, which quantifies the elements by calculating the area under the peak of each identified elements and after taking account for the accelerating voltage of the beam to produce the spectrum, performs calculations to create sensitivity factors that will convert the area under the peak into weight or atomic percent.

Figure 6.14-6.16 show SEM micrographs of fouling deposits from the runs of 10%ATB-90%PFX1, 10%VR-90%PFX1 at 290°C initial surface temperature and 10%VR-90%PFX2 at 310°C initial surface temperature. Figure 6.17 and Figure 6.18 show SEM micrographs of hot filtration insolubles from 10%ATB-90%PFX1 and 10%VR-90%PFX2 blends at 85°C. The fouling deposits and hot filtration solids show significant differences in their microstructure under SEM for both VR and ATB. The hot filtration solids show fine grain-mosaic structure while the fouling deposits show some coarse grain-mosaic structure and some degree of spherical agglomeration.

Figure 6.19 and Figure 6.20 show the EDX plots for the fouling deposits from the runs of 10%ATB-90%PFX1 and 10%VR-90%PFX1 at 290°C initial surface temperature. All peaks are included in the data. The EDX results show noticeable silicon (2.7%) and aluminium (2.1%) content for the deposits originating from ATB, which indicates that clay particles may be present in ATB and contribute to the fouling of ATB blends. This is consistent with results

from the thermal analysis, where the high ash content was found for ATB deposits. For the VR deposit (Figure 6.20), no silicon or aluminum is found. Table 6.10 show EDX results for all the tested fouling deposits, hot filtration insolubles and the n-heptane insolubles. The values shown in each category are averages for several spots or areas of each sample. Again, silicon and aluminium are present for all ATB solids, but are absent for all VR- originating solids.

(a)



(b)

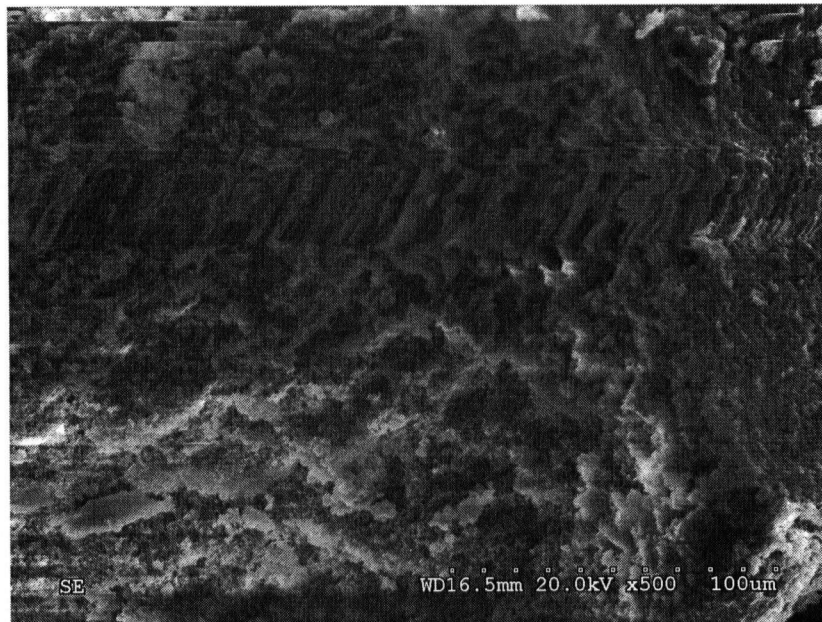


Figure 6.14 SEM Micrographs of Fouling Deposits from the Runs of 10%ATB-90%PFX1 at 290°C Initial Surface Temperature, (a) 45 times, (b) 500 times.

(a)



(b)

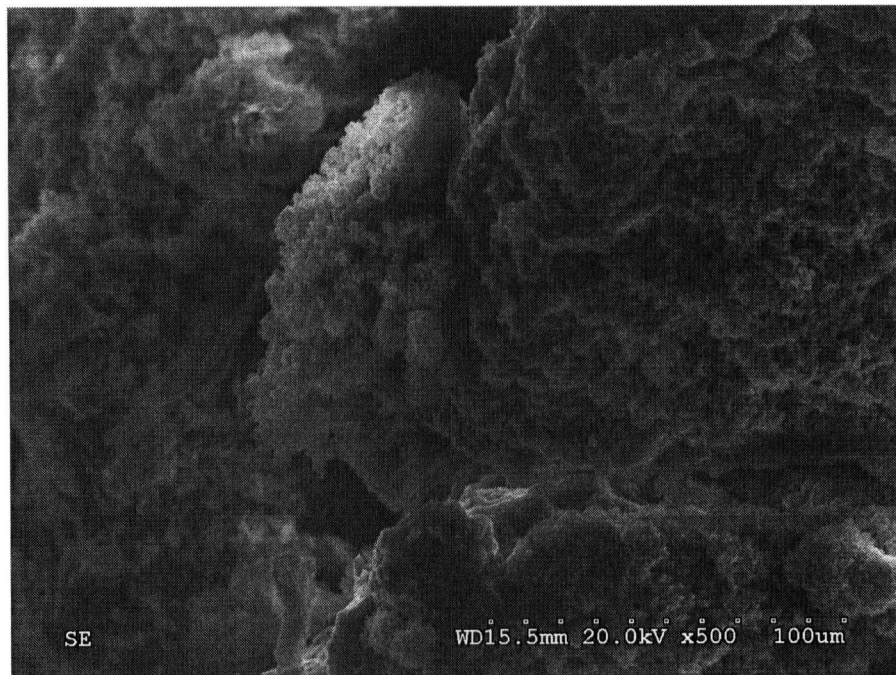


Figure 6.15 SEM Micrographs of Fouling Deposits from the Runs of 10%VR-90%PFX1 at 290°C Initial Surface Temperature, (a) 45 times, (b) 500 times.

(a)



(b)

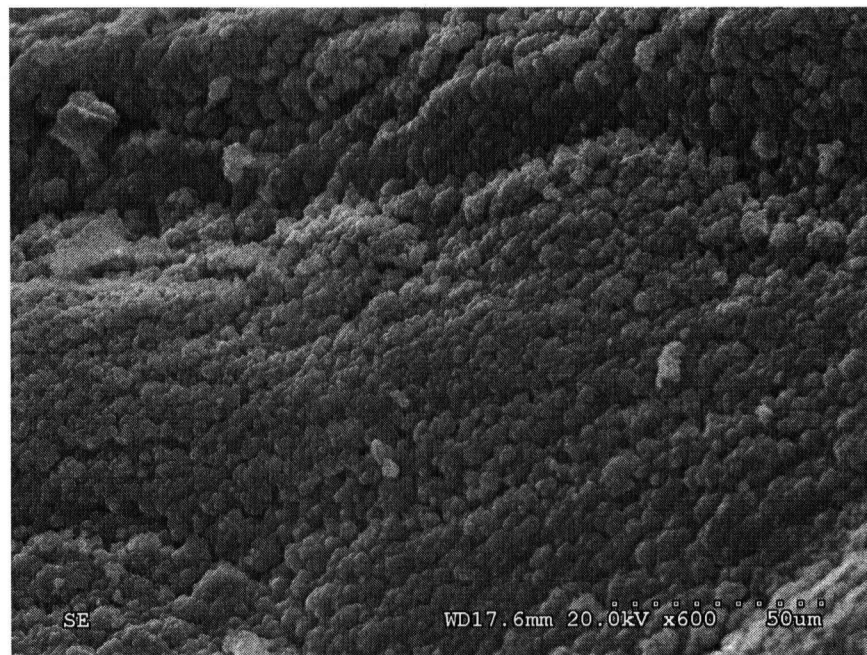
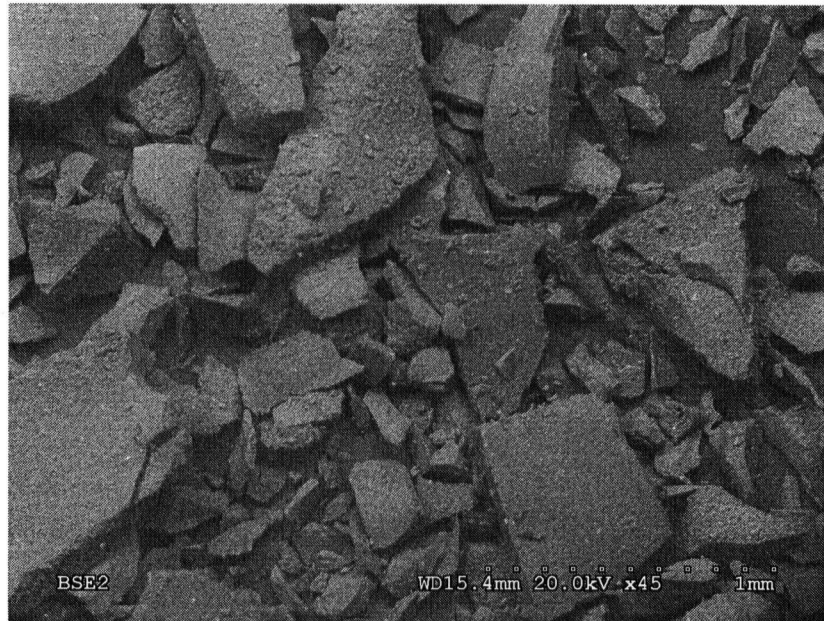


Figure 6.16 SEM Micrographs of Fouling Deposits from the Runs of 10%VR-90%PFX2 at 310°C Initial Surface Temperature, (a) 45 times, (b) 500 times.

(a)

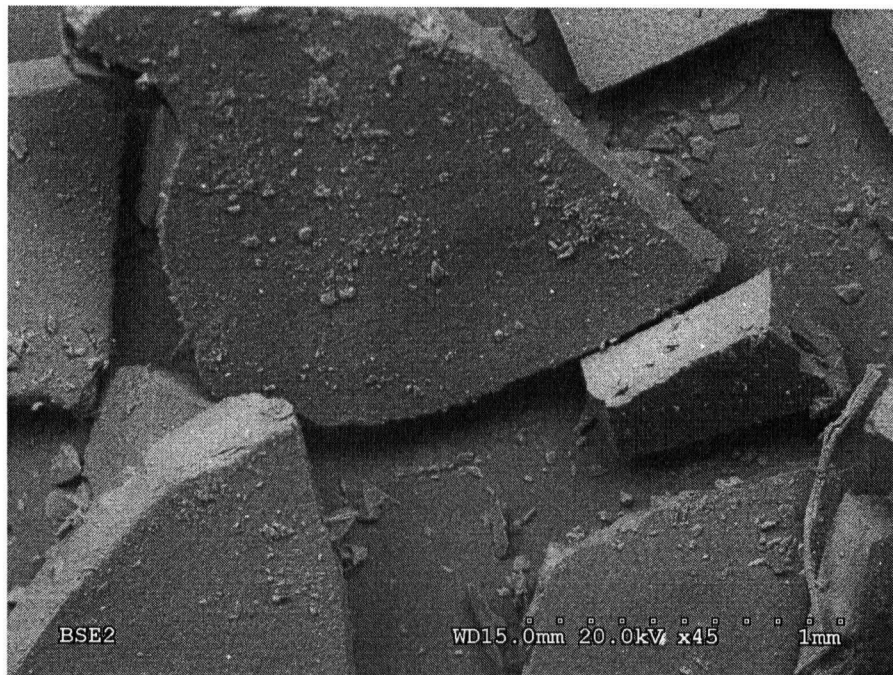


(b)



Figure 6.17 SEM Micrographs of Hot Filtration Insolubles from 10%ATB-90%PFX1 Blends at 85°C, (a) 45 times, (b) 500 times.

(a)



(b)

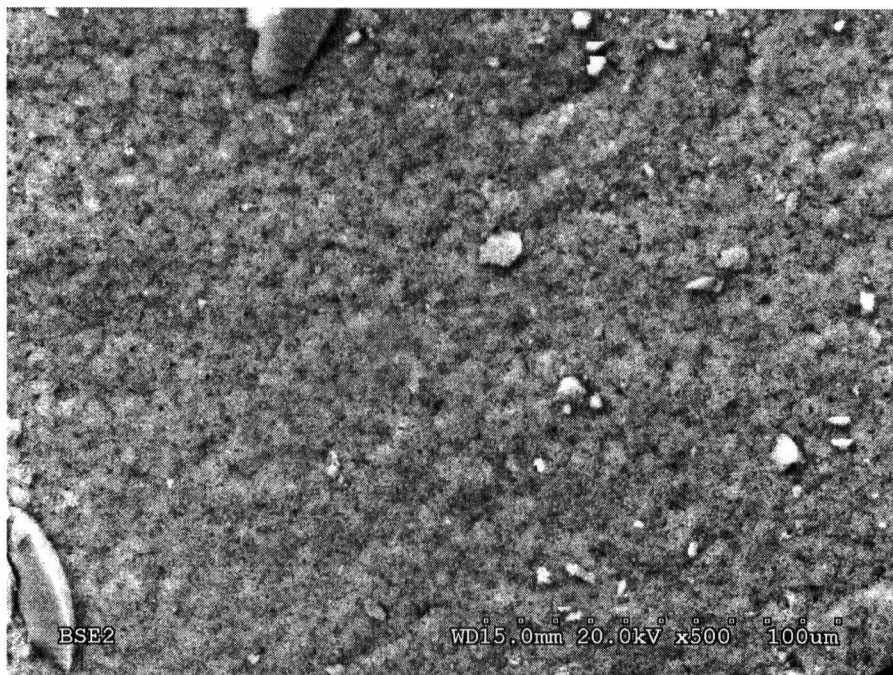
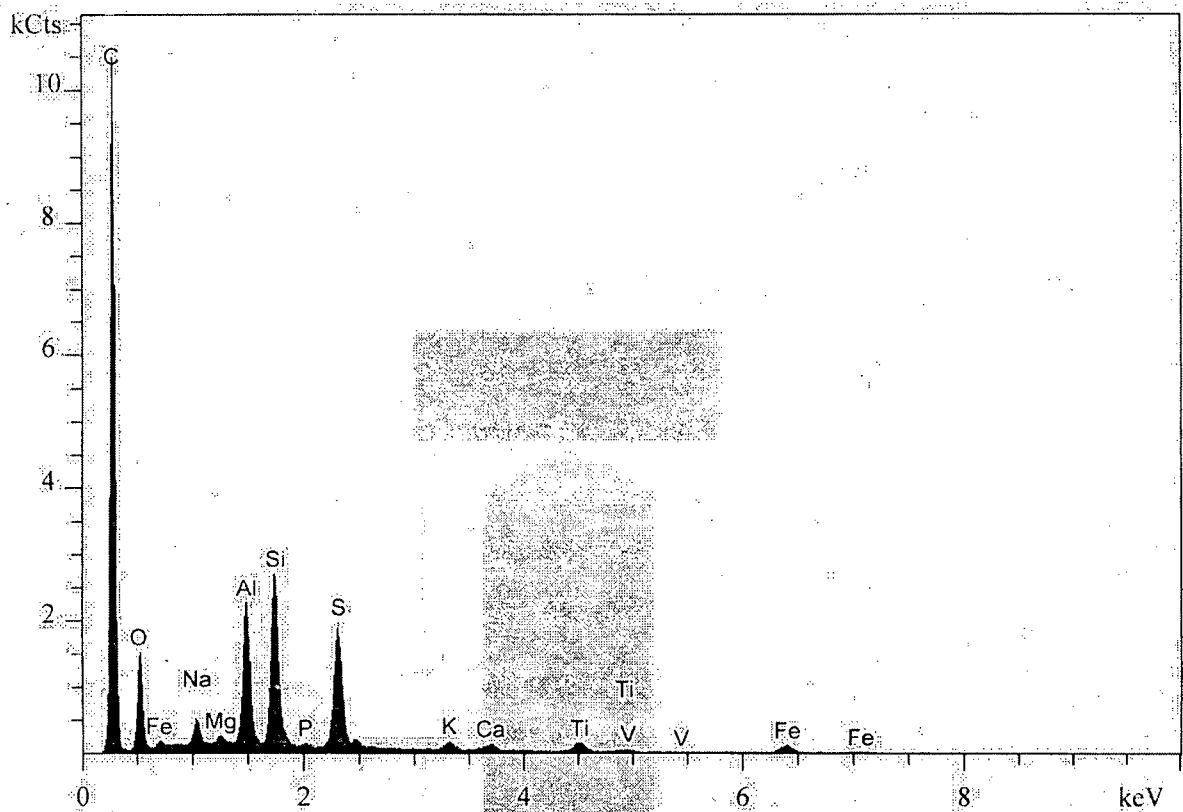


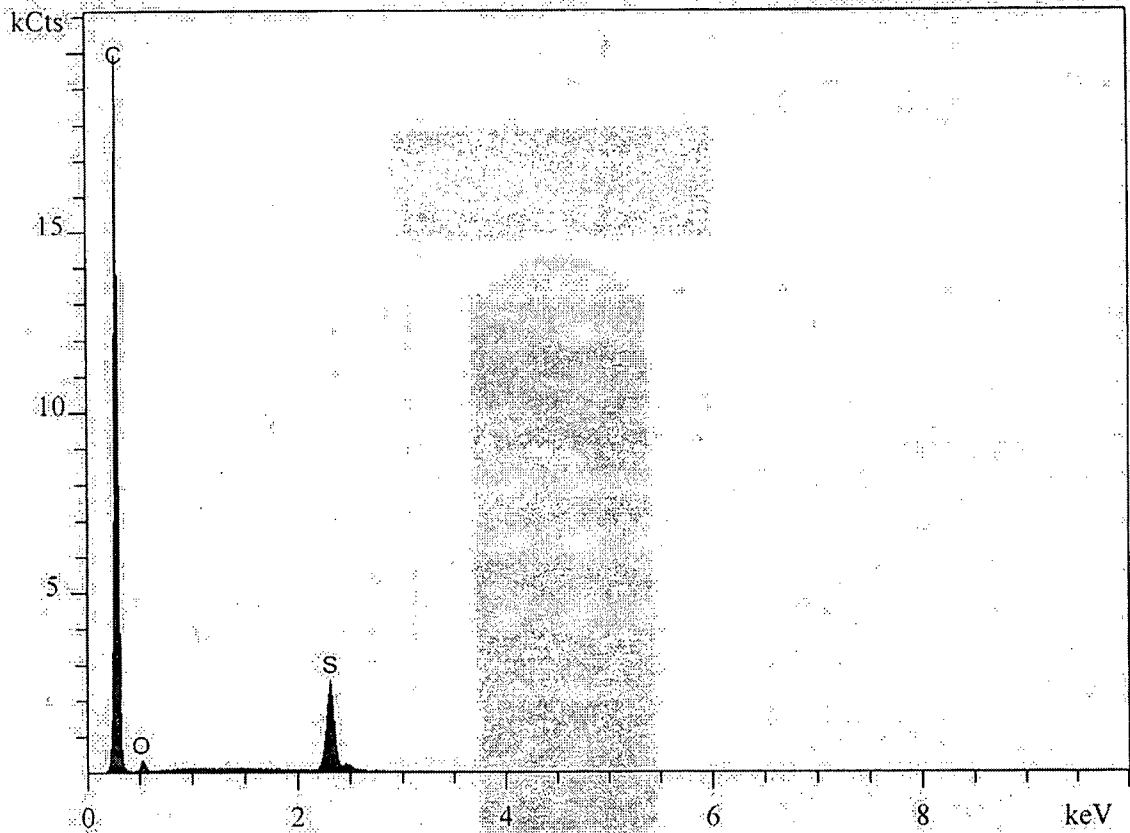
Figure 6.18 SEM Micrographs of Hot Filtration Insolubles from 10%VR-90%PFX2 Blends at 85°C, (a) 45 times, (b) 500 times.



Line	Method	Intensity	K-ratio	ZAF	Concentration	2 Sigma	Z	A	F
C KA	PRZ	578.87	0.272	2.617	71.31 wt%	0.52 wt%	0.974	2.689	1.000
O KA	PRZ	94.42	0.024	8.051	19.34 wt%	0.37 wt%	1.027	7.843	1.000
Na KA	PRZ	33.49	0.003	2.521	0.74 wt%	0.03 wt%	1.130	2.234	0.999
Mg KA	PRZ	13.74	0.001	1.810	0.20 wt%	0.02 wt%	1.109	1.637	0.997
Al KA	PRZ	175.80	0.014	1.517	2.10 wt%	0.03 wt%	1.149	1.324	0.997
Si KA	PRZ	226.52	0.020	1.343	2.66 wt%	0.04 wt%	1.122	1.200	0.998
P KA	PRZ	4.41	0.000	1.319	0.06 wt%	0.01 wt%	1.165	1.136	0.997
S KA	PRZ	172.67	0.019	1.214	2.27 wt%	0.04 wt%	1.140	1.066	0.999
K KA	PRZ	11.30	0.002	1.192	0.19 wt%	0.02 wt%	1.198	0.997	0.998
Ca KA	PRZ	8.95	0.001	1.158	0.16 wt%	0.02 wt%	1.175	0.988	0.998
Ti KA	PRZ	15.26	0.003	1.264	0.37 wt%	0.03 wt%	1.294	0.979	0.998
V KA	PRZ	0.80	0.000	1.292	0.02 wt%	0.03 wt%	1.326	0.978	0.997
Fe KA1	PRZ	9.03	0.004	1.288	0.58 wt%	0.04 wt%	1.315	0.980	1.000

Normalized Factor: 1

Figure 6.19 EDX Plot for the Fouling Deposit from a Run of 10%ATB-90%PFX1 at 290°C Initial Surface Temperature.



Line	Method	Intensity	K-ratio	ZAF	Concentration	2 Sigma	Z	A	F
C KA	PRZ	1088.14	0.532	1.709	90.85 wt%	0.47 wt%	0.992	1.724	1.000
O KA	PRZ	22.75	0.006	10.173	6.11 wt%	0.25 wt%	1.045	9.732	1.000
S KA	PRZ	234.25	0.026	1.151	3.04 wt%	0.04 wt%	1.161	0.992	1.000
Normalized Factor			1						

Figure 6.20 EDX Plot for the Fouling Deposit from a Run of 10%VR-90%PFX1 at 290°C Initial Surface Temperature.

Chapter 6: Thermal Fouling Experimental Results and the Correlation to Stability Criteria

Table 6.10 SEM-EDX Analysis of Fouling Deposits and Solids from Hot Filtration and Precipitation Test \*

Solid Type	C wt%	O wt%	S wt%	Si wt%	Al wt%	Fe wt%	Na wt%	Ti wt%	Mg wt%	K wt%	Ca wt%	P wt%	V wt%
Fouling Deposit (290°C, run10) 10%ATB+90%PFX1	73.62	17.49	2.16	2.52	2.17	0.50	0.63	0.31	0.25	0.12	0.15	0.05	0.03
Fouling Deposit (290°C, run16) 10%ATB+0.1%REF+89.9%PFX1	80.25	9.56	3.52	2.36	1.89	0.93	-	0.77	-	0.42	0.30	-	-
Hot filtration insolubles, 10%ATB+90%PFX1	80.07	17.22	1.63	0.57	0.51	-	-	-	-	-	-	-	-
ATB-heptane insolubles	85.26	13.64	0.78	0.12	0.20	-	-	-	-	-	-	-	-
Fouling Deposit (260°C, run3) 10%VR+90%PFX1	89.33	8.69	1.98	-	-	-	-	-	-	-	-	-	-
Fouling Deposit (290°C, run17) 10%VR+90%PFX1	90.29	6.20	3.51	-	-	-	-	-	-	-	-	-	-
Fouling Deposit (310°C, run24) 10%VR+90%PFX2	89.57	6.83	3.60	-	-	-	-	-	-	-	-	-	-
Hot filtration insolubles, 10%VR+90%PFX2	87.83	4.16	8.01	-	-	-	-	-	-	-	-	-	-
VR-heptane insolubles	87.26	8.95	3.79	-	-	-	-	-	-	-	-	-	-

\*: The values shown in each category are averages for several spots or areas of each sample.

## 6.4 Correlation of Thermal Fouling Data to Stability Criteria and Precipitation Data

### 6.4.1 Correlation of Thermal Fouling Data to the Andersen/Pedersen and the Wiehe Stability Criterion

It was shown previously by Al-Atar and Watkinson [130] for Cold Lake Heavy Oil as the source of the asphaltenes, that the fouling rate for blends under fixed conditions could be correlated with the Wiehe stability criterion. In that work, the values of  $S_{BN}$  and  $I_N$  were obtained by manual titrations, with flocculation point determined by microscopy, as originally proposed by Wiehe and Kennedy [13]. A separate study on crude oils by Brons and Rudy [131] also showed a correlation of extent of fouling and the Wiehe stability criterion. In the present work, the oils used in [130] were titrated automatically, and the trends of fouling rate with stability confirmed.

Additional fouling data were taken in the present study, using both Athabasca and Cold Lake oils with a selection of conditions given in Table 6.1, which were chosen to cover both stable and non-stable blends. Plots of the extent of fouling at 40 hours and the initial fouling rate versus stability criteria are shown in Figure 6.21 and 6.22 for blends using Athabasca Atmospheric Tower Bottoms, in which the asphaltene concentration was held constant at 1.35 % and the initial surface temperature was 290°C, and in Figure 6.23 and 6.24 for diluted Cold Lake Vacuum Residue, where the asphaltene concentration was 1.77 %, and the initial surface temperature was 260°C. Good correlations of extent of fouling at ~ 40 hours and the initial fouling rate with the stability criterion are obtained for both ATB and VR blends. As expected from the data of Figure 5.5, the Andersen/Pedersen stability model gives a similar good correlations.

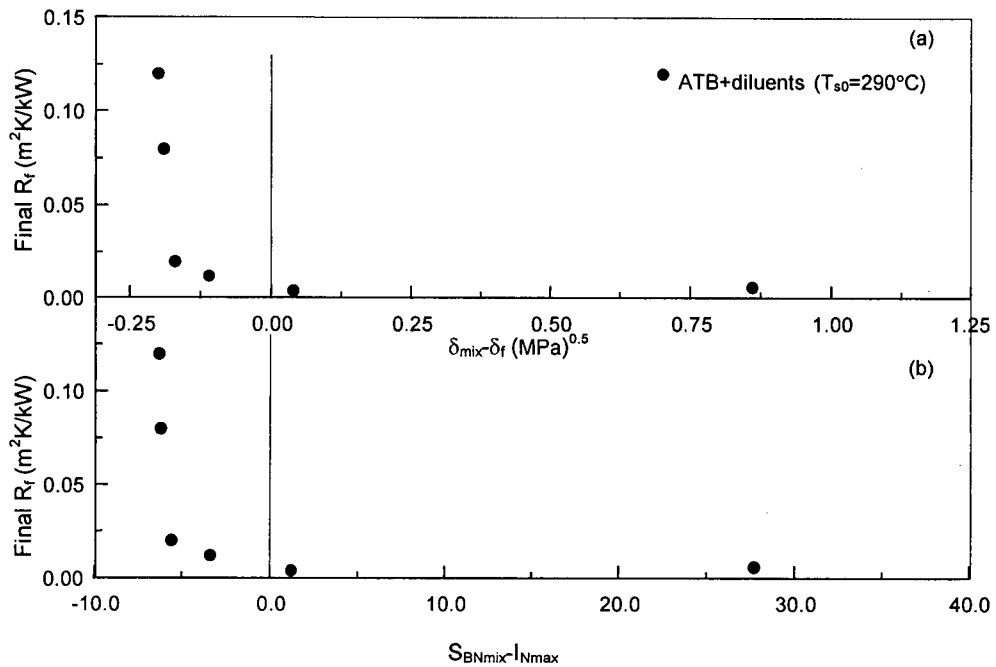


Figure 6.21 Final Fouling Resistance Versus (a) the Andersen Stability Criterion, (b) the Wiehe Stability Criterion for ATB and Various Diluents (n-Heptane as titrant, 25°C).

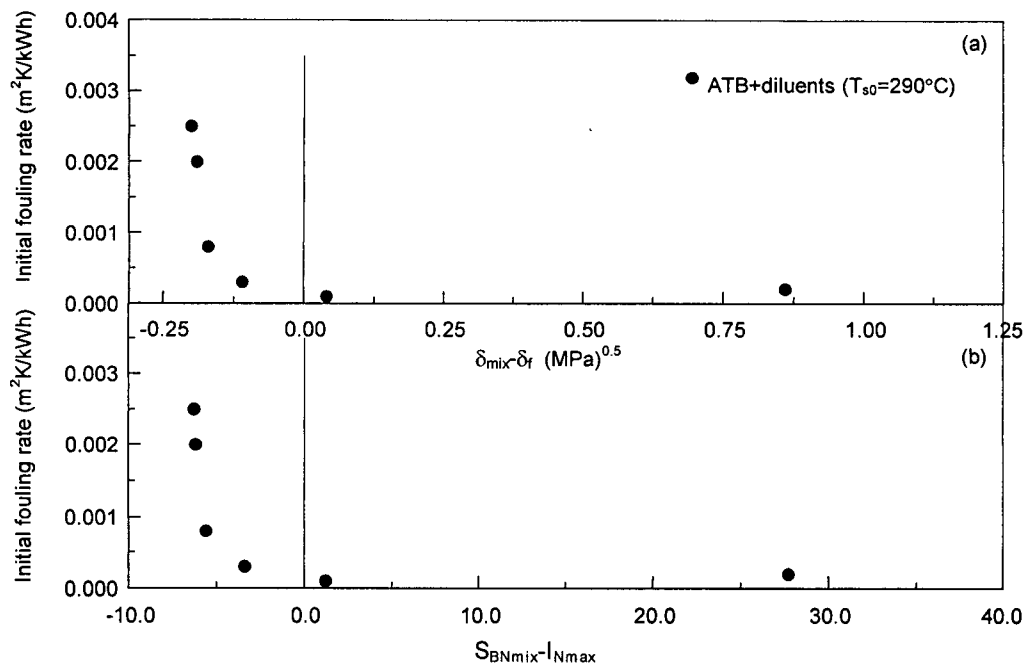


Figure 6.22 Initial Fouling Rate versus (a) the Andersen Stability Criterion, (b) the Wiehe Stability Criterion for ATB and Various Diluents (n-Heptane as Titant, 25°C).

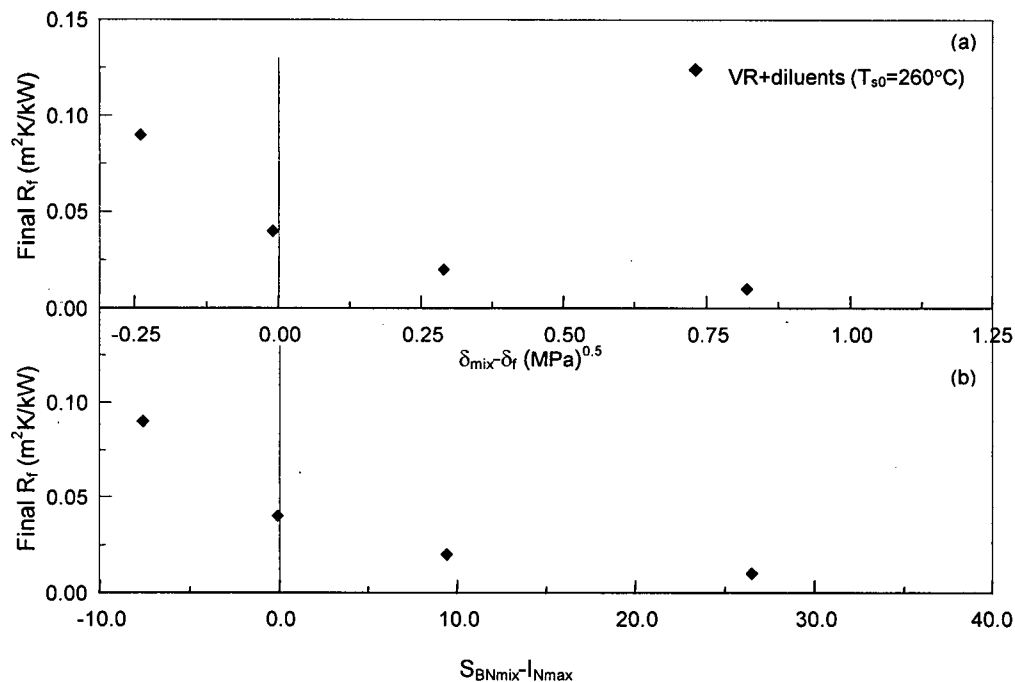


Figure 6.23 Final Fouling Resistance versus (a) the Andersen Stability Criterion, (b) the Wiehe Stability Criterion for VR and Various Diluents (n-Heptane as Titrant, 25°C).

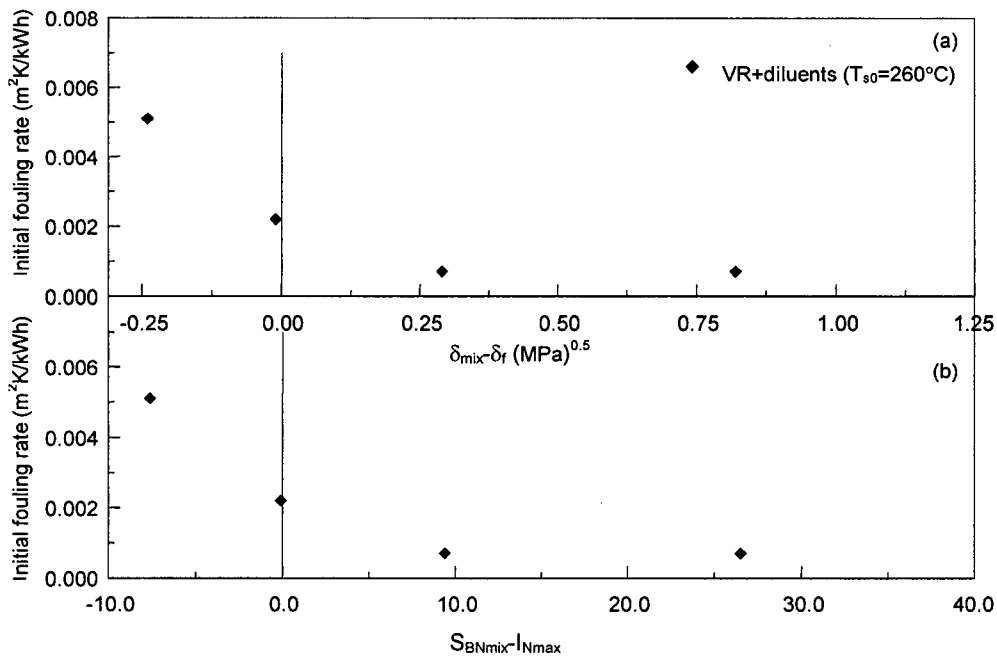


Figure 6.24 Initial Fouling Rate versus (a) the Andersen Stability Criterion, (b) the Wiehe Stability Criterion for VR and Various Diluents (n-Heptane as Titrant, 25°C).

### **6.4.2 Temperature Effect on the Stability Criterion**

As mentioned previously, the hot filtration and fouling tests were conducted at higher temperature (85°C) than the titration experiment (25°C). The temperature effect on solubility parameter was then investigated (25-50°C). The Andersen stability criterion at higher temperature (35°C and 50°C) was then re-calculated and applied for the correlation with initial fouling rate. The results are shown in Table 6.11, Figure 6.25 and Figure 6.26. At the higher temperature of 35°C and 50°C, the stability criteria line was shifted to the right, as shown in Figures 6.25 and Figure 6.26, giving an improved prediction for the “no fouling” region, especially for the VR blends.

Table 6.11 Solubility Parameter for the Mixtures of Thermal Fouling Experiments

Test fluid	Heat flux (kW/m <sup>2</sup> )	Initial fouling rate (m <sup>2</sup> K/kWh)	$\delta_{mix}$ [MPa] <sup>0.5</sup> (25°C)	$\delta_f$ [MPa] <sup>0.5</sup> (25°C)	$\delta_{mix}-\delta_f$ [MPa] <sup>0.5</sup> (25°C)	$\delta_{mix}$ [MPa] <sup>0.5</sup> (35°C)	$\delta_f$ [MPa] <sup>0.5</sup> (35°C)	$\delta_{mix}-\delta_f$ [MPa] <sup>0.5</sup> (35°C)	$\delta_{mix}$ [MPa] <sup>0.5</sup> (50°C)	$\delta_f$ [MPa] <sup>0.5</sup> (50°C)	$\delta_{mix}-\delta_f$ [MPa] <sup>0.5</sup> (50°C)
10%VR+90%PFX	262	0.0051	15.99	16.23	-0.24	15.71	16.04	-0.33	15.28	15.66	-0.38
10%VR+5%REF+85%PFX	248	0.0022	16.22	16.23	-0.01	15.93	16.04	-0.11	15.49	15.66	-0.17
10%VR+45%HVGO+45%PFX	257	0.0007	16.52	16.23	0.29	16.19	16.04	0.15	15.72	15.66	0.06
10%VR+90%HVGO	266	0.0007	17.05	16.23	0.82	16.67	16.04	0.63	16.17	15.66	0.51
10%ATB+90%PFX	316	0.0025	16.0	16.20	-0.2	15.73	16.0	-0.27	15.30	15.59	-0.29
10%ATB+0.1%REF+89.9%PFX	309	0.0020	16.01	16.20	-0.19	15.73	16.0	-0.27	15.30	15.59	-0.29
10%ATB+0.5%REF+89.5%PFX	310	0.0008	16.03	16.20	-0.17	15.75	16.0	-0.25	15.32	15.59	-0.27
10%ATB+2%REF+88%PFX	310	0.0003	16.09	16.20	-0.11	15.81	16.0	-0.19	15.38	15.59	-0.21
10%ATB+5%REF+85%PFX	308	0.0001	16.24	16.20	0.04	15.94	16.0	-0.06	15.50	15.59	-0.09
10%ATB+90%HVGO	326	0.0002	17.06	16.20	0.86	16.68	16.0	0.68	16.18	15.59	0.59

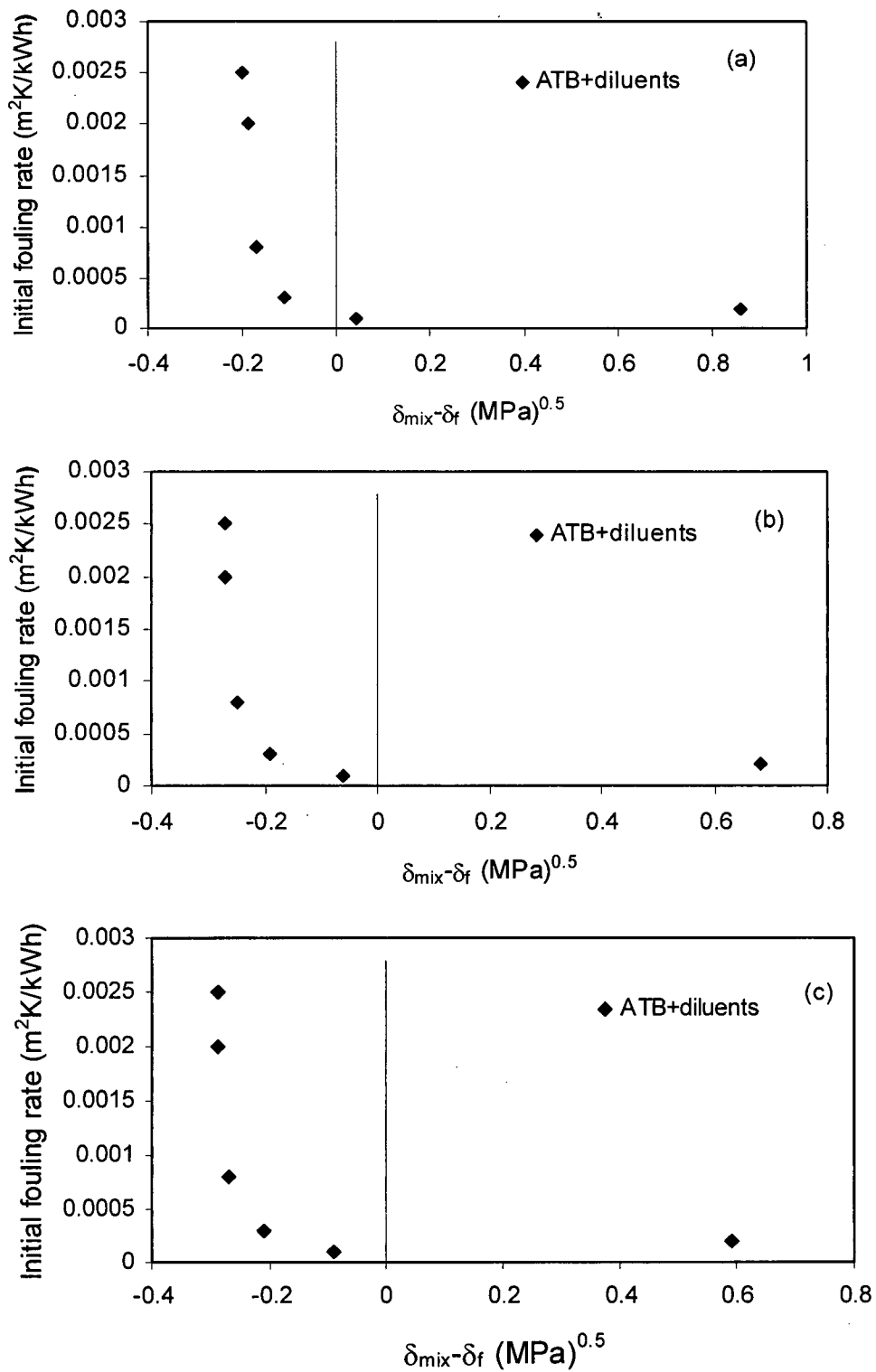


Figure 6.25 Correlation of Initial Fouling Rate with the Andersen Stability Criteria for ATB and Diluents with Solubility Parameters at (a) 25°C, (b) 35°C, and (c) 50°C

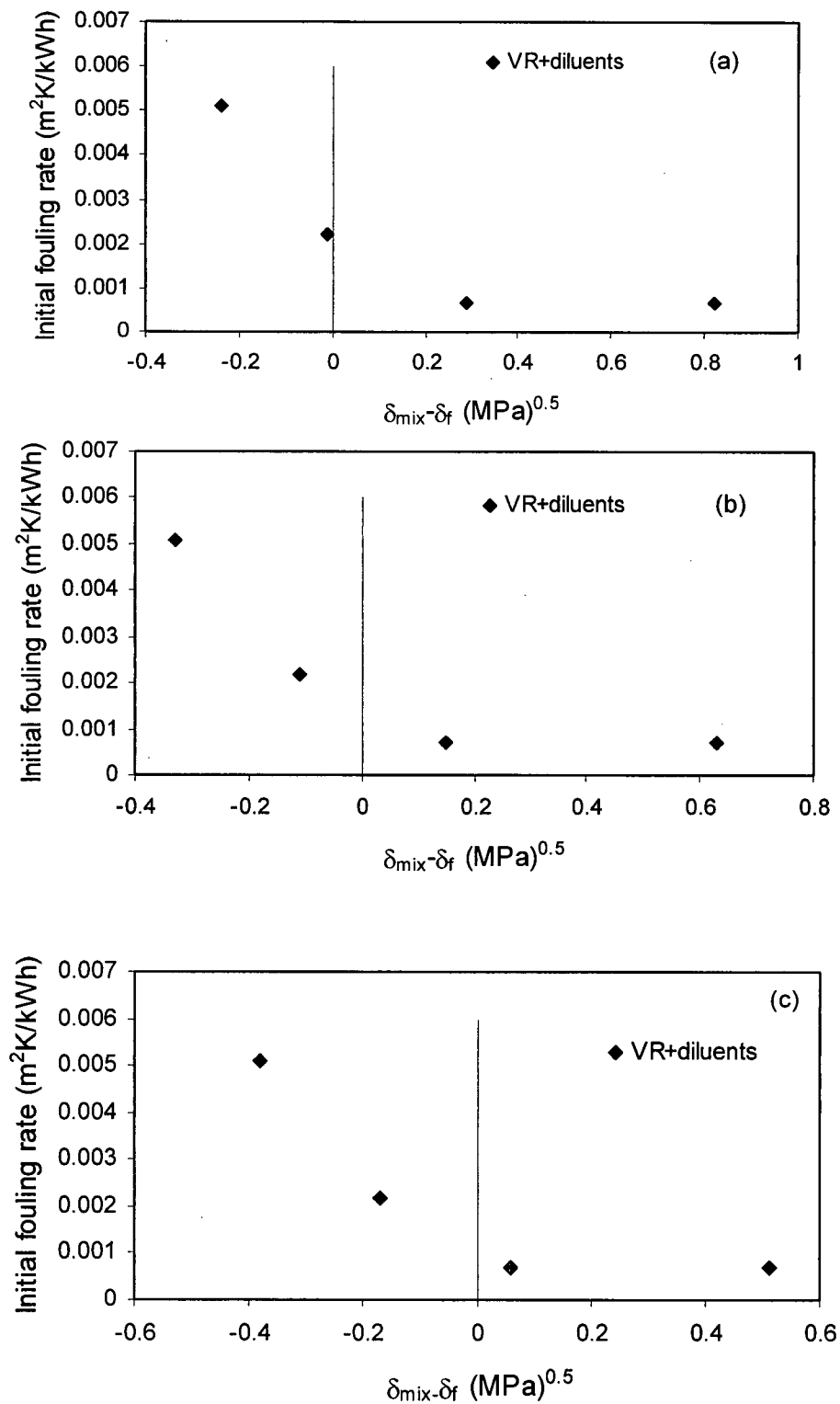


Figure 6.26 Correlation of Initial Fouling Rate with the Andersen Stability Criteria for VR and Diluents with Solubility Parameters at (a) 25°C, (b) 35°C, and (c) 50°C

### 6.4.3 Correlation of Thermal Fouling Data to Colloidal Instability Index

Petroleum asphaltenes are believed to exist in crude oils as a stable colloidal system made up of micelles in which the asphaltenes are peptized by resins and aromatics. Petroleum asphaltenes are held in a delicate balance that can be easily upset by the addition of saturates or the removal of resins or small ring aromatics.

As described previously (Section 5.2.3), the stability of petroleum fractions can be expressed by the Colloidal Instability Index (CII) [109, 132]. Figure 6.27 and Figure 6.28 show the correlation of initial fouling rate versus CII for both ATB and VR blends. As the CII ratio goes up, the initial fouling rate increases. However for ATB, fouling rates at CII below 10 were essentially negligible, and the number of data points was limited. For VR, a smooth trend of fouling rate with CII was obtained, approaching zero for  $CII < 2$ . The CII also correlates well with the amount of hot filtration insolubles, as mentioned in Chapter 5 (Figure 5.7). The good correlation between CII and the initial fouling rate support the fact that the fouling precursors are generated due to the instability or incompatibility of the test solution. It should be noted that for each asphaltene source in Figures 6.27 and 6.28, the asphaltene concentration in the blend is held constant. If the asphaltene concentration is changed, the curves may be expected to shift.

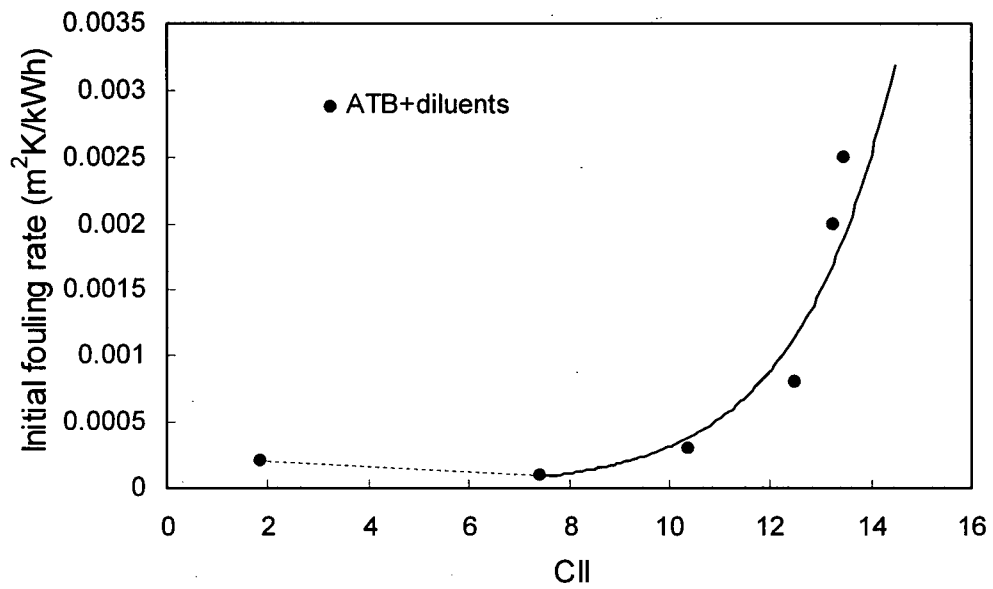


Figure 6.27 Correlation of Initial Fouling Rate with Colloidal Instability Index (CII) for ATB Blends with As=1.35 wt%.

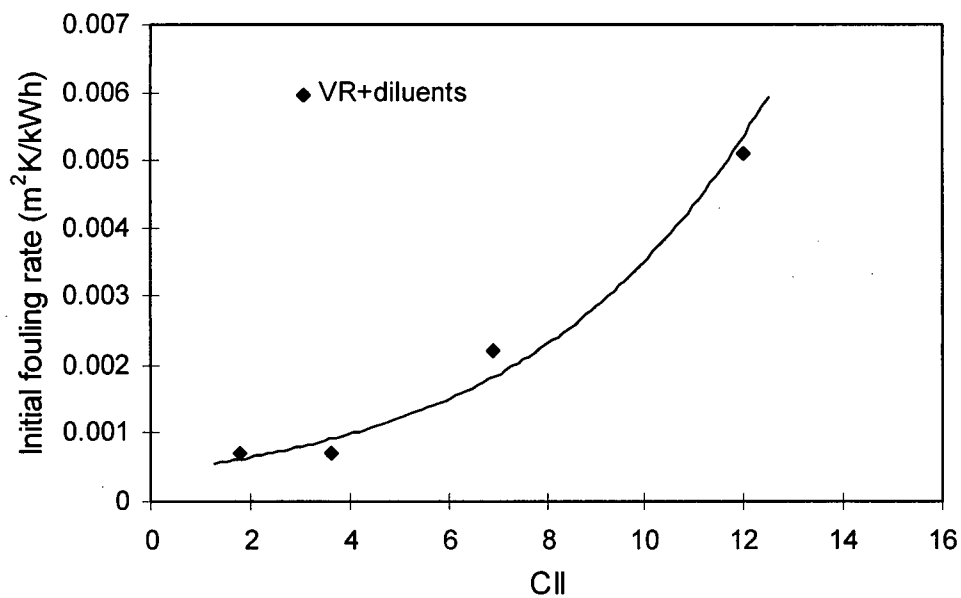


Figure 6.28 Correlation of Initial Fouling Rate with Colloidal Instability Index (CII) for VR Blends with As=1.77 wt%.

#### 6.4.4 Correlation of Thermal Fouling Data to Precipitation Data

The diluents precipitation tests (hot filtration tests) results show that there are insolubles in the test solutions, even at time zero, hence deposition occurs on the probe without an induction period when power to it is turned on. The characterization of hot filtration insolubles has shown that composition is consistent with that of petroleum asphaltenes (Table 6.8).

Figure 6.29 shows a plot of the initial fouling rate data for 10% VR and 10% ATB against the amount of hot filtration insolubles. The Initial fouling rates increase when the amount of hot filtration insolubles goes up for both ATB and VR blends. This suggests that the amount of hot filtration insolubles is a good indicator of the level and severity of fouling. As  $W > 2\%$ , the effect is roughly linear.

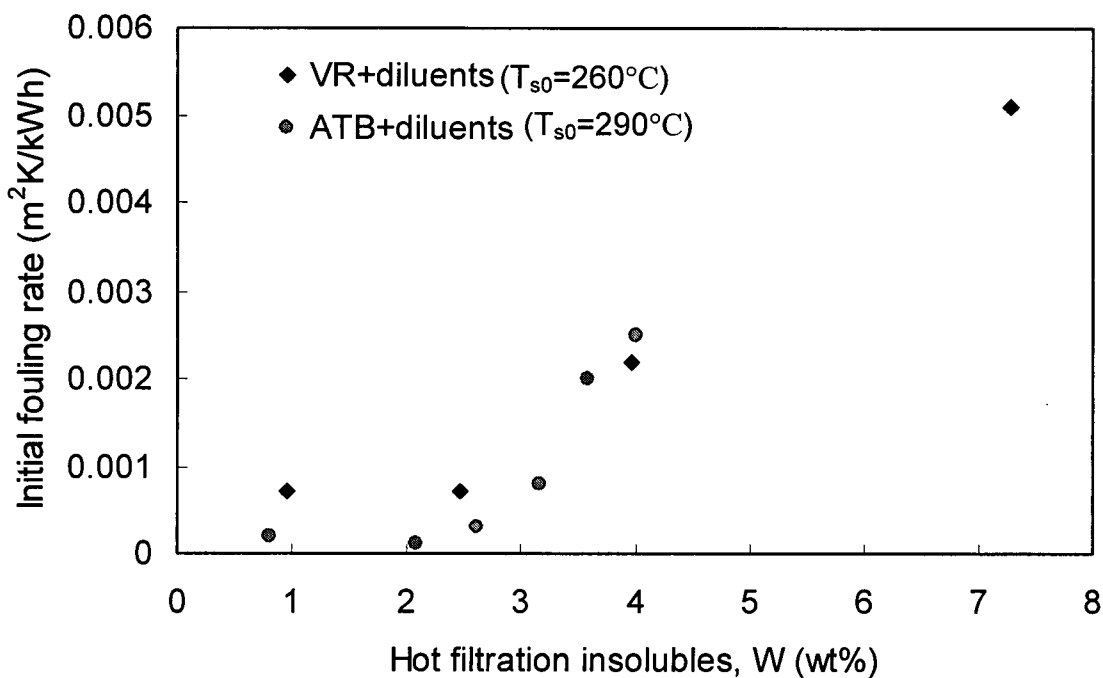


Figure 6.29 The Correlation of Initial Fouling Rate Versus the Amount of Hot Filtration Insolubles for 10% VR or 10% ATB Blends.

#### 6.4.5 Implications of Thermal Fouling Data

Based on the results of this work and previous work completed by Asomaning [54], we may get the following implications for thermal fouling:

- This process is well correlated by the solubility parameter based stability criteria (Andersen/Pedersen and Wiehe stability criterion) and Colloidal Instability Index (CII), which implies that the occurrence of thermal fouling depends on the composition of the test fluid at constant probe surface temperature, bulk temperature and velocity. Small changes in liquid composition which affect fouling can be detected using the flocculation titration. With the addition of small amount (0.5-5%) aromatics and resin rich fraction REF, the extent of thermal fouling and the initial fouling rate decrease dramatically.
- With the addition of pure alkane or multi-component diluents to the asphaltene-containing residue, the asphaltenes may form filtrable aggregated solids. The concentration of the insolubles decrease with raising the bulk temperature. Therefore the extent of thermal fouling and the initial fouling rate decrease with increasing bulk temperature, as also was shown by Asomaning [54].
- The initial fouling rate increase strongly with rising probe surface temperature at constant bulk temperature and velocity.
- At the heated surface, some of the asphaltene solids attach, presumably, via a temperature-sensitive adhesion step. The high apparent activation energy (Table 6.5 and [54]) and negative velocity effect [54] suggest the importance of an adhesion step.
- Attached asphaltene solids age to form coke-like deposits which differ from the original asphaltenes as shown by the deposit characteristics (Table 6.8-6.10 and [54]). The deposits from ATB also reflect the presence of inorganic clays, known to be present in such oils.

## 7. Conclusions and Recommendations

### 7.1 Conclusions

A study of asphaltene precipitation and fouling from blends of heavy oil residues and diluents of varying aromaticities showed:

- The effects of diluent composition on asphaltene precipitation from Cold Lake vacuum residue and Athabasca atmospheric tower bottoms have been determined using the hot filtration method at 60-85°C. Diluents include pure n-alkanes (heptane, decane and dodecane) and multi-component blends with a wide range of saturates, aromatics and resins contents. As found by others, for pure n-alkanes, the amount of asphaltene precipitation decreases as the molecular mass of n-alkanes increases. With the increase of diluent-to-residue ratios  $R$ , the amount of precipitated asphaltene increases sharply at first and then levels off. Similar behaviour was found for the mixtures of both residues with the aliphatic diluent PFX. With more aromatic diluents such as HVGO or the blends of HVGO/PFX=1, the amount of precipitation is reduced and increases in fraction of oil precipitated with diluent to feed ratio are slight. The addition of resin-enriched fluid has a strong inhibition effect on asphaltene precipitation.
- The amount of precipitate decreased and the solubility of asphaltenes in selected mixtures increased monotonically with temperature over the range of 60°C to 300°C. This trend was in agreement with statements of Wiehe [16].
- The original form of scaling equation proposed by Rassamdana et al. [12] for pure n-alkane diluents gave good agreement of the precipitation data for those diluents. For multi-component diluents containing aromatics and resins as well as saturates, an extended equation was developed, which incorporated the density and saturates content

of the diluents. The equation was adapted for different feed oils via the colloidal instability index. It was shown that knowing the SARA analysis of the heavy oil and complex diluent, the suspended asphaltene concentration in resulting mixtures can be calculated using the extended scaling equation.

- Mixture solubility parameters and stability parameters could be readily obtained from automated flocculation titrations. The inhibition effect of aromatic or resin-rich diluents for asphaltene precipitation was also evident in the titrations.
- The stability of oil blends can be predicted by either the Wiehe (Oil Compatibility) model or the Andersen/Pedersen model parameters determined from flocculation titrations. The two models are shown to be related.
- In the isothermal batch experiments, the amount of hot filtration insolubles can be related to the parameters of both models. Good correlation was also found between the amount of hot filtration insolubles and Colloidal Instability Index (CII) of the oil blends. Solubility parameters for all feedstocks were shown to decrease with the increase of temperature over the range 25°C to 50°C, as did the flocculation solubility parameters for ATB and VR. At the higher temperature of flocculation titration, the Andersen stability criterion line was shifted to the right, giving an improved prediction for conditions of no precipitation.
- In thermal fouling tests, for blends with both VR and ATB, fouling is much higher when an aliphatic diluent is used, and decreases as the aromaticity of the diluent is raised. With the addition of a resin and aromatic-rich fluid, the extent of fouling at any time decreases substantially.

- The initial fouling rate increase with rising probe surface temperature was quantified. The magnitude of the fouling activation energy suggest that adhesion of asphaltenes was important in fouling.
- The extent of thermal fouling and the initial fouling rate under otherwise fixed conditions can also be well correlated with several instability criteria, including the Wiehe model or the Andersen/Pedersen model criterion, the Colloidal Instability Index and the amount of suspended insolubles determined from isothermal batch experiments. Using solubility parameters derived from higher flocculation titration temperatures gives improved predictions for compositions with zero initial fouling rate.
- Thermal fouling deposits were characterized by elemental analysis, thermo-gravimetric analysis and scanning electron microscopy. A significant difference was found for the fouling deposits and precipitates recovered by hot filtration from isothermal precipitation tests only in the case of ATB. For ATB, fouling deposits were higher in ash than for VR, and incorporated significant amounts of the aliphatic diluent.

## 7.2 Recommendations

For some oil blends, the amount of hot filtration insolubles was too low to detect with high accuracy levels. It is recommended to use more samples in the filtration tests.

Most of the flocculation titration experiments were done at 25°C, while the hot filtration and fouling experiments were conducted at 85°C. Selected flocculation titration runs were performed at 35°C and 50°C to investigate the temperature effect on solubility parameter and stability prediction model parameter. It was found that model prediction improved for higher titration temperature. Further experiments need to be done to confirm this trend with a modified flow cell which permits titrations at higher temperatures.

In this work, thermal fouling experiments were conducted at constant bulk temperature and velocity. It is recommended to examine this behaviour at higher bulk temperatures and velocity to examine the effect of temperature and flow rates on the fouling behaviour of these mixtures. This would be particularly useful since the solubility of asphaltenes has been shown to increase up to 300°C. The effect of probe surface temperature on fouling was investigated in this work with a limited number of temperature set points. This issue can be investigated further to establish fouling activation over a greater temperature range, and as well for different velocities. The characterization of fouling deposits showed that there was significant difference between the deposits originating from ATB and the ones from VR. It is recommended to conduct further experiments to confirm this result, in order to explain the roles of the diluent and the clays in the ATB.

---

**Nomenclature****Abbreviations**

ATB	Athabasca Atmospheric Tower Bottoms
AFT	Automated Flocculation Titrimeter
CII	Colloidal Instability Index
DAO	De-Asphalted Oil
EDX	Energy-Dispersion X-ray
FO	Fuel Oil
HO	Cold Lake Heavy Oil
HVGO	Heavy Vacuum Gas Oil
OCM	Oil Compatibility Model
PFRU	Portable Fouling Research Unit
PFX	Paraflex
PVT	Pressure Volume Temperature
REF	Resin Enriched Fraction
SEM	Scanning Electron Microscope/Microscopy
SFEF	Supercritical Fluid Extraction and Fractionation
TGA	Thermo-gravimetric Analysis
VR	Cold Lake Vacuum Residue

**Nomenclature**

A	Surface area ( $m^2$ ), Pre-exponent constant in Arrhenius equation
$C_{as}$	Suspended asphaltene concentration (g /L)
$C_{as,cal}$	Calculated suspended asphaltene concentration (g /L )
$C_{as,d}$	Dissolved asphaltene concentration (g /L)
$C_d$	Orifice discharge coefficient
$d_{eq}$	Equivalent diameter of annular test section (m)
E	Activation energy (kJ/mol)
$K_i$	The equilibrium ratio for the solid-liquid equilibrium
$K_H$	Characterization factor, $K_H=10(H/C)/(M^{0.1236}\rho)$
$k_f$	Thermal conductivity of the foulant (kW/mK)
$l_{ij}$	The binary interaction coefficients
m	Mass of deposit per unit surface area ( $kg/m^2$ )
$m_F$	Weight of feed oil (g)
$m_D$	Weight of diluent (g)
$M_{Ai}$	The molecular weight of the ith fraction of asphaltenes in the crude oil
$M_A$	The average molecular weight of all the asphaltene fractions
M	Molecular mass of the diluent
Mw	Molecular weight (g/mol)
$N_{sAi}$	The segment number of the ith fraction of asphaltenes
$n_s(t)$	The number of clusters of size s at time t (cluster size distribution).
Q	Electrical power (kW)
R	Diluent to feed oil ratio ( $cm^3$ diluent/g feed oil); Gas constant (kJ/mol K)
$R_f$	Thermal fouling resistance ( $m^2K/kW$ )

---

$R_f^*$	Asymptotic resistance ( $m^2K/kW$ )
$R_f^\bullet$	Initial fouling rate ( $m^2K/kWh$ )
$s$	The cluster size
$\langle s \rangle$	The mean cluster size
$S_a$	Weight fraction saturates in diluent
$SG$	Specific Gravity at 20 °C (refer to water density at 4°C)
$t$	Time (s, minute, hour)
$T$	Temperature (°C, K)
$T_b$	Bulk fluid temperature (°C)
$T_B$	The volume average boiling point (K)
$T_s, T_{s0}$	Probe surface temperature under fouled and clean conditions (°C)
$U, U_0$	Overall heat transfer coefficient under fouled and clean conditions ( $kW/m^2K$ )
$U_b$	Bulk velocity (m/s)
$V$	Volume ( $m^3$ )
$V_a$	The molar volume of asphaltene ( $m^3/mol$ )
$v_i^l$	The liquid phase molar volume ( $m^3/mol$ ) of component $i$
$v_m$	The molar volume ( $m^3/mol$ ) of the solvent
$V_{fA}^L$	The total volume fraction of asphaltenes in the liquid state in equilibrium with the solid (asphaltene) phase
$V^c$	The total volume of crude oil ( $m^3$ )
$V_L$	The total volume or molar volume of liquid phase ( $m^3$ or $m^3/mol$ )
$V_s$	The total volume of solid phase ( $m^3$ )
$W$	Weight percent of the feed which precipitated ( $((g \text{ asphaltene}/g \text{ feed oil}) \times 100\%)$ )
$W_{At}$	The total weight of asphaltene in the crude oil

$x$	Deposit thickness (m)
$X$	Variable $R/M^{1/4}$ (Equation (4.1))
$X_c$	Value of $X$ at the onset of asphaltene precipitation
$X'$	Variable $X(Sa/\rho_{D,20})^{1.5}$ (Equation (4.7))
$x^*$	The composition of the "solvent" (petroleum fluid diluted with respect to asphaltenes, resins, and micelles)
$X_{al}^*$	The equilibrium concentration of monomeric asphaltenes in the crude oil coexisting with the solid asphaltene phase
$X_{al}^{ons}$	The micellization parameter, which is related to the fugacity of the monomeric asphaltene species calculated from the EOS
$x_i^l$	The liquid-phase mole fraction of component $i$
$x_i^s$	The solid-phase mole fraction of component $i$
$Y$	Variable $WR^2$ (Equation (4.2))
$Y'$	Variable $Y (CII)^2$ (Equation (4.10))
$\beta$	$(\beta=d_1/d_2)$ , ratio of orifice diameter to pipe diameter
$\delta$	Solubility parameter $(MPa)^{0.5}$ , $(cal/ml)^{0.5}$
$\delta_f$	Flocculation onset point solubility parameter, $(MPa)^{0.5}$
$\delta_i^l$	The solubility parameters $(MPa)^{1/2}$ of component $i$
$\mu_{al}^*$	The standard chemical potential of monomeric asphaltene
$\theta$	A complex function of the segment numbers of asphaltenes in both the liquid and solid phase
$\rho$	Density $(kg/m^3)$ , $(g/mL)$
$\rho_f$	Density of the foulant $(kg/m^3)$

---

$\rho_F$	Density of feed oil (g/mL)
$\rho_D$	Density of diluent (g/mL)
$\rho_m$	Mass average density of asphaltene
$\sigma$	The average relative deviation defined by Equation (4.4)
$\varphi_{al}^\beta$	The fugacity coefficient of monomeric asphaltene species in the petroleum fluid medium
$\Phi_{max}$	The maximum volume fraction of asphaltenes soluble in the crude
$\Phi_i, \Phi_j$	The volume fraction of component i and j

**References:**

- [1] Eaton, P. and R. Lux, "Laboratory Fouling Test Apparatus for Hydrocarbon Feedstocks", ASME HTD 35, 33-42, (1984).
- [2] Dickakian, G. B. and S. Seay, "Asphaltene Precipitation Primary Crude Exchanger Fouling Mechanism", Oil and Gas Journal 86, 47-50, (1988).
- [3] Crittenden, B. D., S. T. Kolaczkowski and I. L. Downey, "Fouling of Crude Oil Preheat Trains", Chem. Eng. Res. Des. 70(a), 547-557, (1992).
- [4] Lambourn, G. A. and M. Durrieu, "Fouling in Crude Oil Preheat Trains" in Heat Exchangers Theory and Practice, Taborek Hewitt and Afghan (eds.) Hemisphere Publishing Co., New York, (1983).
- [5] Murphy, G. and J. Campbell, "Fouling in Refinery Heat Exchangers: Causes, Effects, Measurements and Control", in Fouling Mechanisms, M. Bohnet et al. (eds.). 249-261, GRETh Seminar, Grenoble, (1992).
- [6] Brons G, Wiehe, I. A., "Mechanism of Reboiler Fouling during Reforming", Engery & Fuels, 14:2-5, (2000).
- [7] Parker R.J., McFarlane R.A., "Mitigation of Fouling in Bitumen Furnaces by Pigging" Engery & Fuels, 14:11-13, (2000).
- [8] Taher A.Al-Sahhaf, Mohammed A.Fahim, Amal S.Elkilani, "Retardation of Asphaltene Precipitation by Addition of Toluene, Resins, Deasphalted Oil and Surfactants", Fluid Phase Equilibria, 194-197, 1045-1057, (2002).
- [9] Hirschberg, A., L. N. J. deJong, B. A. Schipper and J. G. Meijer, "Influence of Temperature and Pressure on Asphaltene Flocculation", SPE J.24, 283-293, (1984).

- [10] Kawanaka, S., S. J. Park and G. A. Mansoori, "Organic Deposition From Reservoir Fluids: A Thermodynamic Predictive Technique", SPE Reservoir Engineering , 5, 185-192, (1991).
- [11] Victorov, A. I., and A. Firoozabadi, "Thermodynamic Micellization Model of Asphaltene Precipitation from Petroleum Fluids," AIChE J.42, 1753, (1996).
- [12] Rassamdana, H., B. Dabir, M. Nematy, M. Farhani and M. Sahimi, "Asphaltene Flocculation: I. The Onset of Precipitation", AIChE. J 42, 10-22, (1996).
- [13] Wiehe, I. A. and R. J. Kennedy, "Application of the Oil Compatibility Model to Refinery Streams", Energy & Fuels 12, 60-63, (2000).
- [14] Andersen, S.I., Pedersen C., "Thermodynamics of asphaltenes stability by flocculation titration", Proc. Int'l Conf. On Petroleum Phase Behavior and Fouling, AIChE J, pp75-81, (1999).
- [15] Wiehe, I.A., "Tutorial on the Phase Behavior of Asphaltenes and Heavy Oils", (1999).
- [16] Strausz, O. P., T. W. Mojelsky, and E .M. Lown, "The Molecular Structure of Asphaltene: An Unfolding Story", Fuel 71, 1355-1363, (1992).
- [17] Speight, J. G., and S. E. Moschopedis, "Some Observations on the Molecular Nature of Petroleum Asphaltenes", Preprints, Div. of Fuel Chem., ACS, 24, 910, (1979).
- [18] Wiehe, I. A., "Tutorial on the phase behavior of asphaltene and heavy oils", Preprints of AICHE International Conference on Petroleum Phase Behavior and Fouling, Third Int'l Symposium on the Thermodynamics of Asphaltenes and Heavy Oils III, (1999).
- [19] Speight, J.G., "The Chemistry and Technology of Petroleum", Marcel Dekker, New York, (1991).
- [20] Sheu, E.Y., "In Asphaltene-Fundamentals and Applications", Sheu, E.Y., Mullins, O. C., Eds., Plenum: New York, Chapter 1, (1995).

- [21] Sheu, E.Y., "Petroleum Asphaltene-Properties, Characterization and Issues", *Energy & Fuels*, 16, 74-82, (2002).
- [22] Mushrush, G. W. and J. G. Speight, "Petroleum Products:Instability and Incompatibility", *Talor&Francis*, Washington D.C., (1995).
- [23] Acevedo, S. G., Escobar, L., Gutierrezmand H. Rivas, "Isolation and Characterization of Natural Surfactants from Extra Heavy Oils, Asphaltenes and Maltenes," *Fuel*, 71, 619, (1992).
- [24] Strausz, O.P., Peng, P.A., Murgich, J., "About the Colloidal Nature of Asphaltenes and the MW of Covalent Monomeric Units", *Energy & Fuels*, 16, 809-822, (2002).
- [25] Long, R. B., *Advances in Chemistry Series 195*, J. W. Bunger and N. Cc. Li, ed., ACS, Washington, DC, 17, (1981).
- [26] Yen, T. F., " Chemistry of Asphaltenes ", in *Advances in Chemistry Series #195* Bunger, J. W. and Li N. C. (eds.), American Chemical Society, (1981).
- [27] Mitchell, D. L. and J. G. Speight, "The Solubility of Asphaltenes in Hydrocarbon Solvents", *Fuel* 52,149-152, (1973).
- [28] Lian, H., Lin, J. R. and Yen T. F., "Peptization Studies of Asphaltene and Solubility Spectra", *Fuel* 73, 423-427 (1994).
- [29] Laux, H., Rahimian, I., Butz, T., "Thermodynamics and mechanism of stabilization and precipitation of petroleum colloids", *Fuel Process. Technol.*, 53, 69 (1997).
- [30] Moschopedis, S. E., and J. G. Speight, "Investigation of Hydrogen Bonding by Oxygen Functions in Athabasca Bitumen", *Fuel*, 55,187, July, (1976).
- [31] Little, R.C., Singletery, C.R., "Solubility of alkali dinonylnaphthalenesulfonates in different solvents and a theory for the solubility of oil-soluble soaps", *J. Phys. Chem.* 68, 3453, (1964).

- [32] Speight, J. G., "The Molecular Nature of Petroleum Asphaltenes", Arab. J. Sci. Eng., 19, 335, (1994).
- [33] Du, P.C. and Mansoori, G.A.: "Phase Equilibrium Computational Algorithms of Continuous Mixtures", Fluid Phase Equilibria, 30, 57-64, (1986).
- [34] Gray, M. R., "Upgrading Petroleum Residues and Heavy Oils", Marcel and Dekker, New York, (1994).
- [35] Twu, C. H., "Internally Consistent Correlation for Predicting the Critical Properties and Molecular Weights of Petroleum Fractions and Coal-Tar Liquids", Fluid Phase Equil. 16, 137-145, (1984).
- [36] Peramanu, S., Pruden, B.B. and Rahimi, P. "Molecular Weight and Specific Gravity Distributions for Athabasca and Cold Lake Bitumens and Their Saturate, Aromatic, Resin and Asphaltene Fractions", Ind, Eng, Chem. Res. 38, 3121-3130, (1999).
- [37] Dabir, B., Nematy, M., Mehrabi, A. R., Rassamdana, H. and Sahimi, M. "Asphalt Flocculation and Deposition III. The Molecular Weight Distribution", Fuel, 75, 1633-1645, (1996).
- [38] Jiang, T., Wang, R. A. and Yang, G. "Simulated distillation of residue by fractional distraction (I)", Proceedings of International Symposium on Heavy Oil and Residue Upgrading and Utilization. Fushun, P. R. China, P53, (1992).
- [39] Chung, K. H., Xu, C., Hu, Y. and Wang, R., "Supercritical Fluid Extraction Reveals Resid Properties", Oil&Gas Journal, Jan20, v95, n3, 66, (1997).
- [40] Hildebrand, J.H. and R.L. Scott, "Regular Solutions", Prentice-Hall, New York, (1962).
- [41] Andersen, S.I., Ph.D Thesis. Tech. Univ. Denmark, (1990).
- [42] Andersen, S.I., Speight, J.G., Preprints. Div. Pet. Chem. Am. Chem. Soc. 37 (3), 1335, (1992).

- [43] Rogel, E., "Theoretical Estimation of the Solubility Parameter Distribution of Asphaltenes, Resins and Oils from Crude Oils and Related Materials", *Energy & Fuels*, 11, 920-925, (1997).
- [44] Labout, J.W.A., In: Pfeiffer, J.Ph. (Ed.), "The Properties of Asphaltic Bitumen", Elsevier, Amsterdam, (1950).
- [45] Andersen, S.I., "Dissolution of Solid Boscan Asphaltenes in Mixed Solvents", *Fuel Sci. Techn. Int.*, 12, 51-74, (1994).
- [46] Storm, D.A.; Barresi, R.J. Sheu, E.Y. "Flocculation of asphaltenes in heavy oil at elevated temperature", *Fuel Sci. Technol. Int.*, 14, 243-260, (1996).
- [47] Winans, R.E., Hunt, J.E. "An overview of resid characterization by mass spectrometry and small angle scattering techniques", *Prepr. Pap- Am. Chem. Soc., Div. Fuel Chem.*, 44, 725-732, (1999).
- [48] Espinat, D., Ravey, J.C., "Colloidal Structure of Asphaltene Solutions and Heavy Oil Fractions Studied by Small-angle Neutron and X-ray Scattering", Presented at the SPE international symposium on oilfield chemistry, New Orleans, LA, Mar2-5, 1993; Paper 25187, 365-373.
- [49] Andersen, S.I., Stenby, E.H., "Asphaltene precipitation and dissolution investigation of temperature and solvent effects", *Fuel Sci. Technol. Int.*, 14, 261-287, (1996).
- [50] Wiehe, I.A., "Thermal reactivity of heavy oils", 213<sup>th</sup> ACS Presentation, Div. Petr. Chem., San Francisco, (1997).
- [51] Leontaritis, K.J., "The asphaltene and wax deposition envelopes", *Fuel Sci Technol. Int.*, 14,13-30, (1996).

- [52] Low, J.Y., Hood, R.L., Lynch, K.Z., "Valuable products from the bottom of the barrel using ROSE technology", Prepr. Paper. Am. Chem. Soc., Div.Pet.Chem.40, 780-784, (1995).
- [53] Rowlinson, J.S., "Liquid and Liquid Mixtures", Butterworth Scientific Publications, London, 231-235, (1959).
- [54] Asomaning, S., "Heat Exchanger Fouling by Petroleum Asphaltenes", Ph.D Thesis, UBC, (1997).
- [55] Robin King, Summer Essay, "Dependence of Asphaltene Solubility on Temperature in Heavy Oil/Fuel oil Solutions ", UBC (1999).
- [56] Heithaus, J.J., "Measurements and significance of asphaltene peptization", Journal of the Institute of Petroleum, 48 (Feb.), 45, (1962).
- [57] Pauli A.T., "Asphalt compatibility testing using the automated Heithaus titration test", American Chemical Society. Pre-print 212th National Meeting. Orlando FL, August 25-29, 41:4:1276-1281, (1996).
- [58] Hotier, G. and Robin, M., "Effect of different thinners on heavy petroleum products: measuring, interpreting and forecasting asphaltene flocculation", Revue de l' Institut Francaise du Petrole, 38,101, (1983).
- [59] Fuhr, B.J., Klein, L.L., Komishke, B.D., Reichert, C. And Ridley, R.K., "Effects of Diluents and Carbon Dioxide on Asphaltene Flocculation in Heavy Oil Solutions", in Fourth UNITAR/UNDP International Conference on Heavy Crude and Tar Sands, P63, Volume 2, August 7-12, (1988).
- [60] Yang, Z., C. M. Ma, X. S. Lin, J. T. Yang and T. M. Guo, "Experimental and Modeling studies on the Asphaltene Precipitation in Degassed and Gas-Injected Reservoir Oils", Fluid Phase Equilibria, 157,143-158, (1999).

- [61] Hu, Y.-F., Guo, T.-M., "Effect of Temperature and Molecular Weight of n-alkane Precipitants on Asphaltene Precipitation", *Fluid Phase Equilibria*, 192,13-25, (2001).
- [62] Thomas, F.B., Bennion, D.B., Bennion, D.W. and Hunter, B.E., "Experimental and Theoretical Studies of Solids Precipitation from Reservoir Fluid", *Journal of Canadian Petroleum Technology*, 31, 22, (1992).
- [63] Asomaning, S., "Test methods for Determining Asphaltene Stability in Crude Oils", *Petroleum Science and Technology*, 21, 3 & 4, 581-590, (2003).
- [64] Stark, J. L., Asomaning, S., "Crude Oil Blending Effect on Asphaltene Stability in Refinery Fouling", *Petroleum Science and Technology*, 21, 3 & 4, 569-579, (2003).
- [65] Corraera, S., Capuano, F., Panariti, N., "Onset of Asphaltene Precipitation: Analysis of Measurement Methods", 5th International Conference on Petroleum Phase Behavior and Fouling", Banff, Alberta, Canada, June 13-17th, (2004).
- [66] Peramanu, S., Singh, C., Agrawala, M., Yarranton, H.W., "Investigation on the Reversibility of Asphaltene Precipitation", *Energy&Fuels*, 15,910-917, (2001).
- [67] Escobedo, J. and Mansoori, G.A., "Viscometric determination of the onset asphaltene flocculation: A novel method", *SPE Production Facilities*, V10, No2, 115-118, (1995).
- [68] Sivaraman, A., Hu, Y., Jamaluddin, A.K.M., Thomas, F.B. and Bennion, D.B., "Asphaltene Onset, Effects of Inhibitors and EOS Modeling of Solids Precipitation in Live Oil Using Acoustic Resonance Technology", Preprints of AIChE International Conference on Petroleum Behavior and Fouling, Third Int'l Symposium on the Thermodynamics of Asphaltenes and Heavy Oils III, (1999).
- [69] Carrier, H., Plantier, F., Daridon, J-L, Lagourette, B., Lu, Z., "Acoustic Method for Measuring Asphaltene Flocculation in Crude Oils", *Journal of Petroleum Science and Engineering*, 27, 111-117, (2000).

- [70] Jones, G.M., Campbell, J., M., Povey, J.W. and Tong, J., "Development of an Ultrasonic Oil Stability Monitor for the Assessment for Asphaltene Aggregation in Hydrocarbon Streams", Proceedings of an International Conference on Mitigation of heat exchanger fouling and its economic and environmental implications, Banff, AB, Canada, July, 1999.
- [71] Burke, N.E., R.E. Hobbs and S.F. Kashow, "Measurement and Modeling of Asphaltene Precipitation", SPE 18273, 113-126, (1990).
- [72] Monger, T. G. and D. E. Trujillo, "Organic Deposition During CO<sub>2</sub> and Rich-Gas Flooding", SPE 18063,6373, (1988).
- [73] Chung, F., P. Sarathi and R. Jones: "Modeling of Asphaltene and Wax Precipitation", US DOE NiPER-498, 1-43, (1991).
- [74] Novosad, Z. and M.A. Adewumi, "Experimental and Modeling Studies of Asphaltene Phase Equilibria for a Reservoir under CO<sub>2</sub> Injection", SPE 20530, 599-697, (1990).
- [75] Speight, J.G. and Moschopedis, S.E., "On the Molecular Nature of Petroleum Asphaltenes", Chemistry of Asphaltenes, J.W. Bunger and N.C. (eds), Advances in Chemistry Series, American Chemical Soc., Washington, DC, 195, 1, (1981).
- [76] Blažek J., and Šebor, G., "Formation of Asphaltenes and Carbenes During Thermal Conversion of Petroleum Maltenes in the Presence of Hydrogen", Fuel, 72, 199-204, (1993).
- [77] Savage, P.E. and Klein, M.T., "Asphaltene Reaction Pathways 2: Pyrolysis of n-Pentadecyl Benzene", Ind. And Eng. Chem. Res. 26, 488-494, (1987).
- [78] Al-Atar, E., "Effect of Oil Compatibility and Resins/Asphaltenes Ratio on Heat Exchanger Fouling of Mixtures Containing Heavy Oil", M.A.Sc. Thesis, UBC, (2000).

- [79] Kokal, S.L., Najman, S.G.Sayegh and A.E.George, "Measurement and Correlation of Asphaltene Precipitation from Heavy Oils by Gas Injection," J. of Can. Petrol. Technol., 31, 24, (1992).
- [80] Andersen, S. I., "Dissolution of Solid Boscan Asphaltene in Mixed Solvents", Fuel. Sci. Tech. Int 12, 1551, (1994).
- [81] Macmillan, D.J., J.E. Tackett, M.A. Jessee, and T.G. Mongermcclure, "A Unified Approach to Asphaltene Precipitation: Laboratory Measurement and Modeling," J. Petro. Tech. 42, 788, (1995).
- [82] Ferworn, K.A. and W.Y. Sverck, "Thermodynamic and Kinetic Studies of Asphaltene Deposition from Bitumens", Proc. Can. Chem. Eng. Conf., Calgary, (Oct, 1994).
- [83] Lira-Galeana, Firoozabadi, C.A. and Prausnitz, J.M. "Thermodynamics of Wax Precipitation in Petroleum Mixs", AIChE J., 42,239, (1996).
- [84] Leontaritis, K.J. and G. A. Mansoori, "Descriptive accounts of thermodynamic and colloidal models of asphaltene flocculation", SPE Paper 16258,SPE Int. Symp .on Oil Field Chemistry, San Antonio, TX (Feb.4-6), (1987).
- [85] Pan, H.Q., and Firoozabadi, A. "Thermodynamic Micellization Model for Asphaltene Precipitation from Reservoir Crudes at High Pressures and Temperatures," SPE Paper 38857,presented at the SPE Annual Technical Conference, San Antonio, TX (Oct.5-8), (1997).
- [86] Flory, P. J., "Thermodynamicsof Heterogeneous Polymers and Their Solutions",J. Chem. Phys. 12, 425-432, (1944).
- [87] Scott, R. L. and M. Magat, "Thermodynamics of High Polymer Solutions", J. Chem. Phys. 13,172-179, (1945).

- [88] Yarranton, W.H. and J.H. Masliyah, "Molar Mass Distribution and Modeling of Asphaltenes", *AIChE J.*, 42,3533-3543, (1996).
- [89] Hu, Y.-F., Chen, G.-J., Yang, J.-T., Guo, T.-M., "A Study on Application of Scaling Equation for Asphaltene Precipitation", *Fluid Phase Equilibria*, 171,181-195, (2000).
- [90] Wang, J. X., Buckley, J. S., "Asphaltene Stability in Crude Oil and Aromatic Solvents-The Influence of Oil Composition", *Energy & Fuels*, 17, 1445-1451, (2003).
- [91] Buckley, J.S.; Hirasaki, G.J.; Liu, Y.; Vondrasek, S.; Wang, J. X.; Gill, B.S., "Asphaltene Precipitation and Solvent Properties of Crude Oils", *Pet. Sci. Technol.*, 17(3&4), 251-285, (1998).
- [92] Buckley, J.S., "Predicting the Onset of Asphaltene Precipitation from Refractive Index Measurements", *Energy & Fuels*, 13(2), 328-332, (1999).
- [93] Rogel, E., León, O., Contreras, E., Carbognani, L., Torres, G., Espidel, J. and Zambrano, A. "Assessment of Asphaltene Stability in Crude Oils Using Conventional Techniques", *Energy & Fuels*, 17, 1583-1590, (2003).
- [94] Wang, R.-A., "A New Separation Method for Heavy Oils", Chinese Patent, ZL 93117577.1, (1993).
- [95] Warne, G.A., "Administration of Bituminous Oil Sands of Alberta", *J. of Can. Petroleum Tech.*, Jan-Feb, 45-49, (1984).
- [96] Yang G.-H, Wang, R. -A., Xu, Ch-M, "A New Assay Method for Heavy Oils and Petroleum Residual and the Characterization of Chinese Residuals", UNITAR Conference, Beijing, Paper 1998.082, October, (1998).
- [97] Smith, R.G., Scharmm, L.L., "The Influence of Natural Surfactant on Interfacial Charges in Hot Water Process for Recovering Bitumen from Athabasca Oil Sands", *Colloids and Surfaces*, 14, 67-85, (1985).

- [98] Chung, K.H., Dai, Q., "Bitumen – Sand Interaction in Oil Sand Processing", *Fuel*, 74, 1858-1864, (1995).
- [99] Takamura, K., "Microscopic Structure of Athabasca Oil Sands", *Can. J. Chem. Eng.*, 60, 538-545, (1982).
- [100] Watkinson A.P, Navaneetha-Sundaram B, Posarac D. "Fouling of a sweet crude oil under inert and oxygenated conditions", *Energy and Fuels*, 14:64 (2000).
- [101] Kern, D. Q. and Seaton, R. E., " A Theoretical Analysis of Thermal Surface Fouling", *Br. Chem. Eng.* 4, 258-262, (1959).
- [102] Park, S. J., and G.A. Mansoori, "Aggregation and deposition of heavy organics into petroleum crudes", *Energy Sources*, 10,109, (1988).
- [103] Meakin, P., "Phase Transitions and Critical Phenomena" Vol.12, C. Domb and J.L., Lebowitz, eds, Academic Press, London, (1988).
- [104] Sahimi, M., "Structural and dynamical properties of branched polymers and gels and their relation with elastic percolation networks", *Mod. Phys. Lett. B*, 6,507(1992).
- [105] Witten, T. A., and Sander, L. M., "Diffusion-limited aggregation, a kinetic critical phenomenon", *Phys. Rev. Letter*, 47, 1400, (1988).
- [106] Meakin, P., "Formation of fractal clusters and networks by irreversible diffusion-limited aggregation", *Phys. Rev. Letter*, 51,119, (1983).
- [107] Rassamdana H, Sahimi, M., "Asphaltene Flocculation and Deposition: II. Formation and Growth of Fractal Aggregates", *AIChE J.*, 42, 12, 3318-3331, (1996).
- [108] Rassamdana H, Farhani M, Dabir B, Mozaffarian M. "Asphal flocculation and deposition. V. Phase behavior in miscible and immiscible injections", *Energy&Fuels*, 13:176-187, (1999).

- [109] Gastel, C., Smadja R. and Lamminan, K.A., "Contribution a La Connaissance Des Proprietes Des Bitumen Routiers", *Revue Gingirale De Routes Et Des Airodromes* 466,85, (1971).
- [110] Mcketta, J.J., "Petroleum Processing Handbook", Marcel Dekker, New York, (1992).
- [111] Fuhr, B.J., Cathrea, C., Kalya, H., Majeed, A.I., "Properties of asphaltenes from a waxy crude", *Fuel*, 70, 1293-1297, (1991).
- [112] Ali, L.H., Al-Ghannam, K.A., "Investigations into asphaltenes in heavy crude oils. I. Effect of temperature on precipitation by alkane solvents", *Fuel*, 60, 1043-1046, (1981).
- [113] Rogel, E.; León, O.; Espidel, J.; Gonzalez, J., "Asphaltene stability in crude oils", *SPE Production Facilities*, SPE72050, May, (2001).
- [114] Bouts, M. N.; Wiersma, R.J.; Muijs, H. M.; Samuel, A. J., "An evaluation of new asphaltene inhibitors: Laboratory study and field testing", *JPT*, 782, Sept., (1995).
- [115] Thomas, D. C.; Becker, H.L.; Del Real Soria, R. A., "Controlling asphaltene deposition in oil wells", *SPE Production & Facilities*, 119-123, May, (1995).
- [116] Carbognani, L.; Contreras, E.; Guimerans, R.; Leon, O.; Flores, E.; Moya, S. "Physicochemical characterization of crude and solid deposits as a guideline to optimize oil production", 2001 SPE International Symposium on Oilfield Chemistry, Houston, Texas, SPE 64993, (2001).
- [117] Sheu, E.Y., Storm, D.A., in: Sheu, E.Y., Mullins, O.C. (Eds.), "Asphaltenes: Fundamentals and Applications", Plenum Press, New York, 1995, (Chapter 1).
- [118] Rogacheva, O.V., Gimaev, R.N., Gubaidullin, V.Z., Khakimov, D.K., "Study of surfactant activity of asphaltenes in petroleum residues", *Colloid J.USSR*, 23(2), 586-589, (1980).

- [119] Gonzalez, G., Middea, A., "Peptization of asphaltene by various oil soluble amphiphiles", *Colloids and Surfaces*, V52, 207-217, (1991).
- [120] Chang, C.-L., Fogler, H.S., "Stabilization of asphaltenes in aliphatic solvents using alkylbenzene-derived amphiphiles.1.Effect of the chemical structure of amphiphiles on asphaltene stabilization", *Langmuir* 10, 1749, (1994).
- [121] Chang, C.-L., Fogler, H.S., "Stabilization of asphaltenes in aliphatic solvents using alkylbenzene-derived amphiphiles.2.Study of the asphaltene-amphiphile interactions and structures using Fourier transform infrared spectroscopy and small-angle X-ray scattering techniques", *Langmuir* 10, 1758, (1994).
- [122] De Boer, R.B., Leerlooyer, K., Eigner, M.R.B., Van Bergen, R.D., "Screening of crude oils for asphalt precipitation: a review", *SPE Prod. Fac.*55, (1995).
- [123] Pan, H.Q., Firoozabadi, A., "Thermodynamic micellization model for asphaltene precipitation inhibition", *AIChE Journal*. 46,416, (2000).
- [124] Barton, A.F.M., "Handbook of Solubility Parameters and Other Cohesion Parameters", CRC Press, Boca Raton, FL, (1983).
- [125] Asomaning, S., Watkinson, A.P., "Pertroleum stability and heteroatom species effects in fouling of heat exchangers by asphaltene", *Heat Transfer Engineering*, 21:10, (2000)
- [126] Asomaning, S., Yen, A., Weispfennig, K., "Reducing the viscosity of heavy oils with naphtha and its impact on asphaltene stability", *ACS Symposium Series*, 46, 2:117, (2001).
- [127] Sajedi, A-R. Diplomarbeit, Institut fur Erdol-und Erdgsforschung, Clausthal-Zellerfeld, Germany, (1995).
- [128] Asomaning, S., Watkinson AP. In "Understanding Heat Exchanger Fouling", Begell House, New York, pp283-90, (1999).

- [129] Strausz, O.P., and I. Rubinstein in "Atomic and Nuclear Methods in Fossil Fuel Research", Royston, Filby and Carpenter, (eds.), Plenum Publishers, New York, (1980).
- [130] Al-Atar, E, Watkinson AP. "Asphaltene-resin interactions in fouling of unstable oil mixtures", Proc. 4th Int'l Conf.on Heat Exchanger Fouling, Publico Publns. Essen, pp243-8, (2002).
- [131] Brons G, Rudy T.M. , " Fouling of Whole Crudes on Heated Surfaces", Proceedings of the 4<sup>th</sup> International Conference on Heat Exchanger Fouling Fundamental Approaches & Technical Solutions", 249-58, July 8-13, (2001)
- [132] Asomaning, S., A. Yen and C.T. Gallagher, "Predicting the Stability of Asphaltenes in Crude Oils Using the Colloidal Instability Index", Presented at the ACS National Meeting, San Francisco, March 26-30, (2000).

## Appendix A1

Table A1.1 The Amount of Hot Filtration Insolubles (T=85°C) versus Time

W (wt%) Test Fluids	Time (hour)						
	0.0	0.5	1.0	1.5	2.0	2.5	3.0
10%VR+90%PFX	6.22	6.86	6.68	6.74	6.62	6.76	6.80
20%VR+80%PFX	2.56	3.10	3.21	3.16	3.08	3.15	3.06
10%VR+90%HVGO	0.98	1.16	1.18	1.12	1.09	1.15	1.10
20%VR+80%HVGO	0.68	0.75	0.78	0.72	0.77	0.74	0.76
10%ATB+90%PFX	3.41	3.84	3.92	3.88	3.80	3.85	3.81
20%ATB+80%PFX	1.38	1.53	1.59	1.55	1.61	1.56	1.50
10%ATB+90%HVGO	0.73	0.85	0.88	0.81	0.83	0.89	0.86
20%ATB+80%HVGO	0.70	0.75	0.72	0.76	0.73	0.77	0.74

Appendix

Table A1.2 Hot Filtration Experiment Using Several Oil Cuts as Diluents\*

Test fluid	T (°C)	Sa (wt%)	Ar (wt%)	Re (wt%)	As (wt%)	Re/As	CII	W	Cas (g/L)	n-heptane as titrant (25°C)			
										$\delta_{mix}$ [MPa] <sup>0.5</sup>	$\delta_f$ [MPa] <sup>0.5</sup>	S <sub>BNmix</sub>	I <sub>Nmax</sub>
5%VR+95%PFX	85	94.98	2.51	1.63	0.89	1.84	23.18	7.56	3.26	15.83	16.23	20.4	33.2
10%VR+90%PFX	85	90.56	4.41	3.26	1.77	1.84	12.04	6.86	5.97	15.99	16.23	25.6	33.2
15%VR+85%PFX	85	86.14	6.32	4.89	2.66	1.84	7.92	5.72	7.54	16.16	16.23	31.0	33.2
20%VR+80%PFX	85	81.72	8.22	6.52	3.54	1.84	5.78	3.1	5.50	16.33	16.23	36.4	33.2
25%VR+75%PFX	85	77.30	10.13	8.15	4.43	1.84	4.47	1.82	4.07	16.50	16.23	42.0	33.2
30%VR+70%PFX	85	72.88	12.03	9.78	5.31	1.84	3.59	0.83	2.25	16.68	16.23	47.6	33.2
5%VR+95%HVGO	85	65.45	17.0	16.66	0.89	18.82	1.97	1.23	0.54	16.93	16.23	56.0	33.2
10%VR+90%HVGO	85	62.59	18.14	17.50	1.77	9.89	1.81	1.16	1.0	17.05	16.23	59.7	33.2
15%VR+85%HVGO	85	59.72	19.29	18.34	2.66	6.91	1.66	0.88	1.18	17.17	16.23	63.5	33.2
20%VR+80%HVGO	85	56.86	20.43	19.18	3.54	5.42	1.52	0.75	1.35	17.29	16.23	67.4	33.2
25%VR+75%HVGO	85	53.99	21.57	20.02	4.43	4.52	1.40	0.66	1.49	17.41	16.23	71.3	33.2
30%VR+70%HVGO	85	51.12	22.71	20.85	5.31	3.93	1.30	0.56	1.54	17.53	16.23	75.3	33.2
5%VR+47.5%HVGO+47.5%PFX	85	80.22	9.75	9.14	0.89	10.33	1.66	3.14	1.36	16.38	16.23	38.0	33.2
10%VR+45%HVGO+45%PFX	85	76.57	11.28	10.38	1.77	5.86	1.52	2.43	2.13	16.52	16.23	42.6	33.2
15%VR+42.5%HVGO+42.5%PFX	85	72.93	12.80	11.61	2.66	4.37	1.40	1.66	2.20	16.66	16.23	47.1	33.2
20%VR+40%HVGO+40%PFX	85	69.28	14.32	12.85	3.54	3.63	1.30	1.27	2.27	16.81	16.23	51.8	33.2
25%VR+37.5%HVGO+37.5%PFX	85	65.65	15.85	14.08	4.43	3.18	4.29	0.84	1.89	16.95	16.23	56.6	33.2

\*VR: Cold Lake Vacuum residue(Imperial Oil Company)  
 HVGO: Heavy vacuum gas oil (Imperial Oil Company)  
 PFX: Paraflex ( Petro Canada Ltd.)

Table A1.3 Resin Effect on Hot Filtration Insolubles Using REF as Diluent \*

Test fluid	T (°C)	Sa (wt%)	Ar (wt%)	Re (wt%)	As (wt%)	Re/As	CII	W	Cas (g/L)	n-heptane as titrant (25°C)			
										$\delta_{mix}^{0.5}$ [MPa] <sup>0.5</sup>	$\delta_f^{0.5}$ [MPa] <sup>0.5</sup>	S <sub>BNmix</sub>	I <sub>Nmax</sub>
0%REF+10%VR+90%PFX	85	90.56	4.41	3.26	1.77	1.84	12.04	6.86	5.97	15.99	16.23	25.6	33.2
5%REF+10%VR+85%PFX	85	85.63	7.52	5.08	1.77	2.87	6.94	3.61	3.18	16.22	16.23	33.1	33.2
10%REF+10%VR+80%PFX	85	80.71	10.35	6.89	1.77	3.89	4.71	2.18	1.94	16.46	16.23	40.8	33.2
15%REF+10%VR+75%PFX	85	75.79	13.74	8.71	1.77	4.92	3.46	1.95	1.76	16.70	16.23	48.5	33.2
0%REF+15%VR+85%PFX	85	86.14	6.32	4.89	2.66	1.84	7.92	5.72	7.54	16.16	16.23	31.0	33.2
5%REF+15%VR+80%PFX	85	81.22	9.43	6.71	2.66	2.53	5.20	2.79	3.72	16.40	16.23	38.6	33.2
10%REF+15%VR+75%PFX	85	76.29	12.54	8.52	2.66	3.21	3.75	1.68	2.26	16.64	16.23	46.4	33.2
15%REF+15%VR+70%PFX	85	71.37	15.65	10.34	2.66	3.89	2.85	1.59	2.17	16.88	16.23	54.3	33.2
0%REF+20%VR+80%PFX	85	81.72	8.22	6.52	3.54	1.84	5.78	3.1	5.49	16.33	16.23	36.4	33.2
5%REF+20%VR+75%PFX	85	76.80	11.33	8.34	3.54	2.35	4.09	1.89	3.39	16.57	16.23	44.2	33.2
10%REF+20%VR+70%PFX	85	76.84	14.47	10.15	3.54	2.87	3.26	1.29	2.34	16.81	16.23	52.1	33.2
15%REF+20%VR+65%PFX	85	66.95	17.55	11.97	3.54	3.38	2.85	1.16	2.13	17.06	16.23	60.1	33.2

\* VR: Cold Lake Vacuum residue(Imperial Oil Company)

PFX: Paraflex (Petro Canada Ltd.)

REF: Resin enriched fraction (SFEF experiment in China)

Appendix

Table A1.4 Resin Effect on Hot Filtration Insolubles Using REF as Diluent \* (T=85°C)

Test fluid	Sa (wt%)	Ar (wt%)	Re (wt%)	As (wt%)	Re/As	CII	W	Cas (g/L)	n-heptane as titrant (25°C)			
									$\delta_{mix}$ [MPa] <sup>0.5</sup>	$\delta_f$ [MPa] <sup>0.5</sup>	S <sub>BNmix</sub>	I <sub>Nmax</sub>
0%REF+5%VR+47.5%HVGO+47.5%PFX	80.22	9.75	9.14	0.89	10.33	4.29	3.14	1.36	16.38	16.23	38.0	33.2
5%REF+5%VR+45%HVGO+45%PFX	76.07	12.48	10.56	0.89	11.94	3.34	1.86	0.82	16.58	16.23	44.7	33.2
10%REF+5%VR+42.5%HVGO+42.5%PFX	71.92	15.21	11.98	0.89	13.54	2.68	1.38	0.61	16.79	16.23	51.5	33.2
15%REF+5%VR+40%HVGO+40%PFX	67.77	17.94	13.40	0.89	15.14	2.19	1.26	0.57	17.0	16.23	58.4	33.2
0%REF+10%VR+45%HVGO+45%PFX	76.57	11.28	10.38	1.77	5.86	3.62	2.43	2.13	16.52	16.23	42.6	33.2
5%REF+10%VR+42.5%HVGO+42.5%PFX	72.43	14.0	11.80	1.77	6.67	2.87	1.36	1.21	16.73	16.23	49.3	33.2
10%REF+10%VR+40%HVGO+40%PFX	68.28	16.73	13.22	1.77	7.47	2.34	0.98	0.88	16.94	16.23	56.2	33.2
15%REF+10%VR+37.5%HVGO+37.5%PFX	64.13	19.46	14.64	1.77	8.27	1.93	0.92	0.83	17.16	16.23	63.2	33.2
0%REF+15%VR+42.5%HVGO+42.5%PFX	72.93	12.80	11.61	2.66	4.37	3.10	1.66	2.20	16.66	16.23	47.1	33.2
5%REF+15%VR+40%HVGO+40%PFX	68.78	15.53	13.03	2.66	4.91	2.50	0.91	1.22	16.87	16.23	54.0	33.2
10%REF+15%VR+37.5%HVGO+37.5%PFX	64.64	18.26	14.45	2.66	5.44	2.06	0.79	1.07	17.09	16.23	61.0	33.2
15%REF+15%VR+35%HVGO+35%PFX	60.49	20.99	15.87	2.66	5.98	1.71	0.72	0.99	17.31	16.23	68.1	33.2

\* VR: Cold Lake Vacuum residue (Imperial Oil Company)

REF: Resin enriched fraction (SFEEF experiment in China)

HVGO: Heavy vacuum gas oil (Imperial Oil Company)

PFX: Paraflex (Petro Canada Ltd.)

Appendix

Table A1.5 Resin Effect on Hot Filtration Insolubles Using REF as Diluent \*

Test fluid	T (°C)	Sa (wt%)	Ar (wt%)	Re (wt%)	As (wt%)	Re/As	CII	W	Cas (g/L)	n-heptane as titrant (25°C)			
										$\delta_{mix}$ [MPa] <sup>0.5</sup>	$\delta_f$ [MPa] <sup>0.5</sup>	S <sub>BNmix</sub>	I <sub>Nmax</sub>
0%REF+5%VR+95%HVGO	85	65.45	17.0	16.66	0.89	18.82	1.97	1.23	0.54	16.93	16.23	56.0	33.2
5%REF+5%VR+90%HVGO	85	62.08	19.35	17.68	0.89	19.98	1.70	0.82	0.36	17.12	16.23	61.9	33.2
10%REF+5%VR+85%HVGO	85	58.71	21.70	18.71	0.89	21.14	1.48	0.58	0.26	17.30	16.23	67.9	33.2
15%REF+5%VR+80%HVGO	85	55.34	24.04	19.73	0.89	22.29	1.28	0.49	0.22	17.49	16.23	74.0	33.2
0%REF+10%VR+90%HVGO	85	62.59	18.14	17.50	1.77	9.89	1.81	1.16	1.02	17.05	16.23	59.7	33.2
5%REF+10%VR+85%HVGO	85	59.22	20.49	18.52	1.77	10.46	1.56	0.62	0.55	17.24	16.23	65.7	33.2
10%REF+10%VR+80%HVGO	85	55.85	22.84	19.55	1.77	11.04	1.36	0.46	0.41	17.42	16.23	71.8	33.2
15%REF+10%VR+75%HVGO	85	52.48	25.19	20.57	1.77	11.62	1.19	0.40	0.36	17.62	16.23	78.0	33.2
0%REF+15%VR+85%HVGO	85	59.72	19.29	18.34	2.66	6.91	1.66	0.88	1.18	17.17	16.23	63.5	33.2
5%REF+15%VR+80%HVGO	85	56.35	21.63	19.36	2.66	7.29	1.44	0.49	0.66	17.36	16.23	69.6	33.2
10%REF+15%VR+75%HVGO	85	52.98	23.98	20.39	2.66	7.68	1.25	0.36	0.47	17.55	16.23	75.8	33.2
15%REF+15%VR+70%HVGO	85	49.61	26.33	21.41	2.66	8.06	1.09	0.32	0.44	17.74	16.23	82.0	33.2

\* VR: Cold Lake Vacuum residue (Imperial Oil Company)

HVGO: Heavy vacuum gas oil (Imperial Oil Company)

REF: Resin enriched fraction (SFEF experiment in China)

Appendix

Table A1.6 Hot Filtration Experiment Using Several Oil Cuts as Diluents\*

Test fluid	T (°C)	Sa (wt%)	Ar (wt%)	Re (wt%)	As (wt%)	Re/As	CII	W	Cas (g/L)	n-heptane as titrant (25°C)			
										$\delta_{mix}$ [MPa] <sup>0.5</sup>	$\delta_r$ [MPa] <sup>0.5</sup>	S <sub>BNmix</sub>	I <sub>Nmax</sub>
5%ATB+95%PFX	85	95.49	2.85	0.99	0.68	1.47	25.08	5.24	2.26	15.84	16.20	20.5	32.3
10%ATB+90%PFX	85	91.58	5.09	1.98	1.35	1.47	13.14	3.84	3.34	16.0	16.20	26.0	32.3
15%ATB+85%PFX	85	87.67	7.34	2.97	2.03	1.47	8.70	2.48	3.26	16.17	16.20	31.5	32.3
20%ATB+80%PFX	85	83.76	9.58	3.96	2.70	1.47	6.39	1.53	2.70	16.35	16.20	37.1	32.3
25%ATB+75%PFX	85	79.85	11.83	4.95	3.38	1.47	4.96	1.15	2.56	16.52	16.20	42.8	32.3
5%ATB+95%HVGO	85	65.96	17.34	16.02	0.68	23.73	2.0	0.88	0.38	16.94	16.20	56.1	32.3
10%ATB+90%HVGO	85	63.61	18.82	16.22	1.35	12.01	1.85	0.85	0.75	17.06	16.20	60.0	32.3
15%ATB+85%HVGO	85	61.25	20.31	16.42	2.03	8.11	1.72	0.79	1.05	17.18	16.20	63.9	32.3
20%ATB+80%HVGO	85	58.90	21.79	16.62	2.70	6.15	1.60	0.75	1.34	17.30	16.20	67.9	32.3
25%ATB+75%HVGO	85	56.54	23.27	16.82	3.38	4.98	1.49	0.72	1.62	17.43	16.20	72.0	32.3

\* ATB: Athabasca atmospheric tower bottom (Syncrude Canada Ltd.)

PFX: Paraflex (Petro Canada Ltd.)

HVGO: Heavy vacuum gas oil (Imperial Oil Company)

Table A1.7 Resin Effect on Hot Filtration Insolubles Using REF as Diluent \*

Test fluid	T (°C)	Sa (wt%)	Ar (wt%)	Re (wt%)	As (wt%)	Re/As	CII	W	Cas (g/L)	n-heptane as titrant (25°C)			
										$\delta_{mix}$ [MPa] <sup>0.5</sup>	$\delta_f$ [MPa] <sup>0.5</sup>	S <sub>BNmix</sub>	I <sub>Nmax</sub>
0%REF+5%ATB+95%PFX	85	95.49	2.85	0.99	0.68	1.47	25.08	5.24	2.26	15.84	16.20	20.5	32.3
5%REF+5%ATB+90%PFX	85	90.57	5.96	2.81	0.68	4.16	10.42	3.60	1.57	16.06	16.20	27.9	32.3
10%REF+5%ATB+85%PFX	85	85.64	9.07	4.62	0.68	6.84	6.31	2.84	1.25	16.30	16.20	35.4	32.3
15%REF+5%ATB+80%PFX	85	80.72	12.18	6.44	0.68	9.53	4.37	2.32	1.03	16.53	16.20	43.1	32.3
0%REF+10%ATB+90%PFX	85	91.58	5.09	1.98	1.35	1.47	13.14	3.84	3.34	16.00	16.20	26.0	32.3
5%REF+10%ATB+85%PFX	85	86.66	8.20	3.80	1.35	2.81	7.34	2.34	2.06	16.24	16.20	33.5	32.3
10%REF+10%ATB+80%PFX	85	81.73	11.31	5.61	1.35	4.16	4.91	1.78	1.58	16.47	16.20	41.1	32.3
15%REF+10%ATB+75%PFX	85	76.81	14.42	7.43	1.35	5.50	3.58	1.66	1.49	16.71	16.20	48.9	32.3
0%REF+15%ATB+85%PFX	85	87.67	7.34	2.97	2.03	1.47	8.70	2.48	3.26	16.17	16.20	31.5	32.3
5%REF+15%ATB+80%PFX	85	82.75	10.45	4.79	2.03	2.36	5.57	1.72	2.29	16.41	16.20	39.1	32.3
10%REF+15%ATB+75%PFX	85	77.82	13.56	6.60	2.03	3.26	3.96	1.48	1.99	16.65	16.20	46.8	32.3
15%REF+15%ATB+70%PFX	85	72.90	16.67	8.42	2.03	4.16	2.99	1.32	1.79	16.89	16.20	54.7	32.3

\* ATB: Athabasca atmospheric tower bottom (Syncrude Canada Ltd.)

REF: Resin enriched fraction (SFEF experiment in China)

PFX: Paraflex (Petro Canada Ltd.)

Table A1.8 Kinematic Viscosity for Thermal Fouling Test Fluids (85°C)

Test Fluid	Kinematic Viscosity $\times 10^6$ (m <sup>2</sup> /s)
10%VR+90%PFX	4.58
10%VR+5%REF+85%PFX	5.46
10%VR+45%HVGO+45%PFX	4.47
10%VR+90%HVGO	4.32
10%ATB+90%PFX	4.50
10%ATB+0.1%REF+89.9%PFX	4.61
10%ATB+0.5%REF+89.5%PFX	4.80
10%ATB+2%REF+88%PFX	5.02
10%ATB+5%REF+85%PFX	5.38
10%ATB+90%HVGO	4.27

## Appendix A2 Reproducibility of Experiments

### 1. Hot Filtration Experiment

Table A2.1 shows the results of hot filtration insolubles for the duplicate runs with various diluents.

Table A2.1 Hot Filtration Insolubles for the Duplicate Runs with Various Diluents

Test fluid	W (wt%) (1)	W (wt%) (2)
5%VR+95%PFX	7.46	7.67
10%VR+90%PFX	6.98	6.74
10%VR+5%REF+85%PFX	3.73	3.49
5%VR+95%HVGO	1.18	1.27
5%ATB+95%PFX	5.40	5.08
10%ATB+90%PFX	3.71	3.97
10%ATB+5%REF+85%PFX	2.41	2.26
5%ATB+95%HVGO	0.92	0.85

The average absolute and relative deviations are 0.20 (wt%) and 5.89% respectively. This result demonstrates that the hot filtration experimental data is reasonably reproducible.

### 2. Flocculation Titration Experiment

Table A2.2 shows the results of the duplicate runs for flocculation titration experiment.

Table A2.2 The Duplicate Runs for Flocculation Titration Experiment (n-heptane as titrant, 25°C)

Test fluid	Asphaltene precipitation onset, $V_p$ (ml n-heptane) (1)	Asphaltene precipitation onset, $V_p$ (ml n-heptane) (2)
0.5g VR + 3.0ml Toluene	6.9209	6.9012
0.75g VR + 3.0ml Toluene	7.6727	7.6831
1.0g VR + 3.0ml Toluene	8.3222	8.3178
0.5g VR + 3.0ml Toluene+2.0gPFX	6.1842	6.2013
0.5g VR + 3.0ml Toluene+1.0gREF	12.0897	12.0572
0.5g ATB + 3.0ml Toluene	7.5754	7.5996
0.5g ATB + 3.0ml Toluene+2.0gPFX	6.9581	6.9341
0.5g ATB + 3.0ml Toluene+1.0gREF	13.2956	13.2609

The average absolute and relative deviations are 0.021ml and 0.24% respectively. The reproducibility of the flocculation titration experiment is very good.

### 3. Thermal Fouling Experiment

The thermal fouling experiment with 10%VR and 90%PFX was repeated, the results are shown in Table A2.3 and Figure 6.2.

Table A2.3 Test of Reproducibility of Thermal Fouling Experiment

Trial No.	Test fluid	Initial fouling rate (m <sup>2</sup> K/kwh)	Final R <sub>f</sub> (m <sup>2</sup> K/KW) (~40 hours)
1	10%VR+90%PFX	0.0068	0.19
2	10%VR+90%PFX	0.0066	0.20

The average absolute and relative deviations for initial fouling rate and final fouling resistance are 0.0002m<sup>2</sup>K/kwh, 2.9% and 0.01m<sup>2</sup>K/KW, 5.0% respectively. The result indicates that the results of the thermal fouling experiment are reliable and reproducible. Asomaning [54] mentioned that one would expect a rate variance of ±10%.

### Appendix A3 Sample Calculation

#### 1. Bulk Velocity and Reynolds Number in Thermal Fouling

The flow rates are calculated using the following equation:

$$V = C_d A_{or} \left[ \sqrt{\frac{2(\Delta P)}{\rho(1 - \beta^4)}} \right]$$

$$C_d = 0.6102$$

$$d_2 = 0.0158 \text{ m (pipe diameter)}$$

$$\beta = d_1/d_2 = 0.5024$$

$$d_1 = \beta d_2$$

$$A_{or} = 4.7 \times 10^{-5} \text{ m}^2$$

$$\rho = 822 \text{ kg/m}^3 \text{ (10\%VR - 90\%PFX)}$$

For a velocity of 0.75m/s, the volumetric flow rate is as follows,

$$V = u \cdot A_{cr}$$

Where,

$$\begin{aligned} A_{cr} &= \frac{\pi}{4} (d_0^2 - d_i^2) = \frac{\pi}{4} (0.025^2 - 0.0103^2) \\ &= 0.000407 \text{ m}^2 \end{aligned}$$

Where  $d_0$  = annulus outer diameter

$d_i$  = annulus inner diameter

Thus, the volumetric flow rate is

$$V = 0.000306 \text{ m}^3$$

Then the required pressure drop across the orifice flow meter to obtain the desired velocity is:

$$\Delta P = 43808.2$$

Then the required mercury manometer reading is given by:

$$\Delta P = \Delta z (\rho_{\text{Hg}} - \rho_f)g$$

$$\Delta z = 0.349 \text{ m}$$

$$\Delta z = 13.76 \text{ inches}$$

given  $\rho_{\text{Hg}}=13543 \text{ kg/m}^3$

In this work, the digital DP meter was used to measure the pressure drop, the correlation between the mercury manometer reading and DP reading is given by:

$$\Delta z (\text{inch}) = 0.6763 \times dp - 0.3002$$

$$dp = 20.79$$

The bulk Reynolds number is given by:

$$\text{Re} = \frac{u d_{eq}}{\nu}$$

Where  $d_{eq}$  is the equivalent diameter of the annulus,

$$d_{eq} = d_0 - d_1 = 0.025 - 0.0103 = 0.0147 \text{ m}$$

and the kinematic viscosity of the fluid (10%VR - 90%PFX) at 85°C is  $4.58 \times 10^{-6} \text{ m}^2/\text{s}$

$$\text{Re} = \frac{(0.75)(0.0147)}{4.58 \times 10^{-6}} = 2407$$

## 2. Thermal Fouling Resistances

The sample calculation for the thermal fouling resistance is being done for run with 10%VR-90%PFX (run 17). Under clean conditions,  $T_{s0}=291.3^\circ\text{C}$ ,  $T_b=85.2^\circ\text{C}$  and  $Q=1048 \text{ W}$ , under fouled conditions,  $T_s=318.6^\circ\text{C}$ ,  $T_b=85.6^\circ\text{C}$  and  $Q=1046 \text{ W}$ ,

The surface area of the probe is given by:

$$A = \pi r l = 3.14159 \times 0.0107 \times 0.1016 = 3.41 \times 10^{-3} \text{ m}^2$$

Thus the heat flux under clean conditions is given by:

$$Q/A = 1048/3.41 \times 10^{-3} = 307.3 \text{ kW/m}^2$$

the heat flux under fouled conditions is given by:

$$Q/A = 1046/3.41 \times 10^{-3} = 306.7 \text{ kW/m}^2$$

The initial overall heat transfer coefficient is given by:

$$1/U_0 = (291.3 - 85.2)/307.3 = 0.671 \text{ m}^2\text{K/kW}$$

the overall heat transfer coefficient under fouled conditions is given by:

$$1/U = (318.6 - 85.6)/306.7 = 0.760 \text{ m}^2\text{K/kW}$$

Thus the thermal fouling resistance is given by:

$$R_f = 1/U - 1/U_0 = 0.089 \text{ m}^2\text{K/kW}$$

### 3. Initial Fouling Rate

The initial fouling rates were obtained by a fit of the linear section of the fouling resistance-time plots over the first few hours of a run:

$$\frac{dR_f}{dt} = \frac{d}{dt} \left( \frac{1}{U(t)} \right)$$

In case where asymptotic fouling behavior is observed, the Kern-Seaton asymptotic fouling resistance model can be used to fit the data and obtained the initial fouling rate as follows:

$$R_f = R_f^* (1 - \exp(-bt))$$

where  $R_f^*$  is the asymptotic resistance. The initial fouling rate is given by

$$R_{f_0} = b \times R_f^*$$

For thermal fouling test fluid 10%VR+90%PFX1 at  $T_{s0}=260^\circ\text{C}$ ,  $T_b=85^\circ\text{C}$ ,  $v=0.75\text{m/s}$

$$(R_f)_{\text{final}} = 0.09 \text{ m}^2\text{K/kW}$$

Initial fouling rate obtained by a fit of the linear section of the fouling resistance-time ( $R_f$ - $t$ ) plot over the first 5 hours of a run is  $0.0052 \text{ m}^2\text{K/kWh}$ .

Initial fouling rate obtained by the Kern-Seaton asymptotic fouling resistance model is:

$$R_f = 0.10968 * (1 - e^{-0.04629t}), r^2 = 0.9636$$

$$\left(\frac{dR_f}{dt}\right)_{t=0} = 0.10968 * 0.04629 = 0.0051 \text{ m}^2\text{K/kWh}$$

The comparison of the initial fouling rate by two methods is shown in Table A3.1

Table A3.1 The comparison of the initial fouling rate by two methods

Test fluid	$T_{s0}$ (°C)	Initial fouling rate( $\text{m}^2\text{K/kWh}$ )	
		Linear section fit (0-5h)	Asymptotic fouling resistance model
10%VR+90%PFX	260	0.00523	0.00512
10%VR+5%REF+85%PFX	260	0.00242	0.00221
10%VR+45%HVGO+45%PFX	260	0.00067	0.00073
10%VR+90%HVGO	260	0.00075	0.00068
10%ATB+90%PFX	290	0.00232	0.00247
10%ATB+0.1%REF+89.9%PFX	290	0.00194	0.00202
10%ATB+0.5%REF+89.5%PFX	290	0.00076	0.00082
10%ATB+2%REF+88%PFX	290	0.00026	0.00031
10%ATB+5%REF+85%PFX	290	0.0001	0.00012
10%ATB+90%HVGO	290	0.00016	0.00021

The average absolute and relative deviations for two methods  $0.000086 \text{ m}^2\text{K/kWh}$  and 10.4% respectively.

#### 4. Energy of Activation

The activation energies were calculated by solving the Arrhenius type equation,

$$(dR_f/dt)_{t=0} = A \exp(-E/RT)$$

Where E is the activation energy, T is the surface temperature in Kelvin and R the gas constant is 8.314 kJ/kmol K.

#### 5. Colloidal Instability Index (CII)

The colloidal instability index is calculated using the definition:

$$CII = \frac{(\text{Saturates} + \text{Asphaltenes})}{(\text{Aromatics} + \text{Resins})}$$

Table A3.2 Average SARA analysis of test fluids

Test fluid	Saturates, wt%	Aromatics, wt%	Resins, wt%	Asphaltenes, wt%
VR	11.0	38.7	32.6	17.7
ATB	21.2	45.5	19.8	13.5
PFX	99.4	0.6	0	0
HVGO	68.3	15.9	15.8	0
REF	0.9	62.8	36.3	0

For 10%VR – 90%PFX, the CII can be calculated as follows:

$$CII = \frac{(0.1 \times 0.11 + 0.9 \times 0.994) + (0.1 \times 0.177 + 0.9 \times 0)}{(0.1 \times 0.387 + 0.9 \times 0.006) + (0.1 \times 0.326 + 0.9 \times 0)} = 12.04$$

#### 6. Solubility Parameters, The Andersen/Petersen Model and the Wiehe Model Parameters

Based on the flocculation titration experimental results, the Andersen/Pedersen model and the Wiehe (Oil Compatibility) model are applied to calculate the solubility parameter of the feedstocks and the blends.

According to the Andersen/Pedersen approach, asphaltenes will precipitate when the solvent phase or oil reaches conditions where the average solubility parameter of the phase equals a critical solubility parameter obtained through the titration. The critical solubility parameter for the mixture,  $\delta_{cr}$ , is given as

$$\delta_{cr} = \phi_o\delta_o + \phi_p\delta_p + \phi_s\delta_s$$

where  $\delta_o$ ,  $\delta_p$ , and  $\delta_s$  are the solubility parameters of oil, precipitant and solvent respectively and  $\phi_o$ ,  $\phi_p$ ,  $\phi_s$  are volume fractions of the corresponding components such that  $\delta_p=15.2$  (MPa)<sup>0.5</sup> (n-heptane) or  $\delta_p=14.0$  (MPa)<sup>0.5</sup> (iso-octane) and  $\delta_s=18.3$  (MPa)<sup>0.5</sup> are used in this work.  $\sum \phi_i = 1$ . Assuming that the above equation fully describes the onset of asphaltene precipitation, a plot of  $V_p/V_o$  vs  $V_s/V_o$  is a linear function, where the slope,  $s = (\delta_s - \delta_{cr}) / (\delta_{cr} - \delta_p)$ , and the intercept,  $I_y = (\delta_o - \delta_{cr}) / (\delta_{cr} - \delta_p)$ . The criterion for the oil blend to be stable is that  $\delta_o > \delta_{cr}$ .

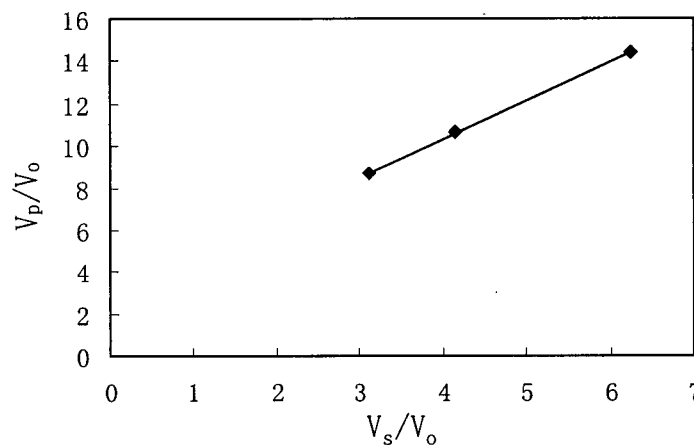
For each oil (such as VR), at least three concentrations of the oil were tested, the result is shown in Table A3.3.

Table A3.3 Flocculation Titration Results for Cold Lake Vacuum Residue

Test fluid	$V_o$ (ml)	$V_s$ (ml)	$V_p$ (ml)	$V_p/V_o$	$V_s/V_o$
0.5gVR+3.0ml Toluene	0.4807	3.0	6.9209	14.3982	6.2412
0.75gVR+3.0ml Toluene	0.7210	3.0	7.6727	10.6415	4.1608
1.0gVR+3.0ml Toluene	0.9614	3.0	8.3222	8.6568	3.1206

A linear equation can be found by plotting  $V_p/V_o$  vs  $V_s/V_o$  :

$$V_p/V_o = 1.835(V_s/V_o) + 2.9609$$



Hence :

$$s = (\delta_s - \delta_{cr}) / (\delta_{cr} - \delta_p) = 1.835$$

$$I_y = (\delta_o - \delta_{cr}) / (\delta_{cr} - \delta_p) = 2.9609$$

$$\delta_{cr} = 16.29 \text{ (MPa)}^{0.5}, \delta_o = 19.52 \text{ (MPa)}^{0.5}$$

The Oil Compatibility Model of Wiehe, expresses the above equation as:

$$\delta_f = \phi_o \delta_o + \phi_H \delta_H + \phi_T \delta_T$$

where  $\delta_f$  is the flocculation solubility parameter, and  $\delta_H$ ,  $\delta_T$ ,  $\delta_o$  are the solubility parameter of n-heptane (precipitant), toluene (solvent) and the oil respectively.  $\delta_H = 15.2 \text{ (MPa)}^{0.5}$  and  $\delta_T = 18.3 \text{ (MPa)}^{0.5}$  are used in this work. The slope and intercept for the flocculation titration plot are defined as :

$$S_{BN} = 100(\delta_o - \delta_H) / (\delta_T - \delta_H)$$

$$I_N = 100(\delta_f - \delta_H) / (\delta_T - \delta_H)$$

where  $S_{BN}$ , and  $I_N$  are defined as the solubility blending number and insolubility number.

For the mixtures of 10%VR-90%PFX,  $\delta_{VR}=19.53 \text{ (MPa)}^{0.5}$ ,  $\delta_{PFX}=15.67 \text{ (MPa)}^{0.5}$ ,  $\delta_{cr}$  or  $\delta_f=16.23 \text{ (MPa)}^{0.5}$ ,

$$\begin{aligned}\delta_{mix} &= \Phi_{VR} \delta_{VR} + \Phi_{PFX} \delta_{PFX} \\ &= \frac{0.1}{1.0402} \times 19.53 + \frac{0.9}{0.8554} \times 15.67 \\ &= \frac{\left( \frac{0.1}{1.0402} + \frac{0.9}{0.8554} \right)}{\left( \frac{0.1}{1.0402} + \frac{0.9}{0.8554} \right)} \times 15.67 \\ &= 15.99 \text{ (MPa)}^{0.5}\end{aligned}$$

According to the Andersen stability criterion,  $\delta_{mix} < \delta_{cr}$ , indicates this oil blend is unstable.

$$\begin{aligned}(S_{BN})_{VR} &= 100(\delta_{VR}-\delta_H)/(\delta_T-\delta_H) \\ &= 100 \times (19.53-15.2)/(18.3-15.2) \\ &= 139.7\end{aligned}$$

$$\begin{aligned}(I_N)_{VR} &= 100(\delta_f-\delta_H)/(\delta_T-\delta_H) \\ &= 100 \times (16.23-15.2)/(18.3-15.2) \\ &= 33.2\end{aligned}$$

$$\begin{aligned}(S_{BN})_{PFX} &= 100(\delta_{PFX}-\delta_H)/(\delta_T-\delta_H) \\ &= 100 \times (15.67-15.2)/(18.3-15.2) \\ &= 15.2\end{aligned}$$

$$(I_N)_{PFX} = 0$$

$$\begin{aligned} S_{BNmix} &= \Phi_{VR} S_{BNVR} + \Phi_{PFX} S_{BNPFX} \\ &= \frac{0.1}{1.0402} \times 139.7 + \frac{0.9}{0.8554} \times 15.2 \\ &= 25.6 \end{aligned}$$

$$I_{Nmax} = 33.2$$

According to the Wiehe stability criterion,  $S_{BNmix} < I_{Nmax}$ , indicates this blend is unstable.